The role of PPARγ in lipid metabolism

Ellen Jeninga

Jeninga, Ellen Helena
The Role of PPARγ in lipid metabolism
Thesis University of Utrecht

ISBN 978-90-393-5049-2

The printing of this thesis was financially supported by contributions of the Department of Metabolic & Endocrine Diseases (UMCU), University of Utrecht and J.E. Jurriaanse Stichting.

Printed by F&N Boekservice, Amsterdam, The Netherlands

Cover: On our way to Le Collet Blanc (France, January 2008)
Photography Nander Wever

The role of PPARγ in lipid metabolism

De rol van PPARγ in de vetstofwisseling

(met een samenvatting in het Nederlands)

Proefschrift

ter verkrijging van de graad van doctor aan de Universiteit Utrecht op gezag van de rector magnificus, prof.dr. J.C. Stoof, ingevolge het besluit van het college voor promoties in het openbaar te verdedigen op dinsdag 19 mei 2009 des middags te 2.30 uur

door

Ellen Helena Jeninga

geboren op 6 april 1980 te Obdam

Promotor: Prof. Dr. R. Berger

Co-promotor: Dr. E. Kalkhoven

"Der Weg ist das Ziel"
Confucius

Aan mijn ouders

Contents

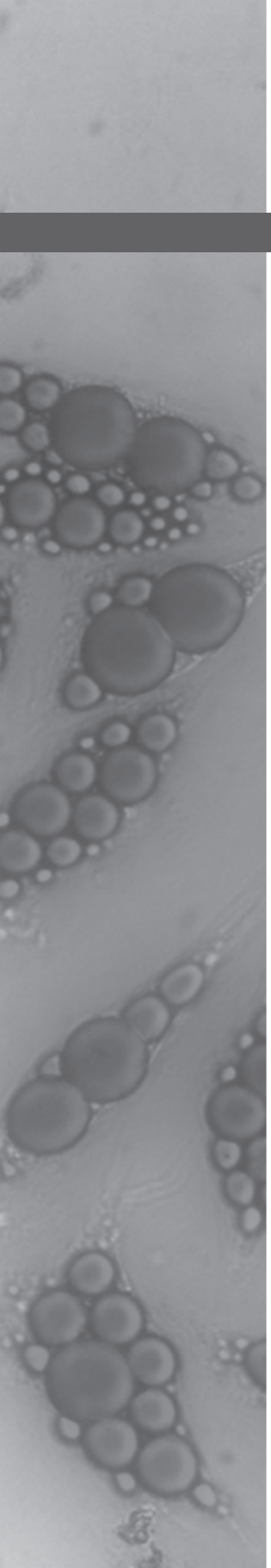

Chapter 1

General Introduction

Introduction

Nowadays the prevalence of overweight and obesity and the herewith associated components of the metabolic syndrome like insulin resistance, type 2 diabetes, dyslipidemia, hypertension and coronary heart disease rapidly increases worldwide (1). Conspicuously, similar metabolic disturbances are observed in patients with lipodystrophy, which is characterized by systemic or localized loss of adipose tissue, indicating an important role for adipose tissue in whole body metabolism

Lipid metabolism in adipocytes

Adipose tissue is the major site of lipid storage in the body and plays a pivotal role in the maintenance of whole body glucose and lipid metabolism. Adipose tissue lipid metabolism, which involves triacylglcerol (TAG) synthesis/storage and lipolysis, is highly regulated by hormones and other factors such as nutritional status and exercise. In the normal physiological state, excess fuel substrates is partitioned to adipose tissue where it is stored as TAGs until its subsequent release as free fatty acids (FFA) in times of energy demand. Dysregulation of these processes can result in an increase in circulating FFAs and lipid accumulation in non-adipose tissues, such as liver, muscle and pancreatic islets, ultimately contributing to dyslipidemia, insulin resistance and diabetes (2).

TAG synthesis and storage

TAG synthesis requires glycerol and fatty acids, which are transformed to glycerol-3-phophate and fatty acyl-CoA to be used as substrates (Figure 1A). Glycerol-3P is derived from glucose through the first step of glycolysis and from glyceroneogenesis. Adipocyte glucose uptake occurs mainly via the GLUT4 receptor and is controlled by insulin. Glyceroneogenesis is the synthesis of glycerol-3P by non-carbohydrate precursors such as pyruvate. The key enzyme in this process is PEPCK. The proportion of Glycerol-3P produced by glycolysis and glyceroneogenesis varies with nutritional status. The fatty acids esterified to the glycerol-3P backbone can be obtained by either *de novo* lipogenesis or the uptake of fatty acids from circulating TAG-rich lipoproteins. Although in human adipose tissue the enzymes for *de novo* lipogenesis (synthesis of fatty acids from non-lipid substrates) are present, the contribution of this pathway to TAG synthesis is considered to be very low. The majority of the fatty acids used for TAG synthesis are derived from the circulating TAG-rich lipoproteins. Fatty acids are released from the TAG-rich lipoproteins through the hydrolysis of TAG by lipoprotein lipase (LPL). The subsequent transport of fatty acids through the adipocyte plasma membrane is regulated and facilitated by fatty acid transporters such as CD36. In the cytoplasm fatty acids and acyl-CoA are esterified into fatty acyl-CoA (FA-CoA) by acyl-coenzyme A synthetase enzymes

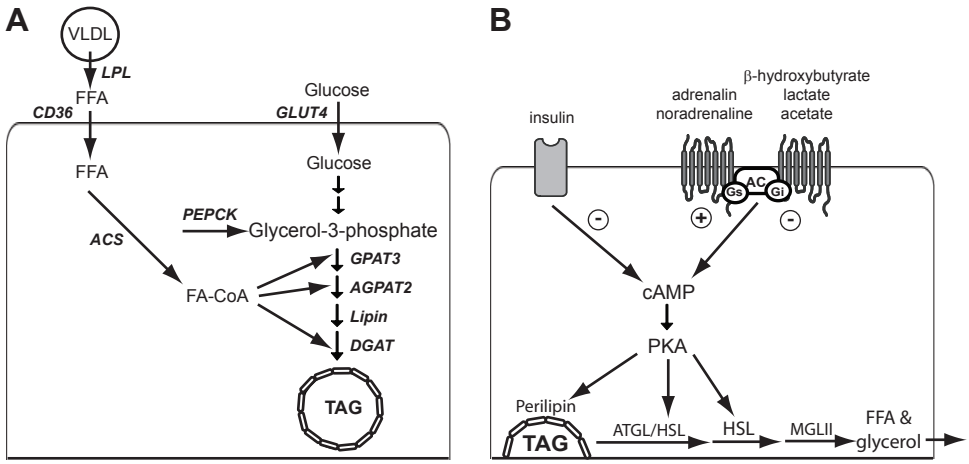

Figure 1. Lipid metabolism in adipocytes.
A, Schematic representation of fatty acid uptake and triacylglycerol (TAG) synthesis. B, FFA release is regulated by lipolysis.

(ACS). These FA-CoAs are subsequently esterified to the glycerol-3P backbone by different enzymes respectively, named glycerol-3-phosphate acyltransferases (GPATs), 1-acylglycerol-3-phophate acyltransferases (AGPATs) and diacylglycerol acyltransferases (DGATs) to TAGs (Figure 1A).

Lipolysis

The regulation of lipolysis provides a main switch between lipid storage and lipid mobilization in times of energy demand and is tightly regulated by hormones, cytokines and other metabolites. The hydrolysis of TAGs occurs in a stepwise fashion via diacylglycerol (DAG) and monoacylglycerol (MAG) with the liberation of a FFA at the first two steps and the release of a FFA and glycerol at the final step. This process is regulated by a number of lipases and lipid droplet proteins. The first step in the hydrolysis of TAG is regulated by a number of lipases including hormone sensitive lipase (HSL) and adipose triglyceride lipase (ATGL), whereas the second and third steps are exclusively regulated by HSL and monoglyceride lipase (MGL) respectively (Figure 1B). The rate-limiting enzyme is HSL and so named of its responsiveness to hormones; like catecholamines and insulin (3). Cathecholamines, such as adrenaline (epinephrine) and noradrenaline (norepinephrine) are the main hormones that markedly stimulate lipolysis in humans are cathecholamines, such as adrenaline and noradrenaline. These cathecholamines bind to β-adrenergic receptors, which are positively coupled to adenylyl cyclase by the stimulatory G-protein complex (G_s). Stimulation of adenylyl cyclase leads to an increase of intracellular cyclic AMP levels (cAMP), which in turn promotes the activation of protein kinase A (PKA). The activation of PKA results in the phosphorylation of

HSL and the lipid droplet protein perilipin, ultimately leading to the hydrolysis of TAGs. Other hormones that may stimulate lipolysis through Gs coupled receptors are thyroid stimulating hormone (TSH), glucagon and cholecystokinin (CCK). In addition the cytokine TNFα has been shown to increase lipolysis rates in humans *in vivo* (4). Insulin is the most potent antilipolytic hormone in adipose tissue. After binding to its receptor at the surface of the adipocyte, it induces a signal transduction cascade including the activation of PI3K and PKB/AKT leading to activation of phosphodiesterase subtype 3B (PDE-3B), causing a lowering of cAMP levels. In addition, other metabolites such as lactate, acetate and the ketone body β-hydroxybutyrate have been shown to inhibit lipolysis in adipocytes via coupling to G_i, which inhibits adenylyl cyclase and counteracts the pro-lipolytic receptors. Interestingly, the expression of a number of genes involved in adipocyte lipid metabolism (e.g. LPL, PEPCK and ATGL) is controlled by the transcription factor PPARγ.

PPARγ, a nuclear receptor

Peroxisome proliferator-activated receptors (PPARs) belong to the nuclear receptor superfamily of ligand inducible transcription factors that were identified in the 1990s in rodents, named after their ability to induce the proliferation of peroxisomes (5). PPARs share a modular structure with other members of the nuclear receptor superfamily. At the N-terminus they contain a ligand-independent activation function 1 (AF-1) domain, which is constitutive active and/or regulated by signal transduction cascades. Centrally located is the highly conserved DNA binding domain (DBD) which contains two zinc fingers that are responsible for DNA binding. A highly flexible region named the hinge region connects the DBD with a C-terminal ligand binding domain (LBD). This LBD mediates ligand-binding and heterodimerisation with RXRα and contains a ligand-dependent activation function (AF-2). PPARs bind as obligate heterodimers with retinoic acid X receptors (RXRs) to PPAR responsive elements (PPREs), which consists of two hexameric direct repeats (AGGTCA) interspaced by one nucleotide (DR-1). Three PPAR subtypes have been identified, encoded by three separate genes. PPARα is mainly expressed in the liver and to a lesser extent in heart and skeletal muscle. This receptor can be activated by fibrates and unsaturated fatty acids and is a major regulator of fatty acid oxidation. This is particularly important in times of energy demand, as PPARα expression and activity increases during fasting and PPARα null mice cannot sustain fasting, while these animals are indistinguishable from wild type mice on a regular diet (6). PPARβ/δ is more ubiquitously expressed and favours fatty acid oxidations in tissues in which PPARα expression is low. Although the natural ligands remain elusive, fatty acids and eicosanoids are able to activate PPARβ/δ (7). Endurance training increases the expression of PPARβ/δ (8) and

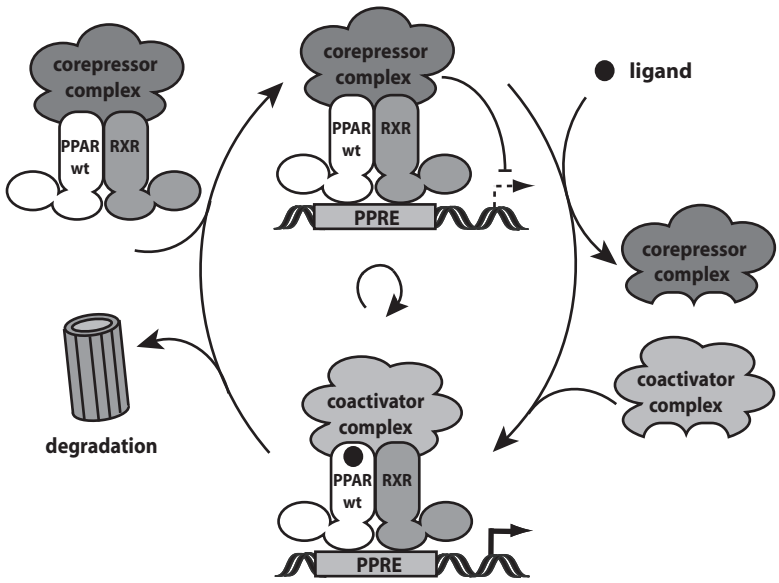

Figure 2. Schematic representation of PPARγ promoter cycling.
PPARγ binds as obligate heterodimer with RXR to a PPRE in the promoter/enhancer region of a target gene. On some PPREs under basal conditions corepressors can repress transcription. Upon binding of ligands corepressors will be released and coactivators recruited and transcription is initiated. Afterwards PPARγ will be degraded and a next round of promoter cycling will take place.

muscle-specific overexpression results in increased oxidative myofiber number and fatty acid oxidation and resistance to muscle fatigue (9).
The third family member is PPARγ and although the *PPARG* gene gives rise to four different mRNA products (PPARγ1-4) by differential promoter usage and alternative splicing, it encodes only two receptor proteins, PPARγ1 and PPARγ2. The PPARγ2 isoform has 30 (or 28 in humans) additional amino acids at the N-terminus and its expression is restricted to adipose tissue, whereas the PPARγ1 isoform is more ubiquitously expressed (e.g. in adipose tissue, skeletal muscle, heart, liver, lower intestine and macrophages). A variety of endogenous ligands have been described for PPARγ, including polyunsaturated fatty acids, eicosanoids and prostaglandin J2 derivatives (10;11). Synthetic agonists include the thiazoledinediones (TZDs) (12) and tyrosine-based agonists (13) that have been shown to lower blood glucose levels and ameliorate insulin sensitivity in patients with type 2 diabetes. From *in vivo* and *in vitro* studies PPARγ has emerged as the master regulator of adipocyte differentiation. Whereas PPARγ homozygous null mice are embryonic lethal due to placental dysfunction, the heterozygous null mice fail to develop adipose tissue (14;15). In addition, PPARγ null ES cells failed to undergo differentiation after hormone treatment (16;17) and ectopic expression of PPARγ in murine cells was sufficient to promote adipogenesis (18). In addition to adipogenesis, PPARγ also

plays an important role in adipocyte glucose and lipid metabolism through the direct regulation of a number of genes involved in these metabolic processes (19;20). On the promoters of some target genes, unliganded PPARγ recruits multiprotein corepressor complexes, containing either NCoR or SMRT, together with histone deacetylases that actively repress transcription. Binding of ligand is the crucial event that switches the function of nuclear receptors from active repression to transcriptional activation and is due to stabilization of the active conformation resulting in reduced corepressor affinity and simultaneously enhanced affinity for coactivators. Corepressors are released and replaced by coactivator complexes, including SRC-1, CBP and TRAP/DRIP/ARC complexes that are involved in transcriptional activation. During transcriptional activation nuclear receptors like PPARγ and their cofactors cycle on and off the promoters of the target genes. As shown in Figure 2, this promoter cycling is a very dynamic process involving ligand binding, cofactor exchange and proteasome dependent receptor degradation and plays an important role in determining the gene transcription rate (21;22). In addition, PPARγ can also regulate gene expression in an indirect ligand dependent manner, e.g. by antagonizing the action of NF-κB activation (23;24).

Genetic variation in PPARγ

Polymorphisms

Since PPARγ was identified as the master regulator of adipogenesis and recognized to play a key role in glucose and lipid metabolism and thereby affecting insulin sensitivity, it was obvious to search for PPARγ mutations in diabetic patients. Yen *et al*. were the first who performed a molecular scanning of the human *PPARG* gene in diabetic Caucasians with or without obesity (25) and reported two polymorphisms: a misssense mutation at codon 12 of PPARγ2 leading to the substitution of a proline for an alanine at this position and a C to T substitution at position 1431 in exon 6 leading to the synonymous His477His polymorphism. Nowadays Pro12Ala is the most extensively studied polymorphism and its frequency has been reported to vary from 2% to 25% depending on ethnicity. Numerous studies have been performed on the possible association of this polymorphism with insulin resistance and initially results have been contradictory. A recruit-by-phenotype approach (26) and two large meta-analysis studies (27;28) however, found a modest but significant increase in diabetes risk for carriers of the proline allele. Since this risk allele has a high frequency this modest effect translates into a large population attributable risk for type II diabetes influencing as much as 25% in the general population. Functional studies on these genetic variants showed for the Ala variant a modest reduction of target gene transactivation in the presence and absence of ligand due to a reduced binding affinity for the cognate promoter elements (29). In addition, a reduced ability to induce adipocyte differentiation (30), altered cofactor binding

and adiponectin signalling (31) were reported for the Ala variant. Although the Ala variant showed reduced adipogenic potential *in vitro*, association studies between the polymorphism and BMI in humans were often contradictory, suggesting the influence of other factors. Several studies have indeed shown the influence of other factors such as physical activity and diet on BMI of the Ala allele carriers (32;33). In addition, Ala/Ala mice were leaner and more insulin sensitive on a regular diet, but this effect was reversed on a high fat diet (31), confirming that the protective role of P12A is highly dependent on gene-nutrient interactions. Next to the influence of gene-environment interactions at the *PPARG* locus, the influence of additional polymorphisms should be taken into account. As mentioned earlier another polymorphism, C1431T, in the *PPARG* gene has been described. Interestingly this polymorphism is in tight allelic disequilibrium with Ala12 (70% Ala carriers) (34) and when this Ala12 variant was on a haplotype with 1431C it conferred greater protection for diabetes compared to the 1431T variant (35). Thus the relationship between the PPARγ P12A polymorphism and insulin sensitivity in humans is complex and is influenced by other genetic and environmental factors.

PPARγ germline mutations

Until now 17 coding sequence mutations and 1 non-coding sequence mutation in the *PPARG* gene have been reported (Figure 3). The majority of these PPARγ mutations are associated with FPLD3. Ten of these mutations are missense mutations, which are either located in the DBD (C142R, C159Y, C190S, C190W, and R194W; PPARγ2 nomenclature) (36-38) or in the LBD (V318M, F388L, D424N, R425C, P495L; PPARγ2 nomenclature) (39-43). In addition, two nonsense mutations (Y355X and R385X;

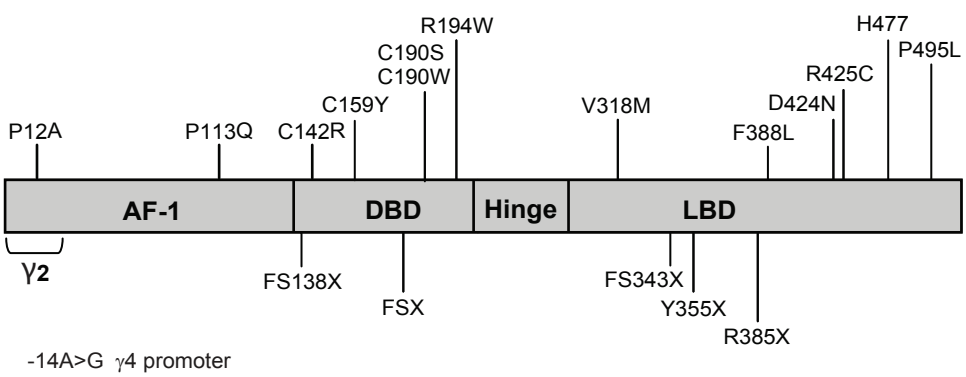

Figure 3. Overview of PPARγ mutations.
Schematic representation of the distinct domains of the PPARγ2 protein (with PPARγ1 missing the first 30 amino acids) and the location of the different mutations. The polymorphisms and missense mutations are depicted above the bar and under the bar are the nonsense mutations (all PPARγ2 nomenclature). In addition, 1 non-coding sequence mutation in the PPARγ4 promoter has been reported and is depicted separately.

PPARγ2 nomenclature) (36;44) two frameshift/premature stop mutations (FS138X and FS343X; PPARγ2 nomenclature) (36;45;46) and a mutation in the PPARγ4 promoter (-14G>A) (47) have been reported. Except for the promoter mutation, all mutations affect protein function resulting in a reduced transcriptional activity. The recently reported crystal structure of the liganded PPARγ/RXRα heterodimer bound to DNA (48) contributed to our comprehension as to how these mutations affect protein function (see Chapter 2). In a study on 358 unrelated German subjects four of the 121 obese subjects harboured a heterozygous mutation in the AF-1 domain at position 113 that substituted a proline into a glutamine (sometimes referred to as P115Q) (49). Although insulin resistant, a fifth subject without severe overweight has been reported to carry the same mutation (50). This suggests that the PPARγ P113Q mutation associates with insulin resistance rather then obesity, which might explain why this mutation has not been found in other studies on obese subjects (51). Furthermore, as the P113Q mutation was detected with high frequency in German obese subjects this strongly suggests a founder effect. *In vitro* experiments showed that the PPARγ P113Q blocked phosphorylation of the serine located next to it (S112) leading to enhanced transcription and a faster adipocyte differentiation (49). A frameshift/premature stop mutation in PPARγ called FSX has been reported in patients with a familial syndrome of insulin resistance (45). These subjects are compound heterozygous for this mutation and a mutation in the *PPP1R3* that encodes an enzyme playing a keyrole in the regulation of glycogen storage in muscle (45).

Lipodystrophies

Human lipodystrophies represent a heterogeneous group of diseases characterized by generalized or partial alterations in body fat amount and/or distribution (52). Despite the marked phenotypic heterogeneity among the different types of lipodystrophies, most of them predispose to metabolic complications such as insulin resistance, type II diabetes, hepatic steatosis and dyslipidemia. The most prevalent form of lipodystrophy is lipodystrophy linked to HAART (highly active anti-retroviral therapy). This acquired form of lipodystrophy develops in 40-50% of HIV-infected patients on HAART and the majority of these patients demonstrate a loss of subcutaneous fat from the face and extremities, while accumulating fat in the dorsocervical region ("buffalo hump"). Unlike the inherited forms of lipodystrophy, acquired partial lipodystrophy linked to HAART can be reversed by attenuation of the therapy. The less common inherited forms of lipodystrophy can be subclassified as generalized or partial with the generalized forms being the most severe (Table 1).

Congenital generalized lipodystrophy (CGL)

CGL is characterized by a near complete absence of adipose tissue from birth or early infancy, leading to a muscular appearance. This rare autosomal recessive disorder has been shown to result from mutations in the *AGPAT-2* (CGL1; MIM 608594), *BSCL2* (CGL2; MIM 269700) or *CAV-1* (CGL3; MIM 612526) genes. CGL type I is caused by homozygous or compound heterozygous mutations in *AGPAT2*, including small deletions, non-sense, splice site, frameshift, missense and 3′ untranslated region mutations (52;53). *AGPAT2* encodes 1-acyl-glycerol-3-phosphate-acyltransferase 2, an enzyme localized in the ER that plays a critical role in the biosynthesis of glycerophosphoslipids and triacylglycerols. While some AGPATs are widely distributed, AGPAT2 is predominantly expressed in adipose tissue. The recently reported AGPAT2$^{-/-}$ mice were lipodystrophic and had similar metabolic complications as observed in humans, emphasizing the importance of this gene in adipose tissue development and whole body metabolism (54). The affected gene in CGL type II is *BSCL2*, which encodes an integral ER membrane protein named seipin. Seipin is mainly expressed in adipose tissue, brain and testis and some *BSCL* mutations have been shown to affect adipocyte differentiation and / or lipid droplet formation (55-57). Very recently a homozygous nonsense mutation in *CAV1* (58) has been reported to result in CGL type III (CGL3). This gene encodes the protein caveolin1, which is typically found in plasma membrane invaginations, known as caveolae. It is highly expressed in adipose tissue and strongly induced during 3T3-L1 differentiation (59). In addition, proteomics analysis revealed that it also localizes to lipid droplets in adipocytes (60). Homozygous deletion of this

	Mode of inheritance	Gene	Clinical features
Generalized lipodystrophy			
CGL1	Autosomal recessive	*AGPAT2*	Acromegaloid features, hepatomegaly, IR, type II DM, dyslipidaemia
CGL2	Autosomal recessive	*BSCL2*	Acromegaloid features, hepatomegaly, IR, dyslipidaemia, mild mental retardation
CGL3	Autosomal recessive	*CAV1*	IR, type II DM, dyslipidaemia
Partial lipodystrophy			
FPLD2	Autosomal dominant	*LMNA*	IR, type II DM, dyslipidaemia, woman often have PCOS
FPLD3	Autosomal dominant	*PPARG*	IR, type II DM, dyslipidaemia, woman often have PCOS
FPLD	Autosomal dominant	*AKT2*	Type II DM, IR, hypertension
MADA	Autosomal recessive	*LMNA*	Mandibular hypoplasia, hyperinsulinemia, IR, type II DM, dyslipidaemia
MADB	Autosomal recessive	*ZMPSTE24*	Mandibular hypoplasia, hyperinsulinemia, IR, type II DM, dyslipidaemia

Table 1. Overview of inherited lipodystrophies.

CGL, congenital generalized lipodystrophy; FPLD, familial partial lipodystrophy disease; MAD, mandibuloacral dysplasia type A and B respectively; IR, insulin resistance; PCOS, polycystic ovarian syndrome.

protein in mice results in lipodystrophy and insulin resistance (61). In some CGL patients no mutations were found in any of these three genes, suggesting the involvement of additional loci.

Partial lipodystrophy
Familial partial lipodystrophies are autosomal dominant disorders and associated with mutations in three different genes *LMNA* (FPLD2; MIM 151660), *PPARG* (FPLD3; MIM 604367) or *AKT2* (FPLD: MIM 164731). Patients with this form of lipodystrophy usually have normal adipose tissue distribution at birth and during childhood, but a subsequent and progressive loss of subcutaneous fat from the extremities and gluteal region together with an accumulation of excess fat in the intra-abdominal region. FPLD2 or Dunnigan variety results from heterozygous missense mutations in exon 8 or 11 of the *LMNA* gene and in 75% of the patients the arginine at position 482 is substituted (R482W/Q/L). Lamin A is a nuclear intermediate filament that, together with lamin-associated proteins, maintains nuclear shape and provides support for chromosomal and replicating DNA. Interestingly, mutations in LMNA have also been described in Mandibuloacral Dysplasia type A (MADA). This is a very rare autosomal recessive inherited disease characterized by mandibular hypoplasia and associated with a partial lipodystrophy similar to that observed in FPLD. Another type of this lipodystrophy-associated disease is Mandibuloacral Dysplasia type B (MADB), caused by mutations in *ZMPSTE24* (62). This gene encodes a zinc metalloprotease involved in prelamin processing. Homozygous deletion of this protein in mice results in lipodystrophy. As both the enzyme involved in the formation of lamin A and mutations in lamina itself is associated with lipodystrophy, this indicates that normal lamin A is essential in adipocyte function. FPLD3 is associated with heterozygous mutations in the PPARG gene, encoding the nuclear transcription factor PPARγ. As PPARγ is mainly expressed in adipose tissue and a key regulator of adipocyte differentiation, maintenance and function, mutations in this protein are likely to affect adipose tissue.
In addition, three different heterozygous missense mutations in *AKT2* have been reported in subjects with severe insulin resistance and some of them presented partial lipodystrophy (63;64). *AKT2* encodes the serine/threonine kinase Akt2, which plays a critical role in the signal tansduction cascade downstream of the insulin receptor. Three mammalian isoforms of Akt (Akt1-3) exist which share about 80% amino acid identity. Akt1 is ubiquitously expressed and Akt3 mainly in brain and testis. Akt2 is predominantly expressed in insulin sensitive tissues (i.e. muscle, liver and adipose tissue) and is the most important isoform in glucose metabolism. Like the patients harbouring mutations in the *AKT2* gene, Akt2 deficient mice showed insulin resistance (65;66). The potential role of Akt in adipogenesis is discussed in Chapter 8.

Aim and outline of this thesis

Regulation of PPARγ expression and activity is critically important in the development of adipose tissue and metabolic homeostasis. The aim of the studies in this thesis was to gain more insight in the role of PPARγ in lipid metabolism. In Chapter 2, we made an overview of the functional data on the natural occurring PPARγ variants reported so far and combined this with novel insights from the crystal structure of the full length PPARγ/RXRα heterodimer bound to DNA. We investigated the functional consequences of two of the FPLD3-associated PPARγ variants. One of these mutations (R425C) is located in the ligand binding domain of PPARγ and described in Chapter 3, while the other mutation (R194W) is located in the DNA binding domain and reported in Chapter 4. A transcriptome analysis in human mature adipocytes treated with the TZD rosiglitazone was performed to obtain more insight in the molecular mechanisms contributing to the insulin sensitizing actions of these drugs. As reported in Chapter 5, this led to the identification of the antilipolytic *GPR81* gene as a novel PPARγ target gene. Furthermore, the PPARγ-mediated regulation of the E3 ubiquitin ligase RNF125 is described in Chapter 6. A novel mutation in the *BSCL2* gene in a patient with congenital generalized lipodystrophy is reported in Chapter 7. Elevated levels of organic acids were measured in the urine of this patient, indicative for mitochondrial dysfunction. In Chapter 8 the findings described in this thesis are discussed and integrated in the current literature.

References

1. James WP 2008 The epidemiology of obesity: the size of the problem. J Intern Med 263:336-352
2. Bays H, Mandarino L, DeFronzo RA 2004 Role of the adipocyte, free fatty acids, and ectopic fat in pathogenesis of type 2 diabetes mellitus: peroxisomal proliferator-activated receptor agonists provide a rational therapeutic approach. J Clin Endocrinol Metab 89:463-478
3. Langin D, Holm C, Lafontan M 1996 Adipocyte hormone-sensitive lipase: a major regulator of lipid metabolism. Proc Nutr Soc 55:93-109
4. Hotamisligil GS, Arner P, Caro JF, Atkinson RL, Spiegelman BM 1995 Increased adipose tissue expression of tumor necrosis factor-alpha in human obesity and insulin resistance. J Clin Invest 95:2409-2415
5. Issemann I, Green S 1990 Activation of a member of the steroid hormone receptor superfamily by peroxisome proliferators. Nature 347:645-650
6. Kersten S, Seydoux J, Peters JM, Gonzalez FJ, Desvergne B, Wahli W 1999 Peroxisome proliferator-activated receptor alpha mediates the adaptive response to fasting. J Clin Invest 103:1489-1498
7. Grimaldi PA 2007 Peroxisome proliferator-activated receptors as sensors of fatty acids and derivatives. Cell Mol Life Sci 64:2459-2464
8. Luquet S, Lopez-Soriano J, Holst D, Fredenrich A, Melki J, Rassoulzadegan M, Grimaldi PA 2003 Peroxisome proliferator-activated receptor delta controls muscle development and oxydative capability. FASEB J 17:2299-+
9. Wang YX, Zhang CL, Yu RT, Cho HK, Nelson MC, Bayuga-Ocampo CR, Ham J, Kang H, Evans RM 2004 Regulation of muscle fiber type and running endurance by PPAR delta. PLoS Biol 2:1532-1539
10. Forman BM, Tontonoz P, Chen J, Brun RP, Spiegelman BM, Evans RM 1995 15-Deoxy-delta 12, 14-prostaglandin J2 is a ligand for the adipocyte determination factor PPAR gamma. Cell 83:803-812
11. Krey G, Braissant O, L'Horset F, Kalkhoven E, Perroud M, Parker MG, Wahli W 1997 Fatty acids, eicosanoids, and hypolipidemic agents identified as ligands of peroxisome proliferator-activated receptors by coactivator-dependent receptor ligand assay. Mol Endocrinol 11:779-791
12. Lehmann JM, Moore LB, Smith-Oliver TA, Wilkison WO, Willson TM, Kliewer SA 1995 An antidiabetic thiazolidinedione is a high affinity ligand for peroxisome proliferator-activated receptor gamma (PPAR gamma). J Biol Chem 270:12953-12956
13. Henke BR, Blanchard SG, Brackeen MF, Brown KK, Cobb JE, Collins JL, Harrington WW, Jr., Hashim MA, Hull-Ryde EA, Kaldor I, Kliewer SA, Lake DH, Leesnitzer LM, Lehmann JM, Lenhard JM, Orband-Miller LA, Miller JF, Mook RA, Jr., Noble SA, Oliver W, Jr., Parks DJ, Plunket KD, Szewczyk JR, Willson TM 1998 N-(2-Benzoylphenyl)-L-tyrosine PPARgamma agonists. 1. Discovery of a novel series of potent antihyperglycemic and antihyperlipidemic agents. J Med Chem 41:5020-5036
14. Kubota N, Terauchi Y, Miki H, Tamemoto H, Yamauchi T, Komeda K, Satoh S, Nakano R, Ishii C, Sugiyama T, Eto K, Tsubamoto Y, Okuno A, Murakami K, Sekihara H, Hasegawa G, Naito M, Toyoshima Y, Tanaka S, Shiota K, Kitamura T, Fujita T, Ezaki O, Aizawa S, Kadowaki T, . 1999 PPAR gamma mediates high-fat diet-induced adipocyte hypertrophy and insulin resistance. Mol Cell 4:597-609
15. Barak Y, Nelson MC, Ong ES, Jones YZ, Ruiz-Lozano P, Chien KR, Koder A, Evans RM 1999 PPAR gamma is required for placental, cardiac, and adipose tissue development. Mol Cell 4:585-595
16. Rosen ED, Sarraf P, Troy AE, Bradwin G, Moore K, Milstone DS, Spiegelman BM, Mortensen RM 1999 PPAR gamma is required for the differentiation of adipose tissue in vivo and in vitro. Mol Cell 4:611-617
17. Rosen ED, Hsu CH, Wang X, Sakai S, Freeman MW, Gonzalez FJ, Spiegelman BM 2002 C/EBPalpha induces adipogenesis through PPARgamma: a unified pathway. Genes Dev 16:22-26
18. Tontonoz P, Hu E, Spiegelman BM 1994 Stimulation of adipogenesis in fibroblasts by PPAR gamma 2, a lipid-activated transcription factor. Cell 79:1147-1156
19. Nielsen R, Pedersen TA, Hagenbeek D, Moulos P, Siersbaek R, Megens E, Denissov S, Borgesen M, Francoijs KJ, Mandrup S, Stunnenberg HG 2008 Genome-wide profiling of PPAR{gamma}:RXR

and RNA polymerase II occupancy reveals temporal activation of distinct metabolic pathways and changes in RXR dimer composition during adipogenesis. Genes Dev 22:2953-2967
20. Lefterova MI, Zhang Y, Steger DJ, Schupp M, Schug J, Cristancho A, Feng D, Zhuo D, Stoeckert CJ, Jr., Liu XS, Lazar MA 2008 PPAR{gamma} and C/EBP factors orchestrate adipocyte biology via adjacent binding on a genome-wide scale. Genes Dev 22:2941-2952
21. Hauser S, Adelmant G, Sarraf P, Wright HM, Mueller E, Spiegelman BM 2000 Degradation of the peroxisome proliferator-activated receptor gamma is linked to ligand-dependent activation. J Biol Chem 275:18527-18533
22. Floyd ZE, Stephens JM 2002 Interferon-gamma-mediated activation and ubiquitin-proteasome-dependent degradation of PPAR gamma in adipocytes. J Biol Chem 277:4062-4068
23. Sethi JK, Hotamisligil GS 1999 The role of TNF alpha in adipocyte metabolism. Semin Cell Dev Biol 10:19-29
24. Ruan H, Lodish HF 2003 Insulin resistance in adipose tissue: direct and indirect effects of tumor necrosis factor-alpha. Cytokine Growth Factor Rev 14:447-455
25. Yen CJ, Beamer BA, Negri C, Silver K, Brown KA, Yarnall DP, Burns DK, Roth J, Shuldiner AR 1997 Molecular scanning of the human peroxisome proliferator activated receptor gamma (hPPAR gamma) gene in diabetic Caucasians: identification of a Pro12Ala PPAR gamma 2 missense mutation. Biochem Biophys Res Commun 241:270-274
26. Tan GD, Neville MJ, Liverani E, Humphreys SM, Currie JM, Dennis L, Fielding BA, Karpe F 2006 The in vivo effects of the Pro12Ala PPARgamma2 polymorphism on adipose tissue NEFA metabolism: the first use of the Oxford Biobank. Diabetologia 49:158-168
27. Altshuler D, Hirschhorn JN, Klannemark M, Lindgren CM, Vohl MC, Nemesh J, Lane CR, Schaffner SF, Bolk S, Brewer C, Tuomi T, Gaudet D, Hudson TJ, Daly M, Groop L, Lander ES 2000 The common PPAR gamma Pro12Ala polymorphism is associated with decreased risk of type 2 diabetes. Nat Genet 26:76-80
28. Ludovico O, Pellegrini F, Di Paola R, Minenna A, Mastroianno S, Cardellini M, Marini MA, Andreozzi F, Vaccaro O, Sesti G, Trischitta V 2007 Heterogeneous effect of peroxisome proliferator-activated receptor gamma2 Ala12 variant on type 2 diabetes risk. Obesity (Silver Spring) 15:1076-1081
29. Deeb SS, Fajas L, Nemoto M, Pihlajamaki J, Mykkanen L, Kuusisto J, Laakso M, Fujimoto W, Auwerx J 1998 A Pro12Ala substitution in PPARgamma2 associated with decreased receptor activity, lower body mass index and improved insulin sensitivity. Nat Genet 20:284-287
30. Masugi J, Tamori Y, Mori H, Koike T, Kasuga M 2000 Inhibitory effect of a proline-to-alanine substitution at codon 12 of peroxisome proliferator-activated receptor-gamma 2 on thiazolidinedione-induced adipogenesis. Biochem Biophys Res Commun 268:178-182
31. Heikkinen S, Argmann C, Feige JN, Koutnikova H, Champy MF, Dali-Youcef N, Schadt EE, Laakso M, Auwerx J 2009 The Pro12Ala PPARgamma2 variant determines metabolism at the gene-environment interface. Cell Metab 9:88-98
32. Luan J, Browne PO, Harding AH, Halsall DJ, O'Rahilly S, Chatterjee VK, Wareham NJ 2001 Evidence for gene-nutrient interaction at the PPARgamma locus. Diabetes 50:686-689
33. Franks PW, Luan J, Browne PO, Harding AH, O'Rahilly S, Chatterjee VK, Wareham NJ 2004 Does peroxisome proliferator-activated receptor gamma genotype (Pro12ala) modify the association of physical activity and dietary fat with fasting insulin level? Metabolism 53:11-16
34. Doney K, Fisher LD, Appelbaum FR, Buckner CD, Storb R, Singer J, Fefer A, Anasetti C, Beatty P, Bensinger W, . 1991 Treatment of adult acute lymphoblastic leukemia with allogeneic bone marrow transplantation. Multivariate analysis of factors affecting acute graft-versus-host disease, relapse, and relapse-free survival. Bone Marrow Transplant 7:453-459
35. Doney AS, Fischer B, Cecil JE, Boylan K, McGuigan FE, Ralston SH, Morris AD, Palmer CN 2004 Association of the Pro12Ala and C1431T variants of PPARG and their haplotypes with susceptibility to Type 2 diabetes. Diabetologia 47:555-558
36. Agostini M, Schoenmakers E, Mitchell C, Szatmari I, Savage D, Smith A, Rajanayagam O, Semple R, Luan J, Bath L, Zalin A, Labib M, Kumar S, Simpson H, Blom D, Marais D, Schwabe J, Barroso I, Trembath R, Wareham N, Nagy L, Gurnell M, O'Rahilly S, Chatterjee K 2006 Non-DNA binding,

dominant-negative, human PPARgamma mutations cause lipodystrophic insulin resistance. Cell Metab 4:303-311
37. Monajemi H, Zhang L, Li G, Jeninga EH, Cao H, Maas M, Brouwer CB, Kalkhoven E, Stroes E, Hegele RA, Leff T 2007 Familial Partial Lipodystrophy Phenotype Resulting from a Single-Base Mutation in Deoxyribonucleic Acid-Binding Domain of Peroxisome Proliferator-Activated Receptor-{gamma}. J Clin Endocrinol Metab 92:1606-1612
38. Ludtke A, Buettner J, Wu W, Muchir A, Schroeter A, Zinn-Justin S, Spuler S, Schmidt HH, Worman HJ 2007 Peroxisome proliferator-activated receptor-gamma C190S mutation causes partial lipodystrophy. J Clin Endocrinol Metab 92:2248-2255
39. Agarwal AK, Garg A 2002 A novel heterozygous mutation in peroxisome proliferator-activated receptor-gamma gene in a patient with familial partial lipodystrophy. J Clin Endocrinol Metab 87:408-411
40. Barroso I, Gurnell M, Crowley VE, Agostini M, Schwabe JW, Soos MA, Maslen GL, Williams TD, Lewis H, Schafer AJ, Chatterjee VK, O'Rahilly S 1999 Dominant negative mutations in human PPARgamma associated with severe insulin resistance, diabetes mellitus and hypertension. Nature 402:880-883
41. Jeninga EH, van Beekum O, van Dijk AD, Hamers N, Hendriks-Stegeman BI, Bonvin AM, Berger R, Kalkhoven E 2007 Impaired peroxisome proliferator-activated receptor gamma function through mutation of a conserved salt bridge (R425C) in familial partial lipodystrophy. Mol Endocrinol 21:1049-1065
42. Hegele RA, Cao H, Frankowski C, Mathews ST, Leff T 2002 PPARG F388L, a transactivation-deficient mutant, in familial partial lipodystrophy. Diabetes 51:3586-3590
43. Ludtke A, Buettner J, Schmidt HH, Worman HJ 2007 New PPARG mutation leads to lipodystrophy and loss of protein function that is partially restored by a synthetic ligand. J Med Genet 44:e88
44. Francis GA, Li G, Casey R, Wang J, Cao H, Leff T, Hegele RA 2006 Peroxisomal proliferator activated receptor-gamma deficiency in a Canadian kindred with familial partial lipodystrophy type 3 (FPLD3). BMC Med Genet 7:3.:3
45. Savage DB, Agostini M, Barroso I, Gurnell M, Luan J, Meirhaeghe A, Harding AH, Ihrke G, Rajanayagam O, Soos MA, George S, Berger D, Thomas EL, Bell JD, Meeran K, Ross RJ, Vidal-Puig A, Wareham NJ, O'Rahilly S, Chatterjee VK, Schafer AJ 2002 Digenic inheritance of severe insulin resistance in a human pedigree. Nat Genet 31:379-384
46. Hegele RA, Ur E, Ransom TP, Cao H 2006 A frameshift mutation in peroxisome-proliferator-activated receptor-gamma in familial partial lipodystrophy subtype 3 (FPLD3; MIM 604367). Clin Genet 70:360-362
47. Al Shali K, Cao H, Knoers N, Hermus AR, Tack CJ, Hegele RA 2004 A single-base mutation in the peroxisome proliferator-activated receptor gamma4 promoter associated with altered in vitro expression and partial lipodystrophy. J Clin Endocrinol Metab 89:5655-5660
48. Chandra V, Huang P, Hamuro Y, Raghuram S, Wang Y, Burris TP, Rastinejad F 2008 Structure of the intact PPAR-gamma-RXR- nuclear receptor complex on DNA. Nature 456:350-356
49. Ristow M, Muller-Wieland D, Pfeiffer A, Krone W, Kahn CR 1998 Obesity associated with a mutation in a genetic regulator of adipocyte differentiation. N Engl J Med 339:953-959
50. Bluher M, Paschke R 2003 Analysis of the relationship between PPAR-gamma 2 gene variants and severe insulin resistance in obese patients with impaired glucose tolerance. Exp Clin Endocrinol Diabetes 111:85-90
51. Meirhaeghe A, Amouyel P 2004 Impact of genetic variation of PPARgamma in humans. Mol Genet Metab 83:93-102
52. Agarwal AK, Barnes RI, Garg A 2004 Genetic basis of congenital generalized lipodystrophy. Int J Obes Relat Metab Disord 28:336-339
53. Agarwal AK, Arioglu E, De Almeida S, Akkoc N, Taylor SI, Bowcock AM, Barnes RI, Garg A 2002 AGPAT2 is mutated in congenital generalized lipodystrophy linked to chromosome 9q34. Nat Genet 31:21-23
54. Cortes VA, Curtis DE, Sukumaran S, Shao X, Parameswara V, Rashid S, Smith AR, Ren J, Esser V, Hammer RE, Agarwal AK, Horton JD, Garg A 2009 Molecular mechanisms of hepatic steatosis and

insulin resistance in the AGPAT2-deficient mouse model of congenital generalized lipodystrophy. Cell Metab 9:165-176
55. Payne VA, Grimsey N, Tuthill A, Virtue S, Gray SL, Dalla NE, Semple RK, O'Rahilly S, Rochford JJ 2008 The human lipodystrophy gene BSCL2/seipin may be essential for normal adipocyte differentiation. Diabetes 57:2055-2060
56. Szymanski KM, Binns D, Bartz R, Grishin NV, Li WP, Agarwal AK, Garg A, Anderson RG, Goodman JM 2007 The lipodystrophy protein seipin is found at endoplasmic reticulum lipid droplet junctions and is important for droplet morphology. Proc Natl Acad Sci U S A 104:20890-20895
57. Fei W, Shui G, Gaeta B, Du X, Kuerschner L, Li P, Brown AJ, Wenk MR, Parton RG, Yang H 2008 Fld1p, a functional homologue of human seipin, regulates the size of lipid droplets in yeast. J Cell Biol 180:473-482
58. Kim CA, Delepine M, Boutet E, El Mourabit H, Le Lay S, Meier M, Nemani M, Bridel E, Leite CC, Bertola DR, Semple RK, O'Rahilly S, Dugail I, Capeau J, Lathrop M, Magre J 2008 Association of a homozygous nonsense caveolin-1 mutation with Berardinelli-Seip congenital lipodystrophy. J Clin Endocrinol Metab 93:1129-1134
59. Scherer PE, Lisanti MP, Baldini G, Sargiacomo M, Mastick CC, Lodish HF 1994 Induction of caveolin during adipogenesis and association of GLUT4 with caveolin-rich vesicles. J Cell Biol 127:1233-1243
60. Brasaemle DL, Dolios G, Shapiro L, Wang R 2004 Proteomic analysis of proteins associated with lipid droplets of basal and lipolytically stimulated 3T3-L1 adipocytes. J Biol Chem 279:46835-46842
61. Razani B, Combs TP, Wang XB, Frank PG, Park DS, Russell RG, Li M, Tang B, Jelicks LA, Scherer PE, Lisanti MP 2002 Caveolin-1-deficient mice are lean, resistant to diet-induced obesity, and show hypertriglyceridemia with adipocyte abnormalities. J Biol Chem 277:8635-8647
62. Miyoshi Y, Akagi M, Agarwal AK, Namba N, Kato-Nishimura K, Mohri I, Yamagata M, Nakajima S, Mushiake S, Shima M, Auchus RJ, Taniike M, Garg A, Ozono K 2008 Severe mandibuloacral dysplasia caused by novel compound heterozygous ZMPSTE24 mutations in two Japanese siblings. Clin Genet 73:535-544
63. George S, Rochford JJ, Wolfrum C, Gray SL, Schinner S, Wilson JC, Soos MA, Murgatroyd PR, Williams RM, Acerini CL, Dunger DB, Barford D, Umpleby AM, Wareham NJ, Davies HA, Schafer AJ, Stoffel M, O'Rahilly S, Barroso I 2004 A family with severe insulin resistance and diabetes due to a mutation in AKT2. Science 304:1325-1328
64. Tan K, Kimber WA, Luan J, Soos MA, Semple RK, Wareham NJ, O'Rahilly S, Barroso I 2007 Analysis of genetic variation in Akt2/PKB-beta in severe insulin resistance, lipodystrophy, type 2 diabetes, and related metabolic phenotypes. Diabetes 56:714-719
65. Garofalo RS, Orena SJ, Rafidi K, Torchia AJ, Stock JL, Hildebrandt AL, Coskran T, Black SC, Brees DJ, Wicks JR, McNeish JD, Coleman KG 2003 Severe diabetes, age-dependent loss of adipose tissue, and mild growth deficiency in mice lacking Akt2/PKB beta. J Clin Invest 112:197-208
66. Cho H, Mu J, Kim JK, Thorvaldsen JL, Chu Q, Crenshaw EB, III, Kaestner KH, Bartolomei MS, Shulman GI, Birnbaum MJ 2001 Insulin resistance and a diabetes mellitus-like syndrome in mice lacking the protein kinase Akt2 (PKB beta). Science 292:1728-1731

Chapter 2

Functional implications of genetic variation in human PPARγ

Ellen H. Jeninga[1,2], Mark Gurnell[3] and Eric Kalkhoven[1,2,4]

[1]Department of Metabolic and Endocrine Diseases, UMC Utrecht, Lundlaan 6, 3584 EA Utrecht, The Netherlands, and [2]Netherlands Metabolomics Centre, The Netherlands; [3]Department of Medicine and Institute of Metabolic Science, University of Cambridge, Addenbrooke's Hospital, Hills Road, Cambridge CB2 0QQ, United Kingdom; [4]Department of Paediatric Immunology, UMC Utrecht, Lundlaan 6, 3584 EA Utrecht, The Netherlands

Submitted

Abstract

Peroxisome proliferator-activated receptor γ (PPARγ) plays a key role in the regulation of lipid and glucose metabolism. Human genetic evidence supporting this view comes from the study of both common (e.g. Pro12Ala polymorphism) and rare (loss-of-function mutations) *PPARG* variants. Indeed, patients harbouring mutant PPARγ exhibit familial partial lipodystrophy type 3 and an extreme monogenic form of the metabolic syndrome. The recent elucidation of the crystal structure of the full-length PPARγ-RXRα heterodimer bound to DNA has shed new light on the functional consequences of these genetic PPARγ alterations and provides novel insights as to why different perturbations of receptor function unite in a common pathway of metabolic dysfunction.

Introduction

As the global prevalence of overweight/obesity increases, the number of individuals diagnosed with the metabolic syndrome (central obesity, insulin resistance/glucose intolerance/diabetes, dyslipidaemia and hypertension) has also risen steeply. Interestingly, systemic or localized loss of fat tissue (lipodystrophy) is associated with a similar metabolic disturbance, indicating that the maintenance and/or distribution of adipose tissue are critically important in metabolic homeostasis. A key regulator of adipocyte differentiation and function is the peroxisome proliferator-activated receptor γ (PPARγ), a nuclear receptor belonging to the superfamily of ligand inducible transcription factors (1). PPARγ directly regulates a large number of target genes that mediate glyceroneogenesis, lipid uptake, lipid synthesis, lipid storage and lipolysis (2-4). In addition, PPARγ also plays a central role in the endocrine function of adipose tissue through its ability to regulate adipo(cyto)kines; for example, the expression of adiponectin, an adipokine that enhances insulin sensitivity, is increased in response to PPARγ activation (5). These PPARγ target genes are regulated by PPAR response elements (PPREs), consisting of two hexameric direct repeats (AGGTCA) interspaced by one nucleotide (DR-1) in their promoter and/or enhancer regions. PPARγ binds these PPREs as an obligate heterodimer with the retinoid acid X receptor (RXR).

Structure and function of PPARγ

The PPARγ protein consists of several functional domains, which exhibit varying degrees of conservation among members of the nuclear receptor family (Figure 1A). Two isoforms of the receptor exist (PPARγ1 and PPARγ2), which differ only in their extreme N-terminal region, with the γ2 protein harbouring an additional 28 amino acids. The poorly conserved N-terminus accomodates activation function 1 (AF-1), the activity of which can be regulated by post-translational modifications (6). Centrally located is the DNA binding domain (DBD), which is highly conserved among species and between nuclear receptors. Zinc coordination by eight of the nine conserved cysteine residues in this domain yields two zinc fingers, which are essential for stabilization of the secondary and tertiary protein structure and ultimately DNA binding (7) (Figure 1B). The recognition α-helix, or P box, which follows directly after the first zinc-nucleated loop, fits into the major groove of the DNA and directly contacts the AGGTCA sequence, while the second α-helix, which is oriented in a perpendicular fashion, stabilizes this interaction. The DBD is linked to the ligand binding domain (LBD) by the variable hinge region. The LBD, which is relatively well conserved in terms of primary amino acid sequence, mediates ligand binding and heterodimerisation with RXRα, and contains the more powerful ligand-dependent activation function (AF-2). A variety of endogenous ligands have been identified for PPARγ, including polyunsaturated fatty acids, eicosanoids and prostaglandin J2 derivatives (8;9). Synthetic agonists

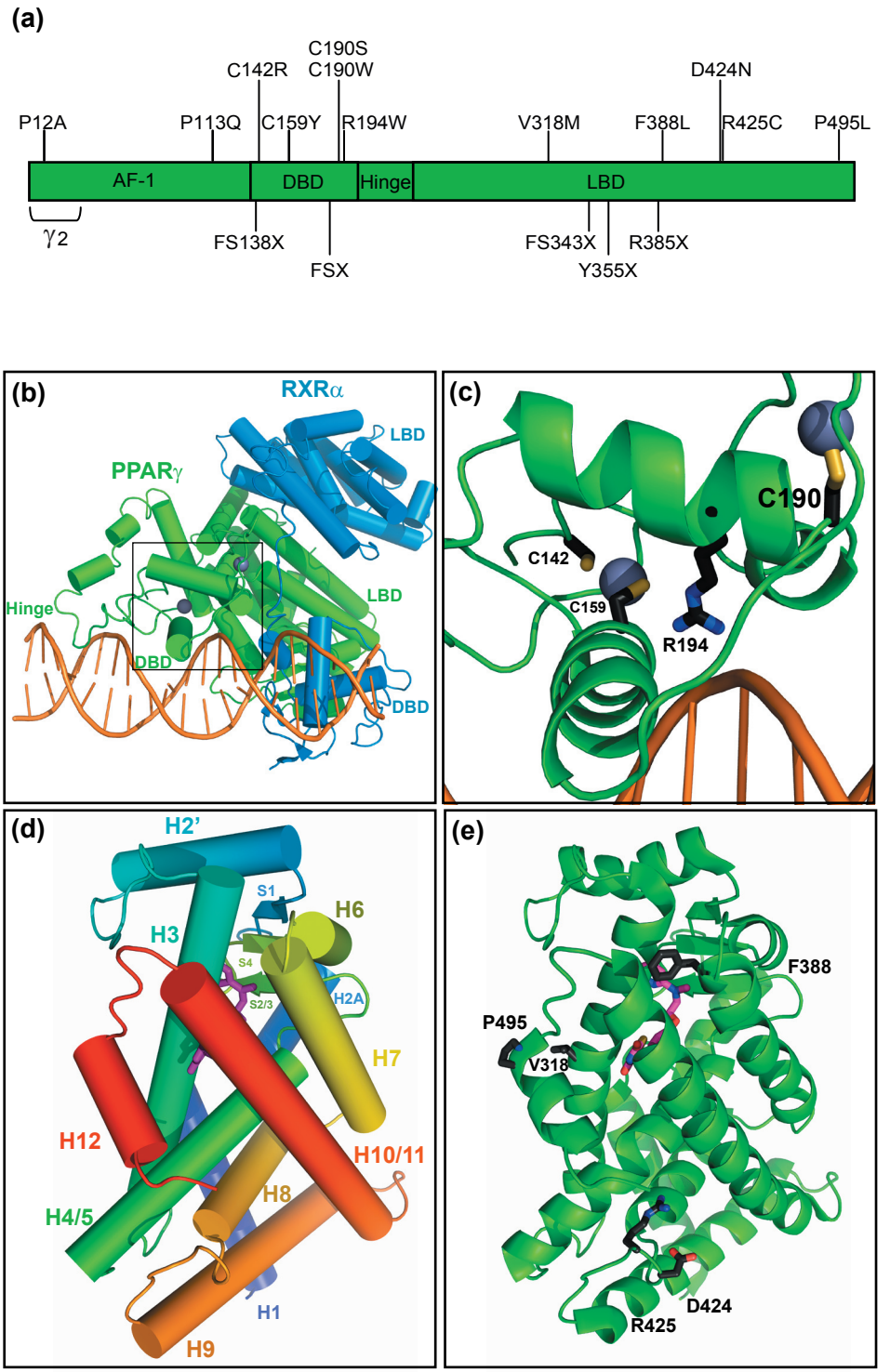
(a)
C190S
C142R
C190W
D424N
P12A
P113Q
C159Y
R194W
V318M
F388L
R425C
P495L
AF-1
DBD
Hinge
LBD
γ2
FS138X
FSX
FS343X
R385X
Y355X
(b)
RXRα
LBD
PPARγ
Hinge
LBD
DBD
DBD
(c)
C190
C142
C159
R194
(d)
H2'
S1
H6
H3
S4
S2/3
H2A
H7
H12
H10/11
H8
H4/5
H1
H9
(e)
F388
P495
V318
D424
R425

⇦ **Figure 1. Structure-function relationships in PPARγ. (a)** Overview of human PPARγ mutations. Schematic representation of the distinct domains of the PPARγ2 protein (with PPARγ 1 missing the first 28 amino acids) and the location of the different natrurally occurring mutations. The missense mutations are depicted above the bar and the nonsense mutations below the bar (all PPARγ2 nomenclature). **(b)** Global structure of the PPARγ-RXRα-DNA structure (20). The DBDs and LBDs of PPARγ (green) and RXRα (blue) are shown, with the zinc ions in the PPARγ DBD (in grey). The hinge region of PPARγ contacts the minor groove of the DNA. Square box indicates the region magnified in panel (c). Figures were generated using PyMOL 1.2 open source software. **(c)** Magnified view of helices of PPARγ-DBD localised around the zinc ions (in grey), with the residues affected in FPLD3 patients indicated in ball-and-stick format. Starting structure of PPARγ was adapted from the Protein Data Bank (PDB) entry 3DZY, chain D (20). **(d)** Global view of 3D-structure of the LBD, which consists of 13 α-helices (H1-H12 and H2') and 4 β-strands (S1-S4) presented as cylinders and arrows respectively. The ligand rosiglitazone is in purple. **(e)** Similar 3D-structure of LBD as shown in (d), but now with the residues affected by missense mutations in FPLD3 patients shown in ball-and-stick format. 3D-structure of the PPARγ-LBD was obtained from the Protein Data Bank (PDB) entry 1FM6, chain D (19).

include the thiazolidinediones (TZDs) (10) and tyrosine-based agonists (11) that have been shown to improve insulin sensitivity and lower blood glucose levels in patients with type 2 diabetes. Ligand binding stabilises the active conformation of the LBD, thereby serving as a "molecular switch" between activation and repression functions of the receptor (12). On the promoters of some target genes, unliganded PPARs recruit corepressors (e.g. N-CoR (nuclear receptor corepressor) and SMRT (silencing mediator for retinoic acid and thyroid receptors)), which are part of multiprotein complexes containing histone deacetylase (HDAC) activity that repress target gene transcription (13). Upon ligand binding, these corepressor complexes are exchanged for coactivator counterparts, including the steroid receptor coactivator-1 (SRC1)/CREB binding protein (CBP) and thyroid hormone receptor associated protein (TRAP) complexes (14), which facilitate transactivation. The interaction of nuclear receptors such as PPARγ with the transcription initiation machinery is a dynamic process in which the receptors and their cofactors cycle on and off the promoters of target genes during transcriptional activation. This process, termed promoter cycling, involves ligand binding, cofactor exchange and proteasome-mediated degradation of transcription factors and plays an important role in determining the rate of gene transcription (15;16).

Crystal structure of the PPARγ-RXRα-DNA complex

Earlier studies have provided structural information on the isolated LBD of PPARγ, either unliganded or in the presence of different ligands (12;17-19), and on the liganded heterodimer of RXRα-PPARγ LBDs (19). The crystal structure of the PPARγ-LBD reveals 13 α-helices and a small four-stranded β-sheet. The ligand binding pocket comprises residues in helices H3, H5, H11 and H12, whereas residues involved in heterodimerisation with RXRα lie in H9, H10 and the loop between H8 and H9 (L8-9) (19). In the liganded, active conformation of the LBD, Helix 12 (H12) (together with residues from helices 3, 4 and 5) forms a charge-

clamp surface that interacts with the LXXLL motif of coactivators. Very recently, Chandra and colleagues (20) reported the 3D-structure of the liganded PPARγ-RXRα heterodimer as a complex on DNA. In addition to confirming earlier findings on the LBD structure, this new structure is unique as it demonstrates for the first time how distinct domains cooperate to modulate receptor properties. As shown in Figure 1B, it has now become clear that the PPARγ LBD is prominently located at the centre of the complex around which all other domains are positioned (20). Previously unsuspected interactions were identified between the PPARγLBD and its own DBD, involving R181 and H183 in the DBD and E455 in the LBD (L9-10) (Note: all numberings are reported relative to the γ2 isoform of the receptor). In addition, the PPARγ LBD clearly interacts with the RXR DBD/hinge region, involving the residues of the PPARγ β-strands (S1-S4). The relevance of this interaction is supported by mutation of one of the β-strand residues (F375A), which results in reduced DNA binding (20). A second important new finding is the interaction of the PPARγ hinge region (also referred to as the C-terminal extension; CTE) with the 5′ extension of the PPRE. This interaction of the RFGR amino acid sequence in the hinge region with the DNA minor groove helps to explain the previously observed polar arrangement of the heterodimer, with PPARγ occupying the 5′ position (21-23). Although present in the crystallized proteins, the AF1 domains of PPARγ and RXRα resisted the attempt to determine their structure. This suggests that these domains are intrinsically flexible, as demonstrated by amide hydrogen/deuterium exchange mass spectrometry (H/D-Ex) (20).

FPLD3-associated mutations in PPARγ

To date one common variant (Pro12Ala) and 16 rare missense and nonsense mutations in the coding region of the *PPARG* gene have been identified (Figure 1A) and analyzed functionally (Table 1) (24-37). In addition, a mutation in the PPARγ4 promoter (-14G>A) has been reported (38). The Pro12Ala polymorphism in the AF-1 region of the PPARγ2 protein is the most frequently found genetic variant of PPARγ, and its frequency has been reported to vary from 2% to 25% depending on ethnicity. Many association studies have examined the link between this polymorphism and insulin resistance, and although some contradictory findings have been reported, a recruit-by-phenotype approach (39) and two large meta-analyses have shown a modest but significant increase in diabetes risk for carriers of the proline allele (40;41). However, since this risk allele occurs with a high frequency in certain populations, this modest effect can translate into a large population attributable risk for type II diabetes (as much as 25%). Functional studies have shown a modest reduction of target gene transactivation by the Ala variant in the absence or presence of ligand, due to reduced DNA binding capacity (27). In addition, Masugi and colleagues showed that the Ala variant has reduced ability to induce adipocyte differentiation compared to its wild type counterpart (42). A second genetic variant in the AF-1 region of the PPARγ protein is the heterozygous mutation of proline 113

Domain	Position[a]	Structure	Primary effect	Activity	Refs
AF1	P12A	-	DNA binding ↓	↓	[27][37]
	P113Q (85)	-	?	↑[b]	[35]
DBD	FS138X (110)	Zinc finger I	DNA binding ↓?	↓	[30]
	C142R (114)	Zinc finger I	DNA binding ↓	↓	[25]
	C159Y (131)	Zinc finger II	DNA binding ↓	↓	[25]
	FSX	Zinc finger II	DNA binding ↓	↓	[36]
	C190S (162)	Zinc finger II	DNA binding ↓	↓	[33]
	C190W (162)	Zinc finger II	DNA binding ↓	↓	[25]
	R194W (164)	Zinc finger II	DNA binding ↓	↓	[34]
LBD	V318M (290)	H3	Ligand binding ↓[c] CoR release ↓[d] CoA recruitment ↓	↓	[26]
	FS343X (315)	H4/5	Dimerisation ↓	↓	[25]
	Y355X (327)	H4/5	Stability ↓	↓	[28]
	R385X (357)	H7	Dimerisation ↓	↓	[25]
	F388L (360)	H7	Ligand binding ↓[c]		[29]
	D424N (396)	Loop 8-9	Ligand binding ↓[c]	↓	[32]
	R425C (397)	Loop 8-9	Ligand binding ↓[c] CoA recruitment ↓ Dimerisation ↓	↓ ↓	[24][31]
	P495L (467)	H12	Ligand binding ↓[c] CoR release ↓ CoA recruitment ↓	↓	[26]

Table 1.

[a] Numbers indicate amino acid position in the γ2 isoform of the receptor, with γ1 position in brackets.

[b] Not based on reporter assays, but accelerated differentiation and greater lipid accumulation in differentiating adipocytes has been shown.

[c] For F388L transcriptional activity is completely rescued by high concentrations of rosiglitazone, while V318M and P495L are completely, and R425C is partially rescued by high concentrations of tyrosine based agonists. D424N is partially rescued by rosiglitazone.

[d] CoR, corepressor; CoA, coactivator.

(P113; often referred to as P115) (35;43). Originally detected among German obese individuals (4 out of 121 subjects) (35), subsequent studies failed to detect other carriers (44-46). These findings suggest that the P113Q mutation is a rare genetic event, and that the original observed high frequency may have been due to a strong founder effect. *In vivo* and *in vitro* experiments have revealed that the transcriptional activity of PPARγ is subject to phosphorylation of an adjacent serine residue (S112) (47;48). Like the artificial S112A mutation (47-49), the P113Q mutant abolishes phosphorylation leading to enhanced transcription and thereby potentially promoting greater adipocyte differentiation (35). This enhanced PPARγ activity did not however appear to translate into improved metabolic function, with three of

the four affected subjects demonstrating concomitant type 2 diabetes. Currently no structural explanations for the functional consequences of the Pro12Ala and P113Q proteins has been provided, due to the lack of structural information on the AF-1 region (20).

Box 1: Familial partial lipodystrophy type 3 (FPLD3)
Familial partial lipodystrophy type 3 (FPLD3; MIM604367) is an autosomal dominantly inherited disorder characterized by diminution of subcutaneous fat in the limbs and gluteal region, with relative sparing/excess of adipose tissue in the subcutaneous and visceral abdominal depots. The majority of FPLD3 patients have profound metabolic complications, in particular severe insulin resistance and early onset type 2 diabetes mellitus, marked dyslipidaemia (characterized by high serum levels of free fatty acids and low levels of high-density lipoprotein cholesterol), and the polycystic ovarian syndrome (PCOS) in affected females. Some subjects also manifest early onset/severe hypertension and hepatic steatosis (58;59). So far, a total of 15 different PPARγ mutations have been reported in affected patients.

The majority of the rare, heterozygous loss-of-function PPARγ mutations reported so far are associated with a distinct clinical phenotype of familial partial lipodystrophy type 3 (FPLD3; see Box 1), in which affected subjects manifest loss of distal limb and gluteal fat, but relative preservation of abdominal adipose tissue. Several of these naturally-occurring mutations involve cysteine residues in the two zinc fingers of the DBD: C142R, C159Y in the first zinc finger and C190W and C190S in the second zinc finger (25;33)(Figure 1c). *In vitro* studies revealed that the DNA binding capacity of the first three mutant proteins was completely abolished (25;33), underscoring the importance of zinc coordination in maintaining the integrity of the DBD structure. In contrast, the C190S mutant exhibited some residual transcriptional function, suggesting that mutation of this cysteine into serine is less deleterious than into a large aromatic tryptophan residue (33). Mutation of the highly conserved hydrophilic arginine at position 194 (R194W), which directly contacts the DNA backbone (20), into a hydrophobic tryptophan residue also resulted in loss of DNA binding (34). Unsurprisingly, deletion of part of the second zinc finger, as observed in the frameshift-premature stop mutant FSX, also led to complete loss of DNA binding capacity (25;36). A second group of FPLD3-associated mutations resides in the ligand binding domain of PPARγ: five missense mutations (V318M, F388L, D424N, R425C and P495L), two nonsense mutations (Y355X and R385X), and one frameshift/premature stop mutation (FS343X) leading to a premature stop codon (24-26;29;32)(Figure 1d and e). The latter three mutations give rise to truncated PPARγ proteins lacking most of the

RXRα dimerisation interface, thereby accounting for their impaired DNA binding (25;28). The loop between helix 8 and 9 of the LBD is part of the RXR dimerisation interface (19;20), and natural point mutations in this loop (D424N and R425C) impair heterodimerisation and subsequent DNA binding (31;32).
In addition to the reduced heterodimerisation capacity observed in some of the LBD mutants, all the missense mutant proteins display reduced ligand binding (Table 1). Since none of the mutated residues appear to directly contact ligands such as oxidized fatty acids and TZDs (17;18;20)(Figure 1e), it seems likely that these mutations affect ligand binding indirectly, i.e. by altering the overall structure of the LBD. Reduced ligand binding affinity, resulting in impaired ligand-dependent coactivator recruitment (CBP, SRC1 and TRAP220), is therefore one of the central mechanisms underlying the reduction in transcriptional activity seen in all natural LBD point mutants. Interestingly, high doses of rosiglitazone completely restored the activity of the F388L mutant, while tyrosine-based agonists completely (V318M, P495L) or partially (R425C) restored the transcriptional activity of the other mutants (29;31;50).

Dominant negative activity versus haplo-insufficiency
FPLD3-associated PPARγ mutations are dominantly inherited. Consistent with this several mutants have been shown to inhibit activity of the wild type receptor in a dominant negative manner. Currently, these mutants can be divided into two groups based on their proposed mechanism of action (Figure 2). The first group comprises missense mutations located in the LBD (V318M, P495L). When expressed at comparable levels, the V318M and P495L mutants inhibited the transcriptional activity of the wild type protein in a dominant negative manner (50). The V318M and P495L receptors showed impaired corepressor release in response to ligand, reminiscent of the impaired corepressor release observed with natural thyroid hormone receptor mutants (51). Indeed, dominant negative activity of the PPARγ mutants was abrogated by the introduction of a second mutation (L346A) that specifically impairs corepressor binding (50). Since the V318M and P495L mutants retain DNA binding capacity, these stable PPARγ-corepressor complexes can compete for DNA binding with the wild type receptor, thereby inhibiting PPARγ target gene regulation. Interestingly, impaired corepressor release may also affect the rate by which PPARγ cycles on and off the promoter during the transcription process. Li and Leff (52) recently showed that the P495L mutant has a reduced promoter cycling rate compared to the wild type receptor suggesting that the majority of PPARγ regulated promoters will be occupied by the mutant protein over time. Both blocking the proteasome and stimulation with supraphysiological ligand concentrations abolished the differences in recycling rates between wild type protein and the P495L mutant (52). The latter observation is consistent with previous reports showing a lack of dominant negative activity at high concentrations of ligand (26;50).

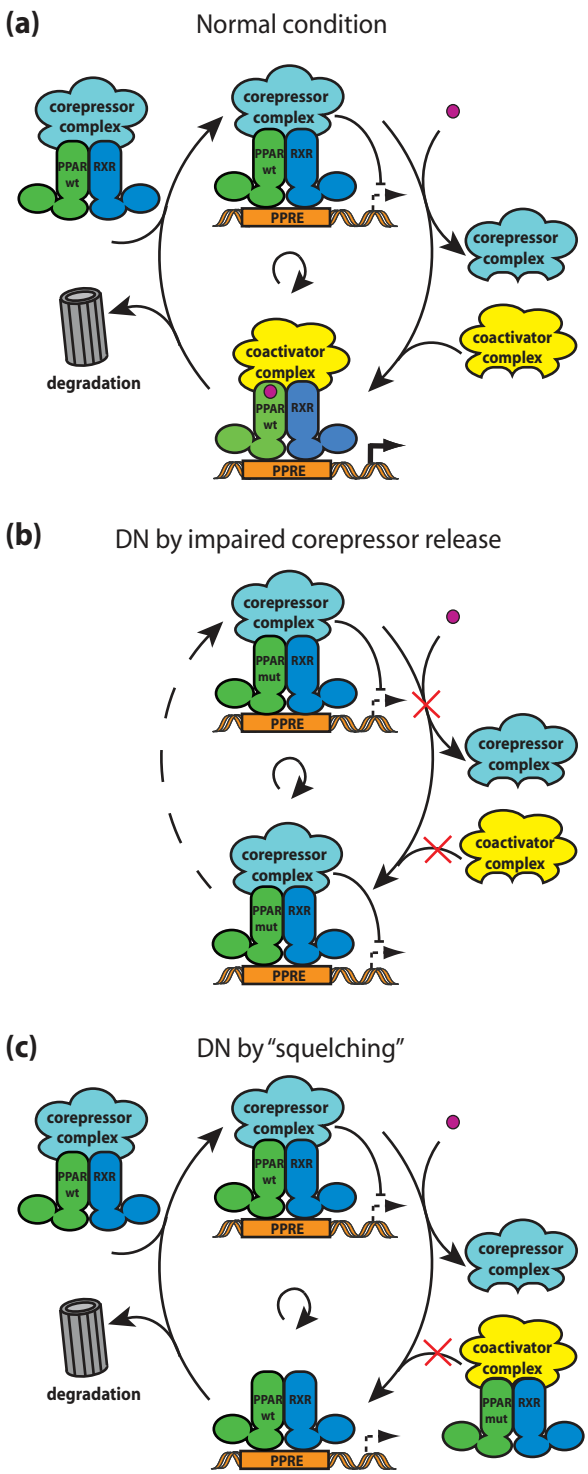

Figure 2. Models representing promoter cycling of wild type and dominant negative mutant PPARγ proteins.
(a) Promoter cycling of wild type PPARγ. PPARγ/RXRα heterodimer binds a PPRE in the promoter of a target gene. Under basal conditions corepressors can repress transcription. Upon binding of endogenous ligands, corepressors will be released and coactivators recruited and transcription is initiated. Afterwards PPARγ will undergo proteasomal degradation and a next round of promoter cycling will take place. **(b)** Dominant negative activity as the result of an impaired corepressor release. PPARγ mutants that display impaired corepressor release (V318M and P495L) are protected from proteasome mediated degradation. Unlike these mutant receptors, the wild type protein will be degraded by the proteasome after ligand binding and activation of transcription. This will result in the majority of PPARγ regulated promoters being occupied by the mutant protein over time. **(c)** Dominant negative activity as a result of "squelching". Mutant PPARγ proteins (C142R, C159Y, C190W, FS343X, R385X) that are not able to bind DNA, but retain the ability to bind coactivators, compete for limiting amounts of coactivators with the wild type protein. Wild type receptors will therefore display reduced ability to initiate transcription.

The second group of PPARγ mutants that exhibits dominant negative activity consists of some DBD mutants (C142R, C159Y, C190W). Unlike the group 1 mutants, these mutants lack the ability to bind DNA but retain the ability to bind cofactors (e.g. CBP, SRC1, TRAP220). They can therefore compete for limiting amounts of cofactor proteins with the wild type receptor, a process referred to as transcriptional "squelching" (53;54). In addition, two LBD truncation mutants (FS343X, R385X) have also been found to repress the activity of wild type PPARγ, despite lacking a key domain (H12) that is necessary for ligand-dependent coactivator recruitment (e.g CBP, SRC-1 and TRAP220) (25). Their dominant negative behaviour may therefore be due to the preserved interactions with coactivators that bind ligand independently to the DBD/hinge region, such as PGC-1α and PDIP1α (25).
In contrast however, other FPLD3-associated mutants appear to lack dominant negative activity, despite residing within similar regions of the LBD and DBD. Together with the FPLD3-associated PPARγ4 promoter (-14A>G) mutation (38), which only reduces the expression of the PPARγ protein, these mutants either harbour multiple defects (R425C) (31), are retained in the cytosol (FSX) (25) or display decreased protein stability (F388L, Y355X) (28;52). These findings indicate that in some FPLD3 patients haploinsufficiency at the *PPARG* locus is sufficient to produce the disease phenotype. It is interesting to speculate whether subjects harbouring dominant negative mutant receptors exhibit more severe or early onset metabolic dysfunction as a consequence of more severe impairment of PPARγ function. However, the limited number of subjects identified to date does not permit a meaningful analysis in this respect, and moreover it is likely that variations in other genetic and environmental factors which impact on metabolic regulation will modify the clinical phenotype in any given individual. In support of this, in the kindred harbouring the FSX mutation, individuals carrying a second 'genetic hit' in an unrelated gene (*PPP1R3*) involved in glycogen synthesis exhibited severe insulin resistance, while a young fit male with only the FSX mutation was unaffected (36). Continued follow-up of this individual will be important to determine whether he goes on to develop evidence of the metabolic syndrome in due course.

Future directions

To date, all of the identified FPLD3-associated mutations reside in either the DBD or the LBD of the PPARγ protein (Figure 1). The recently published 3D-structure of the full-length liganded PPARγ-RXRα heterodimer bound to DNA confirms previous biochemical characterizations of natural PPARγ mutants and extends our understanding as to how these mutations impair PPARγ function (20). Based on this structure, one can hypothesize that mutations in the hinge region, which determines DNA binding polarity, or in the β-strands of the LBD, which contact the RXR DBD, may also lead to FPLD3. Furthermore, several lines of evidence suggest that mutations in the intrinsically unstructured N-terminus of the protein could affect the functional properties of the DBD and LBD, and may therefore

also cause FPLD3. For example, the Pro12Ala mutation affects DNA binding (27) and cofactor interaction (55), whereas mutation of the phosphorylation site S112 (S112A) influences ligand binding affinity (49). While the AF-1 domain is highly dynamic (20), it may become structured upon post-translational modification and/or binding of regulatory proteins (6). Additional 3D-structures, for example using a phospho-mimic mutant of PPARγ (S112E/D) or co-crystalization with an AF1 binding protein (e.g. Tip60 (56)) are needed to establish the structural basis of interdomain communication.

Although crystallographic studies combined with cell-based assays of natural PPARγ variants have contributed enormously to our knowledge of structure-function relationships within this protein, *in vivo* studies are required to investigate the physiological consequences of genetic variation of PPARγ. So far, the limited number of studies in knock-in mice and patients indicate that additional factors influence the development of the insulin resistance phenotype associated with PPARγ mutations. For example, homozygous Pro12Ala mice are more insulin sensitive then Pro12 animals, but this effect is reversed upon high-fat feeding (55). In addition, mice harbouring a heterozygous FPLD3-associated P495L mutation only display the clinical features of their human counterparts when present in the hyperphagic *ob*/*ob* background (57). These data suggest that gene-nutrient interactions play an important role in the development of insulin resistance associated with genetic variants of PPARγ. Furthermore, as already outlined above (FSX kindred), there is clear evidence that gene-gene interactions also play an important role in the development of metabolic dysfunction in affected subjects (36).

The powerful combination of crystallization studies, cell-based assays and *in vivo* investigations (both in mice and humans) will not only help us to design more rational therapeutic approaches to reduce morbidity and mortality in patients harbouring PPARγ mutations, but also help us understand the disease process and unveil mechanisms that are more generally applicable to the common conditions of insulin resistance, glucose intolerance/type 2 diabetes, and dyslipidaemia.

Acknowledgements

The authors thank Dr. A.M.J.J. Bonvin (Bijvoet Center for Biomolecular Research, Utrecht University, The Netherlands) for his expert help in generating Figure 1, and Dr. A. Koppen for critically reading the manuscript. M.G. is supported by the Wellcome Trust and is a National Institutes of Health Research Biomedical Research Centre Investigator.

References

1. Lehrke M, Lazar MA 2005 The many faces of PPARgamma. Cell 123:993-999
2. Anghel SI, Wahli W 2007 Fat poetry: a kingdom for PPARgamma. Cell Res 17:486-511
3. Tontonoz P, Spiegelman BM 2008 Fat and beyond: the diverse biology of PPARgamma. Annu Rev Biochem 77:289-312
4. Nielsen R, Pedersen TA, Hagenbeek D, Moulos P, Siersbaek R, Megens E, Denissov S, Borgesen M, Francoijs KJ, Mandrup S, Stunnenberg HG 2008 Genome-wide profiling of PPAR{gamma}:RXR and RNA polymerase II occupancy reveals temporal activation of distinct metabolic pathways and changes in RXR dimer composition during adipogenesis. Genes Dev 22:2953-2967
5. Scherer PE 2006 Adipose tissue: from lipid storage compartment to endocrine organ. Diabetes 55:1537-1545
6. Beekum OV, Fleskens V, Kalkhoven E 2009 Posttranslational Modifications of PPAR-gamma: Fine-tuning the Metabolic Master Regulator. Obesity (Silver Spring) 17:213-219
7. Khorasanizadeh S, Rastinejad F 2001 Nuclear-receptor interactions on DNA-response elements. Trends Biochem Sci 26:384-390
8. Forman BM, Tontonoz P, Chen J, Brun RP, Spiegelman BM, Evans RM 1995 15-Deoxy-delta 12, 14-prostaglandin J2 is a ligand for the adipocyte determination factor PPAR gamma. Cell 83:803-812
9. Krey G, Braissant O, L'Horset F, Kalkhoven E, Perroud M, Parker MG, Wahli W 1997 Fatty acids, eicosanoids, and hypolipidemic agents identified as ligands of peroxisome proliferator-activated receptors by coactivator-dependent receptor ligand assay. Mol Endocrinol 11:779-791
10. Lehmann JM, Moore LB, Smith-Oliver TA, Wilkison WO, Willson TM, Kliewer SA 1995 An antidiabetic thiazolidinedione is a high affinity ligand for peroxisome proliferator-activated receptor gamma (PPAR gamma). J Biol Chem 270:12953-12956
11. Henke BR, Blanchard SG, Brackeen MF, Brown KK, Cobb JE, Collins JL, Harrington WW, Jr., Hashim MA, Hull-Ryde EA, Kaldor I, Kliewer SA, Lake DH, Leesnitzer LM, Lehmann JM, Lenhard JM, Orband-Miller LA, Miller JF, Mook RA, Jr., Noble SA, Oliver W, Jr., Parks DJ, Plunket KD, Szewczyk JR, Willson TM 1998 N-(2-Benzoylphenyl)-L-tyrosine PPARgamma agonists. 1. Discovery of a novel series of potent antihyperglycemic and antihyperlipidemic agents. J Med Chem 41:5020-5036
12. Nolte RT, Wisely GB, Westin S, Cobb JE, Lambert MH, Kurokawa R, Rosenfeld MG, Willson TM, Glass CK, Milburn MV 1998 Ligand binding and co-activator assembly of the peroxisome proliferator-activated receptor-gamma. Nature 395:137-143
13. Guan HP, Ishizuka T, Chui PC, Lehrke M, Lazar MA 2005 Corepressors selectively control the transcriptional activity of PPARgamma in adipocytes. Genes Dev 19:453-461
14. Perissi V, Rosenfeld MG 2005 Controlling nuclear receptors: the circular logic of cofactor cycles. Nat Rev Mol Cell Biol 6:542-554
15. Dennis AP, O'Malley BW 2005 Rush hour at the promoter: how the ubiquitin-proteasome pathway polices the traffic flow of nuclear receptor-dependent transcription. J Steroid Biochem Mol Biol 93:139-151
16. Muratani M, Tansey WP 2003 How the ubiquitin-proteasome system controls transcription. Nat Rev Mol Cell Biol 4:192-201
17. Waku T, Shiraki T, Oyama T, Fujimoto Y, Maebara K, Kamiya N, Jingami H, Morikawa K 2009 Structural insight into PPARgamma activation through covalent modification with endogenous fatty acids. J Mol Biol 385:188-199
18. Itoh T, Yamamoto K 2008 Peroxisome proliferator activated receptor gamma and oxidized docosahexaenoic acids as new class of ligand. Naunyn Schmiedebergs Arch Pharmacol 377:541-547
19. Gampe RT, Jr., Montana VG, Lambert MH, Miller AB, Bledsoe RK, Milburn MV, Kliewer SA, Willson TM, Xu HE 2000 Asymmetry in the PPARgamma/RXRalpha crystal structure reveals the molecular basis of heterodimerization among nuclear receptors. Mol Cell 5:545-555
20. Chandra V, Huang P, Hamuro Y, Raghuram S, Wang Y, Burris TP, Rastinejad F 2008 Structure of the intact PPAR-gamma-RXR- nuclear receptor complex on DNA. Nature 456:350-356

21. IJpenberg A, Jeannin E, Wahli W, Desvergne B 1997 Polarity and specific sequence requirements of peroxisome proliferator-activated receptor (PPAR)/retinoid X receptor heterodimer binding to DNA. A functional analysis of the malic enzyme gene PPAR response element. J Biol Chem 272:20108-20117
22. Juge-Aubry C, Pernin A, Favez T, Burger AG, Wahli W, Meier CA, Desvergne B 1997 DNA binding properties of peroxisome proliferator-activated receptor subtypes on various natural peroxisome proliferator response elements. Importance of the 5'-flanking region. J Biol Chem 272:25252-25259
23. Hsu MH, Palmer CN, Song W, Griffin KJ, Johnson EF 1998 A carboxyl-terminal extension of the zinc finger domain contributes to the specificity and polarity of peroxisome proliferator-activated receptor DNA binding. J Biol Chem 273:27988-27997
24. Agarwal AK, Garg A 2002 A novel heterozygous mutation in peroxisome proliferator-activated receptor-gamma gene in a patient with familial partial lipodystrophy. J Clin Endocrinol Metab 87:408-411
25. Agostini M, Schoenmakers E, Mitchell C, Szatmari I, Savage D, Smith A, Rajanayagam O, Semple R, Luan J, Bath L, Zalin A, Labib M, Kumar S, Simpson H, Blom D, Marais D, Schwabe J, Barroso I, Trembath R, Wareham N, Nagy L, Gurnell M, O'Rahilly S, Chatterjee K 2006 Non-DNA binding, dominant-negative, human PPARgamma mutations cause lipodystrophic insulin resistance. Cell Metab 4:303-311
26. Barroso I, Gurnell M, Crowley VE, Agostini M, Schwabe JW, Soos MA, Maslen GL, Williams TD, Lewis H, Schafer AJ, Chatterjee VK, O'Rahilly S 1999 Dominant negative mutations in human PPARgamma associated with severe insulin resistance, diabetes mellitus and hypertension. Nature 402:880-883
27. Deeb SS, Fajas L, Nemoto M, Pihlajamaki J, Mykkanen L, Kuusisto J, Laakso M, Fujimoto W, Auwerx J 1998 A Pro12Ala substitution in PPARgamma2 associated with decreased receptor activity, lower body mass index and improved insulin sensitivity. Nat Genet 20:284-287
28. Francis GA, Li G, Casey R, Wang J, Cao H, Leff T, Hegele RA 2006 Peroxisomal proliferator activated receptor-gamma deficiency in a Canadian kindred with familial partial lipodystrophy type 3 (FPLD3). BMC Med Genet 7:3.:3
29. Hegele RA, Cao H, Frankowski C, Mathews ST, Leff T 2002 PPARG F388L, a transactivation-deficient mutant, in familial partial lipodystrophy. Diabetes 51:3586-3590
30. Hegele RA, Ur E, Ransom TP, Cao H 2006 A frameshift mutation in peroxisome-proliferator-activated receptor-gamma in familial partial lipodystrophy subtype 3 (FPLD3; MIM 604367). Clin Genet 70:360-362
31. Jeninga EH, van Beekum O, van Dijk AD, Hamers N, Hendriks-Stegeman BI, Bonvin AM, Berger R, Kalkhoven E 2007 Impaired peroxisome proliferator-activated receptor gamma function through mutation of a conserved salt bridge (R425C) in familial partial lipodystrophy. Mol Endocrinol 21:1049-1065
32. Ludtke A, Buettner J, Schmidt HH, Worman HJ 2007 New PPARG mutation leads to lipodystrophy and loss of protein function that is partially restored by a synthetic ligand. J Med Genet 44:e88
33. Ludtke A, Buettner J, Wu W, Muchir A, Schroeter A, Zinn-Justin S, Spuler S, Schmidt HH, Worman HJ 2007 Peroxisome proliferator-activated receptor-gamma C190S mutation causes partial lipodystrophy. J Clin Endocrinol Metab 92:2248-2255
34. Monajemi H, Zhang L, Li G, Jeninga EH, Cao H, Maas M, Brouwer CB, Kalkhoven E, Stroes E, Hegele RA, Leff T 2007 Familial Partial Lipodystrophy Phenotype Resulting from a Single-Base Mutation in Deoxyribonucleic Acid-Binding Domain of Peroxisome Proliferator-Activated Receptor-{gamma}. J Clin Endocrinol Metab 92:1606-1612
35. Ristow M, Muller-Wieland D, Pfeiffer A, Krone W, Kahn CR 1998 Obesity associated with a mutation in a genetic regulator of adipocyte differentiation. N Engl J Med 339:953-959
36. Savage DB, Agostini M, Barroso I, Gurnell M, Luan J, Meirhaeghe A, Harding AH, Ihrke G, Rajanayagam O, Soos MA, George S, Berger D, Thomas EL, Bell JD, Meeran K, Ross RJ, Vidal-Puig A, Wareham NJ, O'Rahilly S, Chatterjee VK, Schafer AJ 2002 Digenic inheritance of severe insulin resistance in a human pedigree. Nat Genet 31:379-384
37. Yen CJ, Beamer BA, Negri C, Silver K, Brown KA, Yarnall DP, Burns DK, Roth J, Shuldiner AR

1997 Molecular scanning of the human peroxisome proliferator activated receptor gamma (hPPAR gamma) gene in diabetic Caucasians: identification of a Pro12Ala PPAR gamma 2 missense mutation. Biochem Biophys Res Commun 241:270-274
38. Al Shali K, Cao H, Knoers N, Hermus AR, Tack CJ, Hegele RA 2004 A single-base mutation in the peroxisome proliferator-activated receptor gamma4 promoter associated with altered in vitro expression and partial lipodystrophy. J Clin Endocrinol Metab 89:5655-5660
39. Tan GD, Neville MJ, Liverani E, Humphreys SM, Currie JM, Dennis L, Fielding BA, Karpe F 2006 The in vivo effects of the Pro12Ala PPARgamma2 polymorphism on adipose tissue NEFA metabolism: the first use of the Oxford Biobank. Diabetologia 49:158-168
40. Altshuler D, Hirschhorn JN, Klannemark M, Lindgren CM, Vohl MC, Nemesh J, Lane CR, Schaffner SF, Bolk S, Brewer C, Tuomi T, Gaudet D, Hudson TJ, Daly M, Groop L, Lander ES 2000 The common PPAR gamma Pro12Ala polymorphism is associated with decreased risk of type 2 diabetes. Nat Genet 26:76-80
41. Ludovico O, Pellegrini F, Di Paola R, Minenna A, Mastroianno S, Cardellini M, Marini MA, Andreozzi F, Vaccaro O, Sesti G, Trischitta V 2007 Heterogeneous effect of peroxisome proliferator-activated receptor gamma2 Ala12 variant on type 2 diabetes risk. Obesity (Silver Spring) 15:1076-1081
42. Masugi J, Tamori Y, Mori H, Koike T, Kasuga M 2000 Inhibitory effect of a proline-to-alanine substitution at codon 12 of peroxisome proliferator-activated receptor-gamma 2 on thiazolidinedione-induced adipogenesis. Biochem Biophys Res Commun 268:178-182
43. Bluher M, Paschke R 2003 Analysis of the relationship between PPAR-gamma 2 gene variants and severe insulin resistance in obese patients with impaired glucose tolerance. Exp Clin Endocrinol Diabetes 111:85-90
44. Hamer OW, Forstner D, Ottinger I, Ristow M, Bollheimer LC, Scholmerich J, Palitzsch KD 2002 The Pro115Gln polymorphism within the PPAR gamma2 gene has no epidemiological impact on morbid obesity. Exp Clin Endocrinol Diabetes 110:230-234
45. Evans D, Mann WA, de HJ, Michel U, Wendt D, Kortner B, Wolf A, Beisiegel U 2000 Variation in the gene for human peroxisome proliferator activated receptor gamma (PPARgamma) does not play a major role in the development of morbid obesity. Int J Obes Relat Metab Disord 24:647-651
46. Clement K, Hercberg S, Passinge B, Galan P, Varroud-Vial M, Shuldiner AR, Beamer BA, Charpentier G, Guy-Grand B, Froguel P, Vaisse C 2000 The Pro115Gln and Pro12Ala PPAR gamma gene mutations in obesity and type 2 diabetes. Int J Obes Relat Metab Disord 24:391-393
47. Adams M, Reginato MJ, Shao D, Lazar MA, Chatterjee VK 1997 Transcriptional activation by peroxisome proliferator-activated receptor gamma is inhibited by phosphorylation at a consensus mitogen-activated protein kinase site. J Biol Chem 272:5128-5132
48. Hu E, Kim JB, Sarraf P, Spiegelman BM 1996 Inhibition of adipogenesis through MAP kinase-mediated phosphorylation of PPARgamma. Science 274:2100-2103
49. Shao D, Rangwala SM, Bailey ST, Krakow SL, Reginato MJ, Lazar MA 1998 Interdomain communication regulating ligand binding by PPAR-gamma. Nature 396:377-380
50. Agostini M, Gurnell M, Savage DB, Wood EM, Smith AG, Rajanayagam O, Garnes KT, Levinson SH, Xu HE, Schwabe JW, Willson TM, O'Rahilly S, Chatterjee VK 2004 Tyrosine agonists reverse the molecular defects associated with dominant-negative mutations in human peroxisome proliferator-activated receptor gamma. Endocrinology 145:1527-1538
51. Clifton-Bligh RJ, de Zegher F, Wagner RL, Collingwood TN, Francois I, Van Helvoirt M, Fletterick RJ, Chatterjee VK 1998 A novel TR beta mutation (R383H) in resistance to thyroid hormone syndrome predominantly impairs corepressor release and negative transcriptional regulation. Mol Endocrinol 12:609-621
52. Li G, Leff T 2007 Altered promoter recycling rates contribute to dominant-negative activity of human peroxisome proliferator-activated receptor-gamma mutations associated with diabetes. Mol Endocrinol 21:857-864
53. Barettino D, Vivanco Ruiz MM, Stunnenberg HG 1994 Characterization of the ligand-dependent transactivation domain of thyroid hormone receptor. EMBO J 13:3039-3049
54. Zhang X, Jeyakumar M, Bagchi MK 1996 Ligand-dependent cross-talk between steroid and thyroid

hormone receptors. Evidence for common transcriptional coactivator(s). J Biol Chem 271:14825-14833
55. Heikkinen S, Argmann C, Feige JN, Koutnikova H, Champy MF, Dali-Youcef N, Schadt EE, Laakso M, Auwerx J 2009 The Pro12Ala PPARgamma2 variant determines metabolism at the gene-environment interface. Cell Metab 9:88-98
56. van Beekum O, Brenkman AB, Grontved L, Hamers N, van den Broek NJ, Berger R, Mandrup S, Kalkhoven E 2008 The adipogenic acetyltransferase Tip60 targets activation function 1 of PPARgamma. Endocrinology 149:1840-1849
57. Gray SL, Nora ED, Grosse J, Manieri M, Stoeger T, Medina-Gomez G, Burling K, Wattler S, Russ A, Yeo GS, Chatterjee VK, O'Rahilly S, Voshol PJ, Cinti S, Vidal-Puig A 2006 Leptin deficiency unmasks the deleterious effects of impaired peroxisome proliferator-activated receptor gamma function (P465L PPARgamma) in mice. Diabetes 55:2669-2677
58. Semple RK, Chatterjee VK, O'Rahilly S 2006 PPAR gamma and human metabolic disease. J Clin Invest 116:581-589
59. Hegele RA 2005 Lessons from human mutations in PPARgamma. Int J Obes (Lond) 29 Suppl 1: S31-5.:S31-S35

Chapter 3

Impaired PPARγ function through mutation of a conserved salt bridge (R425C) in Familial Partial Lipodystrophy

Ellen H. Jeninga[1], Olivier van Beekum[1], Aalt D.J. van Dijk[2], Nicole Hamers[1], Brenda I. Hendriks-Stegeman[1], Alexandre M.J.J. Bonvin[2], Ruud Berger[1] and Eric Kalkhoven[1]

[1]Department of Metabolic and Endocrine Diseases, UMC Utrecht, Lundlaan 6, 3584 EA Utrecht, The Netherlands; [2]Bijvoet Center for Biomolecular Research, Utrecht University, Padualaan 8, 3584 CH Utrecht, The Netherlands.

Molecular Endocrinology 2007: 21(5):1049-65

Abstract

The nuclear receptor PPARγ plays a key role in the regulation of glucose and lipid metabolism in adipocytes by regulating their differentiation, maintenance and function. A heterozygous mutation in the *PPARG* gene, which changes an arginine residue at position 425 into a cysteine (R425C), has been reported in a patient with familial partial lipodystrophy subtype 3 (FPLD3). The strong conservation of arginine 425 among nuclear receptors that heterodimerise with RXR prompted us to investigate the functional consequences of the R425C mutation on PPARγ function. Here we show that this mutant displayed strongly reduced transcriptional activity compared to wild type PPARγ, irrespective of cell type, promoter context or ligand, whereas transrepression of NF-κB activity remained largely intact. Our data indicate that the reduced transcriptional activity of PPARγ R425C is not caused by impaired corepressor release, but due to reduced dimerisation with RXRα in combination with reduced ligand binding and subsequent coactivator binding. As a consequence of these molecular defects, the R425C mutant was less effective in inducing adipocyte differentiation. PPARγ R425C did not inhibit its wild type counterpart in a dominant negative manner, suggesting a haploinsufficiency mechanism in at least some FPLD3 patients. Using molecular dynamics simulations, substitution of R425 with cysteine is predicted to cause the formation of an alternative salt bridge. This structural change provides a likely explanation how mutation of a single conserved residue in a patient with FPLD3 can disrupt the function of the adipogenic transcription factor PPARγ on multiple levels.

Introduction

The prevalence of obesity and overweight rapidly increases worldwide (1). This is a major health concern, because adiposity is highly associated with insulin resistance, type 2 diabetes, dyslipidemia, hypertension and atherosclerosis (components of the metabolic syndrome). Interestingly, the selective loss of adipose tissue (lipodystrophy) is also frequently associated with marked insulin resistance and complications such as type 2 diabetes, dyslipidemia and hypertension (2). Thus, normal amounts of adipose tissue and normal fat distribution appear to be critical for the optimal regulation of lipid and energy metabolism.

Lipodystrophies represent a heterogeneous group of diseases characterized by altered amounts and / or distribution of body fat and major metabolic complications. The main forms can be classified according to their origin, either genetic or acquired, and subclassified according to the clinical pattern (3;4). Whereas acquired lipodystrophies, like the metabolic syndrome and lipodystrophy due to highly active anti-retroviral therapy (HAART) (5) are fairly common, inherited forms of lipodystrophy are rare. Familial partial lipodystrophy (FPLD) is an autosomal dominantly inherited disorder, characterized by gradual loss of subcutaneous fat from the extremities and an accumulation of excess fat in the intra-abdominal regions (3;4). FPLD subtype 3 (FPLD3, MIM 604367) is associated with mutations in the *PPARG* gene (MIM 601487)(6;7). The majority of FPLD3 patients have profound metabolic disorders, in particular severe insulin resistance (IR) and early onset diabetes mellitus, with polycystic ovarium syndrome seen in female subjects as a direct consequence of IR and marked or extreme dyslipidemia, characterized by high triglycerides and low HDL cholesterol. Some subjects also suffer from hypertension and hepatic steatosis (6;7).

The *PPARG* gene encodes the PPARγ protein, a member of the nuclear receptor superfamily of ligand inducible transcription factors (8-10). Differential promoter usage and alternative splicing of the PPARγ gene generates four mRNA species (PPARγ 1-4), but just two different receptor proteins, PPARγ1 and PPARγ2. The PPARγ2 isoform contains 28 additional amino acids at its N-terminus and its expression is restricted to adipose tissue, while PPARγ1 is more widely expressed (e.g. in adipose tissue, lower intestine and macrophages). PPARγ plays a key role in glucose and lipid metabolism in adipocytes (8-10). Studies in murine cell lines have established that liganded PPARγ is both essential and sufficient for adipogenesis (11), while PPARγ knockout mice fail to develop adipose tissue (12-14). In addition, PPARγ directly regulates the expression of a number of genes involved in net lipid partitioning into mature adipocytes. Besides PPARγ, two closely related receptors have been identified, named PPARα and PPARβ / δ, which are encoded by different genes (10;15). These three related receptors all bind to the PPAR responsive elements (PPRE) in the promoter regions of target genes as obligate heterodimers with retinoic acid X receptors (RXRs), but exhibit different physiological roles due

to their distinct expression patterns and specific activation by different ligands. Like other nuclear receptors, PPARγ consists of distinct functional domains including a constitutively active transactivation domain (AF-1), at the N-terminus, a centrally located highly conserved DNA-binding domain (DBD) composed of two zinc finger motifs, and a C-terminal ligand-binding domain (LBD) that contains a powerful ligand-dependent transactivation function (AF-2). Ligand binding stabilises the active conformation of the PPARγ LBD, thereby serving as a "molecular switch" between activation and repression functions of the receptor (16;17). On some promoters, unliganded PPARγ recruits corepressors like N-CoR and SMRT, which are part of multiprotein complexes containing histone deacetylase (HDAC) activity that repress gene transcription (18-20). Upon ligand binding, these corepressor complexes are released and replaced by coactivator complexes, including the SRC1/CBP and TRAP/DRIP/ARC complexes, that are involved in transcriptional activation (21;22). The endogenous ligands for PPARγ are not firmly established although some natural compounds, like polyunsaturated fatty acids and prostaglandin J2 derivatives (15-deoxy-$D^{12,14}$-PGJ2) have been shown to be able to activate PPARγ (23)(24). Synthetic PPARγ agonists include the thiazolidinediones (TZDs)(25) and tyrosine-based agonists (26), which ameliorate insulin resistance and lower blood glucose levels in patients with type 2 diabetes (8). At least part of this response is thought to occur through indirect regulation of gene expression by PPARγ, e.g. by transrepression of TNFα-induced NF-κB activity (27)(28).

Seven PPARγ missense mutations have been described in patients suffering from FPLD3, which are located either in the DNA binding domain (C142R, C159Y, C190W (PPARγ2 nomenclature)) or in the ligand binding domain (V318M, F388L, R425C, P495L (PPARγ2 nomenclature)) (29-32). In addition, 2 nonsense mutations (R385X, Y355X) and 2 frameshift/premature stop mutations have been reported (32-34). Except for R425C, all mutations have been shown to result in receptors with reduced transcriptional activity and some, but not all mutants inhibited their wild-type counterpart in a dominant negative manner (see also Discussion). The functional consequences of the R425C FPLD3-associated missense mutation, which changes arginine 425 into cysteine, are currently unknown. Interestingly, a structure based sequence alignment of nuclear receptors revealed that this arginine residue is part of a structural signature, which defines nuclear receptors that form heterodimers with RXRα, including the thyroid hormone receptor β (TRβ) (35). Within this subclass of proteins, named class II receptors, R425 is involved in the formation of a conserved salt bridge with a negatively charged residue in helix 4/5 (E352 in PPARγ2). In contrast, the homodimeric class I receptors lack this conserved arginine residue and the internal salt bridge (35).

The strong conservation of arginine 425 in PPARγ2 among class II nuclear receptors together with the lack of functional data on the natural R425C mutation motivated us to investigate the functional consequences of this FPLD3-associated mutant. Here we combine detailed molecular analysis with structural modelling, using

molecular dynamics simulations, to show that the R425C mutation found in a patient with FPLD3 causes aberrant salt bridge formation and thereby abrogates PPARγ transcriptional activity leading to an inhibition of adipocyte differentiation.

Materials and methods

Materials

Rosiglitazone was purchased from Alexis. Pioglitazone, Ciglitazone, Troglitazone and 15-deoxy-$\Delta^{12,14}$-PGJ_2 were from Cayman Chemical Company. GW1929 and TNFα were from Sigma-Aldrich. [^{3}H]-Rosiglitazone was purchased from American Radiolabeled Chemicals, Inc. Fugene®6 transfection reagent was from Roche Applied Biosciences. Anti-PPARγ (sc-7273), anti-RXRα (sc-553) and anti-Gal4 (sc-510) antibodies were from Santa Cruz Biotechnologies. Anti-tropomyosin antibody (T2780) was purchased from Sigma-Aldrich and Roche Applied Biosciences, respectively. Anti-rabbit-HRP (111035144) and anti-mouse-HRP (115035146) were from Jackson Immunoresearch Laboratories Inc. Oil-Red-O was purchased from Sigma-Aldrich (O-0625). Crystal violet was from Chroma-Gesellschaft Schmid&Co.

Plasmids

All recombinant DNA work was performed according to standard procedures (58). The pCDNA3-PPARγ1, pCDNA3-PPARγ2 and pCDNA3-PPARβ/δ constructs were kind gifts from Dr. V.K.K. Chatterjee (48). pCDNA3.1-PPARα expression plasmid was a kind gift from Dr. S. Ali. The reporter containing the human aquaporin promoter (-681/+11) was a kind gift from Dr. N. Maeda (38). The reporter plasmid 2κB-luciferase was a kind gift from Dr. E. Burstein (59). The retroviral pMSCV-vector (Clontech) containing wild type murine PPARγ2 was a kind gift from Dr. B.M. Spiegelman and Dr. R.G. Roeder (60). The bacterial expression vector for GST-SMRT (61) and the 3xPPRE-tk-Luc reporter (23) were kind gifts from Dr. R.M. Evans. The bacterial expression vector for GST-SRC1 (amino acids 570-780) (62), GST-RelA (63) and the 5xGal4-AdMLTATA-Luc (64), 5xGal4-TK-Luc (64) and 3xPPRE-tk-Luc (23) reporters have been described earlier.

The pCDNA-Gal4DBD-PPARγ LBD (amino acids 173-475) expression construct was generated by cloning a *Bam*H1/*Xba*1 fragment from pSG424-PPARγLBD (gift from Dr. V.K.K Chatterjee (48) into the respective sites of pCDNA3-Gal4DBD (64). The expression vector containing the complete coding region of human RXRα was a kind gift from Dr. J.D. Baxter (65). pCDNA3.1-RXRα was generated by PCR amplification of RXRα from this vector using primers containing *Xba*I and *Hind*III-sites and cloned into the respective sites of pCDNA3.1(-). PGEX2TK-GST-CBP was generated by cloning the *Bam*HI/*Eco*RI fragment (amino acids 1-452) from pCDNA3.1-CBP (64) into the pGEX2TK vector. To generate a pCDNA3-

Gal4DBD-SMRT-ID1 construct, the SMRT-ID1 fragment (amino acids 2302-2352) was amplified from the GST-SMRT construct (61) by PCR using primers containing *Bam*H1and *Xba*I-sites respectively and cloned into the pCDNA3-Gal4DBD construct. PCDNA3-VP16 was constructed by amplification of the VP16 from a psG5-VP16 expression construct (66) by PCR using a forward primer containing a H*ind*III-site and a reverse primer containing a stopcodon and *Bam*H1-site. The VP16 cDNA was inserted in the corresponding sites of pCDNA3. PCDNA3-VP16-PPARγLBD was generated by PCR amplification of VP16 activation domain using primers containing *Hind*III and *Bam*H1-sites respectively and insertion into the respective sites of pCDNA-Gal4DBD-PPARγLBD, after removal of the Gal4DBD sequence. All mutations were generated by Quickchange mutagenesis (Stratagene) and verified by sequencing.

Cell culture, transient transfections and reporter assays

The human osteosarcoma cell line U2OS and the human embryonic kidney 293T cell line (HEK293T) were maintained in DMEM Glutamax (Dulbecco) containing 10% foetal calf serum (Gibco Life Technologies), 100 μg of penicillin/ml and 100 μg streptomycin/ml (Gibco Life Technologies). U2OS cells used for NF-κB-luciferase reporter assays were maintained in DMEM Glutamax (Dulbecco) containing 5% dextran-coated charcoal stripped foetal calf serum (67) (Gibco Life Technologies), 100 μg of penicillin/ml and 100 μg streptomycin/ml (Gibco Life Technologies). The murine NIH-3T3 cell line was cultured in the same media but now with 10% bovine serum (Gibco Life Technologies), 100 μg of penicillin/ml and 100 μg streptomycin/ml (Gibco Life Technologies). For luciferase reporter assays cells were seeded in 24-wells plates and transiently transfected using the calcium-phosphate precipitation method. Each well was cotransfected with a reporter construct, PPAR expression constructs and 2 ng pCMV-Renilla (Promega) or 12,5 ng TK-Renilla (Promega) as indicated in the figure legends. The next day, cells were washed twice with HBS (pH 7.05) and subsequently maintained in medium in absence or presence of PPAR ligands for 24 hours. After incubation cells were washed twice with phosphate-buffered saline (PBS) and harvested in passive lysisbuffer (Promega) and assayed for luciferase activity according to the manufacturer's protocol (Promega Dual-Luciferase Reporter Assay System) and for Renilla luciferase activity to correct for transfection efficiency. The relative light units were measured by a Centro LB 960 luminometer (Berthold Technologies).

For western blot analyses of the different PPARγ proteins, U2OS cells were transiently transfected with 2 μg PPARγ expression construct using Fugene®6 transfection reagent and treated as described as above. Cells were lysed in Laemli sample buffer and subjected to SDS-PAGE and transferred to Immobilon membranes (Millipore). α-PPARγ antibody was used to probe for PPARγ protein and ECL (Amersham Biosciences) was used for detection.

GST-pull downs

Recombinant PPARγ2 cDNAs (wild type or mutants) in the pCDNA3 expression vector were transcribed and translated *in vitro* in reticulolysate in the presence of [^{35}S]methionine according to manufacturer's protocol (TNT T7 Quick Coupled Transcription/Translation Kit, Promega). Rosetta pLysS competent bacteria (Novagen) were transformed with GST expression plasmids. GST fusion proteins were induced and purified as described earlier (62). [^{35}S]–labelled proteins were incubated with GST fusion proteins in NETN-buffer (20 mM Tris pH 8.0, 100 mM NaCl, 1 mM EDTA, 0,5% NP40) containing protease inhibitors (Complete, Roche Applied Biosciences). Samples were subsequently washed and subjected to SDS-PAGE. Gels were enhanced with Amplify (Amersham) and dried and the [^{35}S]-labelled proteins were visualized by fluorography. For each assay, at least three independent pull downs were performed.

EMSA

Double-stranded DNA oligomers, containing the PPRE from the rat acyltransferase-coenzyme A oxidase promoter (36), were labelled with [α-^{32}P]dATP using Klenow enzyme and purified using Probe Quant™ G-50 Micro Colums (Amersham Biosciences). *In vitro* translated PPARγ (wild type or mutants) and/or *in vitro* translated RXRα proteins were pre-incubated for 15 minutes at room temperature in absence or presence of 10-fold cold probe (wild type or mutant) in a buffer containing 10 μg BSA, 1 μg poly dI:dC, 40 mM HEPES (pH 7.4), 100 mM KCl, 2 mM DTT and 20% glycerol. For supershift experiments 1 μg of α-RXR or α-PPARγ or α-Gal4 antibodies were added to the pre-incubation mix. Following pre-incubation, purified [^{32}P]-labelled probe was added and incubated for 30 minutes at room temperature, followed by 30 minutes at 4°C. Receptor-DNA complexes were separated from unbound DNA on non-denaturing polyacrylamide gels and visualized by autoradiography. At least three independent experiments were performed.

The complete probe sequences used for binding and competition analysis were as follows: PPRE-wild-type, 5'-CCGGGGACCAGGACAAAGGTCACGAAGCT-3' and PPRE-mutant, 5'-CCGGGGGACCAGCACAAAGCACACGAAGCT-3'

Ligand-binding assay

Filter binding assays were performed as described by Adams *et al.* (68) with minor modifications. Bacterially expressed and purified GST-PPARγ2 fusion proteins were incubated with 10 or 100 nM [^{3}H]-Rosiglitazone in binding buffer (50mM HEPES pH 7.9, 100 mM KCl, 2 mM DTT, 10% glycerol) followed by incubation with an 200-fold excess of competing cold ligand (rosiglitazone). Bound ligand was separated from unbound ligand by passage through a filter membrane (Millipore HA filters, 0.45mm) under vacuum followed by three washes with binding buffer. Filters were then transferred into tubes containing scintillation fluid and counted in a γ-counter.

Binding experiments were performed independently three times.

Differentiation assay
Retrovirus was produced by Fugene transfection of Phoenix Ampho cells with the parental retroviral pMSCV-vector, pMSCV containing either wild type murine PPARγ2, or PPARγ2 R425C and collection of virus supernatants. NIH-3T3 fibroblasts were infected overnight with the virus supernatants in medium containing 4 μg/ml polybrene and infected cells were selected by addition of 2 μg/ml puromycine to the culture medium. Selected cells were grown to confluency and after two days incubated with culture medium containing dexamethasone (250 nM), IBMX (500 μM), insulin (170 nM) and rosiglitazone (2.5 nM) for two days. At day 3, medium was changed for culture medium supplemented with insulin (170 nM) and Rosiglitazone (2.5 nM) and left for a week. Cells were subsequently washed and triglycerides were stained by Oil-Red-O and the cell nuclei by crystal violet. Stained cells were photographed with a light microscope (Zeiss Axiovert 40 CFL) coupled to a digital camera (Canon DSC Powershot G5). Two independent retroviral transductions were performed.
For western blot analyses, differentiated NIH-3T3 cell lines (empty vector, PPARγ wild type or PPARγ2 R425C) were lysed in Laemli sample buffer and samples were subjected to SDS-PAGE and transferred to Immobilon membranes (Millipore). α-PPARγ and α-tropomyosin antibodies were used to probe for PPARγ protein and tropomyosin protein respectively. ECL (Amersham Biosciences) was used for detection.

Quantitative RT PCR
Transduced NIH-3T3 fibroblasts were differentiated as described above. For each cell line (empty vector, PPARγ2 wild type or PPARγ2 R425C), total RNA from three wells was isolated independently using TriPure reagent (Roche Applied Science) and reverse transcribed using MMLV-RT Rnase H Minus Point Mutant (Promega), according to manufacturer's protocol. Transcription levels were determined by real-time PCR using the LightCycler (Roche Applied Science). Briefly, the relative expression of the housekeeping gene *Hprt1* (hypoxanthine-guanine phosphoribos yltransferase 1) was used to calculate the relative expression level of the PPARγ2 target genes *Fabp4*, *Aqp7* and *Gyk* respectively, according to Vandesompele *et al.* (69). The PCR reactions were performed using the DNA Master SYBR-green 1 kit (Roche Applied Science) and contained 5.0 μl 1:40 diluted cDNA, 0.25 pmol/μl. primer, DNA master SYBR-green I solution, and $MgCl_2$ (3.5 mM). Reactions were carried out in triplicate for each sample.
The sequences of the primers are as follows: murine *Hprt1* sense primer; 5'-TCCTCCTCAGACCGCTTTT-3'; anti-sense primer, 5'-CCTGGTTCATCATCGC TAATC-3'; murine *Fabp4* sense primer 5'-GAAAACGAGATGGTGACAAGC-3'; anti-sense primer 5'-TTGTGGAAGTCACGCCTTT-3'; murine *Aqp7* sense

primer, 5′ GGCTTCTCCCTTCCTCTAGTTT-3′; anti-sense primer, 5′- AAGGCC ACTGAGGAAGTCATT-3′; murine *Gyk* sense primer, 5′- TTCCAGGAAATAATA ACTTTGTCAAG-3′; anti-sense primer, 5′- CACTGCACTGAAATACGTGCT-3′.

MD simulations

Molecular dynamics simulations were performed with the GROMACS 3.1.4 package (70;71), using the GROMOS96 43A1 force field (72). The starting structure of the wild type protein was obtained from the protein data bank (PDB) (73), entry 1FM6 (16), chain D or chain X and entry 1FM9 chain D; the mutant protein structure was obtained by replacing Arginine 425 by a Cysteine (for 1FM6 chain D) or by an Alanine (for all three chains). Cofactors and ligands were removed. Each simulation was run for 5.0 ns. A total of seven simulations was thus performed: three for wild type, three for the R425A mutant and one for the R425C mutant.

The starting structure was solvated in a cubic box with a minimum solute-box distance of 14Å, filled with approximately 25000 SPC water molecules (74) and 5 (wild type) or 6 (mutant) additional Na^+ ions to electro-neutralize the system, respectively. Periodic boundary conditions were applied.

Each system was first energy minimized using 1.000 steps of Steepest Descent algorithm. After this, equilibration was performed in five 20 ps phases during which the force constant of the position restraints term for the solute was decreased from 1000 to 0 KJ mol^{-1} nm^{-2} (1000, 1000, 100, 10, 0 KJ mol^{-1} nm^{-2}, respectively). The initial velocities were generated at 300K following a Maxwellian distribution.

Solute, solvent and counterions were independently weakly coupled to reference temperature baths at 300 K ($\tau = 0.1$ ps) (75). The pressure was maintained by weakly coupling the system to an external pressure bath at one atmosphere except for the first 20 ps equilibration part which was performed at constant volume (NVT). The LINCS algorithm (76) was used to constrain bond lengths, allowing an integration time step of 0.002 ps (2 fs) to be used. The non-bonded interactions were calculated with a twin-range cut-off (77) of 0.8 and 1.4 nm. The long-range electrostatic interactions beyond the 1.4 nm cut-off were treated with the generalized reaction field model (78) using a dielectric constant of 54. The non-bonded interaction pair list was updated every 5 steps. Trajectory coordinates and energies were stored at 0.5 ps intervals. The analysis was performed using the set of programs within GROMACS. Figures were generated using MolScript (79) and Raster3D (80).

Results

The FPLD3-associated PPARγ2 R425C displays reduced transcriptional activity

As a first step in our analysis of the FPLD3-associated R425C mutation, its effect on the ability of PPARγ2 to activate transcription was tested in reporter assays. For

this the human osteosarcoma cell line U2OS was used, which lacks endogenous PPARγ expression and displayed the most significant reporter activation by liganded PPARγ among several human cell lines tested. Cells were transfected with expression vectors encoding wild type PPARγ2 or R425C mutant together with a reporter construct containing three copies of the PPRE found in the rat acyl CoA promoter (36). While wild type PPARγ2 readily activated this 3xPPRE-tk-Luc reporter approximately 120-fold upon addition of the synthetic ligand rosiglitazone (1 μM), PPARγ2 R425C only activated this reporter 20-fold (Figure 1A). Figure 1B shows that PPARγ2 R425C was functionally defective at all concentrations of rosiglitazone tested, including saturating amounts. Cotransfection with RXRα did not increase the transcriptional activity of either wild type or mutant PPARγ, indicating that RXRα is not limiting under these experimental conditions (data not shown). Similar results were obtained in 293T cells, indicating that the reduced activity of the R425C mutant is not cell type specific (data not shown).

Since PPARγ can be activated by various ligands (23-26), reporter assays were also performed using several other synthetic and one natural PPARγ ligand. All the TZDs tested (rosiglitazone, pioglitazone, troglitazone and ciglitazone) and the natural ligand 15-deoxy-$\Delta^{12,14}$-PGJ_2 showed similar differences in transcriptional activity between wild type and mutant PPARγ2 (Figure 1C). Interestingly, the impaired activity of the R425C mutant was partially restored by the tyrosine-based agonist GW1929, a strong agonist that is also capable of activating the FPLD3 associated V318M and P495L mutants of PPARγ2 (37).

The reporter construct used above contains three copies of a functional PPRE. In order to test the effect of PPARγ2 R425C on a more "natural" promoter, reporter assays were performed using a luciferase reporter construct containing the promoter of the human adipose aquaporin gene (*AQP7*), which contains a single functional PPRE (38). As shown in Figure 1D, activation of this reporter by wild type PPARγ2 was less pronounced (6- and 12-fold in the absence and presence of rosiglitazone, respectively), compared to the 3xPPRE reporter (Figure 1A). However, mutation of R425 into cysteine reduced the ability of PPARγ2 to activate this natural promoter in a similar fashion (Figure 1D).

Amino acid sequence alignment of PPARs revealed that the arginine at position 425 in PPARγ2 lies within a region that is highly conserved between species and different PPAR family members (Figure 2A). To investigate the effect of the R425C mutation on other PPAR isoforms, analogous mutations were generated in PPARγ1 (R397C), PPARα (R388C) and PPARβ/δ (R361C) and the proteins were subsequently tested for their ability to activate a 3xPPRE reporter construct in U2OS cells. Wild type PPARγ1 activated the 3xPPRE-tk-Luc reporter approximately 70-fold upon addition of rosiglitazone, while the R397C mutant only activated this reporter 15-fold (Figure 2B, left panel). As reported earlier (39), wild type PPARα displayed significant activity in the absence of ligand, which was further increased by addition of the synthetic PPARα-specific ligand WY14643. Mutation of PPARα

R388 into cysteine almost completely inhibited transcriptional activity, both in the absence and presence of ligand (Figure 2B, middle panel). Finally, assays performed with PPARβ/δ showed that this receptor also activated the reporter upon addition of a specific PPARβ/δ ligand (GW501516), albeit significantly less than the PPARγ isoforms or PPARα. Nevertheless, the weak transcriptional activity of PPARβ/δ was clearly inhibited by mutating R361 into cysteine (Figure 2B, right panel).
Collectively, these results suggest that the FPLD3-associated R425C mutation results in reduced transcriptional activity of PPARγ2, independent of ligand type, ligand concentration and promoter used. Furthermore, the reduced transcriptional activity of R425C is not limited to the PPARγ2 protein, since similar effects were observed when analogous mutations were generated in the PPARγ1 isoform as well as in the related PPARα and PPARβ/δ proteins.

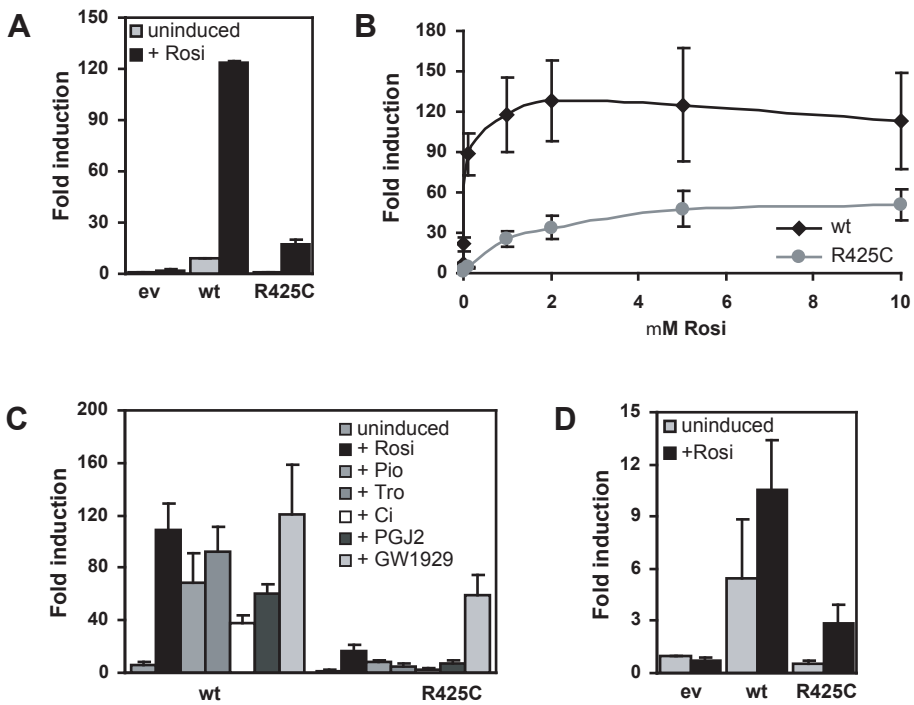

Figure 1. The FPLD3-associated R425C mutation reduces the transcriptional activity of PPARγ2.
A, U2OS cells were transfected with expression vector encoding PPARγ2 wild type (wt) or PPARγ2 R425C respectively, and a 3XPPRE-tk-Luc reporter. Activation of the luciferase reporter, in the absence or presence of 1 μM rosiglitazone, is expressed as fold induction over that with empty vector (ev) in the absence of ligand, after normalisation for Renilla luciferase activity. Results are averages of at least three independent experiments assayed in duplicate ± standard error of the means. B, Dose-response curve of U2OS cells transfected as in panel A. C, Reporter assay as outlined in panel A using the PPARγ ligands, pioglitazone (Pio; 2 μM), troglitazone (Tro; 1.5 μM), ciglitazone (Ci; 6 μM), 15-deoxy-$\Delta^{12,14}$-PGJ_2 (PGJ2; 14 μM) and GW1929 (1 μM), respectively. D, U2OS cells were transfected as in A, but with the human adipose aquaporin (*AQP7*)-Luc reporter instead of the 3xPPRE-tk-Luc reporter.

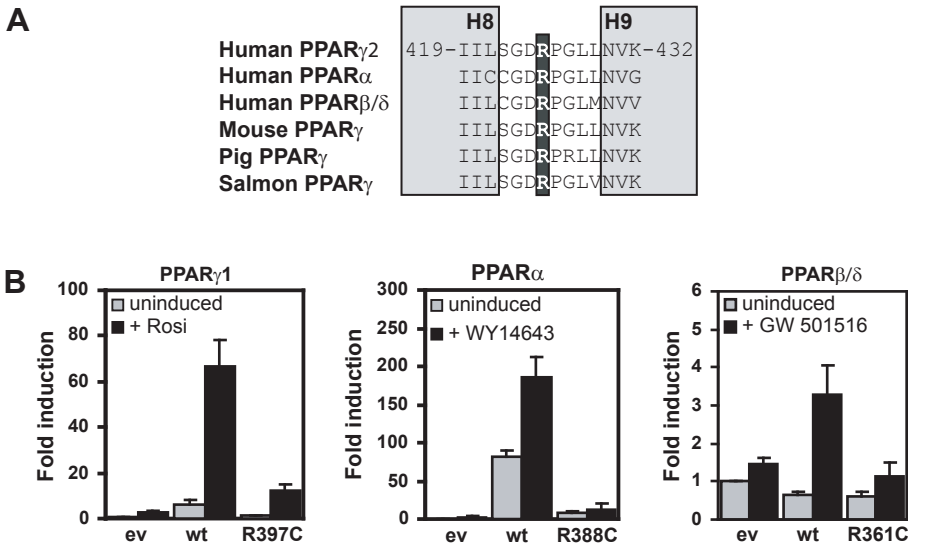

Figure 2. Mutations analogous to R425C in PPARγ2 have similar effects on transcriptional activity of different PPAR proteins.
A, Alignment of the amino acid sequence surrounding R425 in human PPARγ2 (CAA62153), with human PPARα (AAB32649), human PPARβ/δ (AAH02715), mouse PPARγ (AAO45098), pig PPARγ (CAA07225) and salmon PPARγ (CAC02968). Species in which the sequence surrounding R425 was identical to human and mouse (e.g. rat (AADA0119), zebrafish (AAY85274), Xenopus (AAH60474), chicken (AAL85323)) were omitted for reasons of clarity. Also indicated are the boundaries of helix 8 and 9, as defined in the crystal structure of the PPARγ LBD (17). B, U2OS cells were transfected with expression vectors encoding PPARγ1 wt or R397C mutant (left panel), PPARα or R388C mutant (middle panel) or PPARδ or R361C mutant (right panel). Activation of the 3xPPRE-tk-Luc reporter in the absence or presence of rosiglitazone (1 μM) for PPARγ1, WY14643 (100 μM) for PPARα or GW501516 (2.2 nM) for PPARδ, are presented as described in Figure 1A.

Corepressor binding and -release of PPARγ2 R425C is impaired

Mutations in the thyroid hormone receptor β (TRβ) are found in patients with resistance to thyroid hormone (RTH)(40). One RTH-associated mutation changes an arginine at position 383 into a histidine (R383H), resulting in impaired release of the corepressor SMRT (41). Since R383 in TRβ is analogous to R425 in PPARγ2 (Figure 3A), the effect of the R425C mutation in PPARγ2 on binding and release of SMRT was investigated. For this, bacterially expressed and purified GST or GST-SMRT fusion proteins were incubated with *in vitro* translated [^{35}S]methionine-labelled PPARγ2 proteins (wild type or R425C) in the absence or presence of rosiglitazone. As shown in Figure 3B, wild type PPARγ2 interacted with SMRT in the absence of ligand and this interaction was reduced upon addition of rosiglitazone (Figure 3B). The PPARγ2 R425C mutant interacted with SMRT less efficiently, both in the absence and presence of ligand and did not show an obvious impairment of SMRT release in response to ligand (Figure 3B).

To substantiate these *in vitro* results in living cells we performed mammalian two-hybrid assays. For this, an expression vector consisting of the interaction domain 1 (ID1) of SMRT fused to the DNA-binding domain of Gal4 (Gal4DBD) were used, together with an expression vector encoding a fusion protein of PPARγLBD with the activation domain of VP16 (VP16). In the absence of ligand, wild type PPARγLBD clearly interacted with the SMRT-ID1, as demonstrated by the activation of the 5xGal4-TK-Luc reporter (Figure 3C). Upon addition of rosiglitazone this interaction decreased in a dose dependent manner. In contrast, PPARγLBD R425C showed limited interaction with SMRT-ID1, either in the absence or presence of ligand. In contrast, the FPLD3-associated P495L mutant of PPARγ2, which was previously shown to exhibit impaired corepressor release (37), showed a comparable level of transcriptional activity at all concentrations of rosiglitazone. The negative controls, in which VP16 protein was coexpressed with either Gal4DBD or Gal4DBD-SMRT-ID1, displayed negligible luciferase activity.

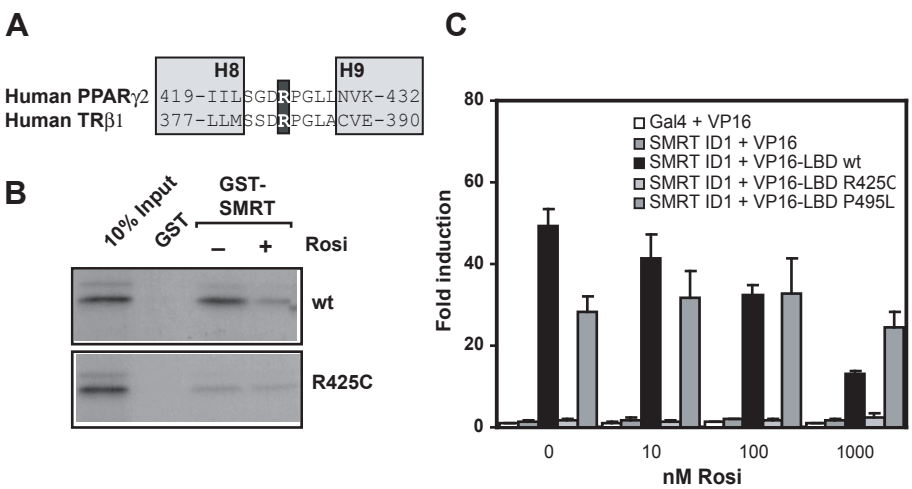

Figure 3. The PPARγ2 R425C mutation affects corepressor binding but not release.
A, Alignment of the amino acid sequence surrounding R425 in human PPARγ2 and human TRβ1 (AAI06930). B, GST fusion proteins coupled to Sepharose beads were incubated with *in vitro* translated [^{35}S]-labelled PPARγ2 proteins (wt or mutant) in the absence or presence of rosiglitazone (1 μM). After extensive washing, samples were boiled and separated on SDS-polyacrylamide gels. Gels were fixed and dried and the labelled proteins were detected by fluorography. The input lanes represent 10% of the total lysate used in each reaction. C, U2OS cells were transfected with Gal4DBD or Gal4DBD-SMRT ID1 (50 ng), VP16 or VP16-PPARγLBD (wt or mutant; 50 ng), 5xGal4-TK-Luc reporter (500 ng) and incubated with different concentrations of rosiglitazone as indicated. Activation of the luciferase reporter, in the absence or presence of rosiglitazone, is expressed as fold induction over that with Gal4DBD+VP16 in the absence of ligand, after normalisation for Renilla luciferase activity. Results are averages of at least three independent experiments assayed in duplicate ± standard error of the means.

Thus, our data indicate that the R425C mutation in PPARγ2 does not impair corepressor release, but rather reduces the affinity for the corepressor. We conclude therefore that in contrast to the natural R383H mutant of TRβ, the reduction in PPARγ-mediated transcription caused by the R425C mutation is unlikely to be caused by impaired corepressor release.

The PPARγ2 R425C mutation results in reduced heterodimerisation with RXRα

The crystal structure of PPARγ-LBD reveals 13 α-helices and a small four-stranded β-sheet (16;17). The arginine at position 425 lies within a highly conserved sequence that is located in a loop between helix 8 and 9, and some of the residues surrounding arginine 425 (G423, D424 and P426) are involved in heterodimerisation with RXRα. This prompted us to investigate whether the PPARγ R425C mutation affected dimerisation with RXRα. First, we studied the effect of this mutation and mutations of the other highly conserved loop residues on *in vitro* heterodimerisation by performing GST-pull down assays. For this, *in vitro* translated [^{35}S]methionine-labelled PPARγ2 proteins (wild type or mutants) were incubated with bacterially expressed and purified GST-RXRα. While wild type PPARγ2 efficiently interacted with RXRα, the R425C mutant protein displayed reduced binding (Figure 4A). Mutation of arginine 425 into alanine (R425A) or lysine (R425K) also decreased the PPARγ2-RXRα interaction. PPARγ2 D424A showed a slightly reduced binding compared to wild type PPARγ2, whereas mutation of glycine 423 or proline 426 into alanine (G423A and P426A, respectively) did not have an appreciable effect on *in vitro* dimerisation with RXRα. As a control, a PPARγ2 mutant was generated (L464R), analogous to the homodimerisation defective mouse ER mutant (L511R) (42). This L464R mutant completely failed to dimerise with RXRα in these *in vitro* assays (Figure 4A).

Next, the effects of the mutants described above on the transcriptional activity of PPARγ2 were studied. Like the R425C mutant (Figure 1), the R425A and R425K mutants displayed strongly reduced ligand-dependent activation of a 3xPPRE-tk-Luc reporter in U2OS cells (Figure 4B). The D424A mutant showed slightly reduced transcriptional activity, while the activity of the G423A and P426A mutants was similar to wild type PPARγ2. Transcriptional activity of the heterodimerisation defective mutant L464R was completely abolished. The expression of all PPARγ proteins was confirmed by Western blot analysis (Figure 4B, lower panel). In general, the observed differences in transcriptional levels between the PPARγ2 mutants reflected the differential effects on heterodimerisation of these mutants (Figure 4A), confirming that heterodimerisation is a prerequisite for the transcriptional activity of the PPARγ2 protein. In addition, mutation of the positively charged arginine at position 425 into a cysteine (R425C), into the uncharged residue alanine (R425A) or into a lysine residue (R425K), which is also positively charged, all affected the *in vitro* RXRα heterodimerisation capacity as well as the transcriptional activity of PPARγ2. These findings point to the specific requirement of the arginine residue at

position 425 for optimal function of PPARγ2 as a transcription factor.
Since PPARγ can only bind to PPRE sequences in the DNA upon heterodimerisation with RXRα, we investigated the effect of the R425C mutant on DNA binding. Electrophoretic mobility shift assays were performed in which *in vitro* translated RXRα and PPARγ2 proteins (either wild type or mutant) were incubated with a [^{32}P]-labelled PPRE sequence. A specific PPARγ2-RXRα heterodimeric complex

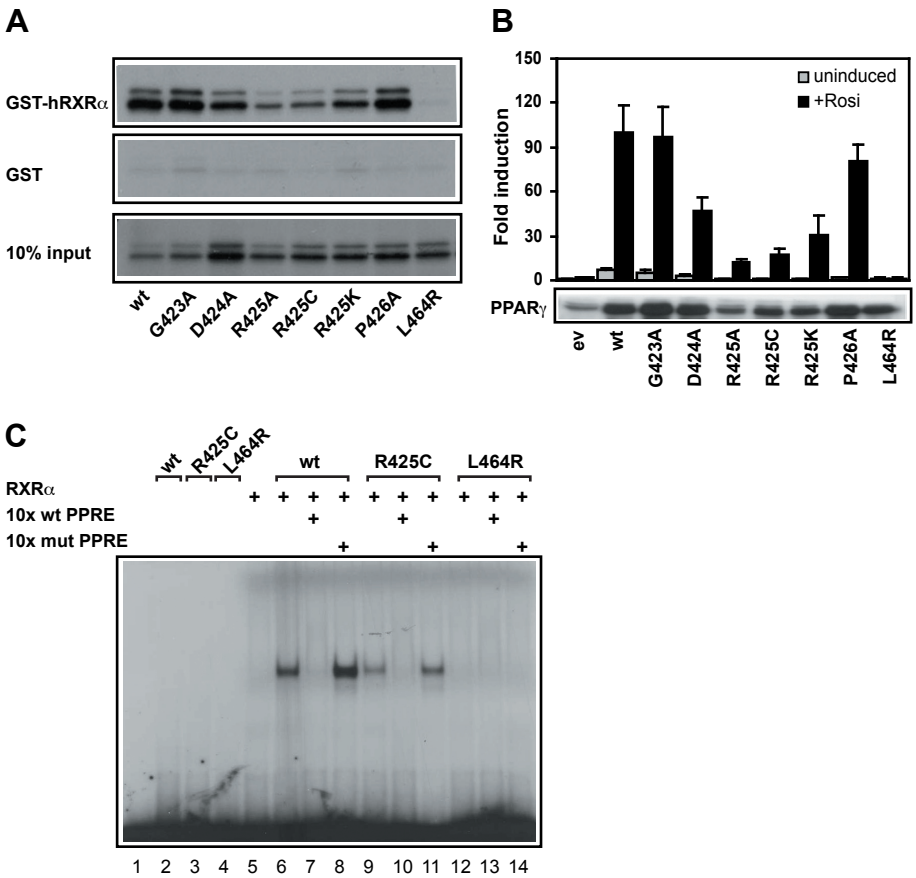

Figure 4. Heterodimerisation of PPARγ2 R425C with RXRα and subsequent DNA binding is impaired.
A, Bacterially expressed and purified GST or GST-RXRα proteins were incubated with *in vitro* translated [^{35}S]methionine-labelled PPARγ2 proteins (wt or mutant). Bound proteins were visualised as described in Figure 3B. B, U2OS cells were transfected with various PPARγ2 mutants. Experiments were performed and data are presented as described in Figure 1A. Expression of the different PPARγ2 proteins was confirmed by western blot analysis using an antibody directed against PPARγ. C, *In vitro* translated RXRα or PPARγ2 (wt or mutant) proteins were incubated with [^{32}P]-labelled probe in absence or presence of 10X unlabelled probe (wt or mutant) as indicated. Protein-DNA complexes were separated from unbound DNA on non-denaturing SDS-polyacrylamide gels and visualized by autoradiography of dried gels.

was formed on the PPRE, as formation of this protein-DNA complex could be diminished by addition of an excess of unlabelled wild type PPRE, but not by an excess of mutant PPRE (Figure 4C). The R425C mutant protein also displayed specific DNA binding in the presence of RXRα, albeit 2.3 fold less than wild type, as determined by densitometric analysis. A similar difference in binding capacity was observed with increasing amounts of PPARγ2 protein (wild type or R425C) (see Supplementary material, Figure S1). Specific antibodies against PPARγ and RXRα supershifted both the wild type and mutant protein-DNA complexes, confirming the heterodimeric composition of both complexes (see Supplementary material, Figure S2). The dimerisation-defective L464R mutant failed to bind the PPRE in the presence of RXRα (Figure 4C). Taken together, these results indicate that heterodimerisation with RXRα and subsequent DNA binding of PPARγ2 is significantly, but not completely impaired by the R425C mutation.

Ligand binding and subsequent coactivator binding of PPARγ2 R425C is reduced

Since heterodimerisation with RXRα and subsequent DNA binding of PPARγ2 R425C is not completely impaired, this suggests that additional molecular defects contribute to the impaired function of this FPLD3-associated mutant. To investigate this, we performed reporter assays in which PPARγ driven transcription is independent of heterodimerisation with RXRα. For this, the mutations described above were introduced into a chimeric Gal4DBD-PPARγ LBD receptor and expressed together with a Gal4 reporter gene in U2OS cells. Both the wild type Gal4-PPARγLBD receptor and the dimerisation defective L464R mutant stimulated transcription from the reporter up to 350-fold in the presence of rosiglitazone, showing that transcriptional activation is indeed independent of heterodimerisation with RXRα in this assay (Figure 5A). In contrast the activity of the R425C mutant, as well as the R425A and R425K mutants, was strongly reduced. The G423A, D4242A and P426A mutants displayed levels of transcription similar to wild type PPARγ. As a control, Western blot analysis was performed and showed comparable amounts of GAL4DBD fusion proteins (Figure 5A, lower panel). These results indicate that the transcriptional defect in the PPARγ2 R425C protein is not only due to reduced heterodimerisation with RXRα.

In order to identify additional defects in the R425C protein, we first performed ligand binding assays. For this, bacterially expressed and purified GST-PPARγ2 fusion proteins (wild type or R425C) were incubated with either 10 nM or 100 nM of [^{3}H]-labelled rosiglitazone. Whereas wild type PPARγ2 protein displayed specific binding of rosiglitazone, the mutant protein showed reduced binding capacity for the ligand at both concentrations tested (Figure 5B). The amounts of the bacterially produced receptors were similar (Figure 5B; inset), indicating that the lower binding capacity for rosiglitazone displayed by the mutant protein was not caused by differences in protein levels. Since a coactivator binding surface is generated in the LBD of PPARγ upon ligand binding, we next examined whether the reduced

affinity for rosiglitazone displayed by the R425C protein also affected interaction with coactivators. For this, bacterially expressed and purified GST-fusion proteins of the coactivators CBP and SRC1 were incubated together with *in vitro* translated [^{35}S]methionine-labelled PPARγ2 wild type or PPARγ2 R425C proteins in the absence or presence of rosiglitazone. As observed before (43-45), wild type PPARγ2 bound to SRC1 in the presence of rosiglitazone in a dose-dependent manner (Figure 5C),

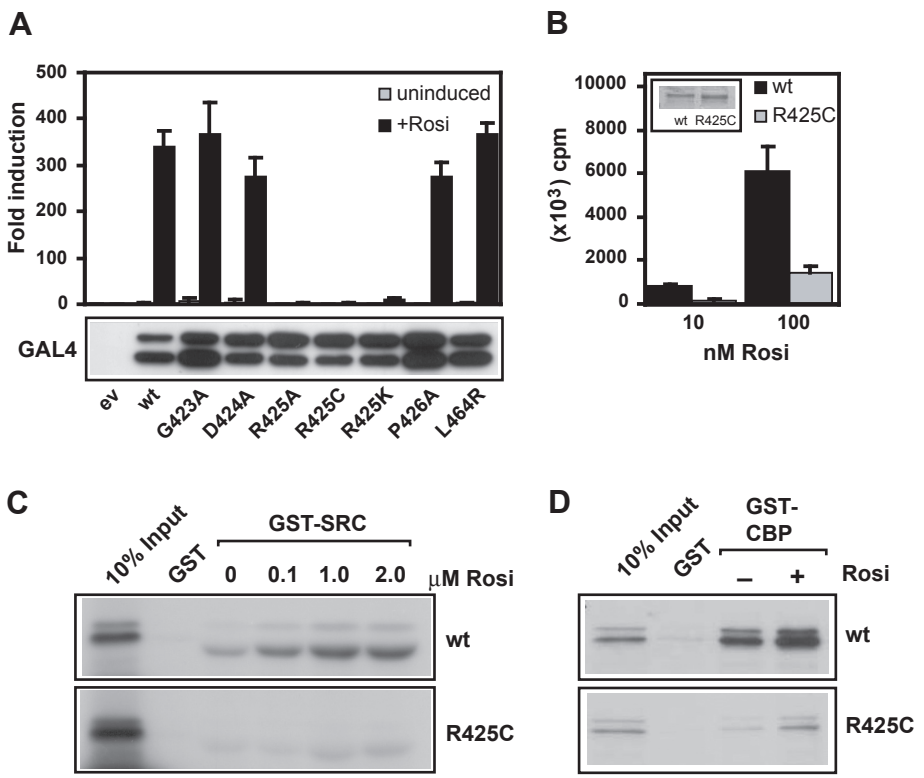

Figure 5. Ligand binding and subsequent coactivator binding of PPARγ2 R425C is reduced.
A, U2OS cells were transfected with 5xGal4-AdMLTATA-Luc reporter (1 μg), empty vector or Gal4DBD-PPARγLBD expression vectors (wt or mutant; 200 ng) and incubated with or without rosiglitazone (1 μM) as indicated. Data are presented as described in figure 1A. Comparable amounts of the different GAL4 DBD fusion proteins were detected by western blot analysis using a GAL4 antibody. B, GST-PPARγ2 (wt or mutant) was incubated with different concentrations of [^{3}H]-rosiglitazone. Bound ligand was measured by a γ-counter. Data are indicated as mean of three separate experiments performed in duplicate. Inset, bacterially expressed and purified PPARγ2 proteins (wt or mutant) were subjected to SDS-PAGE and visualized by Coomassie brilliant blue staining. C, *In vitro* translated [^{35}S]-labelled PPARγ2 proteins (wt or mutant) were incubated with bacterially expressed and purified GST or GST-SRC1 in the absence or presence of increasing concentrations of rosiglitazone (0.1, 1 or 2 μM). Bound proteins were visualised by fluorography of dried gels. D, *In vitro* translated [^{35}S]-labelled PPARγ2 proteins (wt or mutant) were incubated with bacterially expressed and purified GST or GST-CBP in the absence or presence of rosiglitazone (1 μM). Bound proteins were visualised by fluorography of dried gels.

while the interaction between PPARγ2 and CBP was less dependent on the presence of ligand (Figure 5D). Although PPARγ2 R425C also displayed specific binding to SRC1 and CBP under these conditions, these protein-protein interactions were significantly weaker compared to wild type PPARγ2.
In summary, these experiments indicate that in addition to impaired heterodimerisation (Figure 4), the R425C mutation also abrogates ligand binding compared to the wild type protein and as a consequence diminishes ligand-dependent interaction with transcriptional coactivators.

Transrepression of NF-κB by PPARγ R425C remains largely intact and is independent of heterodimerisation with RXRα
In order to examine the effect of the R425C mutation on PPARγ-mediated repression of NF-κB activity, we performed reporter assays in which U2OS cells were transfected with expression vectors encoding wild type PPARγ2 or mutant PPARγ (R425C or L464R) or an empty vector together with a 2κB-luciferase reporter. Upon addition of TNFα, this reporter was activated up to 10-fold and cotransfection of increasing amounts of either wild type PPARγ2 or R425C both reduced this activation in a dose dependent manner. Addition of rosiglitazone enhanced this inhibitory effect to some extent (Figure 6A). Since the R425C mutant displayed reduced dimerisation with RXRα (Figure 4), these results suggest that monomeric forms of the receptor may be sufficient for transrepression of NF-κB activity, as was also shown for other nuclear receptors (46). To investigate this, we employed the PPARγ2 L464R mutant, which displays a complete loss of dimerisation activity (Figure 4). A dose dependent decrease in reporter activation by TNFα was observed upon addition of increasing amounts of L464R mutant, corroborating the hypothesis that PPARγ mediated transrepression of NF-κB is independent of heterodimerisation with RXRα.
In addition, since transcriptional interference between PPARγ and NF-κB occurs through the RelA (p65) subunit of NF-κB (47), we assessed this protein-protein interaction by incubating bacterially expressed GST-RelA fusion proteins with *in vitro* translated PPARγ2 proteins (either wild type, R425C or L464R). As shown in figure 6B, all three PPARγ2 proteins were able to bind to GST-RelA and this interaction was largely rosiglitazone independent.
In summary, although the FPLD3-associated R425C mutation results in reduced transcriptional activity of PPARγ (Figure 1), PPARγ-mediated transrepression of NF-κB activity remains largely intact, especially in the presence of ligand. Furthermore, our data suggest that the PPARγ-mediated transrepression is largely independent of heterodimerisation with RXRα.

Molecular dynamics simulation predicts an alternative salt bridge in PPARγ2 R425C
Since the arginine residue on position 425 in PPARγ2 is involved in the formation of an internal salt bridge (16), the effects of substituting this amino acid by cysteine was examined using several 5 nanosecond (ns) molecular dynamics simulations

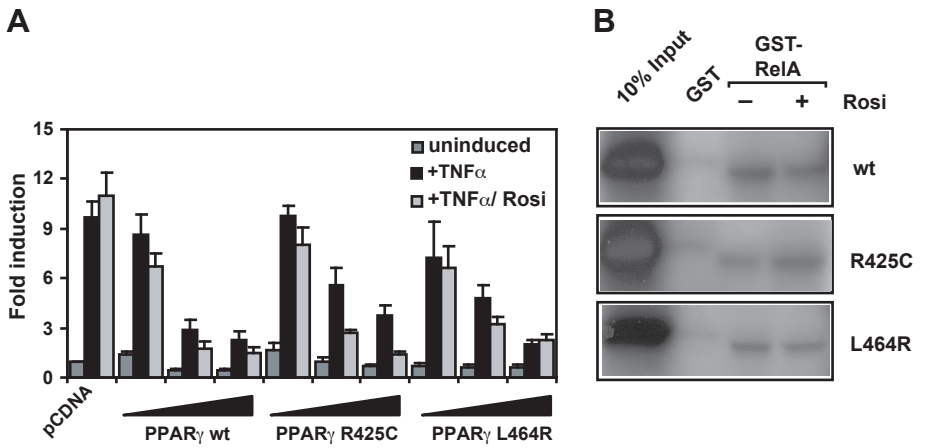

Figure 6. The FPLD3-associated PPARγ R425C mutation is able to transrepress NF-κB activity.
A, U2OS were transfected with empty vector (10 ng), wild type PPARγ2, PPARγ2 R425C and PPARγ2 L464R respectively (10, 50 or 100 ng) and 2κB-luciferase reporter (300 ng). Activation of the luciferase reporter in the absence or presence TNFα (250 units) or TNFα in combination with rosiglitazone (1 μM), respectively, is expressed as fold induction over that of empty vector in the absence of TNFα and rosiglitazone, after normalisation for Renilla luciferase activity. Results are averages of three independent experiments performed in duplicate ± standard error of the means. B, *In vitro* translated [^{35}S]-labelled PPARγ2 proteins (wt, R425C or L464R) were incubated with bacterially expressed and purified GST or GST-RelA in the absence or presence of rosiglitazone (1 μM). Bound proteins were visualised by fluorography of dried gels.

of wild type protein and R425A and R425C mutants starting from various crystal structures of the LBD domain of PPARγ (see Material and Methods). Positional root mean square deviation (RMSD) from the starting structures as well as the various energy terms reached equilibrium in a few ns for all the simulations (see Supplementary material Figure S3 and S4). When analysing the trajectories resulting from the different simulations, there was a clear and consistent difference between wild type PPARγ2 and PPARγ2 R425C with respect to salt bridges that are present. In the wild type protein, R425 (located in the loop between helix 8 and 9) forms a salt bridge with E352 (in helix 4/5), and R471 (in helix 10) forms a salt bridge with D424 (Figure 7A, left panel). In the R425C mutant, however, the salt bridge between R425 and E352 obviously cannot be formed, and this resulted, unexpectedly, in a switch from the R471-D424 salt bridge to a salt bridge between R471 and E352 (Figure 7A, right panel, and Supplementary material Figure S5). A similar change was observed when R425 was mutated into alanine (data not shown). We also compared various structural parameters (RMSDs, angles between helices, solvent accessibility of surface residues). Although in some simulations helix 10 seemed to be deformed in the R425C mutant, we could not find consistent differences between wild type and mutant simulations. The difference in salt bridge pattern was consistently found between on the one hand the three wild type simulations and on the other hand four mutant simulations (both R425A and R425C). The fact

that the same rearrangement is observed in independent simulations starting from various crystal structures, make the observed structural difference between wild type and mutant protein highly significant.
To test the importance of those salt bridges for transcriptional activity, we mutated the individual residues involved in the salt bridge formation to alanine residues and performed reporter assays in U2OS cells. Like R425C, the salt bridge mutants D424A, E352A and R471A all displayed reduced transcriptional activity compared to wild type PPARγ2 (Figure 7B). Western blot analysis was performed as a control

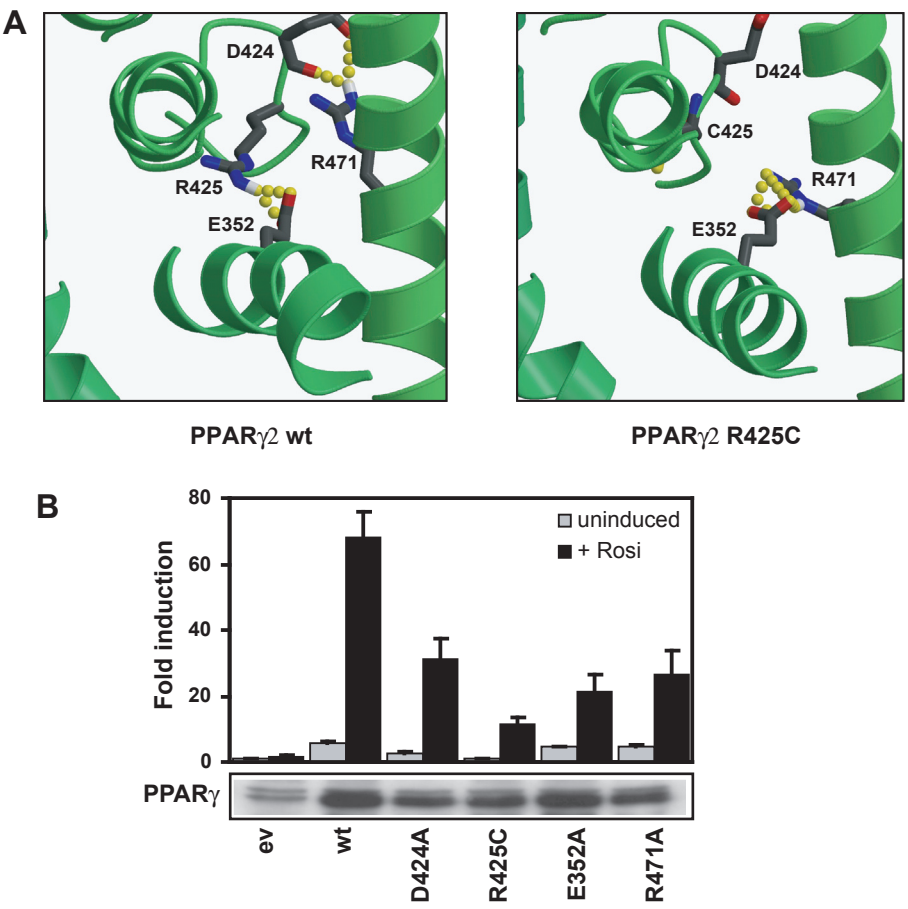

Figure 7. An internal salt bridge in PPARγ2 is disturbed by the substitution of arginine 425 with cysteine.
A, Snapshots from Molecular Dynamics simulations for wild type (left panel) and R425C (right panel) mutant PPARγ. A close-up view of the salt bridges discussed in the text is provided, with residues involved represented in ball-and-stick. B, U2OS cells were transfected with vectors expressing various mutants of PPARγ2. Experiments were performed and data are presented as described in Figure 1A. Expression of the different PPARγ2 proteins was confirmed by western blot analysis using an antibody directed against PPARγ.

and showed comparable expression levels for all PPARγ proteins (Figure 7B, lower panel). These findings suggest that the internal salt bridges between R425 and E352 and between D424 and R471 play an important role in PPARγ2-mediated transcription by maintaining the structural integrity of the ligand binding domain of this receptor.

PPARγ2 R425C and PPARγ1 R397C do not display dominant negative behaviour

All of the FPLD3-associated PPARγ mutations are heterozygous and some of the resulting PPARγ mutant proteins have been shown to inhibit their wild type counterpart in a dominant negative manner (29;37). We therefore examined whether the R425C mutant of PPARγ2 and the same mutant in the context of the PPARγ1 protein (R397C) would inhibit the activity of the respective wild type receptors. For this, reporter assays were performed, using a 1:1 ratio between wild type and mutant receptors and different concentrations of ligand. As shown in figure 8A, PPARγ1 R397C failed to display dominant negative behaviour independent of ligand concentration while the FPLD3-associated PPARγ1 P467L inhibited wild type PPARγ1 at low concentrations of ligand, as reported earlier (37). In addition, the artificial PPARγ1 L468A/E471A mutant displayed a strong dominant negative activity against its wild type protein independent of ligand concentration, as shown earlier (48).

When tested in the context of the PPARγ2 protein, the R-to-C mutant also lacked dominant negative activity, whereas PPARγ2 L496A/E499A was able to inhibit wild type PPARγ2 at all concentrations of rosiglitazone (Figure 8B). Interestingly, whereas PPARγ1 P467L displayed a dominant negative effect over its wild type counterpart (Figure 8A), the same mutant in the context of PPARγ2 (P495L) was not able to

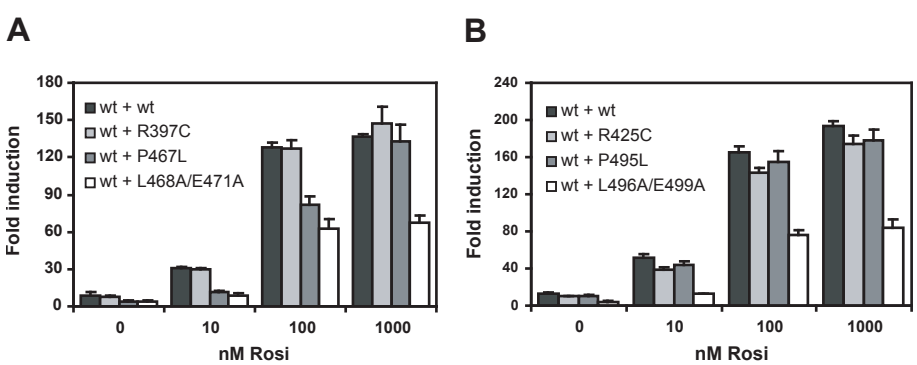

Figure 8. FPLD3-associated R-to-C mutants fail to display dominant negative activity towards wild type PPARγ isoforms.

FPLD3-associated R-to-C mutants fail to display dominant negative activity towards wild type PPARγ isoforms. A, U2OS cells were transfected with equal amounts of wild type and mutant PPARγ1 (both 100 ng), 3xPPRE-tk-Luc reporter (500 ng) and incubated with different concentrations of rosiglitazone, as indicated. B, U2OS were transfected as in panel A, but with PPARγ2 expression vectors. Results are averages of at least three independent experiments assayed in duplicate ± standard error of the means.

inhibit wild type receptor in a dominant negative manner (Figure 8B). In addition, the PPARγ1 P467L mutant was dominant negative over wild type PPARγ2, but PPARγ2 P495L did not display dominant negative activity over wild type PPARγ1 (data not shown). Similar results were obtained in 293T cells, indicating that the observed effects were not restricted to U2OS cells (data not shown).
In summary, these data show that unlike the artificial PPARγ double mutant, the FPLD3-associated PPARγ R-to-C mutant does not exert dominant negative activity over the wild type receptor, whereas dominant negative activity of the FPLD3-associated PPARγ P-to-L mutant appears to be limited to the PPARγ1 isoform under our experimental conditions.

The R425C mutation reduces the ability of PPARγ2 to induce adipocyte differentiation
Having established by *in vitro* and cell-based assays that PPARγ function is affected on multiple levels we investigated the effect of this mutation *in vivo* on adipocyte differentiation. NIH-3T3 fibroblasts were transduced with virus obtained from cells transfected with the parental retroviral pMSCV vector, pMSCV-PPARγ2 or pMSCV-PPARγ2 R425C and stable cell lines were selected. Approximately 20% of the NIH-PPARγ2 cells differentiated into adipocytes, as assessed by staining of triglycerides with Oil-red-O (Figure 9A). Virtually no adipocyte differentiation could be detected in NIH-vector or NIH-PPARγ2 R425C fibroblasts under our experimental conditions. To independently confirm adipocyte differentiation, the mRNA expression of three PPARγ target genes, fatty acid binding protein 4 (*Fabp4*), adipose aquaporin (*Aqp7*) and glycerol kinase (*Gyk*), was determined on the same cell lines by quantitative RT-PCR assays. While a 34-fold increase in *Fabp4* mRNA expression was observed for NIH-PPARγ2 cells, mRNA expression of this gene in NIH-PPARγ2 R425C cells was similar to NIH-vector cells (Figure 9B). The PPARγ2 R425C protein also failed to induce mRNA expression of *Aqp7* and *Gyk*, both of which were significantly upregulated by the wild type receptor (Figure 9B). As shown by Western blot analysis, the PPARγ protein expression levels for wild type and R425C proteins were similar (Figure 9C).
These findings show that the R425C mutation not only compromises the ability of the PPARγ2 protein to activate transiently transfected reporter genes (Figure 1), but also reduces its potential to activate endogenous target genes (*Fabp4*, *Aqp7*, *Gyk*) and promote adipogenesis (Figure 9).

Discussion

The nuclear receptor PPARγ plays a key role in the regulation of glucose and lipid metabolism in adipocytes by regulating their differentiation, maintenance and function (9;10). Compelling genetic evidence for this view comes from human

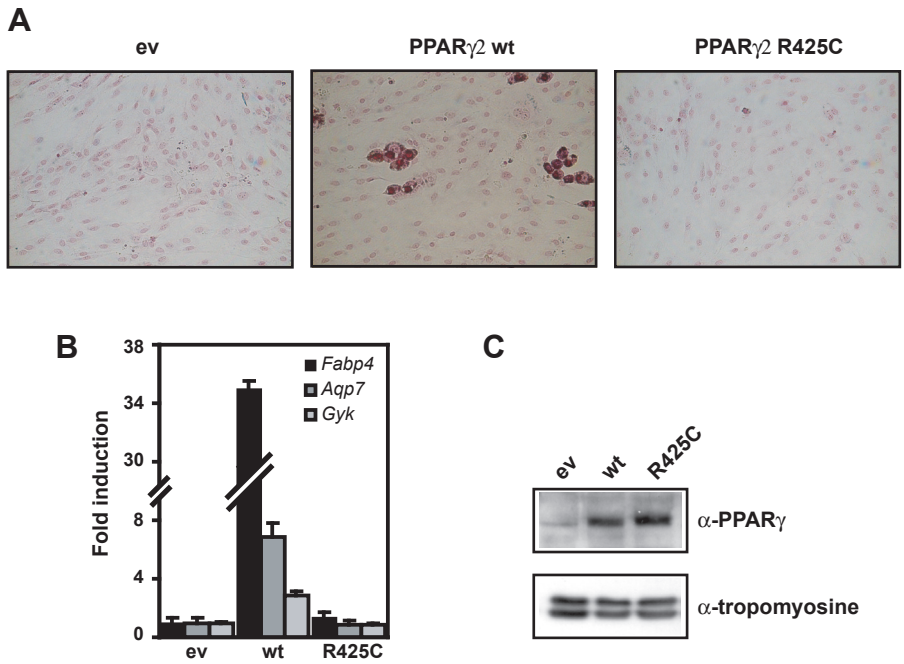

Figure 9. Reduced potential of the PPARγ2 R425C to induce adipocyte differentiation.
A, NIH-3T3 fibroblasts were transduced with retrovirus obtained form cells transfected with pMSCV (empty vector; ev), pMSCV-PPARγ2 or pMSCV-PPARγ2 R425C. After a week of incubation with differentiation medium, triglycerides were stained with Oil-Red-O and cell nuclei with crystal violet. Pictures are representative for three independent experiments. B, mRNA expression of the *Fabp4*, *Aqp7* and *Gyk* genes in NIH-3T3 cell lines described in panel A after differentiation. Expression levels are indicated as fold induction over that with NIH-empty vector cells (ev), after normalisation for the housekeeping gene *Hprt1*. Results are averages of at least three independent experiments assayed in duplicate ± standard deviation. C, Western blot analysis of lysates of the NIH-3T3 cell lines described in panel A with antibodies against PPARγ and tropomyosine (internal control).

FPLD3 patients, harbouring heterozygous mutations in the *PPARG* gene, as they are characterized by aberrant fat distribution and metabolic disturbances, including insulin resistance and dyslipidemia (6;7). In this report, we demonstrate that the FPLD3-associated PPARγ2 R425C mutant displays multiple molecular defects. These defects probably do not involve impaired corepressor release, but comprise a combination of reduced heterodimerisation with RXRα, lower ligand binding affinity and subsequent reduced binding of coactivators, resulting in reduced transcriptional activity and eventually in an impaired ability of the R425C mutant to induce adipocyte differentiation. Interestingly, like the dimerisation defective L464R mutant, the R425C mutant could still transrepress TNFα-induced NF-κB activity. These results are reminiscent of the transrepression of NF-κB activity by monomeric forms of other nuclear receptors, like the glucocorticoid receptor (46),

and indicate that activation and transrepression critically depend on different regions of the receptor (49). Recently, a structure based sequence alignment revealed two sets of differentially conserved residues that divided the entire nuclear receptor superfamily in two classes related to their oligomeric behaviour (35). Nuclear receptors that form homodimers belong to class I, while nuclear receptors that form heterodimers with RXRα, like PPARγ, belong to class II. A differentially conserved arginine (R425 in PPARγ2) defines the signature of these class II receptors, and is involved in the formation of a salt bridge with a negatively charged residue in H4/H5 (E352 in PPARγ2) (16;17). Moreover, the crystal structure of PPARγ LBD revealed an additional internal salt bridge between two different conserved "class II" residues, D424 (L8/9) and R471 (H10). Our molecular dynamics simulations predicted that substitution of PPARγ2 R425 with a cysteine residue would disrupt both internal salt bridges leading to the formation of an alternative salt bridge between R471 and E352. The conserved "salt bridge residues" are structurally important in defining the conformation of the LBD of PPARγ2: both D424 and R471 are involved in dimerisation with RXRα (16), while R425 and E352 form hydrogen bonds with Y505 at the C-terminus of helix 12 leading to the stabilisation of H12, which is important for cofactor binding (39). In addition, destabilisation of H12 could in turn affect heterodimerisation, since an interdimer salt bridge is formed between Y505 (H12) of PPARγ2 and K431 of RXRα (16). Finally, crystallographic studies on PPARα together with a corepressor peptide indicate that the two hydrophobic residues immediately preceding E352 in PPARγ2 are probably part of the corepressor interaction surface (50). Therefore, conformational changes resulting from the simultaneous disruption of both internal salt bridges through the R425C mutation provide a likely explanation for the impaired interactions with cofactors and RXRα, as well as the reduction in ligand binding, despite the fact that R425 is not in the direct vicinity of the ligand binding pocket. The partial restoration of PPARγ2 R425C activity by the tyrosine-based agonist GW1929 might be explained by the benzophenone group in this type of ligand, which is not present in TZDs. This group can make additional hydrophobic interactions with residues in H3, H7 and H10 (16), which could contribute to the active conformation of the LBD structure and thereby partially restore the activity of PPARγ2 R425C, as was observed specifically with this ligand.

Studies on four other mammalian class II nuclear receptors, vitamin D receptor (VDR), TRβ, RXRα and retinoic acid receptor α (RARα), have pointed to the importance of the conserved salt bridge residues for their function. In keeping with our results on the E352A mutation in PPARγ2, the analogous mutant in VDR (E269A) displayed reduced ligand binding and transcriptional activity (51). Unlike the PPARγ2 R425C mutant, however, mutation of the analogous residue in TRβ, as exemplified by the RTH-associated R383H mutant, did not affect activation of target genes, but resulted in impaired corepressor release (41). Furthermore, the R339A mutation reduced the transcriptional activity of RARα, but heterodimerisation

was unaffected (35), which is in contrast to the analogous PPARγ2 mutant (R425A). Finally, the D384A mutant of RXRα (D424A in PPARγ2) displayed reduced ability to homodimerise, but heterodimerisation with RARα was unaffected (52). These findings therefore clearly underscore the important role of the internal salt bridges in maintaining the structural integrity of the LBDs of class II receptors, but also show that the molecular defect(s) caused by their disruption can differ between individual nuclear receptors.

Although the PPARγ2 R425C mutant displays some similarities with other FPLD3-associated PPARγ mutants, the molecular defects are clearly not identical. Based on functional characterisations in combination with studies on dominant negative activity of these different PPARγ mutants, PPARγ mutations can be divided in at least three different subgroups (29-34;37). The first group comprises the missense DNA binding mutants and ligand binding domain (LBD) truncation mutants (C142R, C159Y, C190W, FS343X, R385X). These mutants have no DNA binding capacity, but are still able to recruit coactivators and can therefore compete for common cofactors ("squelching"), which can explain their dominant negative activity. The second group consists of missense mutations located in the LBD (V318M, P495L), which inhibit PPARγ activity through an alternative mechanism. These mutants are transcriptionally inactive due to impaired ligand and coactivator recruitment, but are able to compete for DNA binding with wild type PPARγ. As a consequence the activation of PPARγ target genes is reduced, which could explain the dominant negative activity of these mutants. The third group, represented by the PPARγ R425C mutant, displays both impaired heterodimerisation with RXRα and subsequent DNA binding, as well as impaired ligand and cofactor binding, the combination of which could account for the absence of dominant negative activity. In line with this, addition of an artificial mutation in TRβ, that attenuated heterodimerisation with RXRα and subsequent DNA binding, abrogated the dominant negative activity of three different natural LBD mutants (53;54). This suggests that the combination of either intact DNA binding together with impaired cofactor binding, or intact cofactor binding in combination with impaired DNA binding is a prerequisite for dominant negative activity of TRβ and PPARγ mutants. Like the R425C mutant analysed here, the FPLD3-associated PPARγ2 F388L mutant (30) and the recently published nonsense mutation, which truncates PPARγ2 after residue 355 (Y355X) (33) also lack dominant negative behaviour. Together with the FPLD3-associated PPARγ4 promoter (-14A>G) mutation (55), which only reduces the expression of the PPARγ protein, these findings indicate that in some FPLD3 patients *PPARG* mutations act through a haploinsufficiency mechanism rather than dominant negative activity of the affected gene product.

When the FPLD3-associated PPARγ P-to-L mutant was tested in the context of the PPARγ1 protein (P467L), this protein inhibited wild type PPARγ1 and -γ2 in a dominant negative fashion at low concentrations of rosiglitazone, as described earlier (37). Interestingly, the same amino acid substitution in the context of the

PPARγ2 protein (P495L) resulted in a protein that lacked this capacity, indicating that at least under our experimental conditions the dominant negative activity of the PPARγ P-to-L mutant is isoform specific. These findings suggest that the effect of dominant negative PPARγ mutants might be more pronounced in tissues with a high PPARγ1/-γ2 ratio, but it is currently unknown whether this ratio differs between body fat depots. An important challenge for the future will be to establish how heterozygous *PPARG* mutations can lead to depot-specific effects on adipose tissue, as exemplified by the characteristic aberrant fat distribution in patients suffering from FPLD3 and mice expressing PPARγ mutants (56;57).

Acknowledgements
We would like to thank Drs. S. Ali, J.D. Baxter, E. Burstein, V.K.K. Chatterjee, R.M Evans, M. Gurnell, N. Maeda, M.G. Parker, B.M. Spiegelman and R.G. Roeder for various plasmid constructs. We would also like to thank Drs. J.M. Stephens, G.E. Folkers, P. Muller and M. Agostini for helpful suggestions and Drs. D.A. Baker, P.J. Coffer, L.W. Klomp and M.G. Parker for critical reading of the manuscript. This work was supported by a fellowship from the Royal Netherlands Academy of Arts and Sciences (E.K.) and by a "Jonge Chemici" grant (grant number 700.50.512) from the Netherlands Organization for Scientific Research to A.M.J.J.B.

References

1. Friedman JM 2003 A war on obesity, not the obese. Science 299:856-858
2. Simha V, Garg A 2006 Lipodystrophy: lessons in lipid and energy metabolism. Curr Opin Lipidol 17:162-169
3. Capeau J, Magre J, Lascols O, Caron M, Bereziat V, Vigouroux C, Bastard JP 2005 Diseases of adipose tissue: genetic and acquired lipodystrophies. Biochem Soc Trans 33:1073-1077
4. Garg A 2004 Acquired and inherited lipodystrophies. N Engl J Med 350:1220-1234
5. Nolan D, Mallal S 2004 Complications associated with NRTI therapy: update on clinical features and possible pathogenic mechanisms. Antivir Ther 9:849-863
6. Semple RK, Chatterjee VK, O'Rahilly S 2006 PPAR gamma and human metabolic disease. J Clin Invest 116:581-589
7. Hegele RA 2005 Lessons from human mutations in PPARγamma. Int J Obes (Lond) 29 Suppl 1: S31-5.:S31-S35
8. Willson TM, Brown PJ, Sternbach DD, Henke BR 2000 The PPARs: from orphan receptors to drug discovery. J Med Chem 43:527-550
9. Lehrke M, Lazar MA 2005 The many faces of PPARγamma. Cell 123:993-999
10. Feige JN, Gelman L, Michalik L, Desvergne B, Wahli W 2006 From molecular action to physiological outputs: peroxisome proliferator-activated receptors are nuclear receptors at the crossroads of key cellular functions. Prog Lipid Res 45:120-159
11. Tontonoz P, Hu E, Spiegelman BM 1994 Stimulation of adipogenesis in fibroblasts by PPAR gamma 2, a lipid-activated transcription factor. Cell 79:1147-1156
12. Barak Y, Nelson MC, Ong ES, Jones YZ, Ruiz-Lozano P, Chien KR, Koder A, Evans RM 1999 PPAR gamma is required for placental, cardiac, and adipose tissue development. Mol Cell 4:585-595
13. Kubota N, Terauchi Y, Miki H, Tamemoto H, Yamauchi T, Komeda K, Satoh S, Nakano R, Ishii C, Sugiyama T, Eto K, Tsubamoto Y, Okuno A, Murakami K, Sekihara H, Hasegawa G, Naito M, Toyoshima Y, Tanaka S, Shiota K, Kitamura T, Fujita T, Ezaki O, Aizawa S, Kadowaki T, . 1999 PPAR gamma mediates high-fat diet-induced adipocyte hypertrophy and insulin resistance. Mol Cell 4:597-609
14. Rosen ED, Sarraf P, Troy AE, Bradwin G, Moore K, Milstone DS, Spiegelman BM, Mortensen RM 1999 PPAR gamma is required for the differentiation of adipose tissue in vivo and in vitro. Mol Cell 4:611-617
15. Evans RM, Barish GD, Wang YX 2004 PPARs and the complex journey to obesity. Nat Med 10:355-361
16. Gampe RT, Jr., Montana VG, Lambert MH, Miller AB, Bledsoe RK, Milburn MV, Kliewer SA, Willson TM, Xu HE 2000 Asymmetry in the PPARγamma/RXRalpha crystal structure reveals the molecular basis of heterodimerization among nuclear receptors. Mol Cell 5:545-555
17. Nolte RT, Wisely GB, Westin S, Cobb JE, Lambert MH, Kurokawa R, Rosenfeld MG, Willson TM, Glass CK, Milburn MV 1998 Ligand binding and co-activator assembly of the peroxisome proliferator-activated receptor-gamma. Nature 395:137-143
18. Yu C, Markan K, Temple KA, Deplewski D, Brady MJ, Cohen RN 2005 The nuclear receptor corepressors NCoR and SMRT decrease peroxisome proliferator-activated receptor gamma transcriptional activity and repress 3T3-L1 adipogenesis. J Biol Chem 280:13600-13605
19. Guan HP, Ishizuka T, Chui PC, Lehrke M, Lazar MA 2005 Corepressors selectively control the transcriptional activity of PPARγamma in adipocytes. Genes Dev 19:453-461
20. Chui PC, Guan HP, Lehrke M, Lazar MA 2005 PPARγamma regulates adipocyte cholesterol metabolism via oxidized LDL receptor 1. J Clin Invest 115:2244-2256
21. Westin S, Kurokawa R, Nolte RT, Wisely GB, McInerney EM, Rose DW, Milburn MV, Rosenfeld MG, Glass CK 1998 Interactions controlling the assembly of nuclear-receptor heterodimers and co-activators. Nature 395:199-202
22. Perissi V, Rosenfeld MG 2005 Controlling nuclear receptors: the circular logic of cofactor cycles. Nat Rev Mol Cell Biol 6:542-554
23. Forman BM, Tontonoz P, Chen J, Brun RP, Spiegelman BM, Evans RM 1995 15-Deoxy-delta 12, 14-

prostaglandin J2 is a ligand for the adipocyte determination factor PPAR gamma. Cell 83:803-812
24. Krey G, Braissant O, L'Horset F, Kalkhoven E, Perroud M, Parker MG, Wahli W 1997 Fatty acids, eicosanoids, and hypolipidemic agents identified as ligands of peroxisome proliferator-activated receptors by coactivator-dependent receptor ligand assay. Mol Endocrinol 11:779-791
25. Lehmann JM, Moore LB, Smith-Oliver TA, Wilkison WO, Willson TM, Kliewer SA 1995 An antidiabetic thiazolidinedione is a high affinity ligand for peroxisome proliferator-activated receptor gamma (PPAR gamma). J Biol Chem 270:12953-12956
26. Henke BR, Blanchard SG, Brackeen MF, Brown KK, Cobb JE, Collins JL, Harrington WW, Jr., Hashim MA, Hull-Ryde EA, Kaldor I, Kliewer SA, Lake DH, Leesnitzer LM, Lehmann JM, Lenhard JM, Orband-Miller LA, Miller JF, Mook RA, Jr., Noble SA, Oliver W, Jr., Parks DJ, Plunket KD, Szewczyk JR, Willson TM 1998 N-(2-Benzoylphenyl)-L-tyrosine PPARγamma agonists. 1. Discovery of a novel series of potent antihyperglycemic and antihyperlipidemic agents. J Med Chem 41:5020-5036
27. Sethi JK, Hotamisligil GS 1999 The role of TNF alpha in adipocyte metabolism. Semin Cell Dev Biol 10:19-29
28. Ruan H, Lodish HF 2003 Insulin resistance in adipose tissue: direct and indirect effects of tumor necrosis factor-alpha. Cytokine Growth Factor Rev 14:447-455
29. Barroso I, Gurnell M, Crowley VE, Agostini M, Schwabe JW, Soos MA, Maslen GL, Williams TD, Lewis H, Schafer AJ, Chatterjee VK, O'Rahilly S 1999 Dominant negative mutations in human PPARγamma associated with severe insulin resistance, diabetes mellitus and hypertension. Nature 402:880-883
30. Hegele RA, Cao H, Frankowski C, Mathews ST, Leff T 2002 PPARγ F388L, a transactivation-deficient mutant, in familial partial lipodystrophy. Diabetes 51:3586-3590
31. Agarwal AK, Garg A 2002 A novel heterozygous mutation in peroxisome proliferator-activated receptor-gamma gene in a patient with familial partial lipodystrophy. J Clin Endocrinol Metab 87:408-411
32. Agostini M, Schoenmakers E, Mitchell C, Szatmari I, Savage D, Smith A, Rajanayagam O, Semple R, Luan J, Bath L, Zalin A, Labib M, Kumar S, Simpson H, Blom D, Marais D, Schwabe J, Barroso I, Trembath R, Wareham N, Nagy L, Gurnell M, O'Rahilly S, Chatterjee K 2006 Non-DNA binding, dominant-negative, human PPARγamma mutations cause lipodystrophic insulin resistance. Cell Metab 4:303-311
33. Francis GA, Li G, Casey R, Wang J, Cao H, Leff T, Hegele RA 2006 Peroxisomal proliferator activated receptor-gamma deficiency in a Canadian kindred with familial partial lipodystrophy type 3 (FPLD3). BMC Med Genet 7:3.:3
34. Savage DB, Agostini M, Barroso I, Gurnell M, Luan J, Meirhaeghe A, Harding AH, Ihrke G, Rajanayagam O, Soos MA, George S, Berger D, Thomas EL, Bell JD, Meeran K, Ross RJ, Vidal-Puig A, Wareham NJ, O'Rahilly S, Chatterjee VK, Schafer AJ 2002 Digenic inheritance of severe insulin resistance in a human pedigree. Nat Genet 31:379-384
35. Brelivet Y, Kammerer S, Rochel N, Poch O, Moras D 2004 Signature of the oligomeric behaviour of nuclear receptors at the sequence and structural level. EMBO Rep 5:423-429
36. Tugwood JD, Issemann I, Anderson RG, Bundell KR, McPheat WL, Green S 1992 The mouse peroxisome proliferator activated receptor recognizes a response element in the 5′ flanking sequence of the rat acyl CoA oxidase gene. EMBO J 11:433-439
37. Agostini M, Gurnell M, Savage DB, Wood EM, Smith AG, Rajanayagam O, Garnes KT, Levinson SH, Xu HE, Schwabe JW, Willson TM, O'Rahilly S, Chatterjee VK 2004 Tyrosine agonists reverse the molecular defects associated with dominant-negative mutations in human peroxisome proliferator-activated receptor gamma. Endocrinology 145:1527-1538
38. Kondo H, Shimomura I, Kishida K, Kuriyama H, Makino Y, Nishizawa H, Matsuda M, Maeda N, Nagaretani H, Kihara S, Kurachi Y, Nakamura T, Funahashi T, Matsuzawa Y 2002 Human aquaporin adipose (AQPap) gene. Genomic structure, promoter analysis and functional mutation. Eur J Biochem 269:1814-1826
39. Molnar F, Matilainen M, Carlberg C 2005 Structural determinants of the agonist-independent association of human peroxisome proliferator-activated receptors with coactivators. J Biol Chem

280:26543-26556
40. Yen PM 2003 Molecular basis of resistance to thyroid hormone. Trends Endocrinol Metab 14:327-333
41. Clifton-Bligh RJ, de Zegher F, Wagner RL, Collingwood TN, Francois I, Van Helvoirt M, Fletterick RJ, Chatterjee VK 1998 A novel TR beta mutation (R383H) in resistance to thyroid hormone syndrome predominantly impairs corepressor release and negative transcriptional regulation. Mol Endocrinol 12:609-621
42. Fawell SE, Lees JA, White R, Parker MG 1990 Characterization and colocalization of steroid binding and dimerization activities in the mouse estrogen receptor. Cell 60:953-962
43. Chen S, Johnson BA, Li Y, Aster S, McKeever B, Mosley R, Moller DE, Zhou G 2000 Both coactivator LXXLL motif-dependent and -independent interactions are required for peroxisome proliferator-activated receptor gamma (PPARγamma) function. J Biol Chem 275:3733-3736
44. Schulman IG, Shao G, Heyman RA 1998 Transactivation by retinoid X receptor-peroxisome proliferator-activated receptor gamma (PPARγamma) heterodimers: intermolecular synergy requires only the PPARγamma hormone-dependent activation function. Mol Cell Biol 18:3483-3494
45. Gelman L, Zhou G, Fajas L, Raspe E, Fruchart JC, Auwerx J 1999 p300 interacts with the N- and C-terminal part of PPARγamma2 in a ligand-independent and -dependent manner, respectively. J Biol Chem 274:7681-7688
46. Heck S, Bender K, Kullmann M, Gottlicher M, Herrlich P, Cato AC 1997 I kappaB alpha-independent downregulation of NF-kappaB activity by glucocorticoid receptor. EMBO J 16:4698-4707
47. Suzawa M, Takada I, Yanagisawa J, Ohtake F, Ogawa S, Yamauchi T, Kadowaki T, Takeuchi Y, Shibuya H, Gotoh Y, Matsumoto K, Kato S 2003 Cytokines suppress adipogenesis and PPAR-gamma function through the TAK1/TAB1/NIK cascade. Nat Cell Biol 5:224-230
48. Gurnell M, Wentworth JM, Agostini M, Adams M, Collingwood TN, Provenzano C, Browne PO, Rajanayagam O, Burris TP, Schwabe JW, Lazar MA, Chatterjee VK 2000 A dominant-negative peroxisome proliferator-activated receptor gamma (PPARγamma) mutant is a constitutive repressor and inhibits PPARγamma-mediated adipogenesis. J Biol Chem 275:5754-5759
49. Pascual G, Fong AL, Ogawa S, Gamliel A, Li AC, Perissi V, Rose DW, Willson TM, Rosenfeld MG, Glass CK 2005 A SUMOylation-dependent pathway mediates transrepression of inflammatory response genes by PPAR-gamma. Nature 437:759-763
50. Xu HE, Stanley TB, Montana VG, Lambert MH, Shearer BG, Cobb JE, McKee DD, Galardi CM, Plunket KD, Nolte RT, Parks DJ, Moore JT, Kliewer SA, Willson TM, Stimmel JB 2002 Structural basis for antagonist-mediated recruitment of nuclear co-repressors by PPARαlpha. Nature 415:813-817
51. Vaisanen S, Duchier C, Rouvinen J, Maenpaa PH 1999 The importance of the putative helices 4 and 5 of human vitamin D(3) receptor for conformation and ligand binding. Biochem Biophys Res Commun 264:478-482
52. Vivat-Hannah V, Bourguet W, Gottardis M, Gronemeyer H 2003 Separation of retinoid X receptor homo- and heterodimerization functions. Mol Cell Biol 23:7678-7688
53. Collingwood TN, Adams M, Tone Y, Chatterjee VK 1994 Spectrum of transcriptional, dimerization, and dominant negative properties of twenty different mutant thyroid hormone beta-receptors in thyroid hormone resistance syndrome. Mol Endocrinol 8:1262-1277
54. Nagaya T, Jameson JL 1993 Thyroid hormone receptor dimerization is required for dominant negative inhibition by mutations that cause thyroid hormone resistance. J Biol Chem 268:15766-15771
55. Al Shali K, Cao H, Knoers N, Hermus AR, Tack CJ, Hegele RA 2004 A single-base mutation in the peroxisome proliferator-activated receptor gamma4 promoter associated with altered *in vitro* expression and partial lipodystrophy. J Clin Endocrinol Metab 89:5655-5660
56. Tsai YS, Maeda N 2005 PPARγamma: a critical determinant of body fat distribution in humans and mice. Trends Cardiovasc Med 15:81-85
57. Gray SL, Dalla NE, Vidal-Puig AJ 2005 Mouse models of PPAR-gamma deficiency: dissecting PPAR-gamma's role in metabolic homoeostasis. Biochem Soc Trans 33:1053-1058

58. Ausubel FM, Brent R, Kingston R, Moore D, Seidman JJ, Smith J, Struhl K 1993 Current Protocols in Molecular Biology. New York: John Wiley & Sons
59. Burstein E, Hoberg JE, Wilkinson AS, Rumble JM, Csomos RA, Komarck CM, Maine GN, Wilkinson JC, Mayo MW, Duckett CS 2005 COMMD proteins, a novel family of structural and functional homologs of MURR1. J Biol Chem 280:22222-22232
60. Ge K, Guermah M, Yuan CX, Ito M, Wallberg AE, Spiegelman BM, Roeder RG 2002 Transcription coactivator TRAP220 is required for PPAR gamma 2-stimulated adipogenesis. Nature 417:563-567
61. Chen JD, Evans RM 1995 A transcriptional co-repressor that interacts with nuclear hormone receptors. Nature 377:454-457
62. Kalkhoven E, Valentine JE, Heery DM, Parker MG 1998 Isoforms of steroid receptor co-activator 1 differ in their ability to potentiate transcription by the oestrogen receptor. EMBO J 17:232-243
63. Wissink S, van Heerde EC, Schmitz ML, Kalkhoven E, van der BB, Baeuerle PA, van der Saag PT 1997 Distinct domains of the RelA NF-kappaB subunit are required for negative cross-talk and direct interaction with the glucocorticoid receptor. J Biol Chem 272:22278-22284
64. Kalkhoven E, Teunissen H, Houweling A, Verrijzer CP, Zantema A 2002 The PHD type zinc finger is an integral part of the CBP acetyltransferase domain. Mol Cell Biol 22:1961-1970
65. Ribeiro RC, Feng W, Wagner RL, Costa CH, Pereira AC, Apriletti JW, Fletterick RJ, Baxter JD 2001 Definition of the surface in the thyroid hormone receptor ligand binding domain for association as homodimers and heterodimers with retinoid X receptor. J Biol Chem 276:14987-14995
66. Butler AJ, Parker MG 1995 COUP-TF II homodimers are formed in preference to heterodimers with RXR alpha or TR beta in intact cells. Nucleic Acids Res 23:4143-4150
67. van der BB, Rutteman GR, Blankenstein MA, de Laat SW, van Zoelen EJ 1988 Mitogenic stimulation of human breast cancer cells in a growth factor-defined medium: synergistic action of insulin and estrogen. J Cell Physiol 134:101-108
68. Adams M, Matthews C, Collingwood TN, Tone Y, Beck-Peccoz P, Chatterjee KK 1994 Genetic analysis of 29 kindreds with generalized and pituitary resistance to thyroid hormone. Identification of thirteen novel mutations in the thyroid hormone receptor beta gene. J Clin Invest 94:506-515
69. Vandesompele J, De Preter K, Pattyn F, Poppe B, Van Roy N, De Paepe A, Speleman F 2002 Accurate normalization of real-time quantitative RT-PCR data by geometric averaging of multiple internal control genes. Genome Biol 3:RESEARCH0034
70. Lindahl E, Hess B, van der Spoel D 2001 GROMACS 3.0: a package for molecular simulation and trajectory analysis. J Mol Model 7:306-317
71. Berendsen HJC, Vanderspoel D, Vandrunen R 1995 Gromacs - A Message-Passing Parallel Molecular-Dynamics Implementation. Comput Phys Commun 91:43-56
72. Daura X, Jaun B, Seebach D, van Gunsteren WF, Mark AE 1998 Reversible peptide folding in solution by molecular dynamics simulation. J Mol Biol 280:925-932
73. Berman HM, Westbrook J, Feng Z, Gilliland G, Bhat TN, Weissig H, Shindyalov IN, Bourne PE 2000 The Protein Data Bank. Nucleic Acids Res 28:235-242
74. Berendsen HJC, Postma JPM, van Gunsteren WF 1981 Interaction models for water in relation to protein hydration.; 331-342
75. Berendsen HJC, Postma JPM, van Gunsteren WF, DiNola A, Haak JR 1984 Molecular dynamics with coupling to an external bath. 81 ed.; 3684-3690
76. Hess B, Bekker H, Berendsen HJC, Fraaije JGEM 1997 LINCS: A linear constraint solver for molecular simulations. J Comput Chem 18:1463-1472
77. Vangunsteren WF, Berendsen HJC 1990 Computer-Simulation of Molecular-Dynamics - Methodology, Applications, and Perspectives in Chemistry. Angewandte Chemie-International Edition in English 29:992-1023
78. Tironi IG, Sperb R, Smith PE, Vangunsteren WF 1995 A Generalized Reaction Field Method for Molecular-Dynamics Simulations. J Chem Phys 102:5451-5459
79. Kraulis PJ 1991 Molscript - A Program to Produce Both Detailed and Schematic Plots of Protein Structures. J Appl Crystallogr 24:946-950
80. Merritt EA, Murphy MEP 1994 Raster3D Version-2.0 - A Program for Photorealistic Molecular Graphics. Acta Crystallogr D 50:869-873

Supplemental Figures

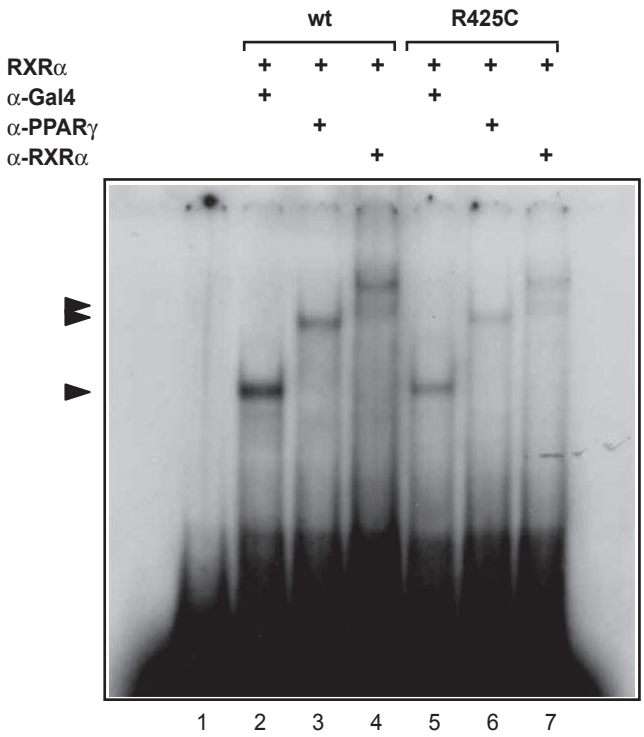

Supplementary Figure S1.
In vitro translated RXRα or PPARγ2 (wt or mutant) proteins were incubated with [32P]-labelled probe in the presence of antibodies against PPARγ or RXRα, or an irrelevant antibody (α-Gal4) as indicated. Protein-DNA complexes were separated from unbound DNA on non-denaturing SDS-polyacrylamide gels and visualized by autoradiography of dried gels. Note that both antibodies (α-PPARγ and α-RXRα) can supershift the protein-DNA complexes, confirming the heterodimeric composition of the complexes.

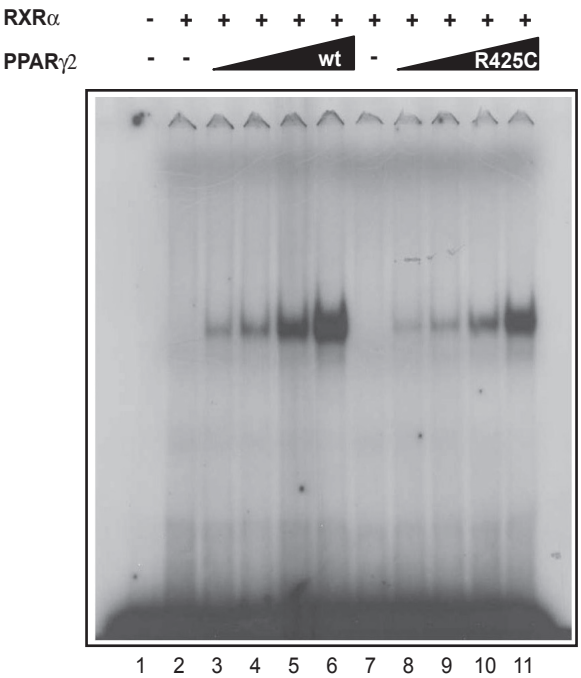

Supplementary Figure S2.
Increasing amounts of *in vitro* translated RXRα or PPARγ2 (wt or mutant) proteins were incubated with [32P]-labelled probe as indicated. Protein-DNA complexes were separated from unbound DNA on non-denaturing SDS-polyacrylamide gels and visualized by autoradiography of dried gels. PPARγ2 R425C displyas reduced DNA binding compared to wild type PPARγ2, independent of the concentration of PPARγ2 protein (either wild type or mutant).

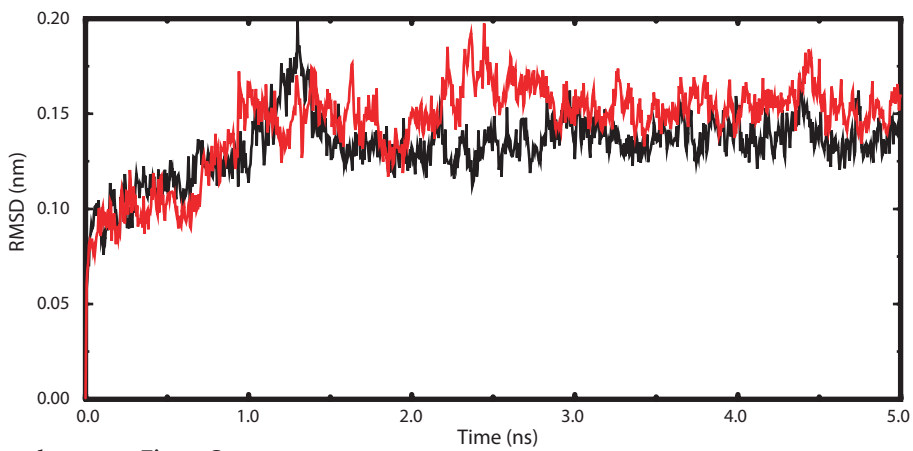

Supplementary Figure S3.
Positional root mean-square deviation (RMSD) of structures from the respective starting structure versus simulation time. The RMSD values of the secondary structure elements subjected to least-squares superposition of backbone atoms are shown for the wild type (black line) and Cys mutant (red line) MD simulations (starting from crystal structure 1FM6 chain D). Note that the RMSD values reach a plateau after approximately 1 ns which indicates that the systems are stable within the timeframe of the simulation.

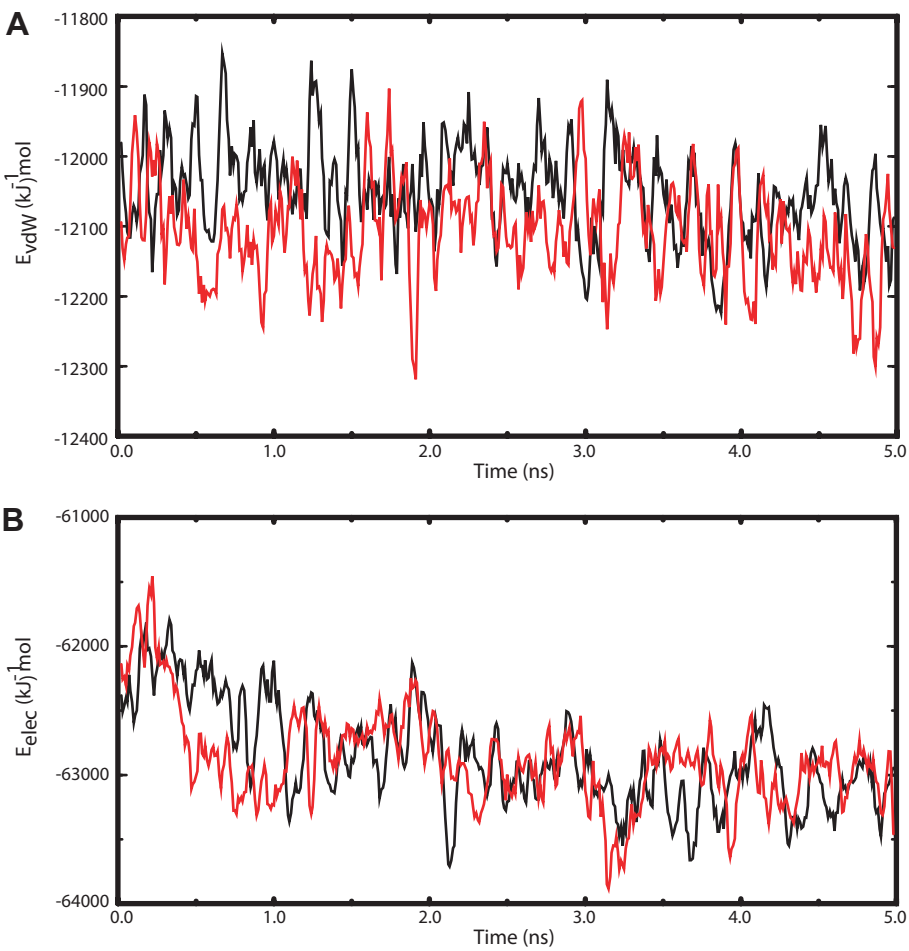

Supplementary Figure S4.
Non-bonded energies (sum of protein-protein and protein-solvent energy terms) versus simulation time. Van der Waals energy (A) and Coulomb energy (B) are shown for the wild type (black line) and Cys mutant (red line) simulation (starting from crystal structure 1FM6 chain D); these values were smoothed for clarity using a 0.05-ns averaging window. Note that the electrostatic energies reach a plateau after 1 to 2 ns which indicates that the systems have reached an equilibrium and are stable within the timeframe of the simulation.

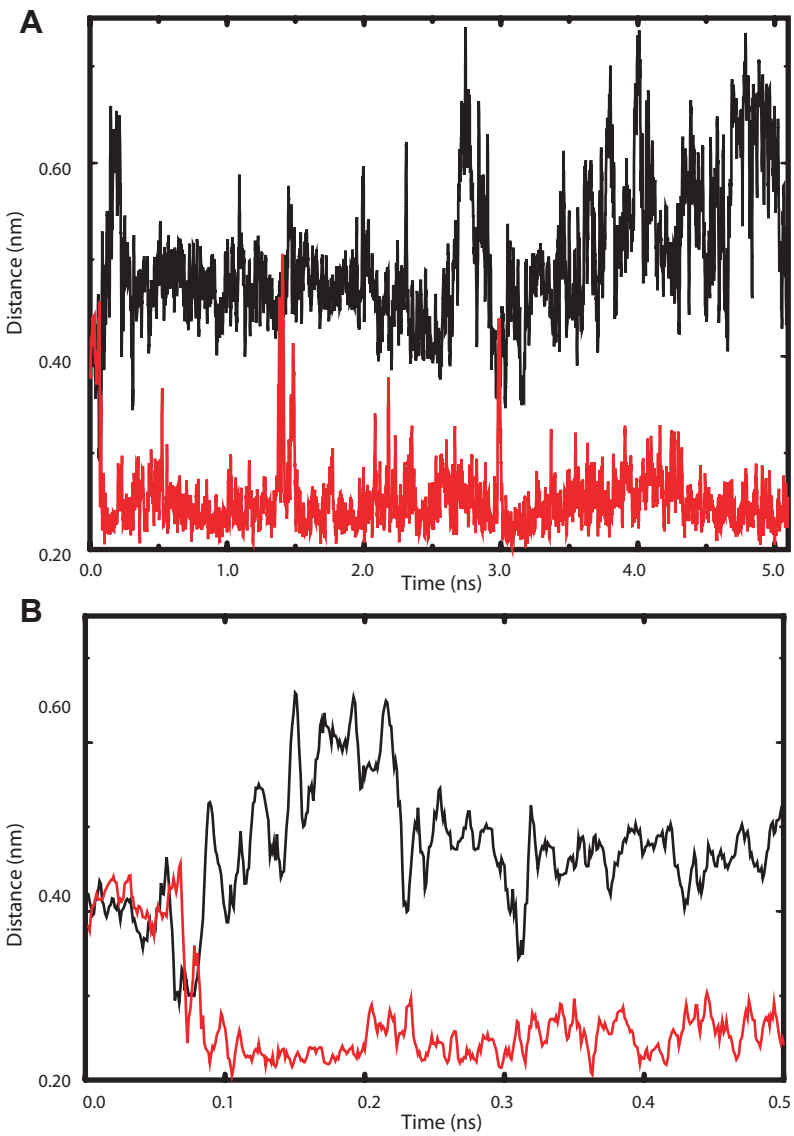

Supplementary Figure S5.
Alternative salt bridge formation in PPARγ R425C. Minimum distance between R471 guanidinium and E352 carboxylate groups is shown for wildtype (black line) and Cys mutant (red line) MD simulation (starting from crystal structure 1FM6 chain D). (A) Complete simulation (0.1 ns equilibration and 5.0 ns simulation). (B) Detailed view of the first 500 ps which shows that the salt bridge switch occurs during the first 100 ps. Distance values were smoothed for clarity using a 0.05-ns averaging window. In the R425C mutant, the carboxylate group of E352 can no longer hydrogen bond to the side chain of residue 425; instead a conformational switch is observed after ~ 0.08 ns leading to the formation of a stable hydrogen bond between the guanidinium group of R471 and the carobxylate group of E352.

Chapter 4

Familial partial lipodystrophy phenotype resulting from a single-base mutation in DNA binding domain of peroxisome proliferator-activated receptor gamma

Houshang Monajemi[1], Lin Zhang[2*], Gang Li[2*], Ellen H. Jeninga[3*], Henian Cao[4], Mario Maas[5], C.B. Brouwer[6], Eric Kalkhoven[3], Erik Stroes[1], Robert A. Hegele[4], Todd Leff[2]

[1]Department of vascular medicine, and [5]radiology, Academic Medical Center, Amsterdam, The Netherlands; [2]Department of Pathology, Center for Integrative Metabolic & Endocrine Research, Wayne State University School of Medicine, Detroit, Michigan, USA; [3]Department of Metabolic and Endocrine Diseases, UMC Utrecht, The Netherlands; [4]Robarts Research Institute and Schulich School of Medicine, London, Ontario, Canada; [6]Department of Internal Medicine, Onze Lieve Vrouwe Gasthuis, Amsterdam, The Netherlands

Journal of Clinical Endocrinology & Metabolism 2007: 92(5):1606-12

Abstract

Context: Familial partial lipodystrophy (FPLD) results from coding sequence mutations either in LMNA, encoding nuclear lamin A/C, or in *PPARG*, encoding peroxisome proliferator-activated receptor gamma (PPARγ). The LMNA form is called FPLD2 (MIM 151660) and the PPARG form is called FPLD3 (MIM 604367).
Objective: To investigate whether the clinical phenotype of this proband is due to mutation(s) in PPARγ.
Design: Case report
Setting: Academic medical center
Patient: A 31-yr-old female with the clinical phenotype of FPLD3; i.e lipodystrophy and early childhood diabetes with extreme insulin resistance and hypertriglyceridemia leading to recurrent pancreatitis.
Results: The proband was heterozygous for a novel C>T mutation in PPARG gene that led to the substitution of arginine 194 in PPARγ2 isoform, a conserved residue located in the zinc finger structure involved in DNA binding, by tryptophan (R194W). The mutation was absent from the genomes of 100 healthy Caucasians. In vitro analysis of the mutated protein showed that R194W (and R166W in PPARγ1 isoform) could not bind to DNA and had no transcriptional activity. Furthermore, R194W had no dominant negative activity.
Conclusions: The R194W mutation in PPARG disrupts its DNA binding activity and through haploinsufficiency leads to clinical manifestation of FPLD3 and the associated metabolic disturbances.

Introduction

Dunnigan-type familial partial lipodystrophy results from rare coding sequence mutations either in *LMNA*, encoding nuclear lamin A/C, or in *PPARG*, encoding peroxisome proliferator-activated receptor gamma (PPARγ) (1;2). The *LMNA* and *PPARG* forms are called FPLD2 (MIM 151660) and FPLD3 (MIM 604367), respectively. These mutations underlie profound redistribution of fat stores, characterized by lipoatrophy of the extremities and gluteal region in combination with lipohypertrophy in face, neck, trunk and central adipose stores. This redistribution can be accompanied by a variety of clinical characteristics, including severe insulin resistance, often with acanthosis nigricans, and hypertriglyceridemia, sometimes associated with pancreatitis and eruptive xanthomata (3). The core clinical phenotype is fat loss with subsequent development of secondary metabolic disturbances that are characteristic of the insulin resistance syndrome.
The presence of lipodystrophy in subjects with dysfunctional *PPARG* missense mutations, such as R425C, F388L, E138fsDAATG, V290M, P467L and Y355X (4-9) and in PPARγ-deficient murine models (10;11) has confirmed the central role of PPARγ in adipogenesis. PPARγ interacts with retinoid X receptor (RXR), binds DNA as a heterodimer and subsequently regulates transcription of PPARγ-responsive genes. Heterozygous loss of function or haploinsufficiency is clinically important when gene dosage is strictly regulated. Here, we show that a heterozygous mutation of a conserved arginine residue into tryptophan in the PPARγ (referred as R166W in PPARγ1 and R194W in PPARγ2 isoform) zinc finger II region disrupts DNA binding and transcriptional activity and thus underlies FPLD3.

Methods

Study subject
The study was approved by the University of Western Ontario Ethics Review Panel (protocol 07920E) and the subject gave informed consent to participate.

Magnetic Resonance Imaging
MRI was performed using a 1.5 Tesla scanner (Signa, GE Medical Systems, Milwalkee, WI, USA) with a neck coil and body coil. Axial and sagittal T1 weighted images of the c-Spine, Axial T1 weighted images of the abdomen and the lower leg were acquired according to the procedure described earlier.

DNA sequence analysis
After DNA sequencing showed no mutation in *LMNA*, we amplified and sequenced the 6 exons of *PPARG* plus >100 bp at intron-exon boundaries and

~700 bp of the promoter (5;7). The R194W mutation was genotyped by scoring the electropherogram tracing of exon 4 sequences from the Applied Biosystems 3730 Automated DNA Sequence Analyser (ABI, Mississauga, ON). Genomic DNA from 100 healthy Caucasian subjects was studied, permitting 70% power to exclude a mutation with frequency >2% in the healthy population (two-tailed alpha<0.05).

PPARgamma clones
A cDNA encoding full length human PPARγ1 was cloned into the pTRE-shuttle2 eukaryotic expression vector (Clontech, Palo Alto, CA). A double-FLAG epitope tag (MDYKDHDGDYKDHD) was added to the N-terminus of the clone. The pCDNA3-PPARγ1 and pCDNA3-PPARγ2 constructs were kind gifts from Dr. V.K.K. Chatterjee. The R194W mutation was introduced using the QuickChange Site-Directed Mutagenesis Kit (Stratagene, La Jolla, CA) and verified by sequencing.

Electrophoretic mobility shift assays (EMSA)
EMSA experiments were performed as described (12). In short, a radiolabelled double-stranded DNA oligomer, containing the PPRE from the rat acyltransferase-coenzyme A oxidase promoter, was incubated with *in vitro* translated PPARγ (wild type or mutants) and/or *in vitro* translated RXRα proteins. For supershift experiments 1 μg of α-RXR (sc-553; Santa Cruz Biotechnologies), α-PPARγ (sc-7273) or α-Gal4 (sc-510) antibodies were added. Receptor-DNA complexes were separated from unbound DNA on native gels and visualized by autoradiography. At least three independent experiments were performed. The complete probe sequences used for binding and competition analysis were as follows: PPRE-wild-type, 5′-CCGGGGACCAGGACAAAGGTCACGAAGCT-3′ and PPRE-mutant, 5′-CCGGGGGACCAGCACAAAGCACACGAAGCT-3′. Western blot analyses of the different in vitro translated PPARγ proteins was performed as described (13). α-PPARγ antibody (sc-7196) was used to probe for PPARγ protein and ECL (Amersham Biosciences) was used for detection.

Cell culture, reporter assays and dominant negative assays
NIH 3T3 mouse fibroblasts and human U2OS osteosarcoma cells were maintained in DMEM Glutamax (Dulbecco) containing 10% foetal calf serum (Gibco Life Technologies), 100 μg of penicillin/ml and 100 μg streptomycin/ml (Gibco Life Technologies). NIH 3T3 mouse fibroblasts were grown in 24-well plates (1.0×10^5 cells/well) in DMEM+10% fetal calf serum. Cells were transfected with 25 ng WT or R194W expression plasmid, 6 ng of pTET-off, 25 ng of pRXR, 2 ng of a β-galactosidase control plasmid and 200 ng of the PPAR-dependent luciferase reporter pFATP-Luc (i.e. three copies of the mouse FATP gene PPRE inserted upstream of the minimal thymidine kinase promoter). Cells were transfected for 4 h with Lipofectamine-plus and then treated with DMSO or increasing doses of rosiglitazone for 16 h. Transfections were performed in triplicate. Mixing experiments examining

dominant negative activity (Fig. 4E) were conducted as described above except with the amounts of PPARγ plasmids: NIH 3T3 cells that were transfected with the combination of 5 ng of WT PPARγ and increasing amounts of WT, the R194W mutant, or the dominant-negative mutant P467L (5, 10, or 20 ng; indicated in the figure as 1:1, 1:2 and 1:4 respectively), in the presence or absence of rosiglitazone (Fig. 4E and 4F).

U2OS were also seeded in 24-wells plates and transiently transfected using the calcium-phosphate precipitation method. Each well was cotransfected with 1 μg reporter construct, 10 ng pCDNA-PPARγ expression constructs and 2 ng pCMV-Renilla (Promega). After washing, cells were maintained in medium in presence or absence of rosiglitazone (1 mM) for 24 h. Activities of luciferase plus β-galactosidase (NIH-3T3) or luciferase plus renilla (U2OS) were measured with the Dual-light assay system (ABI, Foster City, CA) or Dual-Luciferase Reporter Assay System (Promega), respectively, using a 96-well luminometer (Berthold Technologies, Bad Wildbad, Germany).

Results

Patient medical history and clinical evaluation

The proband was a 31-yr-old Turkish female living in The Netherlands. Menarche occurred at age 11, followed by regular menstrual cycles. At age 15, she was diagnosed with diabetes with severe insulin resistance. Despite insulin therapy, she developed severe hypertriglyceridemia, with plasma concentration > 50 mmol/L, leading to eruptive xanthomas on her trunk and extremities. At age 17, her menstrual cycle became irregular and her extremities and face developed excessive hair growth, leading to the diagnosis of polycystic ovarian syndrome (PCOS). At age 19, she became pregnant after in vitro fertilization and gave birth to a healthy son. Subsequently, she was hospitalized twice more for pancreatitis at ages 20 and 22. During outpatient follow-up, her insulin dose was increased >300 U per day. At the end of 2005, she was referred to the Academic Medical Center, Amsterdam for management of refractory hypertriglyceridemia despite fibrate and insulin treatment. On examination, she was mildly obese (weight 68 kg; height 167 cm and body mass index [BMI], 25 kg/m^2). Her resting blood pressure was 130/70 mm Hg. She had excess subcutaneous (sc) fat on the face, neck, trunk, and abdomen, with lack of sc fat on the gluteal region and extremities (Figure 1). This was confirmed with magnetic resonance imaging (Figure 2), which showed excessive and relatively symmetrical deposition of sc fat on the face, neck, and upper trunk, with disproportionate depletion of sc fat in the lower body. Furthermore, she had acanthosis nigricans on her feet, axillae and neck. She was also hirsute. Measurements from fasting plasma: glucose 8.8 mmol/L; HbA1c 8.2%:

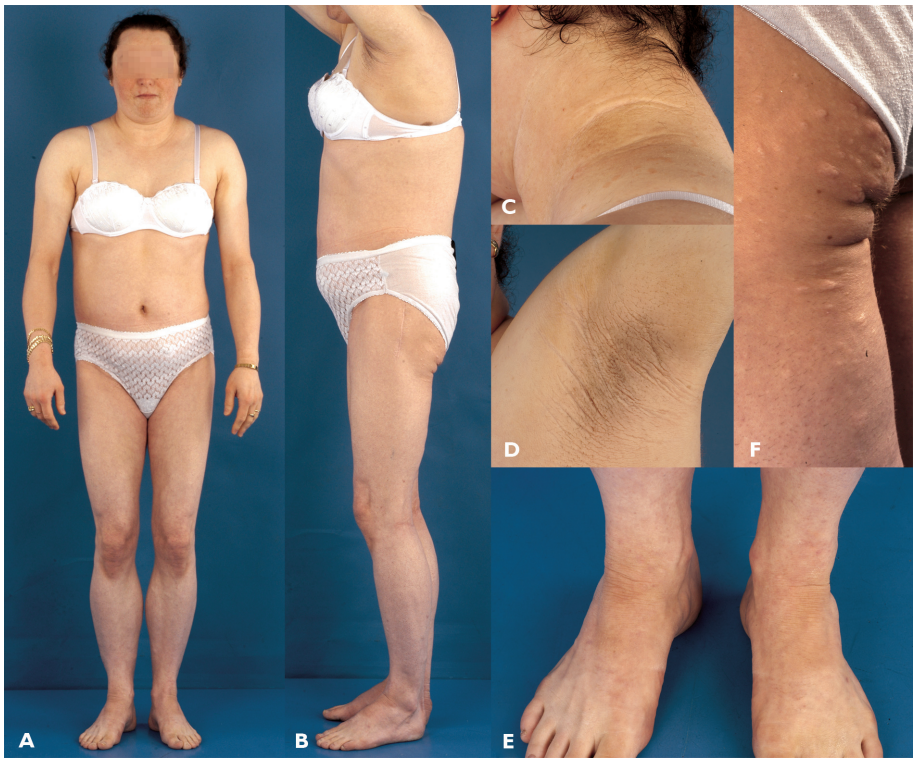

Figure 1. Clinical aspects of the proband.
(A and B) showing the masculine appearance with a clear trunk-sparing lipodystrophy; (C-E), acanthosis nigricans on her neck, axilla and feet; (F), eruptive xanthoma.

insulin 1074 pmol/L (reference 34-172); C-peptide 950 pmol/L (reference 176-664); total cholesterol 9.42 mmol/L; HDL cholesterol 1.33 mmol/L; and triglyceride 35.0 mmol/L. *APOE* genotype was E3/E3. Lipoprotein lipase (LPL) activity was normal and no genomic DNA sequence changes were seen in the *LPL* gene (data not shown). The free androgen index was 134 (normal ratio 0-8). At the time of these measurements, she was being treated with multiple daily insulin injections totaling 300 U/day, ciprofibrate 100 mg and cyproterone 50 mg daily.
Her 53 year-old father had a history of type 2 diabetes and dyslipidemia, but was not lipodystrophic clinically. Her mother died at age 20 from meningitis. The proband's sister, half-sister and two half-brothers were healthy; none had criteria for metabolic syndrome diagnosis. None of the family members were willing to participate in additional clinical or genetic testing.

DNA sequence analysis
In the genome of the proband, we found a heterozygous nucleotide substitution

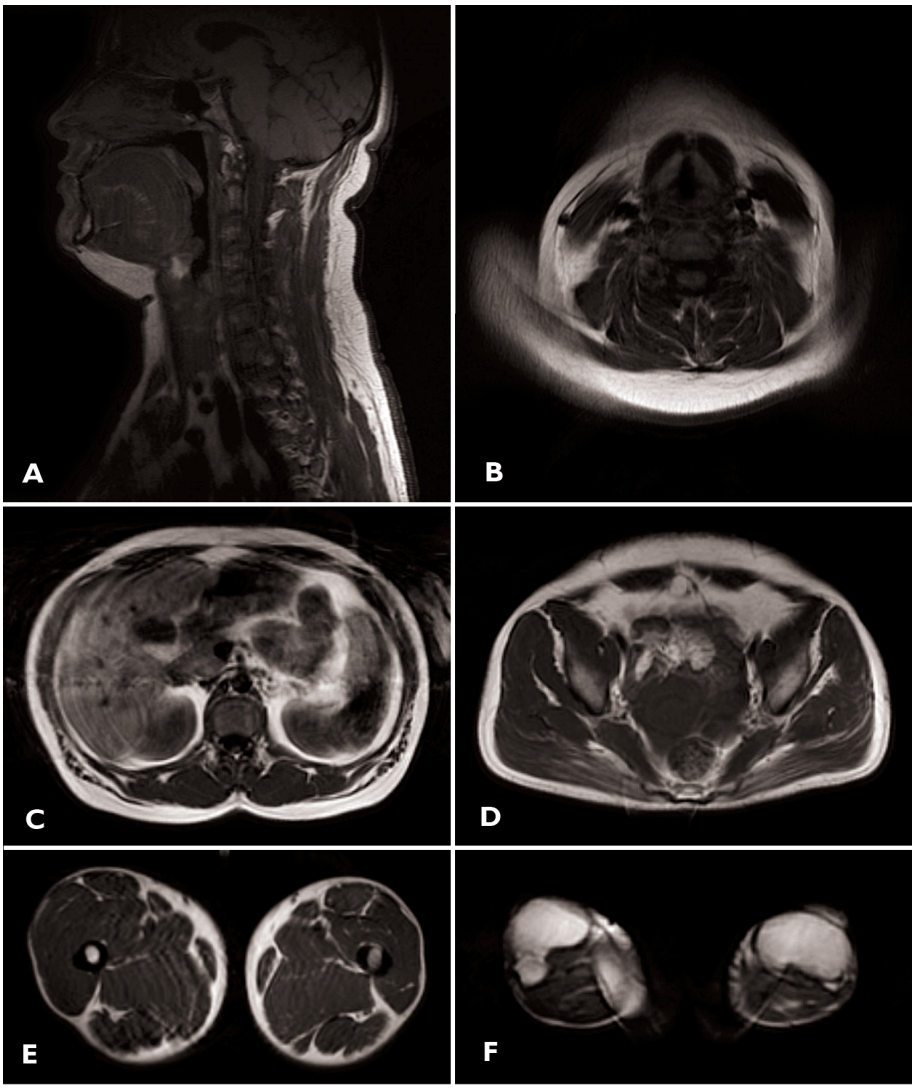

Figure 2. Magnetic resonance imaging (MRI) scans.
T1 weighted images were obtained; (A and B), scans of the neck showing a layer of sc fat measuring 2.52 cm; (C), cross section at the abdomen, showing a symmetrical layer of sc fat measuring 1.09 cm; (D), cross section at the gluteal region, showing sc fat measuring 0.80 cm; (E), cross section at the level of upper leg region, showing a dorsal layer of sc fat measuring 0.64 cm; (F) cross section at the level of lower leg region, showing a dorsal layer of sc fat measuring 0.56 cm.

C>T at position 1762 in the PPARγ isoform 4 (Figure 3). All other regions analysed were free of DNA sequence changes. This mutation was absent from the genomes of 100 normal Caucasian controls. This mutation causes an amino acid substitution R194W in PPARγ isoform 2 (R166W in PPARγ isoform 1).

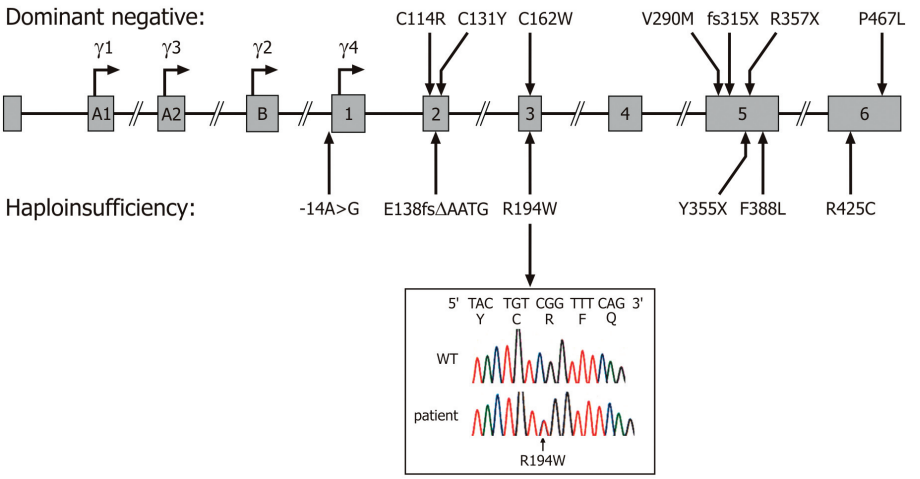

Figure 3. Reported *PPARG* mutations in FPLD3 and genomic DNA sequence electropherograms of heterozygous R194W mutation.
Schematic genomic map of *PPARG*, showing the positions of known mutations, and the disease mechanism indicated. Coding exons are shown with Arabic numerals, while non-coding exons are designated alphabetically. The start of transcription for γ1, γ2, γ3 and γ4 isoforms is shown. The electropherogram tracing shows both alleles from proband (R194W) compared to corresponding genomic DNA sequence from a healthy subject. The position of the mutation is indicated by the arrow. Normal nucleotide and amino acid sequence is shown above the WT electropherogram tracing. Note that the mutation numbers refer to gamma 1 isoform in a few and to gamma 2 isoform in other subjects.

R194W mutant PPARγ does not bind DNA and is transcriptionally inactive

The location of the mutation within the DNA binding domain of PPARγ suggested that it might influence DNA binding. To investigate this possibility, the binding of the R166W as well as R194W mutant to a standard PPRE sequence was assessed using an electrophoretic mobility shift assay (EMSA). While PPARγ wild type in the presence of RXRα was capable of binding to PPARγ response element, the R166W mutant had no detectable DNA binding activity (Figure 4A). As expected, lack of DNA binding was also observed in the PPARγ2 isoform (Figure 4B).

The transcriptional activity of the R194W mutant PPARγ was assessed by transient transfection of PPARγ expression plasmids into NIH 3T3 cells and analysis of luciferase activity from a PPAR responsive reporter. The R194W mutant receptor was inactive at all doses of the ligand rosiglitazone (Figure 4C). In addition, U2OS cells were transfected with PPARγ1 (WT and R166W) or PPARγ2 isoform (WT and R194W). Whereas both WT isoforms had a slight basal expression level that was highly induced by rosiglitazone, both mutant isoforms displayed no transcriptional activity in the absence or presence of exogenous ligand (Figure 4D).

R194W mutant PPARγ displays no dominant-negative activity

To investigate if the R194W receptor had dominant-negative activity against WT PPARγ, a mixing experiment was performed in which an increasing amount of mutant or wild-type receptor were mixed with a fixed amount of WT PPARγ (Figure 4E). While simply increasing the amount of the WT receptor caused a significant increase in transcriptional activity (WT+WT), the addition of increasing amounts of R194W PPARγ to a fixed amount of WT receptor resulted in no change in total PPARg transcriptional activity (WT+R194W). For comparison, the same experiment was conducted with the P467L that has dominant-negative activity(4). Increasing amounts of P467L PPARγ caused a dose-dependent decrease in WT PPARγ transcriptional activity (WT+P467L). When the cells were treated with high concentration of rosiglitazone (Figure 4F), the dominant negative activity of P467L was abolished as described earlier(4). Together, these findings indicate that the R194W mutant does not possess any dominant-negative activity against the WT PPARγ receptor.

Discussion

The principal findings of this study are: 1) association of a novel heterozygous PPARγ missense mutation, R194W (R166W in gamma1 isoform), with FPLD3, including fat redistribution, severe insulin resistance, hypertriglyceridemia, hirsutism and acanthosis nigricans; and 2) functional analysis showing that the R194W mutant is transcriptionally inactive, independent of PPARγ isoform (γ1 and γ2) and cell type (NIH-3T3 and U2OS)

The substitution of a hydrophilic arginine to a hydrophobic tryptophan within an α-helix would predict disrupted structure and decreased DNA binding, as was seen with EMSA. The importance of the conserved arginine residue is underscored by natural mutations in other nuclear receptors causing hormone resistance. For instance, a R614H mutation and deletion of this amino acid (D614) in the androgen receptor (AR) have been reported in two patients with complete androgen insensitivity (14). Furthermore, mutation of the analogous residue (R477H) in the glucocorticoid receptor (GR) was detected in a patient with primary cortisol resistance (15). In addition, mutation of this conserved arginine residue in the photoreceptor-specific nuclear receptor PNR into tryptophan (R104W) (16) or glutamine (R104Q) (17) were found in patients with enhanced S-cone syndrome. DNA binding of the AR D614 and R614H mutants and the GR R477H mutant was impaired (14;15) analogous to the PPARγ R194W mutant, emphasizing the importance of this conserved arginine residue in nuclear receptor signaling.

R194W brings the number of reported *PPARG* mutations associated with clinical phenotypes to fourteen. Only the PPARγ2 P115Q mutation was not associated with

FPLD3 (18). Two PPARγ missense mutations (P467L and V290M), along with the recently published subjects by Agostini et al (C114R, C131Y, C162W, FS315X and R357X) act via a dominant negative mechanism (19), while five (-14A>G, F388L, E138fsDAATG, Y355X and R194W) caused FPLD3 through haploinsufficiency (5;7;20) (Figure 3). The R425C mutation (9) also lacks dominant negative activity (E.H. Jeninga et al., submitted). All patients with *PPARG* haploinsufficiency mutations were ascertained based upon a diagnosis of FPLD; almost every patient with a *PPARG* mutation had partial lipodystrophy as a core phenotype. FPLD3 has proven to be a useful and appropriate clinical designation; the term acknowledges the centrality of lipodystrophy, while concurrently distinguishing FPLD3 from phenotypically similar but molecularly distinct forms of lipodystrophy, such as FPLD2 due to *LMNA* mutations.

Mutations can lead to disease through either i) loss of function; ii) gain of function; or iii) dominant negative activity. According to the "classical" dominant negative hypothesis, the mutant allele eliminates the WT function by direct interference. For instance, in the case of nuclear receptors the mutant receptor competes with the WT for binding DNA. However, there is some evidence that nuclear receptors can also have indirect dominant negative activity by affecting the bioavailability of other components of the transcriptional machinery, such as coactivators, and hence could interfere with the WT allele. We have shown that R194W has neither

Figure 4. *PPARG* R194W mutation is transcriptionally inactive.
A, In vitro translated RXRα and/or PPARγ1 (wt or R166W) proteins were incubated with [^{32}P]-labelled probe in absence or presence of 10X unlabelled probe as indicated. Protein-DNA complexes were separated from unbound DNA on native gels and visualized by autoradiography of dried gels. To analyse the specificity of the binding the same experiment was performed in the presence of antibodies against PPARγ or RXRα, or an irrelevant antibody (α-Gal4) as indicated (the right panel). Expression of the different PPARγ proteins was confirmed by western blot analysis using an antibody directed against PPARγ. B, Competition and supershift EMSA as described in (A) was performed for PPARγ2 isoform using in vitro translated PPARγ2 (wt or R194W) proteins. C, The R194W mutant does not respond to rosiglitazone. NIH 3T3 cells were transfected with WT, R194W mutant or empty vector, together with a PPAR responsive reporter construct and a β-galactosidase reference plasmid. After transfection, NIH3T3 cells were treated with the indicated dose of rosiglitazone for 16h. Data are presented as a percentage of the maximum level of transcription achieved in the rosiglitazone curve (10 μM). 0% was defined separately for each curve as the lowest level of transcription for that curve. The data points are means ± SD (n=3). D, U2OS cells were transfected with expression vectors encoding PPARγ1 (wild type or mutant) or PPARγ2 (wild type or mutant) and a 3xPPRE-tk-luc reporter. Activation of the luciferase reporter, in the absence or presence of 1 μM rosiglitazone, is expressed as fold induction over that with empty vector (pCDNA) in the absence of ligand, after normalisation for Renilla luciferase activity. Results are averages of at least three independent experiments performed in duplicate ± standard error of the means. E, R194W has no dominant negative activity. Increasing amounts of R194W or P467L mutant receptors were cotransfected with a fixed amount of WT PPARγ. Data are normalized to the transcriptional activity of WT receptor alone (1:0) and are presented as means ± SD (n=3).The legend indicates the molar ratios of the two transfected receptors (WT+WT or WT + mutant). * indicates $p<0.05$, § indicates $p<0.01$ relative to the wild-type receptor alone (1:0). F, The same experiment (as described in E) was performed in the presence of a saturating amount (20 mM) of rosiglitazone. Under this condition P467L had no dominant negative activity as was published in the original article(4).

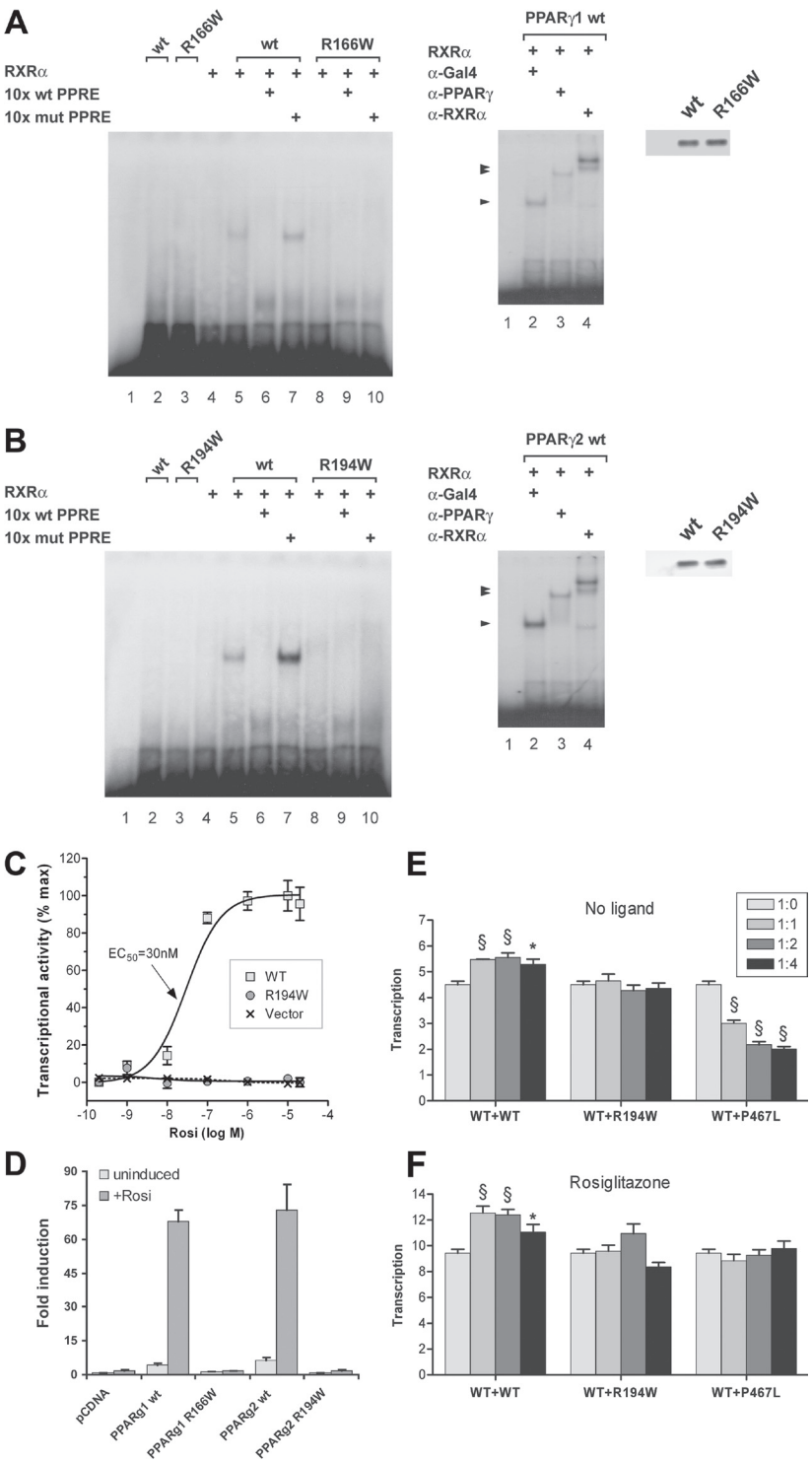
A
wt
R166W
wt
R166W
RXRα
10x wt PPRE
10x mut PPRE
1 2 3 4 5 6 7 8 9 10
PPARγ1 wt
RXRα
α-Gal4
α-PPARγ
α-RXRα
1 2 3 4
wt
R166W
B
wt
R194W
wt
R194W
RXRα
10x wt PPRE
10x mut PPRE
1 2 3 4 5 6 7 8 9 10
PPARγ2 wt
RXRα
α-Gal4
α-PPARγ
α-RXRα
1 2 3 4
wt
R194W
C
Transcriptional activity (% max)
EC50=30nM
WT
R194W
Vector
Rosi (log M)
D
Fold induction
uninduced
+Rosi
pCDNA
PPARg1 wt
PPARg1 R166W
PPARg2 wt
PPARg2 R194W
E
No ligand
1:0
1:1
1:2
1:4
Transcription
WT+WT
WT+R194W
WT+P467L
F
Rosiglitazone
Transcription
WT+WT
WT+R194W
WT+P467L

direct (figure 4 A) nor indirect (Figure 4E) dominant negative activity under our experimental conditions. With haploinsufficiency, 50% reduced gene expression results from one nonfunctional allele, whereas dominant negative mutations induce even greater reduction in gene expression. How do these two mechanisms underlie the same phenotype? One possibility is that subjects with either mutation type might have slightly different clinical phenotypes that are not easily discerned using current methods. For instance, hypertension in human subjects with dominant negative mutations seems to be more severe than in subjects with haploinsufficiency mutations (21). Additional pedigrees with *PPARG* would allow for better comparisons of these two mechanisms *in vivo*.

Since the first publication on familial partial lipodystrophy by Dunnigan and Kobberling (22), awareness of this condition by clinicians has increased. Several mutations both in *LMNA* and *PPARG* have been described. Yet, many such patients are probably overlooked, because of clinical similarities with the common obesity-related metabolic syndrome that currently is endemic to westernized societies, largely due to lifestyle changes. Careful physical examination of patients with insulin resistance and hypertriglyceridemia could help identify partial lipodystrophy. In summary, in a proband with FPLD3 we found a novel *PPARG* mutation that fails to bind DNA and is transcriptionally inactive. Human *PPARG* mutations will improve our understanding of mechanisms involved in lipodystrophy and insulin resistance.

Acknowledgements

This work was supported by operating grants from the Heart and Stroke Foundation of Ontario, the Ontario Research and Development Challenge Fund (Project #0507), Genome Canada, the Canadian Institutes of Health Research (MT14030), the Blackburn Group and the American Diabetes Association (TL). Dr. Hegele is a Career Investigator of the Heart and Stroke Foundation of Ontario and holds the Edith Schulich Vinet Canada Research Chair (Tier I) in Human Genetics and the Jacob J. Wolfe Distinguished Medical Research Chair. Dr. Kalkhoven is supported by a fellowship from the Royal Netherlands Academy of Arts and Sciences. We would like to thank Dr. V.K.K. Chatterjee for plasmid constructs.

References

1. Hegele RA. Monogenic forms of insulin resistance: apertures that expose the common metabolic syndrome. Trends Endocrinol Metab 2003; 14:371-377.
2. Agarwal AK, Garg A. Genetic basis of lipodystrophies and management of metabolic complications. Annu Rev Med 2006; 57:297-311.
3. Kobberling J, Dunnigan MG. Familial partial lipodystrophy: two types of an X linked dominant syndrome, lethal in the hemizygous state. J Med Genet 1986; 23:120-127.
4. Savage DB, Tan GD, Acerini CL, Jebb SA, Agostini M, Gurnell M, Williams RL, Umpleby AM, Thomas EL, Bell JD, Dixon AK, Dunne F, Boiani R, Cinti S, Vidal-Puig A, Karpe F, Chatterjee VK, O'Rahilly S. Human metabolic syndrome resulting from dominant-negative mutations in the nuclear receptor peroxisome proliferator-activated receptor-gamma. Diabetes 2003; 52:910-917.
5. Hegele RA, Cao H, Frankowski C, Mathews ST, Leff T. PPARG F388L, a transactivation-deficient mutant, in familial partial lipodystrophy. Diabetes 2002; 51:3586-3590.
6. Hegele RA, Ur E, Ransom TP, Cao H. A frameshift mutation in peroxisome-proliferator-activated receptor-gamma in familial partial lipodystrophy subtype 3 (FPLD3; MIM 604367). Clin Genet 2006; 70:360-362.
7. Francis GA, Li G, Casey R, Wang J, Cao H, Leff T, Hegele RA. Peroxisomal proliferator activated receptor-gamma deficiency in a Canadian kindred with familial partial lipodystrophy type 3 (FPLD3). BMC Med Genet 2006; 7:3.
8. Barroso I, Gurnell M, Crowley VE, Agostini M, Schwabe JW, Soos MA, Maslen GL, Williams TD, Lewis H, Schafer AJ, Chatterjee VK, O'Rahilly S. Dominant negative mutations in human PPARgamma associated with severe insulin resistance, diabetes mellitus and hypertension. Nature 1999; 402:880-883.
9. Agarwal AK, Garg A. A novel heterozygous mutation in peroxisome proliferator-activated receptor-gamma gene in a patient with familial partial lipodystrophy. J Clin Endocrinol Metab 2002; 87:408-411.
10. Rosen ED, Sarraf P, Troy AE, Bradwin G, Moore K, Milstone DS, Spiegelman BM, Mortensen RM. PPAR gamma is required for the differentiation of adipose tissue in vivo and in vitro. Mol Cell 1999; 4:611-617.
11. Barak Y, Nelson MC, Ong ES, Jones YZ, Ruiz-Lozano P, Chien KR, Koder A, Evans RM. PPAR gamma is required for placental, cardiac, and adipose tissue development. Mol Cell 1999; 4:585-595.
12. Kalkhoven E, Valentine JE, Heery DM, Parker MG. Isoforms of steroid receptor co-activator 1 differ in their ability to potentiate transcription by the oestrogen receptor. EMBO J 1998; 17:232-243.
13. Kalkhoven E, Teunissen H, Houweling A, Verrijzer CP, Zantema A. The PHD type zinc finger is an integral part of the CBP acetyltransferase domain. Mol Cell Biol 2002; 22:1961-1970.
14. Beitel LK, Kazemi-Esfarjani P, Kaufman M, Lumbroso R, DiGeorge AM, Killinger DW, Trifiro MA, Pinsky L. Substitution of arginine-839 by cysteine or histidine in the androgen receptor causes different receptor phenotypes in cultured cells and coordinate degrees of clinical androgen resistance. J Clin Invest 1994; 94:546-554.
15. Ruiz M, Lind U, Gafvels M, Eggertsen G, Carlstedt-Duke J, Nilsson L, Holtmann M, Stierna P, Wikstrom AC, Werner S. Characterization of two novel mutations in the glucocorticoid receptor gene in patients with primary cortisol resistance. Clin Endocrinol (Oxf) 2001; 55:363-371.
16. Haider NB, Jacobson SG, Cideciyan AV, Swiderski R, Streb LM, Searby C, Beck G, Hockey R, Hanna DB, Gorman S, Duhl D, Carmi R, Bennett J, Weleber RG, Fishman GA, Wright AF, Stone EM, Sheffield VC. Mutation of a nuclear receptor gene, NR2E3, causes enhanced S cone syndrome, a disorder of retinal cell fate. Nat Genet 2000; 24:127-131.
17. Hayashi T, Gekka T, Goto-Omoto S, Takeuchi T, Kubo A, Kitahara K. Novel NR2E3 mutations (R104Q, R334G) associated with a mild form of enhanced S-cone syndrome demonstrate compound heterozygosity. Ophthalmology 2005; 112:2115.
18. Ristow M, Muller-Wieland D, Pfeiffer A, Krone W, Kahn CR. Obesity associated with a mutation in a genetic regulator of adipocyte differentiation. N Engl J Med 1998; 339:953-959.

19. Agostini M, Schoenmakers E, Mitchell C, Szatmari I, Savage D, Smith A, Rajanayagam O, Semple R, Luan J, Bath L, Zalin A, Labib M, Kumar S, Simpson H, Blom D, Marais D, Schwabe J, Barroso I, Trembath R, Wareham N, Nagy L, Gurnell M, O'Rahilly S, Chatterjee K. Non-DNA binding, dominant-negative, human PPARgamma mutations cause lipodystrophic insulin resistance. Cell Metab 2006; 4:303-311.
20. Al-Shali K, Cao H, Knoers N, Hermus AR, Tack CJ, Hegele RA. A single-base mutation in the peroxisome proliferator-activated receptor gamma4 promoter associated with altered in vitro expression and partial lipodystrophy. J Clin Endocrinol Metab 2004; 89:5655-5660.
21. Hegele RA. Lessons from human mutations in PPARgamma. Int J Obes (Lond) 2005; 29 Suppl 1: S31-S35.
22. Dunnigan MG, Cochrane MA, Kelly A, Scott JW. Familial lipoatrophic diabetes with dominant transmission. A new syndrome. Q J Med 1974; 43:33-48.

Chapter 5

Peroxisome Proliferator-Activated receptor γ (PPARγ) regulates expression of the anti-lipolytic G-protein-coupled receptor 81 (GPR81/Gpr81)

Ellen H. Jeninga[1,2], Anne Bugge[3], Ronni Nielsen[3], Sander Kersten[4], Christian Dani[5], Martin Wabitsch[6], Ruud Berger[1,2], Hendrik G. Stunnenberg[7], Susanne Mandrup[3] and Eric Kalkhoven[1,2,8]

[1] Dept. Metabolic & Endocrine Diseases, UMC Utrecht, Utrecht, The Netherlands; [2]Netherlands Metabolomics Centre, The Netherlands; [3]Dept. of Biochemistry & Molecular Biology, University of Southern Denmark, Odense, Denmark; [4]Nutrition, Metabolism & Genomics group, Wageningen University, Wageningen, The Netherlands; [5]ISBDC, Université de Nice Sophia-Antipolis, CNRS, Nice, France; [6]Division of Pediatric Endocrinology, Dept. of Pediatrics and Adolescent Medicine, University of Ulm, Ulm, Germany; [7]Dept. of Molecular Biology, Nijmegen Center for Molecular Life Sciences, Nijmegen, The Netherlands; [8]Dept. of Pediatric Immunology, UMC Utrecht, Utrecht, The Netherlands.

Submitted

Abstract

The ligand-inducible nuclear receptor PPARγ plays a key role in the differentiation, maintenance and function of adipocytes and is the molecular target for the insulin sensitizing thiazoledinediones (TZDs). Although a number of PPARγ target genes that may contribute to the reduction of circulating FFAs after TZD treatment have been identified, the relevant PPARγ target genes that may exert the anti-lipolytic effect of TZDs are unknown. Here we identified the anti-lipolytic human G protein-coupled receptor 81 (GPR81), GPR109A and the (human-specific) GPR109B genes as well as the mouse Gpr81 and Gpr109A genes as novel TZD-induced genes in mature adipocytes. GPR81/Gpr81 is a direct PPARγ target gene, since mRNA expression of GPR81/Gpr81 (and GPR109A/Gpr109A) increased in mature human and murine adipocytes as well as *in vivo* in epididymal fat pads of mice upon rosiglitazone stimulation, while siRNA- mediated knockdown of PPARγ in differentiated 3T3-L1 adipocytes showed a significant decrease in Gpr81 protein expression. In addition, ChIP-seq analysis in differentiated 3T3-L1 cells revealed a conserved PPAR:RXR binding site in the proximal promoter of the Gpr81 gene, which was proven to be functional by EMSA and reporter assays. Importantly, siRNA-mediated knock down of Gpr81 partly reversed the inhibititory effect of TZDs on lipolysis in 3T3-L1 adipocytes. The coordinated regulation of the GPR81/Gpr81 and GPR109A/Gpr109A genes (and GPR109B in humans) by TZD-induced PPARγ activation presents a novel mechanism by which these drugs may lower circulating FFA levels and thereby ameliorate insulin resistance in obese patients.

Introduction

Due to a high calorie diet and a sedentary lifestyle, obesity and its associated comorbidities like hypertension, type II diabetes and atherosclerosis rapidly increase worldwide (1). Adipose tissue is the major site of lipid storage in the body and plays a pivotal role in the regulation of whole body metabolic homeostasis and therefore in the pathophysiology of obesity (2). After a meal, excess fuel substrates are partitioned to adipose tissue where they are processed and stored as triglycerides (TAG). Conversely, during fasting TAGs are hydrolized to free fatty acids (FFA) and glycerol, and the FFA released into the blood stream can subsequently be used by other organs as energy substrates. The latter process, termed lipolysis, is tightly regulated by hormones and cytokines (3). The three main hormones that regulate lipolysis in humans are insulin, which inhibits lipolysis, and catecholamines (adrenaline, noradrenaline) and glucagon which stimulate lipolysis. In rodents, inhibition of lipolysis by adenosine presents an additional regulatory pathway. Lipolysis is deregulated in obesity: basal lipolysis rates are increased (4), while the stimulation of lipolysis by catecholamines (5) as well as the anti-lipolytic action of insulin (6) are inhibited. The impairment of hormonal control of lipolysis may be due to high levels of TNFα, which is over-produced by adipose tissue in obese humans and rodents (7). Deregulated lipolysis results in increased circulating FFA levels and lipid accumulation in non-adipose tissues, ultimately contributing to insulin resistance and other obesity-related metabolic disorders (8).

One of the key regulators of adipocyte differentiation, maintenance and function is peroxisome proliferator-activated receptor γ (PPARγ), a member of the nuclear hormone receptor superfamily of ligand inducible transcription factors (9). PPARγ exists in two isoforms, PPARγ1 and PPARγ2. PPARγ2 has an additional 30 amino acids at the N-terminus and its expression is restricted to adipose tissue while PPARγ1 is more widely distributed (e.g. adipocytes, lower intestine, monocytes and macrophages). *In vitro* and *in vivo* studies showed that PPARγ is both necessary and sufficient to induce adipogenesis (9). PPARγ bind as an obligate heterodimer with the retinoic acid X receptors (RXRs) to PPAR responsive elements (PPREs), which consist of two direct repeats of 6 nucleotides (AGGTCA) interspaced by one nucleotide (DR-1). Upon binding of ligand these proteins undergo a conformational change, which allows the interaction with so-called coactivators, starting a cascade of protein interactions and modifications that finally results in the induction of specific target genes (10). Although the endogenous ligands for PPARγ have not been firmly established, natural compounds like polyunsaturated fatty acids and eicosanoids have been shown to activate PPARγ. In addition, the antidiabetic drugs, such as thiazolidinediones (TZDs) act as high affinity PPARγ ligands (11). Administration of these TZDs to obese and/or insulin resistant patients has been shown to reduce circulating FFAs and thereby improve insulin sensitivity. Part of these effects may be explained by the stimulatory effect of TZDs on adipocyte differentiation,

thereby increasing lipid storage capacity in adipose tissue. In addition, PPARγ also regulates a number of genes essential for the adipocytic phenotype, such as genes involved in lipid uptake, lipid synthesis, lipid droplet stabilization, glycerol/FA recycling and FA oxidation (12). Since elevated levels of serum FFAs promote insulin resistance (13), an important potential mechanism for the beneficial effects of TZDs is therefore the net partitioning of lipids in adipose tissue. Consistent with this notion genes encoding proteins involved in lipid uptake in adipocytes, such as lipoprotein lipase (LPL), CD36 and the oxidized LDL receptor (OLR) have been reported to be directly regulated by PPARγ (9). In addition, PPARγ directly regulates the expression of the lipid-droplet proteins perilipin and S3-12 (14), and genes (potentially) involved in the 'futile cycle' (9;15;16), the re-esterification of fatty acids and glycerol to triglycerides, which may be particularly important in rodents (17). Several findings suggest that PPARγ and TZDs may also be implicated in the process of lipolysis. First, the TZD troglitazone has been shown to lower basal lipolysis rates in differentiated adipocytes ((18-20); this manuscript), as well as TNFα-activated lipolysis (21;22). Secondly, introduction of a dominant-negative form of PPARγ in mature adipocytes resulted in increased lipolysis, suggesting that PPARγ normally inhibits this process (23). Finally, treatment of diabetic patients with TZDs has been shown to restore insulin-mediated suppression of lipolysis (24-27). However, the relevant PPARγ target genes which may exert the anti-lipolytic effect of TZDs are unknown.

To identify novel target genes that may play a role in the effects of TZDs on lipid metabolism, we performed a transcriptome analysis in human adipocytes treated with the TZD rosiglitazone. In this study we show that TZDs induce the expression of two anti-lipolyitic G-protein-coupled receptors, GPR81/Gpr81 and GPR109A/Gpr109A, in human and murine adipocytes. In addition, a third anti-lipolytic GPR, the human-specific GPR109B, is also induced by rosiglitazone. This PPARγ-mediated activation may occur through a conserved PPRE located in the GPR81 promoter. The coordinated regulation of these genes by TZD-induced PPARγ activation presents a novel mechanism by which these drugs may lower circulating FFA levels and thereby ameliorate insulin resistance in obese patients.

Materials and methods

Materials

Rosiglitazone was purchased from Alexis. Anti-PPARγ antibody (2345S) was from Cell Signalling, anti-GPR81 antibody (NLS2095) was from Novus Biologicals, anti-GPR109A (GTX12610) was from Genetex and anti-tubulin (T5168) was from Sigma. Anti-PPARγ (sc-7196) and anti-RXR (sc-774) were used for ChIP assays. Anti-PPARγ (sc-7273), anti-RXRα (sc-553) and anti-Gal4 (sc-510) antibodies used for EMSA were from Santa Cruz Biotechnologies.

Plasmids
All recombinant DNA work was performed according to standard procedures (28). The murine GPR81 reporter, GPR81(-1059/+28)-luc, was generated by inserting the respective promoter into XhoI/HindIII site of the PGL3-basic vector (Promega). All mutations were generated by Quickchange mutagenesis (Stratagene) and verified by sequencing. All other plasmids have been described earlier (29).

Cell culture, differentiation and reporter assays
Culturing of cells was performed as described (29)(30)(31). Differentiation of 3T3-L1 (29), the human multipotent adipose derived stem cells (hMADs) (31) and the human Simpson-Golabi Behmel Syndrome cell line (SGBS) (30) has been described earlier. Reporter assays were performed exactly as described (29).

Micro-array analysis
3T3-L1, SGBS and hMADs were differentiated as described above and at day 6, 8 and 17 respectively treated with Rosiglitazone or DMSO for 6 hours. Micro-array experiments were performed as described before (32). In short, total RNA was isolated using TRIzol reagent. Concentrations and purity were determined on a NanoDrop ND-1000 spectrophotometer (Isogen). RNA integrity was checked on an Agilent 2100 bioanalyzer (Agilent Technologies) with 6000 Nano Chips. Part of the RNA samples from four 6 cm dishes was used for quantitative RT-PCR (see RT-PCR section). Remaining RNA samples from four 6 cm dishes were pooled and used for micro-array analysis. Samples were hybridized on Human NUGO arrays from Affymetrix. A detailed description of the analysis method is available on request.

Animal study
Animal study was performed as described earlier (32). In short, Sv129 male mice were purchased at The Jackson Laboratory (Bar Harbor, ME). At 20 weeks of age, the diet of half of the mice group was supplemented with rosiglitazone (0.01% w/w) for a week. At the end of the experiment epididymal white adipose tissue was dissected, weighed, and used for RNA isolation. The animal experiments were approved by the animal experimentation committee of Wageningen University.

RNA isolation and real-time PCR
3T3-L1 fibroblasts were differentiated as described above. Three independent samples of total RNA were extracted at different time points using TRIzol reagent (Invitrogen). cDNA was synthesized using the superscript first strand synthesis system (Invitrogen) according to manufacturer's protocol. Gene expression levels were determined by quantitative real-time PCR with the MyIq cycler (Bio-Rad) using SYBR-green (Bio-Rad) and normalized to *TFIIb* expression.
The primers used were murine TFIIb forward primer; 5'-TCCTCCTCAGACCGCT TTT-3';reverseprimer,5'-CCTGGTTCATCATCGCTAATC-3';murineGpr81forward

primer 5′-GGTGGCACGATGTCATGTT-3′; reverse primer 5′-GACCGAGCAGA ACAAGATGATT-3′; murine Gpr109A forward primer, 5′-TCCAAGTCTCCAAA GGTGGT-3′; reverse primer, 5′-TGTTTCTCTCCAGCACTGAGTT-3′; murine Fapb4 forward primer, 5′- GAAAACGAGATGGTGACAAGC-3′; reverse primer, 5′-TTGTGGAAGTCACGCCTTT-3′; human 36B4 forward primer, 5′-CGGGAAGG CTGTGGTGCTG-3′; reverse primer 5′- GTGAACACAAAGCCCACATTCC-3′; human GPR109A forward primer, 5′- TTCAGAGAATGCGATTTAGGG-3′; reverse primer 5′-ACACCTTGCAACCAGTCTCC-3′; human GPR109B forward primer, 5′-TTCTGTGGGGCATCACTGT-3′; reverse primer, 5′-GCCATTCTGGATC AGCAACT-3′; human GPR81 forward primer, 5′- ATTTGGCCGTGGCTGATTTC-3′; reverse primer, 5′- ACCGTAAGGAACACGATGCTC-3′.

Western blot analysis

For Western blot analyses, differentiated 3T3-L1 cells were lysed in RIPA lysis buffer (200 mM Tris-HCl pH 8,0; 0,1% SDS, 1% Triton X-100; 10 mM EDTA; 150 mM NaCl; 1% NaDOC containing protease inhibitors). Total cell lysate was diluted in 4x Laemli sample buffer and subjected to SDS-PAGE and transferred to Immobilon membranes (Millipore). α-PPARγ, α-GPR81, α-GPR109A, α-FABP4 and α-tubulin antibodies were used to probe for the respective proteins. ECL Plus (Perkin Elmer) was used for detection and signals were quantified using a densitometer.

Chromatin immunoprecipitation (ChIP) and sequencing (ChIP-seq)

ChIP assays were performed exactly as described earlier (33). The primers used for ChIP assays were as follows: murine Gpr81 forward primer 5′-AGTGCCAGAGAGGGGAGACT-3′; reverse primer 5′-CGTTTCTCTGCAGACC TTCC-3′; murine beta-globin forward primer primer 5′-CCTGCCCTCTCTA TCCTGTG-3′; reverse primer 5′-GCAAATGTGTTGCCAAAAAG-3′; human GPR81 forward primer 5′-CTGGAGAGCACACAAAGCTG-3′; reverse primer 5′-CCACTCCAGGAAATGTTTGG-3′; human Beta-globin forward primer 5′-TGGTATGGGGCCAAGAGATA-3′; reverse primer 5′-TAGATGCCTCTGCCC TGACT-3′. ChIP-seq was performed as described earlier (12).

EMSA

EMSAs were performed as described earlier (29). The sequences of the double-stranded DNA oligomers, containing the wild type or mutant PPRE from the mouse G-protein-coupled receptor 81 promoter (between -128 and -98 of the *Gpr81* gene) used, were as follows: mGpr81-wild-type, 5′-CCGGGGACGGGTAGTCAG GCAAAGGTTAGGGAGGA-3′ and mGpr81-mutant A, 5′-CCGGGGACGGCAAG TCACCCAAAGGTTAGGGAGGA-3′ and mGpr81-mutant B, 5′-CCGGGACGGGT AGTCTCGCAAACCTTAGGGAGGA-3′

siRNA transfection in differentiated adipocytes
3T3-L1 cells were differentiated as described above. At day 6 cells were detached using 5x trypsin/EDTA (Gibco Life Technologies), washed in medium containing 4% glycerol. For each reaction 2 million of cells were resuspended in buffer L (AMAXA Cell line Nucleofector kit L) and control (D-001210-01-20; Dharmacon), murine specific PPARγ (#2 J-040712-06 Dharmacon) or custom-made Gpr81 (5'-ACCTGGAAGTCAAGCACTATT; Dharmacon) siRNA oligonulceotides were delivered into adipocytes (500 nM of each siRNA/ 2 million cells) by electroporation (AMAXA Nucleofector II). Cells were reseeded and 20 hours post electroporation cells were incubated with 1 μM rosiglitazone for an additional 28 hours. Subsequently, cells were harvested for Western blot analysis and media (n=4) were collected for glycerolmeasurements. Glycerol levels were determined according to the manufacturers instructions (Instruchemie).

Results

GPR109A, GPR109B and GPR81 are regulated by rosiglitazone in mature adipocytes
To identify novel TZD-regulated genes in mature human adipocytes, we performed transcriptome analysis in differentiated human multipotent adipose derived stem cells (hMADs) (31). Out of 361 genes that were upregulated after 6 hours of treatment with the TZD rosiglitazone (data not shown) we selected the human specific G-protein-coupled receptor 109B (GPR109B) to explore in more detail. Together with GPR109A and GPR81, GPR109B belongs to the class A rhodopsin-like G-protein-coupled receptors (GPCRs). GPR109A (also called puma-g) and the human specific GPR109B are 96% homologous (34) and expressed in adipose tissue, spleen and immune cells (35)(36)(37), whereas GPR81 expression is almost exclusively restricted to adipose tissue (38)(39). GPR109A has been identified as the receptor for the anti-lipolytic drug nicotinic acid (NA), and in GPR109A knockout mice it has been shown that GPR109A was the receptor mediating the lipid-lowering effects of NA (35)(36)(37). Recently the ketone body β-hydroxybutyrate was reported as an endogenous agonist for GPR109A (40). In addition, very recently two reports (41)(42) showed that GPR81 functions as a receptor for lactate, which reduces lipolysis *in vitro* and *in vivo* (43)(44). Interestingly, the GPR81, GPR109A and GPR109B genes are colocalized on human chromosome 12 and share synteny with murine GPR81 and GPR109A on mouse chromosome 5 (Figure 1A; (45)). For this reason, expression of the GPR109A and GPR81 genes, which were not represented on the microarray, was determined together with the GPR109B gene in differentiated hMADs cells. Using quantitative RT-PCR, mRNA expression of these three genes was found to increase 4- to 5-fold after treatment with rosiglitazone for 6 hours (Figure 1B, left panel). The same experiment was performed in another

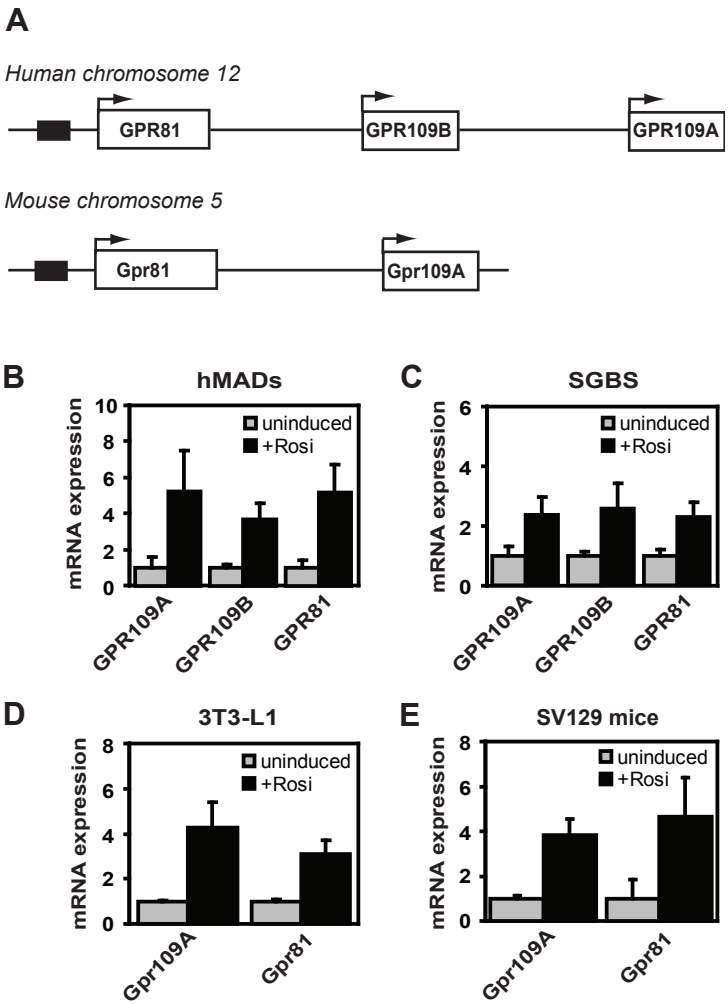

Figure 1. GPR109A/Gpr109A, GPR81/Gpr81 and GPR109B are induced by the PPARγ ligand rosiglitazone in mature adipocytes and *in vivo* in adipose tissue.
A, Schematic representation of the genomic arrangement of the GPR-family in human and mouse. GPR109A, GPR109B and GPR81 mRNA expression in fully differentiated hMADs (B) and SGBS cells (C) after treatment with 1 μM rosiglitazone for 6 hours. D, GPR109A and GPR81 mRNA expression in fully differentiated murine 3T3-L1 cells after incubation with 1 μM rosiglitazone for 6 hours. Relative mRNA expression levels were related to untreated cells and normalized for the 36B4 or TFIIb reference gene for human and murine adipocytes respectively. E, GPR109A and GPR81 mRNA expression levels in epididymal fat pads of control or rosiglitazone treated male SV129 mice. Relative mRNA expression levels were related to control mice and normalized for the TFIIb reference gene.

human adipocyte cell line, the Simpson-Golabi Behmel syndrome (SGBS) cell line (30). In these cells a similar mRNA expression profile was observed (Figure 1C). To investigate whether conserved mechanisms of regulation exist in mouse adipocytes, we examined the effect of rosiglitazone treatment on Gpr81 and Gpr109A mRNA expression in differentiated 3T3-L1 adipocytes. As was observed for the human adipocytes, treatment of murine adipocytes with rosiglitazone stimulated the mRNA expression levels of Gpr81 and Gpr109A up to 4-fold (Figure 1D). Finally, we examined the effect of rosiglitazone treatment on the mRNA expression of Gpr81 and Gpr109A in mouse adipose tissue *in vivo*. For this Sv129 male mice received a diet supplemented with rosiglitazone for 1 week, RNA was isolated from epididymal fat pads and subjected to quantitative RT-PCR analysis. As shown in Figure 1E, mRNA expression of both Gpr109A and Gpr81 was upregulated in epididymal fat pads of the mice administered rosiglitazone compared to control mice.
In summary, rosiglitazone treatment induces the mRNA expression of the human GPR109A, GPR109B and GPR81 genes in differentiated adipocytes. A conserved regulatory mechanism may underlie this induction, since the mouse Gpr109A and Gpr81 genes were also significantly upregulated, *in vitro* and *in vivo*, upon rosiglitazone treatment.

GPR81 and GPR109A mRNA and protein expression increase during 3T3-L1 differentiation

Since PPARγ plays an essential role in adipogenesis and the expression of known PPARγ target genes increases during differentiation we studied the protein and mRNA expression levels of Gpr81 and Gpr109A during differentiation of 3T3-L1 pre-adipocytes into mature adipocytes. At different time points of differentiation cells were harvested to determine mRNA and protein expression levels. Quantitative RT-PCR showed that mRNA expression of both Gpr81 and Gpr109A steadily increased during adipocyte differentiation, starting at day 2 (Figure 2). In addition, protein expression levels of GPR81 and GPR109A were determined during adipogenesis. Protein expression of GPR81 could be detected from day 4 onwards, while expression of the Gpr109A protein was observed slightly earlier (day 3). As a control, protein expression levels of PPARγ and the well established PPARγ target gene Fabp4 were determined and showed a similar increase during adipocyte differentiation (Figure 2). In conclusion, Gpr81 and Gpr109A mRNA and protein expression clearly increased during differentiation of 3T3-L1 adipocytes.

siRNA mediated knockdown of PPARγ in mature adipocytes decreases GPR81 protein expression

To investigate whether the activation of the Gpr81 and Gpr109A genes by rosiglitazone is mediated by PPARγ, we reduced expression of the PPARγ protein in mature 3T3-L1 adipocytes by siRNA-mediated knockdown. As described earlier

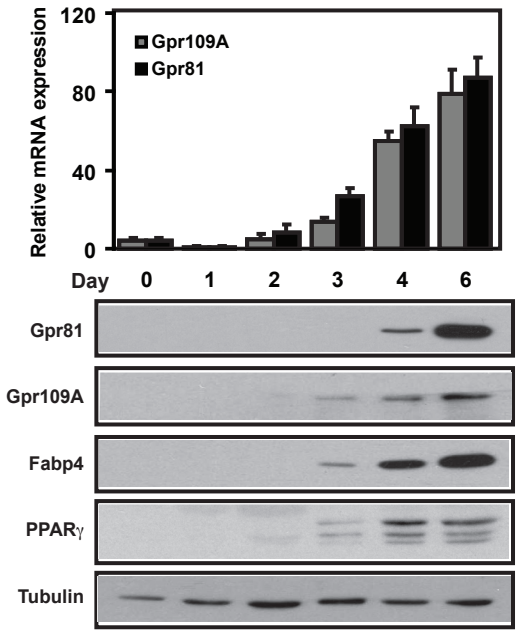

Figure 2. mRNA and protein expression of GPR109A and GPR81 increases during differentiation of 3T3-L1 adipocytes.
GPR109A, GPR81 and Fabp4 mRNA expression (upper panel) and protein expression levels (lower panels) at day 0, 1, 2, 3, 4 and 6 respectively of differentiating 3T3-L1 cells. Relative mRNA expression levels were related to undifferentiated cells (day 0) and normalized for the TFIIb reference gene. Tubulin protein expression was used as a loading control in Western blot analysis.

(46), rosiglitazone treatment resulted in reduced PPARγ protein levels (Figure 3, lane 1 and 2). Electroporation of siRNA oligonucleotides directed against PPARγ significantly reduced, but did not completely abolish PPARγ protein expression in the absence and presence of rosiglitazone (Figure 3). In agreement with the mRNA expression data (Figure 1B), the expression of the Gpr81 and Gpr109A proteins increased in the presence of rosiglitazone in these cells (Figure 3, lane 1 and 2). Knockdown of PPARγ resulted in a significant reduction (5-fold, as determined by densitometry) of both basal and rosiglitazone-induced Gpr81 protein expression compared to 3T3-L1 adipocytes treated with non-targeting siRNA oligonucleotides. In the case of Gpr109A, a 2-fold reduction of rosiglitazone-induced protein expression was observed upon knockdown of the PPARγ protein. These results indicate that the PPARγ protein is essential for the activation of the Gpr81 gene- and to a lesser extent the Gpr109A gene- by rosiglitazone.

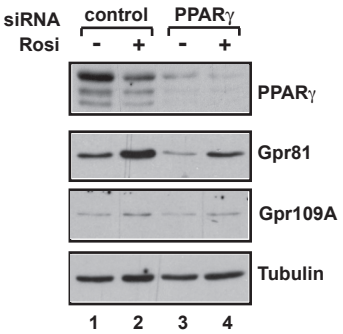

Figure 3. siRNA mediated PPARγ knockdown reduces GPR81 and GPR109A protein expression.
Differentiated 3T3-L1 adipocytes (day 6) were electroporated with control or PPARγ siRNA. Twenty hours after electroporation medium was replaced by medium with or without 1 μM rosiglitazone and incubated for an additional 28 hours. Cells were lysed and subjected to Western blot analysis. α-tubulin was used as a loading control. This blot is a representative of at least three independently performed experiments.

Endogenous PPARγ and RXR bind to the proximal promoter of GPR81

The rapid activation of the Gpr81 and Gpr109A genes by rosiglitazone (Figure 1) together with the essential role of the PPARγ protein in this process (Figure 3) prompted us to examine whether PPARγ and its heterodimeric partner RXR are recruited to the proximal promoter of the Gpr81 and/or Gpr109A genes. Very recently, a genome-wide analysis of PPARγ and RXR binding during 3T3-L1 differentiation by ChIP sequencing technology was reported (12). Detailed analysis of the chromosomal region surrounding the Gpr81 and Gpr109A genes revealed clear PPARγ and RXR binding in the proximal promoter (-294/-55) of Gpr81, suggesting a PPARγ:RXR binding site at this location. Interestingly, no significant peaks in close proximity of the Gpr109A gene were observed (Figure 4A). The recruitment of PPARγ and RXR to the proximal promoter of the Gpr81 in mature 3T3-L1 adipocytes (day 6) was confirmed by ChIP-PCR (Figure 4B). In addition, the recruitment in preadipocytes (day 0), in which PPARγ expression is low, was negligible and neither PPARγ nor RXR were detected on an arbitrary gene region of the beta-globin gene on chromosome 7, which served as a negative control (Figure 4B).

Since the proximal promoter region of the Gpr81 gene is well conserved between human and mouse, we investigated if PPARγ/RXR also binds to the proximal promoter of the human GPR81 gene in SGBS preadipocytes (day 0) and mature SGBS adipocytes (day 8). Interestingly, both PPARγ and RXR were recruited to the proximal promoter of GPR81 in differentiated SGBS cells, but not in preadipocytes (day 0) (Figure 4C). Also in this case binding of PPARγ and RXR was absent in the negative control (human beta-globin; Figure 4C). Taken together these results indicate that a PPARγ/RXR heterodimer binds to the proximal promoter of the mouse Gpr81 gene as well as the human GPR81 gene.

Identification of a functional PPRE in the proximal promoter of GprR81

In order to identify the PPRE in the proximal promoter of Gpr81, we subjected the sequence underneath the peaks (-294/-55) of the ChIP-seq data (Figure 4A)

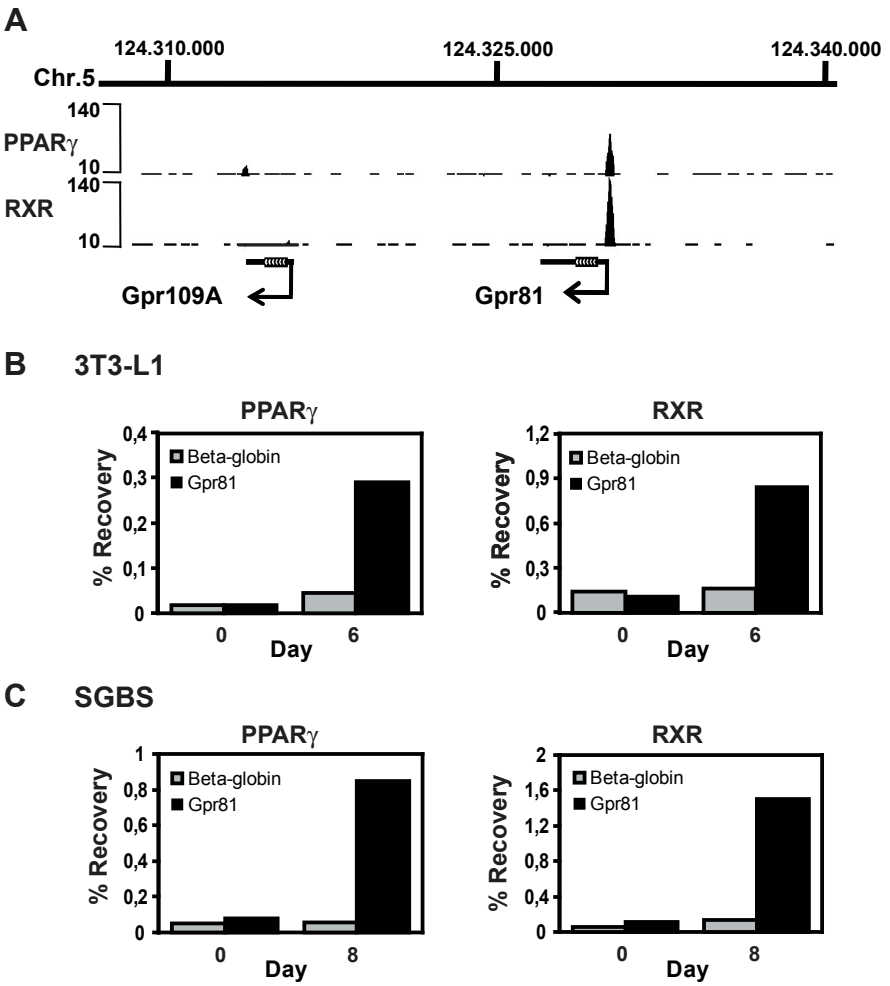

Figure 4. PPARγ and RXR are recruited to the proximal promoter of GPR81.
A, ChIP-seq data of differentiated 3T3-L1 adipocytes (day 6) viewed in the UCSC browser showing PPARγ and RXR binding sites for GPR81. B, ChIP-PCR for PPARγ and RXR was performed in 3T3-L1 (B) and SGBS (C) at the days indicated. As a negative control the arbitrary gene, beta-globin was used. Results are indicated as % of immunoprecipitated chromatin compared to the input.

to an *in silico* promoter analysis (NHR scan; (47)). A potential PPRE was detected, which was conserved between human and mice (Figure 5A). To assess if PPARγ/RXRα binds to this potential PPRE we first performed electrophoretic mobility shift assays. A ^{32}P labelled probe containing the PPRE was incubated with *in vitro* translated PPARγ2 and/or RXRα. As shown in Figure 5B, a specific PPARγ2-RXRα heterodimeric complex was formed on the Gpr81 PPRE, as formation of this protein-DNA complex could be diminished by addition of an excess of unlabelled wild type

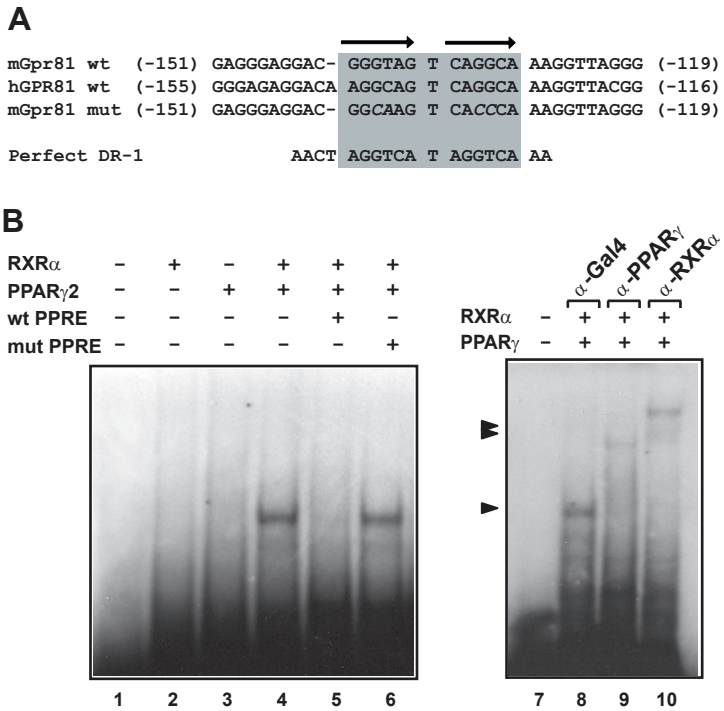

Figure 5. Identification of the PPRE in the proximal promoter of GPR81.
A, Alignment of the murine, human GPR81 and perfect PPRE. Electrophoretic mobility shift assay using a ^{32}P labelled fragment from the proximal GPR81 promoter containing the PPRE incubated with *in-vitro* translated PPARγ2 and/or RXRα proteins in the presence or absence of an excess of unlabelled wild-type or mutant fragment (B) or α-Gal4, α-PPARγ or α-RXRα antibody respectively (C). Protein-DNA complexes were separated from unbound DNA on non-denaturing polyacrylamide gels and visualized by autoradiography of dried gels.

PPRE, but not by an excess of mutant PPRE (Figure 5B). Specific antibodies against PPARγ and RXRα, but not an antibody directed against an irrelevant protein (Gal4), supershifted the protein-DNA complex, confirming the heterodimeric composition of the complex (Figure 5B; right panel).
Next, we fused the 5′-flanking region and start site of the mouse Gpr81 gene (-1059/+28) to a luciferase gene. The activity of this reporter was determined in human osteosarcoma (U2OS) cells, which express negligible levels of endogenous PPARγ protein, but display a robust response upon overexpression of the protein (29). As shown in Figure 6A, transfection of cells with an expression vector encoding PPARγ2 markedly activated the reporter gene compared to empty vector control (pCDNA). Activation of PPARγ by rosiglitazone further enhanced the PPARγ-mediated activation of the reporter. Mutation of the potential PPRE completely abolished the PPARγ mediated activation of the reporter, both in the absence and presence of rosiglitazone (Figure 6A).

To examine the regulation of the Gpr81 promoter in more detail we tested the ability of the PPARγ1 isoform, as well as three PPARγ2 mutants to activate this reporter. As shown in Figure 6B, PPARγ1 activated the reporter to a comparable level as PPARγ2, suggesting there is no isoform specificity for this PPRE. The two natural PPARγ2 mutants R425C and P495L displayed reduced and negligible activity, respectively, in agreement with their activity on other promoters (29)(48). The heterodimerization defective mutant L464R failed to activate the reporter (Figure 6B), confirming that dimerization of PPARγ and RXRα is a prerequisite for binding to the Gpr81 PPRE (Figure 5B and C).
Taken together these results indicate that PPARγ activates transcription of the Gpr81 gene by binding of a PPARγ/RXR heterodimer to a conserved PPRE located in the proximal promoter (-141/ -129) of the gene.

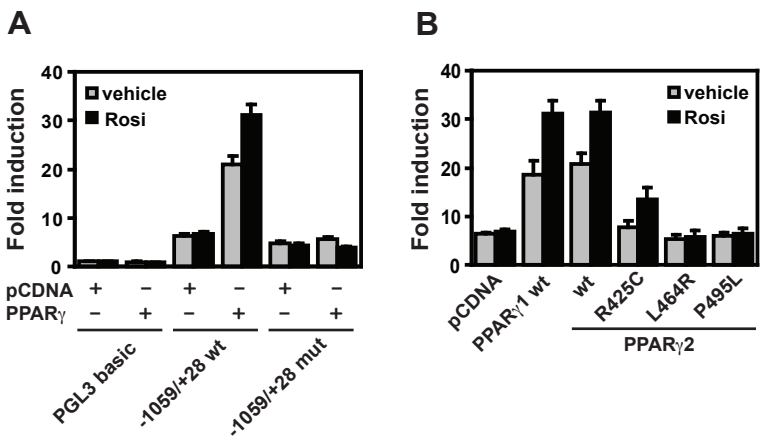

Figure 6. The identified PPRE in the proximal promoter of GPR81 is functional in cells.
A, U2OS cells were cotransfected with a reporterconstruct (pGL3-GPR81(-1059/+28)) containing wild-type or mutant PPRE together with empty (pCDNA) or PPARγ encoding expression vectors. Activation of the luciferase reporter in the absence or presence of 1μM rosiglitazone is expressed as fold induction over that with empty reporter cotransfected with pCDNA in the absence of rosiglitazone after normalisation for Renilla luciferase activity. B, U2OS cells were transfected with the GPR81(-1059/+28) reporter and expression vectors encoding wild type PPARγ1, PPARγ2 or mutant PPARγ2. Activation of the luciferase reporter is expressed as described above. Results are averages of at least three independently performed experiments assayed in duplicate ± standard error of the means.

siRNA mediated knockdown of both Gpr81 and PPARγ in mature adipocytes increased lipolysis

Next, we wished to establish the relevance of the PPARγ-mediated upregulation of the Gpr81 gene in the anti-lipolytic action of TZDs. For this, we reduced Gpr81

or PPARγ protein expression by siRNA-mediated knockdown in mature 3T3-L1 adipocytes and determined glycerol levels as a measure for lipolyis. In agreement with previous studies (19)(18)(20), TZD treatment decreased glycerol levels by twofold (Figure 7B). Partial knock down of PPARγ increased lipolysis, and reduced the effect of rosiglitazone treatment (35% reduction; Figure 7B, right panel). Similarly, knock down of Gpr81, which was also partial (Figure 7A), resulted in a slight increase in glycerol levels, and a 35% reduction of the rosiglitazone-mediated inhibition (Figure 7B, right panel). Taken together, these data suggest that the anti-lipolytic action of rosiglitazone is partly mediated through the PPARγ-mediated regulation of the Gpr81 gene in mature adipocytes.

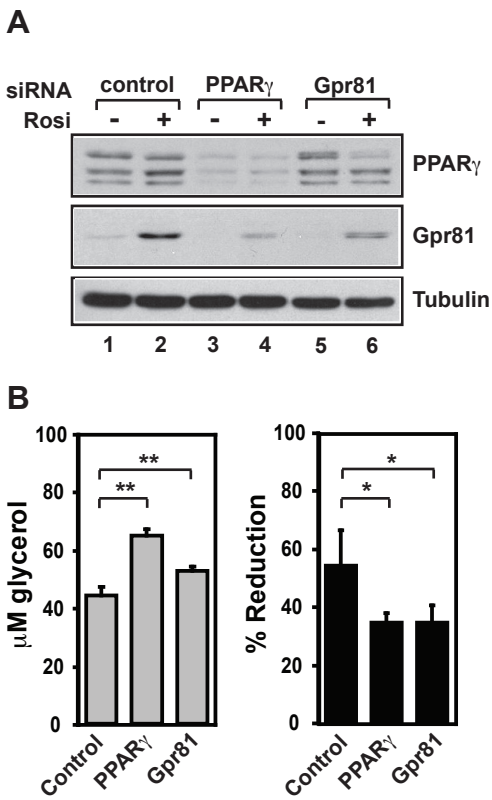

Figure 7. GPR81 contributes to the anti-lipolytic action of rosiglitazone.
siRNA-mediated knock down of PPARγ or Gpr81 win differentiated 3T3-L1 adipocytes was performed as described in Figure 3. (A) Cells were lysed and subjected to Western blot analysis, using α-tubulin as a loading control. (B) Media were collected (n=4) and glycerol levels were determined, as a measure for lipolysis. Indicated is the fold reduction upon rosiglitazone treatment over vehicle treated cells.

Discussion

PPARγ plays a key role in (pre)adipocyte biology by regulating their differentiation, maintenance and lipid metabolism. The insulin-sensitizing TZDs have been shown to be high affinity ligands for PPARγ and are administered to patients with insulin resistance. This class of antidiabetic drugs increases systemic insulin sensitivity in diabetic animal models and humans (49). The number of target genes which help to explain the beneficial effects of these ligands is however limited. Here we present compelling evidence that the anti-lipolytic G-protein-coupled receptor 81 (GPR81/Gpr81) is a novel direct PPARγ target gene in human and murine adipocytes. Interestingly, in addition to the Gpr81/GPR81 gene, expression of the anti-lipolytic Gpr109A/GPR109A gene (and the GPR109B gene in human adipocytes) was also stimulated by TZD-activated PPARγ, but a functional PPRE could only be identified in the proximal promoter of the Gpr81 gene (Figure 1A and 4A). It is possible that this site also controls the Gpr109A/GPR109A promoter which is 16 Kb further downstream. Of note, the genome-wide profiles of PPARγ:RXR in 3T3-L1 have unequivocally shown that only a very small percentage of PPARγ:RXR target sites lie in the proximal promoters (12;50). Distal gene regulation has been proposed to occur via a mechanism by which a transcription factor bound to a distal site directs looping, thereby bringing coactivators and chromatin remodelers at the distal sites in proximity of TSS of target genes and facilitating recruitment of RNA polymerase II (51). The rapid increase (within 6 hours) and synchronous induction of GPR81/Gpr81 and GPR109A/Gpr109A in mature adipocytes observed in our studies support the direct regulation of both genes by PPARγ. Alternatively, PPARγ could regulate the GPR109A/Gpr109A gene (and the GPR109B gene in humans) in an indirect manner. Future studies are therefore required to establish the exact molecular mechanisms underlying the regulation of the GPR109A/Gpr109A gene. Based on the data presented here showing that PPARγ directly regulates the antilipolytic GPR81, GPR109A and GPR109B genes in adipocytes together with previous reports showing that TZDs reduce lipolysis in these cells (18-22), we propose the following model for the anti-lipolytic effect of TZDs in adipocytes. Administration of TZDs to mature adipocytes activates PPARγ leading to increased transcription of GPR81 and GPR109A (and GPR109B in humans) and subsequent increase in protein expression of both receptors. GPR109A and GPR81 couple to members of the G_i family of G proteins (39;45). In adipocytes activation of G_i preferentially results in the inhibition of adenylyl cyclases, which counteracts the activity of pro-lipolytic receptors (e.g. β-adrenergic and glucagon receptors). As a result, intracellular cAMP levels will be lowered and Protein kinase A will be less active. PKA phosphorylates a number of proteins, most notably hormone sensitive lipase (HSL) and perilipin, which are required for hydrolysis of TAGs. Phosphorylation of perilipin allows access to the TAG containing droplets by the

now activated HSL and a second lipase, ATGL, which hydrolyses the TAG in FFA and glycerol. Our data in mature 3T3-L1 adiopocytes suggest that the PPARγ-mediated upregulation of Gpr81 and Gpr109A contributes to the anti-lipolytic action of TZDs *in vitro*. It is therefore tantalizing to speculate that also *in vivo* the insulin-sensitizing, antidiabetic and hypolipidemic actions of TZDs are partly mediated via PPARγ-mediated upregulation of the Gpr81 and Gpr109A genes in rodents and the GPR81, GPR109A and GPR109B genes in humans. Investigations on the effects of TZDs in Gpr81 knockout mice, Gpr109A knock out mice and double knock out animals will help to establish the importance of these GPCRs in mediating the lipid lowering effects of these drugs.

Acknowledgements
This work was partly funded by a short-term fellowship of the Federation of European Biochemical Societies (to E.H.J). We thank Shohreh Keshtkar and Dr. Guido Hooiveld (Nutrition, Metabolism & Genomics group, Wageningen University, Wageningen, The Netherlands) for their help with micro-array analysis and Dr. Thomas Åskov Pedersen (Department of Biochemistry and Molecular Biology, University of Southern Denmark, Odense, Denmark) for his help in analysing the ChIP seq data.

References

1. James WP 2008 The epidemiology of obesity: the size of the problem. J Intern Med 263:336-352
2. Rosen ED, Spiegelman BM 2006 Adipocytes as regulators of energy balance and glucose homeostasis. Nature 444:847-853
3. Duncan RE, Ahmadian M, Jaworski K, Sarkadi-Nagy E, Sul HS 2007 Regulation of lipolysis in adipocytes. Annu Rev Nutr 27:79-101
4. Reynisdottir S, Langin D, Carlstrom K, Holm C, Rossner S, Arner P 1995 Effects of weight reduction on the regulation of lipolysis in adipocytes of women with upper-body obesity. Clin Sci (Lond) 89:421-429
5. Large V, Peroni O, Letexier D, Ray H, Beylot M 2004 Metabolism of lipids in human white adipocyte. Diabetes Metab 30:294-309
6. Jensen MD, Haymond MW, Rizza RA, Cryer PE, Miles JM 1989 Influence of body fat distribution on free fatty acid metabolism in obesity. J Clin Invest 83:1168-1173
7. Hotamisligil GS, Shargill NS, Spiegelman BM 1993 Adipose expression of tumor necrosis factor-alpha: direct role in obesity-linked insulin resistance. Science 259:87-91
8. Bays H, Mandarino L, DeFronzo RA 2004 Role of the adipocyte, free fatty acids, and ectopic fat in pathogenesis of type 2 diabetes mellitus: peroxisomal proliferator-activated receptor agonists provide a rational therapeutic approach. J Clin Endocrinol Metab 89:463-478
9. Lehrke M, Lazar MA 2005 The many faces of PPARγ. Cell 123:993-999
10. Glass CK, Rosenfeld MG 2000 The coregulator exchange in transcriptional functions of nuclear receptors. Genes Dev 14:121-141
11. Lehmann JM, Moore LB, Smith-Oliver TA, Wilkison WO, Willson TM, Kliewer SA 1995 An antidiabetic thiazolidinedione is a high affinity ligand for peroxisome proliferator-activated receptor γ (PPAR γ). J Biol Chem 270:12953-12956
12. Nielsen R, Pedersen TA, Hagenbeek D, Moulos P, Siersbaek R, Megens E, Denissov S, Borgesen M, Francoijs KJ, Mandrup S, Stunnenberg HG 2008 Genome-wide profiling of PPAR{γ}:RXR and RNA polymerase II occupancy reveals temporal activation of distinct metabolic pathways and changes in RXR dimer composition during adipogenesis. Genes Dev 22:2953-2967
13. Boden G 1997 Role of fatty acids in the pathogenesis of insulin resistance and NIDDM. Diabetes 46:3-10
14. Dalen KT, Schoonjans K, Ulven SM, Weedon-Fekjaer MS, Bentzen TG, Koutnikova H, Auwerx J, Nebb HI 2004 Adipose tissue expression of the lipid droplet-associating proteins S3-12 and perilipin is controlled by peroxisome proliferator-activated receptor-γ. Diabetes 53:1243-1252
15. Kershaw EE, Schupp M, Guan HP, Gardner NP, Lazar MA, Flier JS 2007 PPARγ regulates adipose triglyceride lipase in adipocytes in vitro and in vivo. Am J Physiol Endocrinol Metab 293:E1736-E1745
16. Yajima H, Kobayashi Y, Kanaya T, Horino Y 2007 Identification of peroxisome-proliferator responsive element in the mouse HSL gene. Biochem Biophys Res Commun 352:526-531
17. Tan GD, Debard C, Tiraby C, Humphreys SM, Frayn KN, Langin D, Vidal H, Karpe F 2003 A "futile cycle" induced by thiazolidinediones in human adipose tissue? Nat Med 9:811-812
18. Lenhard JM, Kliewer SA, Paulik MA, Plunket KD, Lehmann JM, Weiel JE 1997 Effects of troglitazone and metformin on glucose and lipid metabolism: alterations of two distinct molecular pathways. Biochem Pharmacol 54:801-808
19. Wang P, Renes J, Bouwman F, Bunschoten A, Mariman E, Keijer J 2007 Absence of an adipogenic effect of rosiglitazone on mature 3T3-L1 adipocytes: increase of lipid catabolism and reduction of adipokine expression. Diabetologia 50:654-665
20. McTernan PG, Harte AL, Anderson LA, Green A, Smith SA, Holder JC, Barnett AH, Eggo MC, Kumar S 2002 Insulin and rosiglitazone regulation of lipolysis and lipogenesis in human adipose tissue in vitro. Diabetes 51:1493-1498
21. Souza SC, Yamamoto MT, Franciosa MD, Lien P, Greenberg AS 1998 BRL 49653 blocks the lipolytic actions of tumor necrosis factor-alpha: a potential new insulin-sensitizing mechanism for

thiazolidinediones. Diabetes 47:691-695
22. Okazaki H, Osuga J, Tamura Y, Yahagi N, Tomita S, Shionoiri F, Iizuka Y, Ohashi K, Harada K, Kimura S, Gotoda T, Shimano H, Yamada N, Ishibashi S 2002 Lipolysis in the absence of hormone-sensitive lipase: evidence for a common mechanism regulating distinct lipases. Diabetes 51:3368-3375
23. Tamori Y, Masugi J, Nishino N, Kasuga M 2002 Role of peroxisome proliferator-activated receptor-γ in maintenance of the characteristics of mature 3T3-L1 adipocytes. Diabetes 51:2045-2055
24. Miles JM, Wooldridge D, Grellner WJ, Windsor S, Isley WL, Klein S, Harris WS 2003 Nocturnal and postprandial free fatty acid kinetics in normal and type 2 diabetic subjects: effects of insulin sensitization therapy. Diabetes 52:675-681
25. Boden G, Cheung P, Mozzoli M, Fried SK 2003 Effect of thiazolidinediones on glucose and fatty acid metabolism in patients with type 2 diabetes. Metabolism 52:753-759
26. Mayerson AB, Hundal RS, Dufour S, Lebon V, Befroy D, Cline GW, Enocksson S, Inzucchi SE, Shulman GI, Petersen KF 2002 The effects of rosiglitazone on insulin sensitivity, lipolysis, and hepatic and skeletal muscle triglyceride content in patients with type 2 diabetes. Diabetes 51:797-802
27. Racette SB, Davis AO, McGill JB, Klein S 2002 Thiazolidinediones enhance insulin-mediated suppression of fatty acid flux in type 2 diabetes mellitus. Metabolism 51:169-174
28. Ausubel FM, Brent R, Kingston R, Moore D, Seidman JJ, Smith J, Struhl K 1993 Current Protocols in Molecular Biology. New York: John Wiley & Sons
29. Jeninga EH, van Beekum O, van Dijk AD, Hamers N, Hendriks-Stegeman BI, Bonvin AM, Berger R, Kalkhoven E 2007 Impaired peroxisome proliferator-activated receptor γ function through mutation of a conserved salt bridge (R425C) in familial partial lipodystrophy. Mol Endocrinol 21:1049-1065
30. Wabitsch M, Brenner RE, Melzner I, Braun M, Moller P, Heinze E, Debatin KM, Hauner H 2001 Characterization of a human preadipocyte cell strain with high capacity for adipose differentiation. Int J Obes Relat Metab Disord 25:8-15
31. Rodriguez AM, Elabd C, Delteil F, Astier J, Vernochet C, Saint-Marc P, Guesnet J, Guezennec A, Amri EZ, Dani C, Ailhaud G 2004 Adipocyte differentiation of multipotent cells established from human adipose tissue. Biochem Biophys Res Commun 315:255-263
32. Stienstra R, Duval C, Keshtkar S, van der LJ, Kersten S, Muller M 2008 Peroxisome proliferator-activated receptor γ activation promotes infiltration of alternatively activated macrophages into adipose tissue. J Biol Chem 283:22620-22627
33. Nielsen R, Grontved L, Stunnenberg HG, Mandrup S 2006 Peroxisome proliferator-activated receptor subtype- and cell-type-specific activation of genomic target genes upon adenoviral transgene delivery. Mol Cell Biol 26:5698-5714
34. Lee DK, Nguyen T, Lynch KR, Cheng R, Vanti WB, Arkhitko O, Lewis T, Evans JF, George SR, O'Dowd BF 2001 Discovery and mapping of ten novel G protein-coupled receptor genes. Gene 275:83-91
35. Wise A, Foord SM, Fraser NJ, Barnes AA, Elshourbagy N, Eilert M, Ignar DM, Murdock PR, Steplewski K, Green A, Brown AJ, Dowell SJ, Szekeres PG, Hassall DG, Marshall FH, Wilson S, Pike NB 2003 Molecular identification of high and low affinity receptors for nicotinic acid. J Biol Chem 278:9869-9874
36. Tunaru S, Kero J, Schaub A, Wufka C, Blaukat A, Pfeffer K, Offermanns S 2003 PUMA-G and HM74 are receptors for nicotinic acid and mediate its anti-lipolytic effect. Nat Med 9:352-355
37. Soga T, Kamohara M, Takasaki J, Matsumoto S, Saito T, Ohishi T, Hiyama H, Matsuo A, Matsushime H, Furuichi K 2003 Molecular identification of nicotinic acid receptor. Biochem Biophys Res Commun 303:364-369
38. Schaub A, Futterer A, Pfeffer K 2001 PUMA-G, an IFN-γ-inducible gene in macrophages is a novel member of the seven transmembrane spanning receptor superfamily. Eur J Immunol 31:3714-3725
39. Ge H, Weiszmann J, Reagan JD, Gupte J, Baribault H, Gyuris T, Chen JL, Tian H, Li Y 2008 Elucidation of signaling and functional activities of an orphan GPCR, GPR81. J Lipid Res 49:797-

803
40. Taggart AK, Kero J, Gan X, Cai TQ, Cheng K, Ippolito M, Ren N, Kaplan R, Wu K, Wu TJ, Jin L, Liaw C, Chen R, Richman J, Connolly D, Offermanns S, Wright SD, Waters MG 2005 (D)-beta-Hydroxybutyrate inhibits adipocyte lipolysis via the nicotinic acid receptor PUMA-G. J Biol Chem 280:26649-26652
41. Cai TQ, Ren N, Jin L, Cheng K, Kash S, Chen R, Wright SD, Taggart AK, Waters MG 2008 Role of GPR81 in lactate-mediated reduction of adipose lipolysis. Biochem Biophys Res Commun %19;377:987-991
42. Liu C, Wu J, Zhu J, Kuei C, Yu J, Shelton J, Sutton SW, Li X, Yun SJ, Mirzadegan T, Mazur C, Kamme F, Lovenberg TW 2008 Lactate inhibits lipolysis in fat cells through activation of an orphan G-protein coupled receptor, GPR81. J Biol Chem
43. Boyd AE, III, Giamber SR, Mager M, Lebovitz HE 1974 Lactate inhibition of lipolysis in exercising man. Metabolism 23:531-542
44. De Pergola G, Cignarelli M, Nardelli G, Garruti G, Corso M, Di Paolo S, Cardone F, Giorgino R 1989 Influence of lactate on isoproterenol-induced lipolysis and beta-adrenoceptors distribution in human fat cells. Horm Metab Res 21:210-213
45. Offermanns S 2006 The nicotinic acid receptor GPR109A (HM74A or PUMA-G) as a new therapeutic target. Trends Pharmacol Sci 27:384-390
46. Hauser S, Adelmant G, Sarraf P, Wright HM, Mueller E, Spiegelman BM 2000 Degradation of the peroxisome proliferator-activated receptor γ is linked to ligand-dependent activation. J Biol Chem 275:18527-18533
47. Sandelin A, Wasserman WW 2005 Prediction of nuclear hormone receptor response elements. Mol Endocrinol 19:595-606
48. Barroso I, Gurnell M, Crowley VE, Agostini M, Schwabe JW, Soos MA, Maslen GL, Williams TD, Lewis H, Schafer AJ, Chatterjee VK, O'Rahilly S 1999 Dominant negative mutations in human PPARγ associated with severe insulin resistance, diabetes mellitus and hypertension. Nature 402:880-883
49. Rosen ED, Spiegelman BM 2001 PPARγ : a nuclear regulator of metabolism, differentiation, and cell growth. J Biol Chem 276:37731-37734
50. Lefterova MI, Zhang Y, Steger DJ, Schupp M, Schug J, Cristancho A, Feng D, Zhuo D, Stoeckert CJ, Jr., Liu XS, Lazar MA 2008 PPAR{γ} and C/EBP factors orchestrate adipocyte biology via adjacent binding on a genome-wide scale. Genes Dev 22:2941-2952
51. West AG, Fraser P 2005 Remote control of gene transcription. Hum Mol Genet 14 Spec No 1:R101-11.:R101-R111

Chapter 6

Peroxisome Proliferator-Activated receptor γ (PPARγ) regulates expression of the E3 ubiqituin ligase RNF125 (RNF125/Rnf125)

Ellen H. Jeninga[1,2], Anne Bugge[3], Ronni Nielsen[3], Sander Kersten[4], Ruud Berger[1,2], Susanne Mandrup[3] and Eric Kalkhoven[1,2,5]

[1]Dept. Metabolic & Endocrine Diseases, UMC Utrecht, Utrecht, The Netherlands; [2]Netherlands Metabolomics Centre, Utrecht, The Netherlands; [3]Dept. of Biochemistry & Molecular Biology, University of Southern Denmark, Odense, Denmark; [4]Nutrition, Metabolism & Genomics group, Wageningen University, Wageningen, The Netherlands; [5]Dept. of Pediatric Immunology, UMC Utrecht, Utrecht, The Netherlands

Manuscript in preparation

Abstract

PPARγ, a member of the nuclear receptor superfamily of ligand-inducible transcription factors, plays a keyrole in the differentiation, maintenance and function of adipocytes and is the molecular target for the insulin-sensitizing TZDs. Despite the fact that a number of PPARγ target genes have been characterized, the underlying molecular mechanisms whereby TZDs improve insulin sensitivity remain unclear. In order to unravel mechanisms by which TZD action in adipocytes influences insulin sensitivity, we searched for novel PPARγ target genes using transcriptome analysis in human adipocytes treated with the TZD rosiglitazone. We identified the E3 ubiquitin ligase ring finger protein 125 (RNF125/TRAC-1) as a novel PPARγ target gene. We demonstrate that rosiglitazone rapidly induced the expression of RNF125/Rnf125 in both human and murine adipocytes and that the expression of Rnf125 increased subsequent to PPARγ expression during adipocyte differentiation of 3T3-L1 cells. Furthermore, ChIP-seq analysis in differentiated 3T3-L1 adipocytes revealed three PPARγ:RXR binding sites in the promoter of the *Rnf125* gene and binding of PPARγ/RXR heterodimers to all three was confirmed by ChIP-PCR and EMSA. As ubiquitination has been implicated in the regulation as well as activation of proteasome-dependent degradation of target proteins, the direct regulation of E3 ubiquitin ligases such as RNF125 by PPARγ presents a novel mechanism by which TZDs may exert their insulin-sensitizing effects.

Introduction

The incidence of obesity is increasing dramatically in industrialized countries and this is a major health concern as it comes with pathological consequences such as type 2 diabetes and cardiovascular disease (1-3). Adipose tissue is the major site for storage of lipids and plays an essential role in regulating whole body lipid and glucose homeostasis. Supporting this notion, loss of adipose tissue in lipodystrophy as well as its expansion in obesity both result in metabolic pathologies. One of the key regulators in adipocyte differentiation, maintenance and function is the peroxisome proliferator activated receptorγ (PPARγ), a ligand inducible nuclear hormone receptor (4;5). PPARγ exists in two isoforms, PPARγ1 and PPARγ2, which are derived from the *PPARG* gene by differential promoter usage and/or mRNA splicing. PPARγ2 has an additional 30 amino acids at the N-terminus and its expression is restricted to adipose tissue, whereas PPARγ1 is more ubiquitously expressed. An important role for PPARγ in adipogenesis has been established by several *in vitro* and *in vivo* studies showing that it is both necessary and sufficient to induce adipogenesis (6-9). PPARγ binds to retinoic acid X receptors (RXRs) and as obligate heterodimers to PPAR responsive elements (PPREs), which are often degenerate variants of two direct repeats of 6 nucleotides (AGGTCA) interspaced by one nucleotide (DR-1) (1). In the absence of ligand most heterodimers are bound to DNA in association with corepressors, histone deacetylases and chromatin remodelers to maintain active repression of target genes (10). Ligand binding stabilizes the active conformation of the receptor resulting in the release of corepressors and subsequent recruitment of coactivators thereby initiating a cascade of protein interactions and modifications that finally results in the induction of specific target genes (10). Although a range of naturally occurring compounds including polyunsaturated fatty acids and eicosanoids (11;12) can activate PPARγ, the physiological relevance of these compounds has to be determined. In addition, PPARγ is the molecular target of the insulin sensitizing thiazoledinediones (TZDs) (13). TZD treatment has been shown to improve systemic insulin sensitivity in diabetic animal models and humans (14). The primary mode of action of TZDs is thought to occur through the direct regulation of a number of adipocyte-specific genes, including genes involved in adipocyte differentiation, lipid uptake, lipid droplet stabilization and lipid and glucose metabolism (15). Next to these effects, TZDs have been shown to induce an anti-inflammatory response. At least part of the anti inflammatory effects are thought to be mediated through the transrepression of NF-κB either by PPAR-independent (16;17) or PPAR-dependent mechanisms (18;19), resulting in decreased expression of target genes for cytokines and growth factors.

To further unravel the mechanisms by which TZDs mediate their insulin sensitizing effects in adipocytes, we performed a micro-array analysis in human differentiated adipocytes treated with the TZD rosiglitazone for 6 hours. We show that rosiglitazone

rapidly induced the expression of the E3 ubiquitin ligase RNF125/Rnf125 in both human and murine adipocytes. ChIP-seq analysis revealed three PPARγ:RXR binding sites in the promoter of the *Rnf125* gene, two of these are located in the distal promoter (>25 Kb upstream of the TSS) and the third one in close proximity of the TSS. To our knowledge this is the first report showing that TZD mediated activation of PPARγ induces the expression of an E3 ubiquitin ligase.

Materials and methods

Materials

Rosiglitazone was purchased from Alexis. Anti-PPARγ antibody (2345S) was from Cell Signalling, anti-RNF125 antibody was a kind gift from Dr. Arimoto (20) and anti-tubulin (T5168) was from Sigma. Anti-PPARγ (sc-7196) and anti-RXR (sc-774) were used for ChIP assays. Anti-PPARγ (sc-7273), anti-RXRα (sc-553) and anti-Gal4 (sc-510) antibodies used for EMSA were from Santa Cruz Biotechnologies.

Plasmids

All recombinant DNA work was performed according to standard procedures (21). The murine Rnf125 reporter, Rnf125(-1100/+68)-luc, was generated by inserting the respective promoter into KpnI/BglII site of the PGL3-basic vector (Promega). All mutations were generated by Quickchange mutagenesis (Stratagene) and verified by sequencing. All other plasmids have been described earlier (22).

Cell culture and differentiation

The human osteosarcoma cell line U2OS was maintained in DMEM Glutamax (Dulbecco) containing 10% foetal calf serum (Gibco Life Technologies), 100 μg /ml penicillin and 100 μg/ml streptomycin (Gibco Life Technologies). The murine 3T3-L1 cell line was cultured in the same media but now with 10% bovine serum (Gibco Life Technologies), 100 μg/ml penicillin and 100 μg/ml streptomycin (Gibco Life Technologies). Two days post-confluence (day 0) cells were induced to differentiate by changing the medium to culture medium containing 3-isobutyl-1-methylxanthine (IBMX; 500 μM), Dexamethasone (Dex; 1 μM) and insulin (1 μg/ml). After 48 hours (day 2) the medium was replaced by culture medium supplemented with insulin (1 μg/ml) and maintained for 4 days. The human multipotent adipose derived stem cells (hMADs) were maintained in DMEM low glucose (Dulbecco) supplemented with 10% foetal calf serum (Gibco Life Technologies), 100 μg of penicillin/ml and 100 μg streptomycin/ml (Gibco Life Technologies). When cells reached confluence (day 0), medium was replaced by DMEM/Ham's F12 (1/1) containing insulin (5 μg/ml), human transferrin (10 μg/ml), T3 (0,2 nM), rosiglitazone (0,5 μM), Dex (1 μM), IBMX (100 μM). At day 3 the medium was changed for DMEM/Ham's

F12 (1/1) supplemented with insulin (5 μg/ml), human transferrin (10 μg/ml), T3 (0,2 nM) and rosiglitazone (0,5 μM). At day 10, medium was replaced by DMEM/ Ham's F12 (50/50) medium containing insulin (5 μg/ml), human transferrin (10 μg/ml) and T3 (0,2 nM) and cells were left for a week. The human Simpson-Golabi Behmel Syndrome cell line (SGBS) was maintained in DMEM Glutamax (Dulbecco) supplemented with 10% foetal calf serum (Gibco Life Technologies), 100 μg of penicillin/ml and 100 μg streptomycin/ml (Gibco Life Technologies). When cells reached confluence (day 0) the medium was replaced by DMEM/ Nutrient Mix F12 (1/1) containing biotin (33 mM), pantothenate (17 mM), insulin (20 nM), human transferring (10 μg/ml), cortisol (100 nM), T3 (0,2 nM), Dex (25 nM), IBMX (500 μM) and rosiglitazone (2 μM). At day 4 DMEM/Nutrient Mix F12 (1/1) medium containing biotin (33 mM), pantothenate (17 mM), insulin (20 nM), human transferring (10 μg/ml), cortisol (100 nM) and T3 (0.2 nM) was added and cells were grown for an additional 4 days.

Micro-array

3T3-L1, SGBS and hMADs were differentiated as described above and at day 6, 8 and 17 respectively treated with Rosiglitazone or DMSO for 6 hours. Micro-array experiments were performed as described before (23). In short, total RNA was isolated using TRIzol reagent. Concentrations and purity were determined on a NanoDrop ND-1000 spectrophotometer (Isogen). RNA integrity was checked on an Agilent 2100 bioanalyzer (Agilent Technologies) with 6000 Nano Chips. Part of the RNA samples from four 6 cm dishes was used for quantitative RT-PCR (see RT-PCR section). Remaining RNA samples from four 6 cm dishes were pooled and used for micro-array analysis. Samples were hybridized on Human NUGO arrays from Affymetrix. A detailed description of the analysis method is available on request.

RNA isolation and real-time PCR

3T3-L1 fibroblasts were differentiated as described above. Three independent samples of total RNA were extracted at different time points using TRIzol reagent (Invitrogen). cDNA was synthesized using the superscript first strand synthesis system (Invitrogen) according to manufacturer's protocol. Gene expression levels were determined by quantitative real-time PCR with the MyIq cycler (Bio-Rad) using SYBR-green (Bio-Rad) and normalized to *TFIIb* expression. The primers used were murine TF-IIb forward primer; 5'-TCCTCCTCAGACCGCTTTT-3'; reverse primer, 5'-CCTGGTTCATCATCGC TAATC-3'; murine Rnf125 forward primer 5'-TCCATTTTGTCAGCGGGAACT-3'; reverse primer 5'-GGCTTTCATCAGGTCGTGAAT-3'; murine PPARγ forward primer, 5'- CGCTGATGCACTGCCTATGA-3'; reverse primer, 5'- AGAGGTCCAC AGAGCTGATTCC-3'.; human 36B4 forward primer, 5'-CGGGAAGGC TGTGGTGCTG-3'; reverse primer 5'- GTGAACACAAAGCCCACATTCC-3'; human RNF125 forward primer; 5'- TACCCGATGAGAATTCCAAGC-3';

reverse primer 5′-TCTTCGGATAAGAGCTTCCTCA-3′.

Western blot analysis
For Western blot analyses, differentiated 3T3-L1 cells were lysed in 2X Laemli sample buffer and subjected to SDS-PAGE and transferred to Immobilon membranes (Millipore). α-PPARγ, α-RNF125 and α-tubulin antibodies were used to probe for the respective proteins. ECL Plus (Perkin Elmer) was used for detection.

Chromatin immunoprecipitation (ChIP) and sequencing (ChIP-seq)
ChIP assays were performed as described earlier (24). Briefly, chromatin of 3T3-L1 preadipocytes (day 0) and differentiated adipocytes (day 6) was fragmented. Chromatin was incubated overnight at 4°C with Prot A beads (Amersham Biosciences), antibody against PPARγ or RXR and 1 μg/μl BSA. The next day after extensive washing chromatin was eluted from the beads and decrosslinked overnight at 65°C at 950 rpm. Subsequently, chromatin was purified using phenol:chloroform extraction and precipitated. Precipitated DNA was solved in water and analyzed using quantitative RT-PCR. The primers used for ChIP assays were as follows: murine RNF125 PPRE A forward primer 5′-AGCTGCTGTCTGGAAATGGT-3′; reverse primer 5′-TGCCTGAGTAGTCACCAGCTT-3′; murine RNF125 PPRE B forward primer 5′-AAGCCTGGGAGAGAGAGAGG-3′; reverse primer 5′-CTAGGCAAGGCACTTTGCTG-3′; murine RNF125 PPRE C forward primer 5′-CCTCGTCTTGAAATATTGA-3′; reverse primer 5′-ACTCTATCCGGCCTCCAAGT-3′; murine beta-globin forward primer primer 5′-CCTGCCCTCTCTATCCTGTG-3′; reverse primer 5′-GCAAATGTGTTGCCAAAAAG-3′. ChIP-seq was performed as described earlier (15).

Reporter assays
U2OS cells were seeded in 24-wells plates and transiently transfected using the calcium-phosphate precipitation method. Each well was cotransfected with 1 μg reporter construct, 50 ng pCDNA-PPARγ or pCDNA (empty vector) and 2 ng pCMV-Renilla (Promega). The next day, cells were washed twice with HBS (pH 7.05) and subsequently maintained in medium in absence or presence of 1 μM Rosiglitazone for 24 hours. After incubation cells were washed twice with phosphate-buffered saline (PBS) and harvested in passive lysisbuffer (Promega) and assayed for luciferase activity according to the manufacturer's protocol (Promega Dual-Luciferase Reporter Assay System) and for Renilla luciferase activity to correct for transfection efficiency. The relative light units were measured by a Centro LB 960 luminometer (Berthold Technologies).

EMSA
EMSAs were performed as described earlier (22). The sequences of the double-stranded DNA oligomers, containing the wild type or mutant PPRE from the

mouse Rnf125 promoter used, were as follows: mRNF125 PPRE A -wild-type, 5'- CCGGGGAGTGGGGAAAGGGTCAGGC -3' and mRNF125 PPRE A -mutant, 5'- CCGGGGAGTGCCGAAAGCCTCAGGC -3'; mRNF125 PPRE B -wild-type, 5'- CCGGGCAGCAGGAATTAGGTCATTG -3' and mRNF125 PPRE B -mutant, 5'- CCGGGCAGCACCAATTACCTCATTG -3'; mRNF125 PPRE C -wild-type, 5'- CCGGCTAAATGGTCATAGGTCGGCT -3' and mRNF125 PPRE C -mutant, 5'- CC GGCTAAATCCTCATACCTCGGCT -3'.

Results

PPARγ regulates the expression of RNF125 in adipocytes

In order to identify novel TZD-regulated genes in mature human adipocytes, we performed transcriptome analysis in differentiated human multipotent adipose derived stem cells (hMADs) (25) stimulated with the TZD rosiglitazone for 6 hours. Out of a number of upregulated genes, the 10 genes with the highest fold induction are listed in Table 1. Among these genes are the already identified PPARγ target genes, UCP-1 (26), PCK1 (27), PDK4 (28) and the recently identified GPR109B (chapter 5). Out of these 10 highly upregulated genes we selected the E3 ubiquitin ligase RNF125 to investigate in more detail. First, we confirmed this regulation of RNF125 mRNA expression in differentiated hMADs cells treated with rosiglitazone for 6 hours using quantitative RT-PCR (Figure 1A). The same experiment was performed in another human adipocyte cell line, the Simpson-Golabi Behmel syndrome (SGBS) cell line (29). In these cells RNF125 mRNA expression also increased upon rosiglitazone treatment, albeit to a lesser extent then observed in hMADs (Figure 1A). To examine whether the regulation of Rnf125 is conserved in mouse adipocytes, we performed the same experiment in the murine adipocyte cell line, 3T3-L1. Like for the human mature adipocytes, the mRNA expression level of

	Gene name	Description	Fold induction
1	UCP-1	uncoupling protein 1	54
2	PKP2	plakophilin 2	21
3	MAGEE2	melanoma antigen family E, 2	14
4	PCK1	phosphoenolpyruvate carboxykinase 1	11
5	RNF125	ring finger protein 125	10
6	PDK4	pyruvate dehydrogenase kinase, isozyme 4	8
7	DLL1	delta-like 1	7
8	ST3GAL4	ST3 beta-galactoside alpha-2,3-sialyltransferase 4	7
9	GPR109B	G protein-coupled receptor 109B	5
10	STX11	syntaxin 11	5

Table 1. List of most upregulated annotated genes.
Transcriptome analysis in differentiated hMADs stimulated or not with rosiglitazone for 6 hours was performed. Of the annotated genes that were significantly upregulated, the 10 genes with the highest induction are listed.

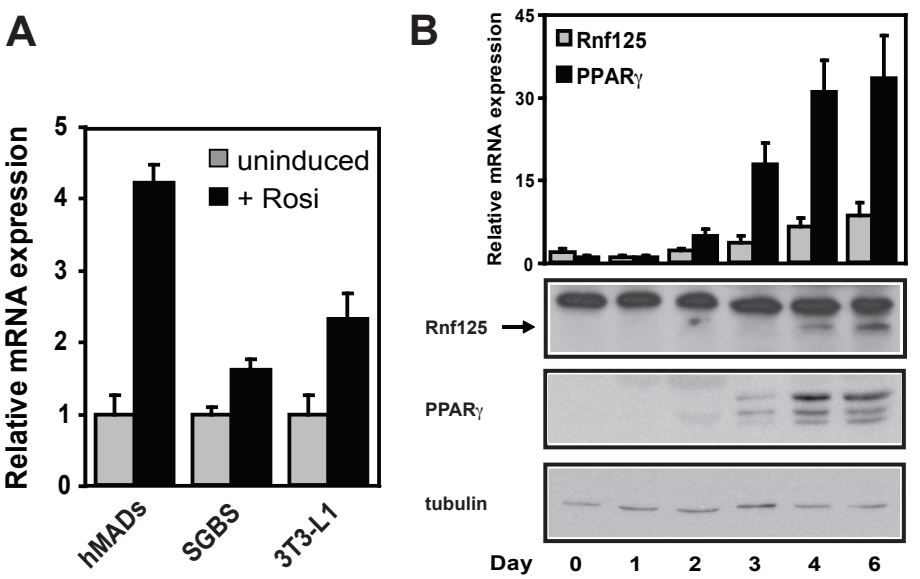

Figure 1. RNF125/Rnf125 expression is induced by the PPARγ ligand rosiglitazone in mature adipocytes and during adipogenesis.
A, mRNA expression levels in human (hMADs and SGBS) and murine (3T3-L1) adipocytes treated with 1 μM rosiglitazone for 6 hours. Relative mRNA expression levels were related to untreated cells and normalized for the 36B4 or TFIIb reference gene for human and murine adipocytes respectively. B, Rnf125 and PPARγ mRNA expression (upper panel) and protein expression (lower panel) at different time points of 3T3-L1 differentiation. Relative mRNA levels were related to undifferentiated 3T3-L1 cells at day 1 and normalized for the TFIIb reference gene. Tubulin was used as a loading control in Western blot analysis.

Rnf125 increased after rosiglitazone treatment of murine adipocytes (Figure 1A). Since PPARγ plays an essential role in adipogenesis and the expression of known PPARγ target genes increases during differentiation, we studied the mRNA and protein expression of Rnf125 during differentiation of 3T3-L1 preadipocytes into adipocytes. Rnf125 mRNA expression increases from day 2 of differentiation and this occured simultaneously with the increase in PPARγ mRNA expression during differentiation as determined by quantitative RT-PCR (Figure 1B). In addition, protein expression of Rnf125 and PPARγ was examined at the same time points. As shown in Figure 1B, Rnf125 protein expression could be detected from day 4 onwards, whereas PPARγ protein expression could be detected somewhat earlier (day 3; Figure 1B).
In conclusion, treatment of human and murine adipocytes with the TZD rosiglitazone induces mRNA expression of RNF125 and Rnf125, respectively. Furthermore, the mRNA and protein expression of Rnf125 increased during differentiation.

Endogenous PPARγ and RXRα bind to three different sites in the promoter of Rnf125

The rapid induction of RNF125/Rnf125 in mature adipocytes by rosiglitazone and the increase in mRNA and protein expression of Rnf125 following PPARγ expression during differentiation suggest a direct regulation of this gene by PPARγ. Therefore the next step in our analysis was to investigate whether PPARγ and its heterodimeric partner RXR are recruited to the promoter of the Rnf125 gene. Very recently, Nielsen et al. (15) reported a genome-wide analysis of PPARγ and RXR binding during differentiation of 3T3-L1 cells by ChIP sequencing. Detailed analysis of the region on chromosome 18 in which the Rnf125 gene is located revealed three PPARγ:RXR binding sites in differentiated 3T3-L1 cells (Figure 2A). Two of these sites (peak A and B) are located in the distal promoter region and one site (peak A) close to the transcriptional startsite (TSS) of Rnf125 isoform 1 (Figure 2A). Furthermore PPARγ and RXR peaks were absent in undifferentiated 3T3-L1 cells (day 0) in which PPARγ expression is low (data not shown). The recruitment of endogenous PPARγ and

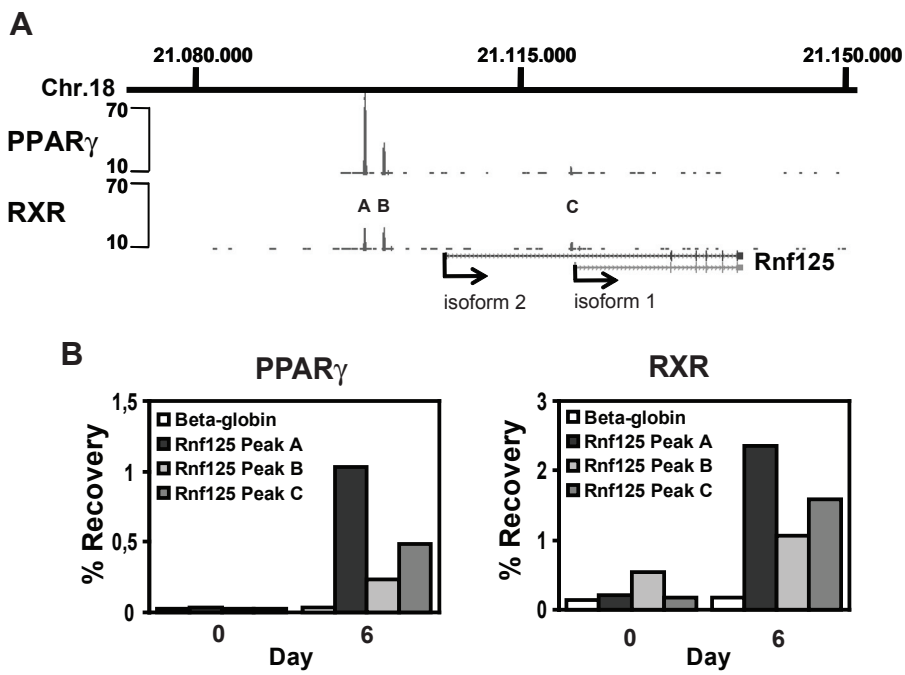

Figure 2. PPARγ and RXR are recruited to three different sites in the promoter of Rnf125.
A, ChIP-seq data of differentiated 3T3-L1 adipocytes (day 6) viewed in the UCSC browser showing PPARγ and RXR binding sites for Rnf125. On the x-axis the Rnf125 gene with its two transcripts, encoding isoform 1 (233 aa) and isoform 2 (140 aa) respectively, is indicated. On the y-axis, the Yaxis number that correlates to the number of sequences counted in a sliding window of 100 basepairs is indicated. B, ChIP-PCR for PPARγ and RXR was performed in undifferentiated (day 0) and differentiated (day 6) 3T3-L1 cells. The arbitrary beta-globin gene was used as a negative control. Results are expressed as % of immunoprecipitated chromatin compared to the input.

RXR to these sites in differentiated 3T3-L1 cells (day 6) was confirmed by ChIP-PCR (Figure 2B). In addition, recruitment of endogenous PPARγ and RXR to these sites in undifferentiated 3T3-L1 cells (day 0) in which PPARγ expression is low, as well as to an arbitrary gene (beta-globin) was negligible.
In summary, our ChIP-seq and ChIP-PCR data suggest binding of PPARγ/RXR heterodimers at three different sites in the promoter of the murine *Rnf125* gene in mature adipocytes.

Identification of PPREs upstream of the Rnf125 gene
In order to identify the PPREs in the promoter of Rnf125, we subjected the sequences underneath the peaks of the ChIP-seq data (Figure 2A) to an *in silico* promoter analysis (NHR scan; (30;30)). Potential PPREs were detected and are depicted in figure 3A. To establish if PPARγ/RXRα bound to these PPREs, we performed electrophoretic mobility shift assays using three different ^{32}P labelled probes containing the respective PPREs. As shown in figure 3B, PPARγ/RXRα heterodimers bind specifically to the PPREs (lane 4, 10 and 16 for PPRE A, B and C respectively), as formation of the protein-DNA complexes was abrogated by addition of an excess of unlabelled wild type PPRE (lane 5 (A), 11 (B) and 17 (C)), but not by an excess of unlabelled mutant PPRE (lane 6 (A), 12 (B) and 18 (C)). Furthermore, addition of specific antibodies against PPARγ and RXRα, but not an antibody directed against an irrelevant protein (Gal4), supershifted the protein-DNA complex, confirming the heterodimeric composition of the complex (Figure 3C). These results suggest that we identified three PPREs upstream of the *Rnf125* gene.

The conserved PPRE in the proximal promoter of Rnf125 (PPRE C) is functional
The identified PPRE (C) near the TSS of the murine Rnf125 encoding isoform 1 (Figure 2A) shares 85% sequence identity with a perfect PPRE in the TSS of the human RNF125 gene, as assessed by NHR scan (Figure 4A). As binding of the PPARγ/RXR heterodimer to PPRE C was confirmed *in vitro* (Figure 3B), the next step in our analysis was to asses whether this PPRE is functional *in vivo*. Therefore we fused the 5' flanking region and startsite of the mouse Rnf125 gene (-1100/+68) to a luciferase reporter. Cotransfection of human osteosarcoma (U2OS) cells with this reporter construct and expression vectors encoding PPARγ2 activated this reporter gene significantly compared to empty vector control (pCDNA), as shown in figure 4B. Addition of the PPARγ ligand rosiglitazone only slightly increased the activity of the reporter. Mutation of the PPRE reduced the PPARγ2 mediated activation of the reporter significantly in both the absence and presence of rosiglitazone (Figure 4B).
To investigate the regulation of this PPRE in the promoter of Rnf125 in more detail we tested the ability of the PPARγ1 isoform, as well as three PPARγ2 mutants to activate this reporter. Although PPARγ1 activated the reporter to a comparable level

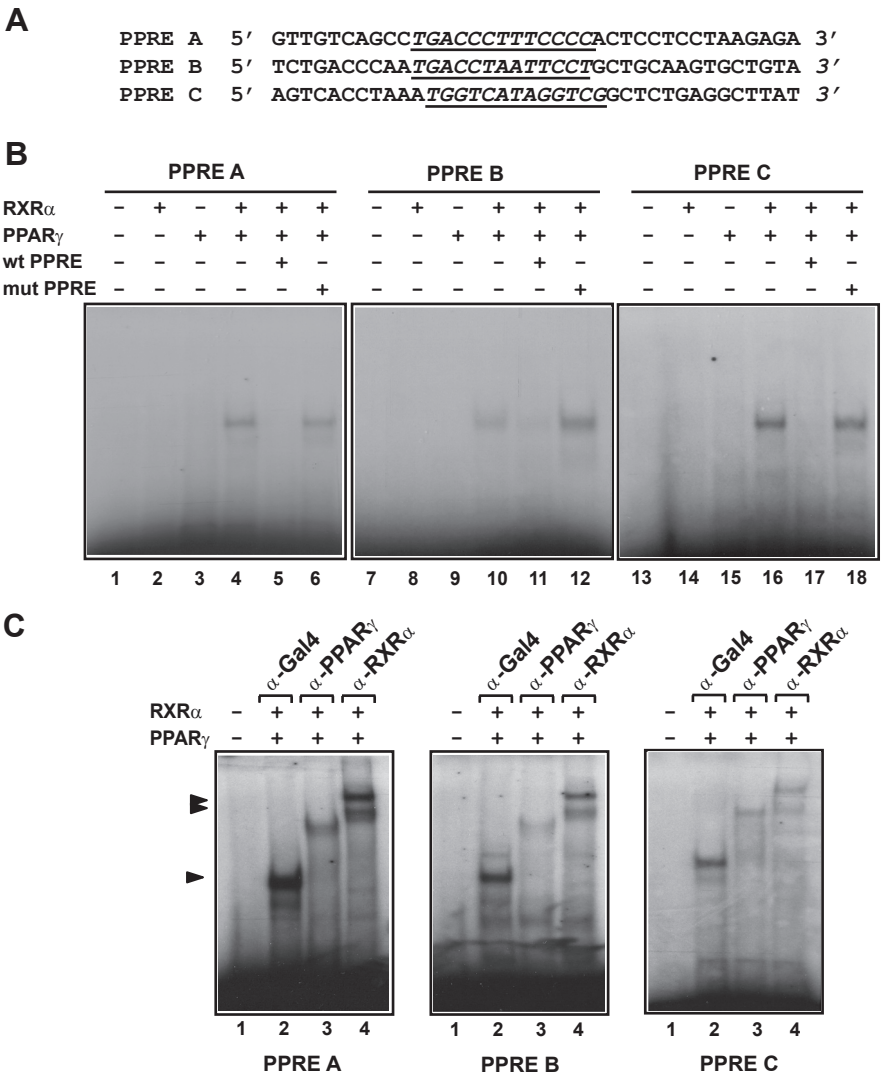

Figure 3. Identification of the three PPREs in the promoter of Rnf125.
A, A PPRE was predicted for each site in the promoter of Rnf125 by NHR scan. Electrophoretic mobility shift assays using ^{32}P labelled probes containing the respective PPREs incubated with *in vitro* translated PPARγ and/or RXRα proteins in the presence or absence of an excess of unlabelled wild type or mutant probe (B) or α-Gal4, α-PPARγ or α-RXRα antibody respectively (C). Protein-DNA complexes were separated from unbound DNA on non-denaturing polyacrylamide gels and visualized by autoradiography of dried gels.

as PPARγ2 in the absence of rosiglitazone, the activity of PPARγ1 was somewhat higher in the presence of rosigitazone compared to PPARγ2 (Figure 4C). In keeping with their activity on other promoters (22;31), the two natural PPARγ2 mutants R425C and P495L displayed reduced and negligible activity, respectively. The heterodimerization defective mutant L464R failed to activate the reporter (Figure 4C), confirming that dimerization of PPARγ and RXRα is a prerequisite for binding to the Rnf125 PPRE (Figure 3B and C).
Taken together these results suggest that binding of a PPARγ/RXR heterodimer to a conserved PPRE located in the proximal promoter (-384/ -366) of the Rnf125 gene controls the regulation of the gene.

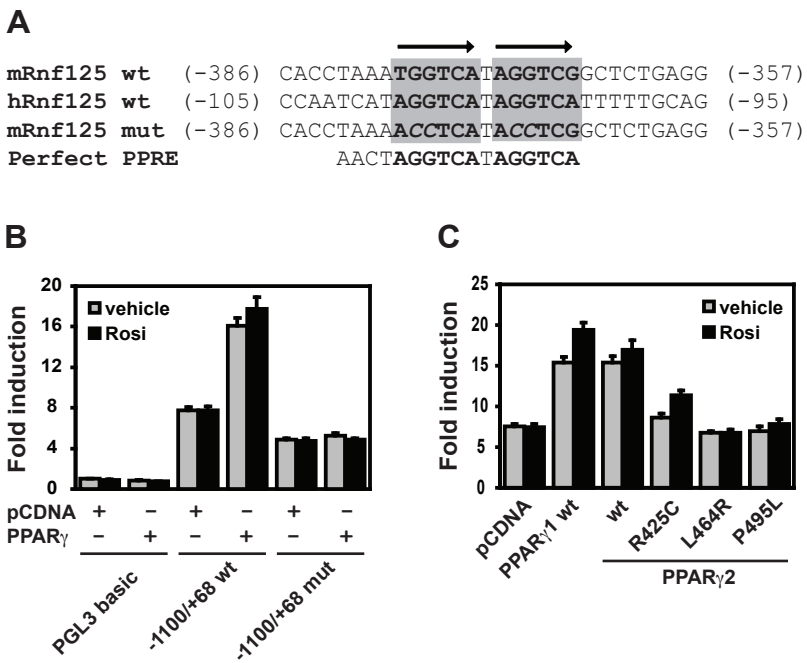

Figure 4. The conserved PPRE near the TSS of Rnf125 is functional in cells.
A, Alignment of the PPRE near the TSS of the murine Rnf125 and human RNF125 gene together with a perfect PPRE. B, Reporter assays were performed in U2OS cotransfected with a reporterconstruct (pGL3-Rnf125(-1100/+68)) containing wild type or mutant PPRE and empty (pCDNA) or PPARγ expression vectors. C, U2OS cells were transfected with Rnf125(-1100/+68) reporter together with expression vectors encoding PPARγ1 or PPARγ2 (wild type or mutant). Activation of the luciferase reporter in the presence or absence of 1 μM rosiglitazone is expressed as fold induction over that of empty reporter in the absence of 1 μM rosiglitazone after normalisation for Renilla luciferase activity.

Discussion

PPARγ plays an essential role in adipocytes, as it regulates adipocyte differentiation, maintenance and metabolism. The insulin-sensitizing TZDs have been shown to be high affinity ligands for PPARγ which improve systemic insulin sensitivity in diabetic animal models and humans (14). Although a number of PPARγ target genes that might contribute to the insulin sensitizing effects of TZDs have been identified during the last decade might, the underlying molecular mechanisms remain poorly understood. The data presented in this report indicate that the E3 ubiquitin ligase ring finger protein 125 (RNF125/Rnf125) is a novel direct PPARγ target gene. Interestingly, we identified three different PPARγ:RXR sites in the promoter of the *Rnf125* gene (Figure 2B and 3B), which according to Ensembl gives rise to two transcripts, encoding Rnf125 isoform 1 and Rnf125 isoform 2, proteins of 233 and 140 amino acids respectively (Supplemental figure 1). However, the existence of two Rnf125 isoforms is questionable since (i) the human and rat RNF125/Rnf125 gene have only one transcript encoding the long isoform (murine isoform 1; Supplemental figure 1), (ii) murine isoform 2 lacks the RING domain which has been shown to be required for E3 ligase activity (20;32), (iii) murine Rnf125 isoform 1 (Figure 1B), but not Rnf125 isoform 2 (data not shown) could be detected by Western blot analysis in 3T3-L1 adipocytes and moreover (iv) analysis of RNA polymerase II (RNAPII) occupancy, which provide a direct readout of transcriptional activation by transcription factors showed RNAPII occupancy in Rnf125 isoform 1, but not in the gene region assigned to isoform 2. These findings suggest that at least in adipocytes only Rnf125 isoform 1 is expressed. It is possible that this isoform is regulated by all three identified PPREs. Consistent with this hypothesis, recent studies have shown that only a small percentage of PPARγ:RXR target sites are located in the proximal promoter (<1 Kb upstream of TSS) and that many known PPARγ target genes contained multiple PPARγ:RXR binding sites in the promoter (15;33). In addition, Lefterova *et al.* showed that PPARγ:RXR sites in distal promoters might be functional as a large number of PPARγ:RXR sites located > 10 Kb from a TSS were enriched for H3K9Ac, a signature for enhancers (34), in adipocytes but not preadipocytes (33). In these cases transcription factors bound to distal sites might direct looping of the chromatin by which it brings coactivators and chromatin remodelers at the distal sites in proximity of the TSS of the target genes, thereby facilitating recruitment of RNA polymerase II (35).

To our knowledge this is the first report showing that PPARγ regulates an E3 ubiquitin ligase, indicating that PPARγ, next to regulation at a transcriptional level, may also regulate proteins at the post-translational level, at least by ubiquitination. The E3 ubiquitin ligase RNF125 was first identified in a retroviral vector-based T cell surface activation marker screen and therefore also named TRAC-1 (T cell RING (really interesting new) protein identified in activation screen) (36). Highest expression of RNF125 was observed in spleen, liver, thymus and peripheral blood

lymphocytes (32;36), but in these reports adipose tissue was not tested. RNF125 has been shown to function as a positive regulator of the T-cell response (TCR) in T-cells (32) and to down-modulate HIV-1 replication in primary peripheral blood mononuclear cells (PBMC) (37). In addition, RNF125 has been shown to inhibit pathogen induced cytokine production by RIG signalling through ubiquitin conjugation to RIG-I (retinoic acid-inducible gene I) itself, as well as to MDA5 (a protein related to RIG-I) and IPS-1 (a downstream protein of RIG-I signalling) (20). Interestingly, this group also showed a substantial increase in the release of the cytokine IFNγ in the presence of polyI:C after siRNA mediated knockdown of Rnf125 in MEFs, which are capable to differentiate into mature adipocytes. Since it is known that TZDs induce an anti-inflammatory response in adipocytes, it is possible that this occurs by PPARγ mediated upregulation of RNF125. Alternatively, RNF125 might modulate the activity or degradation of important adipocyte specific proteins. Further studies aimed at identifying the substrates for RNF125 in adipocytes are needed to understand the relevance of TZD induced PPARγ mediated regulation of this gene.

Acknowledgements
We thank Shohreh Keshtkar and Dr. Guido Hooiveld (Nutrition, Metabolism & Genomics group, Wageningen University, Wageningen, The Netherlands) for their help with micro-array analysis and Dr. Thomas Askov Pedersen (Department of Biochemistry and Molecular Biology, University of Southern Denmark, Odense, Denmark) for his help in analysing the ChIP seq data. We would also like to thank Dr. Christian Dani and Prof. Dr. Martin Wabitsch for the hMADs and SGBS cell lines, respectively and Prof. H.G. Stunnenberg for sharing ChIP-seq data prior to publication. This work was partly funded by a short-term fellowship of the Federation of European Biochemical Societies (to E.H.J).

References

1. IJpenberg A, Jeannin E, Wahli W, Desvergne B 1997 Polarity and specific sequence requirements of peroxisome proliferator-activated receptor (PPAR)/retinoid X receptor heterodimer binding to DNA. A functional analysis of the malic enzyme gene PPAR response element. J Biol Chem 272:20108-20117
2. James WP 2008 The epidemiology of obesity: the size of the problem. J Intern Med 263:336-352
3. Hossain P, Kawar B, El Nahas M 2007 Obesity and diabetes in the developing world--a growing challenge. N Engl J Med 356:213-215
4. Anghel SI, Wahli W 2007 Fat poetry: a kingdom for PPARgamma. Cell Res 17:486-511
5. Tontonoz P, Spiegelman BM 2008 Fat and beyond: the diverse biology of PPARgamma. Annu Rev Biochem 77:289-312
6. Tontonoz P, Hu E, Spiegelman BM 1994 Stimulation of adipogenesis in fibroblasts by PPAR gamma 2, a lipid-activated transcription factor. Cell 79:1147-1156
7. Barak Y, Nelson MC, Ong ES, Jones YZ, Ruiz-Lozano P, Chien KR, Koder A, Evans RM 1999 PPAR gamma is required for placental, cardiac, and adipose tissue development. Mol Cell 4:585-595
8. Kubota N, Terauchi Y, Miki H, Tamemoto H, Yamauchi T, Komeda K, Satoh S, Nakano R, Ishii C, Sugiyama T, Eto K, Tsubamoto Y, Okuno A, Murakami K, Sekihara H, Hasegawa G, Naito M, Toyoshima Y, Tanaka S, Shiota K, Kitamura T, Fujita T, Ezaki O, Aizawa S, Kadowaki T, . 1999 PPAR gamma mediates high-fat diet-induced adipocyte hypertrophy and insulin resistance. Mol Cell 4:597-609
9. Rosen ED, Sarraf P, Troy AE, Bradwin G, Moore K, Milstone DS, Spiegelman BM, Mortensen RM 1999 PPAR gamma is required for the differentiation of adipose tissue in vivo and in vitro. Mol Cell 4:611-617
10. Glass CK, Rosenfeld MG 2000 The coregulator exchange in transcriptional functions of nuclear receptors. Genes Dev 14:121-141
11. Kliewer SA, Sundseth SS, Jones SA, Brown PJ, Wisely GB, Koble CS, Devchand P, Wahli W, Willson TM, Lenhard JM, Lehmann JM 1997 Fatty acids and eicosanoids regulate gene expression through direct interactions with peroxisome proliferator-activated receptors alpha and gamma. Proc Natl Acad Sci U S A 94:4318-4323
12. Forman BM, Tontonoz P, Chen J, Brun RP, Spiegelman BM, Evans RM 1995 15-Deoxy-delta 12, 14-prostaglandin J2 is a ligand for the adipocyte determination factor PPAR gamma. Cell 83:803-812
13. Lehmann JM, Moore LB, Smith-Oliver TA, Wilkison WO, Willson TM, Kliewer SA 1995 An antidiabetic thiazolidinedione is a high affinity ligand for peroxisome proliferator-activated receptor gamma (PPAR gamma). J Biol Chem 270:12953-12956
14. Rosen ED, Spiegelman BM 2001 PPARgamma : a nuclear regulator of metabolism, differentiation, and cell growth. J Biol Chem 276:37731-37734
15. Nielsen R, Pedersen TA, Hagenbeek D, Moulos P, Siersbaek R, Megens E, Denissov S, Borgesen M, Francoijs KJ, Mandrup S, Stunnenberg HG 2008 Genome-wide profiling of PPAR{gamma}:RXR and RNA polymerase II occupancy reveals temporal activation of distinct metabolic pathways and changes in RXR dimer composition during adipogenesis. Genes Dev 22:2953-2967
16. Straus DS, Pascual G, Li M, Welch JS, Ricote M, Hsiang CH, Sengchanthalangsy LL, Ghosh G, Glass CK 2000 15-deoxy-delta 12,14-prostaglandin J2 inhibits multiple steps in the NF-kappa B signaling pathway. Proc Natl Acad Sci U S A 97:4844-4849
17. Rossi A, Kapahi P, Natoli G, Takahashi T, Chen Y, Karin M, Santoro MG 2000 Anti-inflammatory cyclopentenone prostaglandins are direct inhibitors of IkappaB kinase. Nature 403:103-108
18. Sethi JK, Hotamisligil GS 1999 The role of TNF alpha in adipocyte metabolism. Semin Cell Dev Biol 10:19-29
19. Ruan H, Lodish HF 2003 Insulin resistance in adipose tissue: direct and indirect effects of tumor necrosis factor-alpha. Cytokine Growth Factor Rev 14:447-455
20. Arimoto K, Takahashi H, Hishiki T, Konishi H, Fujita T, Shimotohno K 2007 Negative regulation of the RIG-I signaling by the ubiquitin ligase RNF125. Proc Natl Acad Sci U S A 104:7500-7505
21. Ausubel FM, Brent R, Kingston R, Moore D, Seidman JJ, Smith J, Struhl K 1993 Current Protocols

in Molecular Biology. New York: John Wiley & Sons
22. Jeninga EH, van Beekum O, van Dijk AD, Hamers N, Hendriks-Stegeman BI, Bonvin AM, Berger R, Kalkhoven E 2007 Impaired peroxisome proliferator-activated receptor gamma function through mutation of a conserved salt bridge (R425C) in familial partial lipodystrophy. Mol Endocrinol 21:1049-1065
23. Stienstra R, Duval C, Keshtkar S, van der LJ, Kersten S, Muller M 2008 Peroxisome proliferator-activated receptor gamma activation promotes infiltration of alternatively activated macrophages into adipose tissue. J Biol Chem 283:22620-22627
24. Nielsen R, Grontved L, Stunnenberg HG, Mandrup S 2006 Peroxisome proliferator-activated receptor subtype- and cell-type-specific activation of genomic target genes upon adenoviral transgene delivery. Mol Cell Biol 26:5698-5714
25. Rodriguez AM, Elabd C, Delteil F, Astier J, Vernochet C, Saint-Marc P, Guesnet J, Guezennec A, Amri EZ, Dani C, Ailhaud G 2004 Adipocyte differentiation of multipotent cells established from human adipose tissue. Biochem Biophys Res Commun 315:255-263
26. Sears IB, MacGinnitie MA, Kovacs LG, Graves RA 1996 Differentiation-dependent expression of the brown adipocyte uncoupling protein gene: regulation by peroxisome proliferator-activated receptor gamma. Mol Cell Biol 16:3410-3419
27. Tontonoz P, Hu E, Devine J, Beale EG, Spiegelman BM 1995 PPAR gamma 2 regulates adipose expression of the phosphoenolpyruvate carboxykinase gene. Mol Cell Biol 15:351-357
28. Degenhardt T, Saramaki A, Malinen M, Rieck M, Vaisanen S, Huotari A, Herzig KH, Muller R, Carlberg C 2007 Three members of the human pyruvate dehydrogenase kinase gene family are direct targets of the peroxisome proliferator-activated receptor beta/delta. J Mol Biol 372:341-355
29. Wabitsch M, Brenner RE, Melzner I, Braun M, Moller P, Heinze E, Debatin KM, Hauner H 2001 Characterization of a human preadipocyte cell strain with high capacity for adipose differentiation. Int J Obes Relat Metab Disord 25:8-15
30. Sandelin A, Wasserman WW 2005 Prediction of nuclear hormone receptor response elements. Mol Endocrinol 19:595-606
31. Tanaka Y, Naruse I, Maekawa T, Masuya H, Shiroishi T, Ishii S 1997 Abnormal skeletal patterning in embryos lacking a single Cbp allele: a partial similarity with Rubinstein-Taybi syndrome. Proc Natl Acad Sci U S A 94:10215-10220
32. Zhao H, Li CC, Pardo J, Chu PC, Liao CX, Huang J, Dong JG, Zhou X, Huang Q, Huang B, Bennett MK, Molineaux SM, Lu H, Daniel-Issakani S, Payan DG, Masuda ES 2005 A novel E3 ubiquitin ligase TRAC-1 positively regulates T cell activation. J Immunol 174:5288-5297
33. Lefterova MI, Zhang Y, Steger DJ, Schupp M, Schug J, Cristancho A, Feng D, Zhuo D, Stoeckert CJ, Jr., Liu XS, Lazar MA 2008 PPAR{gamma} and C/EBP factors orchestrate adipocyte biology via adjacent binding on a genome-wide scale. Genes Dev 22:2941-2952
34. Roh TY, Wei G, Farrell CM, Zhao K 2007 Genome-wide prediction of conserved and nonconserved enhancers by histone acetylation patterns. Genome Res 17:74-81
35. West AG, Fraser P 2005 Remote control of gene transcription. Hum Mol Genet 14 Spec No 1:R101-11.:R101-R111
36. Chu P, Pardo J, Zhao H, Li CC, Pali E, Shen MM, Qu K, Yu SX, Huang BC, Yu P, Masuda ES, Molineaux SM, Kolbinger F, Aversa G, de Vries J, Payan DG, Liao XC 2003 Systematic identification of regulatory proteins critical for T-cell activation. J Biol 2:21
37. Shoji-Kawata S, Zhong Q, Kameoka M, Iwabu Y, Sapsutthipas S, Luftig RB, Ikuta K 2007 The RING finger ubiquitin ligase RNF125/TRAC-1 down-modulates HIV-1 replication in primary human peripheral blood mononuclear cells. Virology 368:191-204

Supplemental Figures

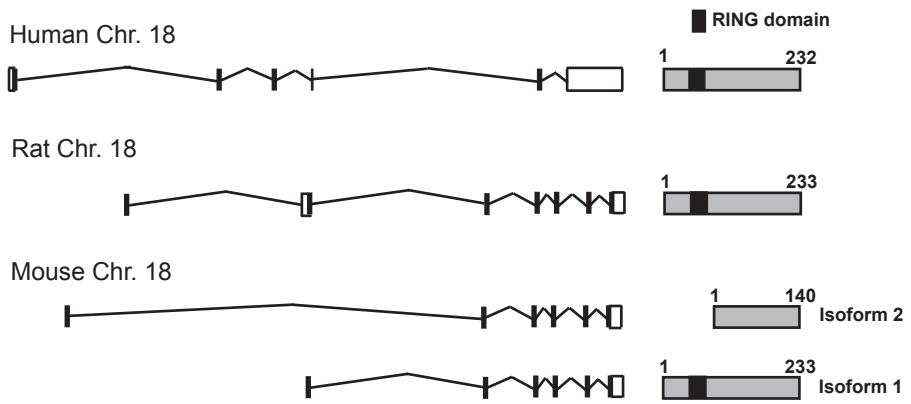

Supplemental Figure S1. RNF125 transcripts in human, mouse and rat.
Schematic representation of transcripts (left) and encoded proteins (right) of the human, murine and rat *RNF125*/*Rnf125* gene according to Ensembl.

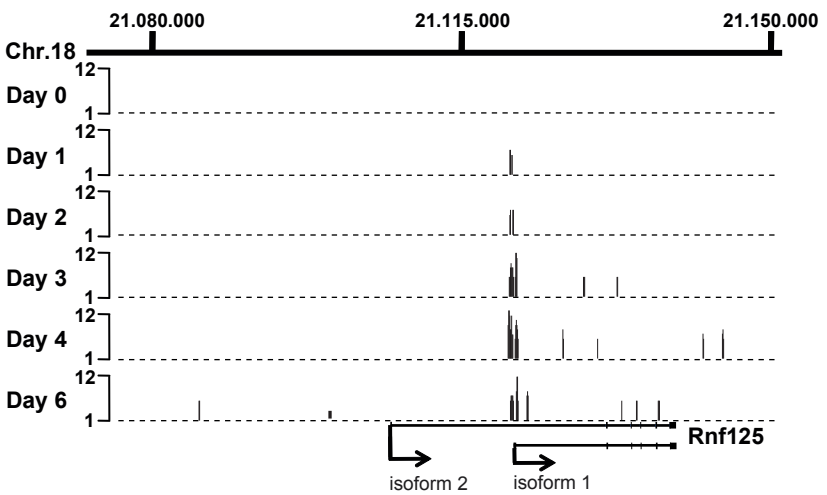

Supplemental Figure S2. RNAPII occupancy at Rnf125 gene during 3T3-L1 differentiation.
ChIP-seq data at day 0,1,2,3,4 and 6 respectively of differentiating 3T3-L1 cells viewed in the UCSC browser showing RNA polymerase II (RNAPII) occupancy at the Rnf125 gene.

Chapter 7

Abnormal urinary organic acids levels in a patient with congenital generalized lipodystrophy resulting from a novel mutation in BSCL2

Ellen H. Jeninga[1,2], Monique de Vroede[3], Nicole Hamers[1,2], Johannes M.P.J. Breur[4], Nanda M. Verhoeven-Duif[1,2], Ruud Berger[2] and Eric Kalkhoven[1,2,5]

[1]Dept. Metabolic & Endocrine Diseases, UMC Utrecht, The Netherlands; [2]Netherlands Metabolomics Centre, The Netherlands; [3]Dept. of Pediatric Endocrinology, UMC Utrecht, The Netherlands; [4]Dept. of Pediatric Cardiology, UMC Utrecht, The Netherlands; [5]Dept. Pediatric Immunology, UMC Utrecht, The Netherlands

Manuscript in preparation

Abstract

Context: Congenital generalized lipodystrophy (CGL) results from mutations in *AGPAT2*, encoding 1-acyl-glycerol-3-phosphate-acyltransferase 2 (CGL1; MIM 608594), *BSCL2*, encoding seipin (CGL2; MIM 269700) or *CAV1*, encoding caveolin1 (CGL3; MIM 612526)
Objective: To investigate whether the clinical phenotype of the proband is caused by mutation(s) in *BSCL2*
Design: Case report
Patients and Settings: A 7-day old child of consanguineous Turkish parents was admitted to hospital for feeding problems and weight loss. Physical examination showed the generalized loss of subcutaneous fat and a strikingly enlarged liver, suggestive for congenital generalized lipodystrophy.
Results: A homozygous mutation in the acceptor splice site of exon 5 of the *BSCL2* gene was found in the genome of the proband. This mutation affects RNA splicing and results in aberrant seipin proteins, which were normally expressed and localized to the endoplasmic reticulum like wild type protein. Examination of organic acids in urine of the patient showed that these were highly elevated compared to age-dependent reference values.
Conclusions: Here we report abnormal organic acid levels in urine of a patient with congenital generalized lipodystrophy (CGL) resulting from a novel mutation in *BSCL2*. This is indicative for mitochondrial dysfunction and suggests for the first time an association between CGL and mitochondrial dysfunction.

Introduction

Adipose tissue plays an essential role in whole body metabolism as illustrated by lipodystrophies in which the lack of adipose tissue results in many metabolic complications such as severe insulin resistance, hypertriglyceridemia and hepatic steatosis (1). Lipodystrophies can be classified as acquired or genetic and subclassified as partial or generalized. Genetic lipodystrophies are the most severe and either autosomal dominant or recessive. Congenital generalized lipodystrophy (CGL), also known as Berardinelli-Seip syndrome is an autosomal dominant inherited disorder and is characterized by a near complete absence of adipose tissue, from birth or early infancy. Lipids are stored aberrantly in muscle and liver resulting in extreme insulin resistance. In addition to hepatomegaly and generalized muscular hypertrophy, patienst have acromegaloid features such as enlarged hands and feet, acanthosis nigricans and excessive body hair (2;3). A few patients develop hypertrophic cardiomyopathy. Up to date CGL has been associated with mutations in three different genes; *AGPAT2* (4), *BSCL2* (5) and *CAV1* (6). Several mutations in patients have been reported in *AGPAT2,* which encodes the 1-acyl-glycerol-3-phosphate-acyltransferase 2, an enzyme involved in the synthesis of triglycerides and predominantly expressed in adipose tissue (7). Very recently CGL has been reported to be associated with a nonsense mutation in *CAV1*, which encodes caveolin1, a highly conserved protein that is the key component of membrane invaginations known as caveolae (8). Loss of this protein in mice leads to lipodystrophy and insulin resistance (9). Magré *et al.* were the first who reported several mutations, such as nonsense, frameshift, deletion, insertion and missense mutations, associated with CGL in *BSCL2* and called the protein 'seipin' (5). Seipin is an integral ER membrane protein and mainly expressed in adipose tissue, brain and testis (5;10). Lundin *et al.* determined the membrane topology of seipin showing that this protein spans the ER membrane twice with the C- and N-termini facing the cytoplasm and a glycolisation site in the luminal segment (11). Here we report a novel mutation in *BSCL2* and show for the first time abnormalities in urinary organic acids suggestive for mitochondrial dysfunction.

Subject and Methods

Study subject
The patient had been referred to the University Medical Centre Utrecht for clinical evaluation and informed consent for this study was obtained from the parents of the patient.

Isolation of genomic DNA and RNA, RT-PCR and mutation analysis
Genomic DNA was isolated from EDTA containing blood samples. Exons, including

the intron boundaries of *BSCL-2* were amplified by PCR. RNA was isolated form EDTA containing blood samples and used for cDNA synthesis using oligo(dT) primers and Superscript II (Invitrogen). RT-PCR was performed using primers located in exon 4 (forward) and exon 6 (reverse). PCR products were purified and sequenced using a BigDye Terminator v1.1 cycle sequencing kit (Applied Biosystems). The sequence products were purified and analyzed on an ABI Prsim 3730 DNA analyzer (Applied Biosystems). Primer sequences are available upon request.

Plasmids
All recombinant DNA work was performed according to standard procedures (12). The pLPS-seipin-EGFP expression construct (13) was a kind gift of Dr. K. Wagner (medical University, Graz, Austria). The pEBB-Flag-seipin wild type construct was generated by PCR amplification of full length seipin from this vector using primers containing *BamH1* and *Not1* restriction sites and cloned into the respective sites of pEBB-Flag. The pEBB-Flag-seipin ΔExon 5 and FS constructs were generated by Quickchange mutagenesis (Stratagene) and the sequences were verified by sequencing. pEBB-HA-seipin wild type, ΔExon 5 and FS were generated according to using the same procedures as described above, but cloned in the pEBB-HA vector.

Western blot analysis
The human osteosarcoma cell line U2OS was maintained in DMEM Glutamax (Dulbecco) containing 10% foetal calf serum (Gibco Life Technologies), 100 μg of penicillin/ml and 100 μg streptomycin/ml (Gibco Life Technologies). U2OS were transiently transfected with Seipin expression constructs using PEI transfection reagent. Cells were lysed in 2X Laemli sample buffer and subjected to SDS-PAGE and transferred to Immobilon membranes (Millipore). Anti-Flag M2 antibody (F3165, Sigma) was used to probe for the respective proteins. ECL Plus (Perkin Elmer) was used for detection.

Immunofluorescence microscopy
Immunofluorescence microscopy was performed as described earlier (14). Briefly, U2OS cells were grown on coverslips and transiently transfected with seipin expression constructs using PEI transfection reagent. Cells were washed, fixed, permeabilized, blocked in BSA and subsequently incubated with mouse-anti-HA (H9658, Sigma) and rabbit-anti-calreticuline (ALX-210-126-R100, Alexis Biochemicals) antibodies. As secondary antibodies Alexa Fluor 568 anti-mouse (A11031, Invitrogen) and Alexa Fluor 488 anti-rabbit (A11034, Invitrogen) were used, respectively. The coverslips were washed and mounted with FlourSave reagent (Calbiochem). Images were analysed on a confocal laserscanning microscope (Zeiss LSM 710 Meta).

Organic acid measurement in urine patient
Organic acid profiles in urine were analyzed by gas chromatography and flame ionisation detection after ethoximation and formation of TMS eters. The identities of the increased components were confirmed by mass spectrometry.

Results

Patient medical history and clinical evaluation
The patient is the third child of consanguineous Turkish parents. Family history is uneventful. He was born after a normal pregnancy with a birth weight of 3360gr. He was first admitted at the age of seven days for feeding problems and weight loss. Physical examination was remarkable for the generalized absence of subcutaneous fat and a strikingly enlarged liver (Figure 1). Laboratory examination included severe hypertriglyceridemia (7.4 mmo/l), low HLD cholesterol (0.5 mmol/l), impaired liver function and hyperglycemia (Figure 1E). Liver biopsy showed micro and macrovesicular steatosis. Serum leptin concentration was undetectable. At age 4 weeks, he was started on a low fat diet supplemented with medium chain triglycerides, protein, essential fatty acids and vitamins. Insulin was administered intravenously and later on subcutaneously in doses exceeding 2 U/kg and was discontinued after 1 month. Subsequently two short courses of insulin were necessary during upper respiratory tract infection. During the first months, the diet resulted in an impressive decrease in serum lipid concentration and improvement of liver function (Figure 1E), but at the age of 10 months, liver function again deteriorated and metformin was added. During an additional work up at age 4 months, hypertrophic cardiomyopathy was found on ultrasound examination.
At present, he is 15 months old and has normal height and weight for age. His physical examination, in addition to the lipodystrophy is remarkable for muscle hypertrophy, acanthosis nigricans, large hands and feet and enlarged external genitalia (Figure 1). He is mildly retarded.

Identification of a homozygous mutation in the acceptor splice site of exon 5 of BSCL2
In the genome of the proband we found a homozygous nucleotide substitution in the acceptor splicesite of exon 5 (IVS4 -2A→C) of *BSCL2* (Figure 2B). The clinically unaffected grandfather, father, mother and an older brother (I.1; II.1; II.2 and III.2 respectively) were heterozygous for the same nucleotide substitution and the clinically unaffected grandmother and oldest brother (I.2 and III.1 respectively) had two wild type alleles (Figure 2A). All other regions analysed were devoid of DNA sequence changes.
Since the mutation is located in a splice site, we next examined whether this mutation affects RNA splicing. RT-PCR analysis resulted in a single PCR product

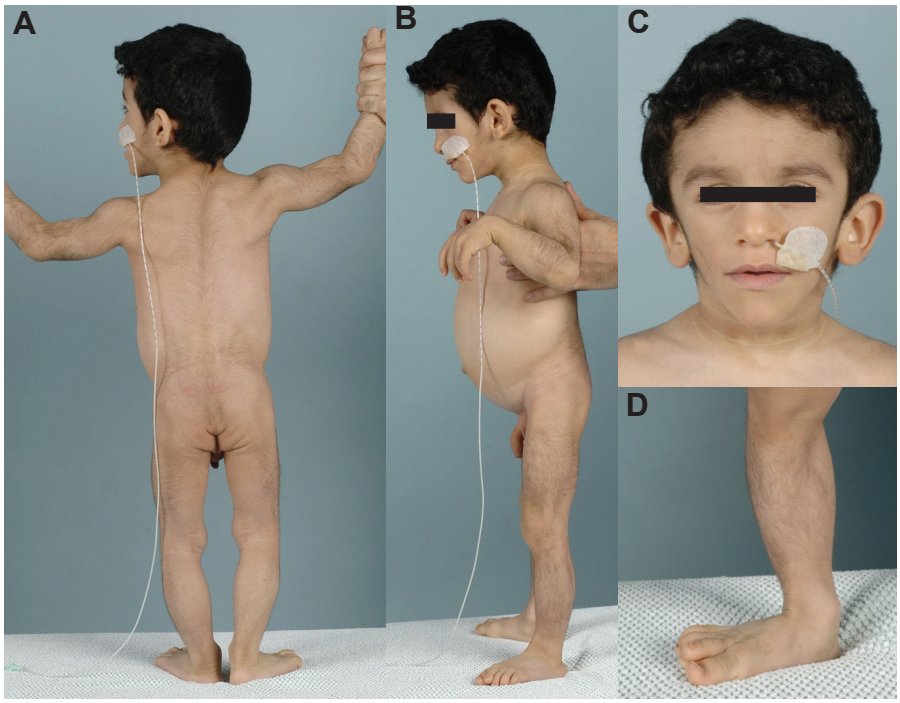

E

	1 weeks	4 months	10 months	14 months	Reference values
HbA1c			6.3	5.5	4.0-6.0 %
Alkaline phosphatase	589	335	324	226	0-295 U/L
gamma-GT	175	101	205	156	0-55 U/L
ASAT	117	25	103	69	0-47 U/L
ALAT	363	34	122	101	0-45 U/L
Cholesterol	3.9	5.8	6.4	6.3	3.5-6.5 mmol/L
Triglycerides	7.4	5.3	3.8	4.5	0.34-2.08 mmol/L
HDL-cholesterol	0.5	0.5	0.5	0.4	0.90-2.12 mmol/L
LDL-cholesterol		>5	4.2		0.0-3.5 mmol/L
Insuline			214	336	5-25 mIU/L
C-Peptide			9100	4550	400-1200 pmol/L

Figure 1. Clinical aspects of the proband.
Photographs of the proband showing the absence of subcutaneous fat, muscular hypertrophy (A,B,D), enlarged hands and feet (B,D), hirsutism and acanthosis nigricans (D). E, Table of biochemical features of the proband as measured in blood samples of the patient at 1 week, 4, 6, 10 and 14 months of age respectively. *Patient was started on a special diet at 4 weeks of age. **At 10 months of age patient was started on metformin.

with homozygous wild type sample (I.2), while RNA from the proband resulted in two smaller bands, suggesting that two aberrant mRNA products are formed. RNA from the heterozygous mother (II.2) displayed next to the two aberrant bands a band similar to the wild type band, albeit to a lesser intensity. Sequencing of the two aberrant mRNA products revealed that the smaller band is the result of an exon

5 skipping (ΔV147-S191). The other product is the result of a cryptic acceptor site in exon 5 resulting in a partly deletion and frameshift (ΔV147-A173+1) ultimately leading to a premature stopcodon in exon 6 (Fs → stop L223+1).

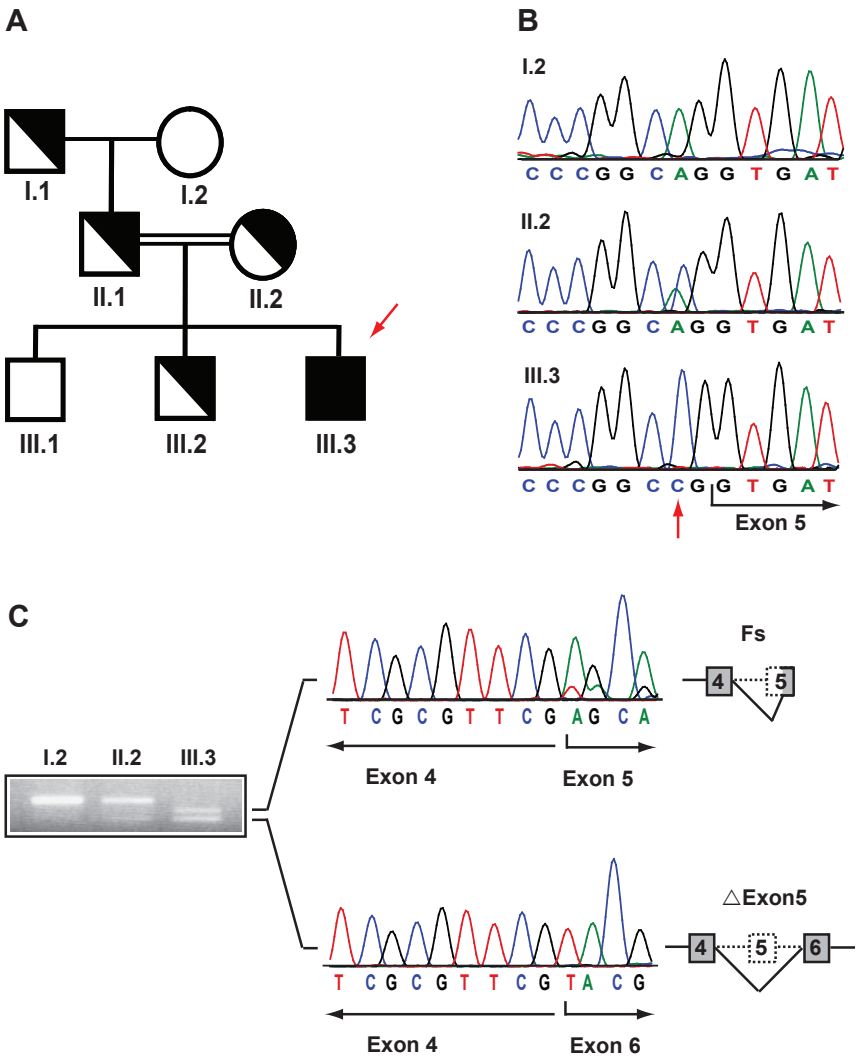

Figure 2. A novel homozygous mutation at the intron-exon boundary of exon 5 of the *BSCL2* gene affects RNA splicing.

A, Family pedigree with the affected proband indicated as a filled symbol and marked with an arrow. Half-filled symbols are clinically unaffected subjects harbouring a heterozygous mutation; unfilled symbols are clinically unaffected subjects harbouring the wild type sequence. B, DNA sequencing chromotagrams of the intron-exon boundary of exon 5 of the *BSCL2* gene illustrating the A→C nucleotide substitution at position -2 of IVS4 (IVS4 -2A→C). C, DNA gel analysis and DNA sequencing chromatograms of PCR products after PCR amplification of cDNA synthesized from patients RNA using primers encompassing exon 5, showing that the mutation affects RNA splicing.

Expression and cellular localisation of aberrant seipin proteins

To investigate the subcellular localization of the aberrant seipin proteins, U2OS cells transfected with expression vectors encoding wild type (FL) and mutant (ΔExon5 and Fs) seipin proteins were used for confocal immuno-fluorescence microscopy. Like the wild type protein, seipin-ΔExon5 and seipin-Fs both localized to the endoplasmic reticulum as it colocalized with the ER marker calreticuline (Figure 3A). Furthermore, this colocalisation pattern was absent in the empty vector negative control (Figure 3A). In parallel, protein expression levels were determined by Western blot analysis and showed similar expression levels for the different seipin proteins (Figure 3B). In contrast to wild type and ΔExon5 seipin protein, a high molecular weight complex could not be detected for seipin-Fs, which is consistent with its lack of transmembrane domain 2 (15).

In conclusion, the mutant seipin proteins (seipin-ΔExon5 and seipin-Fs) are normally expressed and localize to the ER like wild type protein.

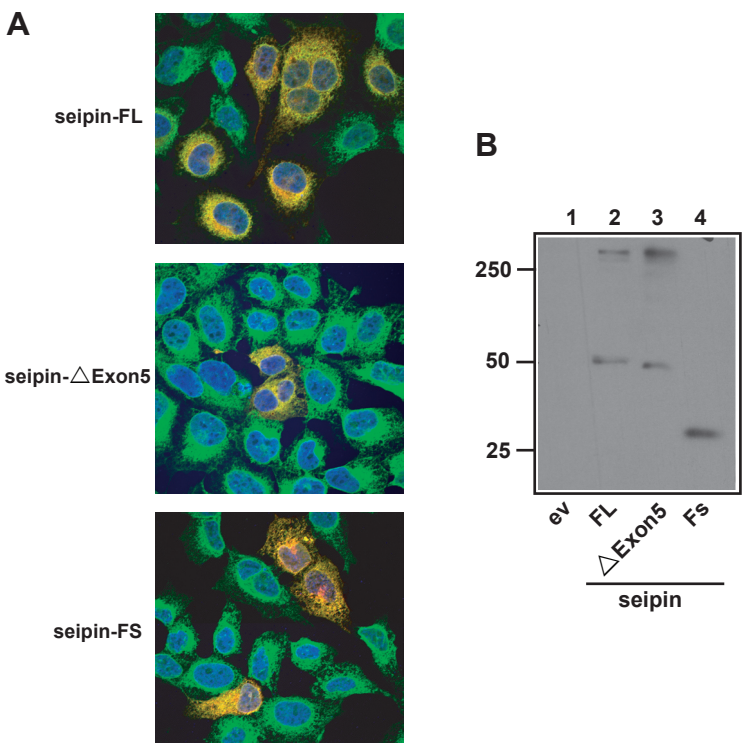

Figure 3. Aberrant seipin proteins are expressed and colocalize with the ER.
A, U2OS cells were transiently transfected with expression vectors encoding wild type (wt) or mutant HA-seipin proteins (ΔExon5 and Fs respectively). Cells were immunostained with HA-antibody (seipin) and calreticulum-antibody (ER-marker) and proteins were visualized by confocal immunofluorescence microscopy. The yellow pattern as observed in the merged images is suggestive for colocalization of the seipin proteins (wild type and mutants) with the ER. B, U2OS cells were transiently transfected with expression vectors encoding empty vector (ev), wild type (wt) or mutant Flag-seipin proteins (ΔExon5 and Fs respectively) and protein expression was assessed by Western blot analysis using α-Flag antibody.

Abnormal organic acid levels in the urine of the proband

Before the diagnosis of CGL was made (age 3 weeks), urinary organic acids were analysed to investigate the possibility of a mitochondrial disorder. Ethylmalonic acid was increased and fumaric acid, 2-ketoglutaric acid and citric acid were mildly increased. Lactic acid was normal. The analysis of organic acids was repeated at ages 6 weeks 49 weeks, showing a consistent pattern with most prominent abnormalities at age 49 weeks (Table 1).

	1 weeks	4 months	10 months	14 months	Reference values
HbA1c			6.3	5.5	4.0-6.0 %
Alkaline phosphatase	589	335	324	226	0-295 U/L
gamma-GT	175	101	205	156	0-55 U/L
ASAT	117	25	103	69	0-47 U/L
ALAT	363	34	122	101	0-45 U/L
Cholesterol	3.9	5.8	6.4	6.3	3.5-6.5 mmol/L
Triglycerides	7.4	5.3	3.8	4.5	0.34-2.08 mmol/L
HDL-cholesterol	0.5	0.5	0.5	0.4	0.90-2.12 mmol/L
LDL-cholesterol		>5	4.2		0.0-3.5 mmol/L
Insuline			214	336	5-25 mIU/L
C-Peptide			9100	4550	400-1200 pmol/L

Table 1. Concentrations of organic acids in urine of the patient.

Levels of lactic acid, ethylmalonic acid, fumaric acid, citric acid and 2-ketoglutaric levels in urine samples of the patient at ages 3, 6 and 49 weeks expressed in mmol/mol creatinine. Age-dependent reference values are indicated between brackets (24), *(18).

Discussion

Here we report a novel homozygous mutation in an acceptor splice site of the *BSCL2* gene, encoding the integral ER membrane protein seipin, in the genome of a patient with congenital generalized lipodystrophy type II (CGL2). We show that this mutation affects RNA splicing, resulting in the expression of aberrant seipin proteins. Consistent with the preservation of transmembrane domain 1, which has been shown to be critical for ER retention (15), the aberrant proteins localized to the ER like wild type protein. Very recently, Szymanski *et al.* showed that seipin predominantly localized at the ER-lipid droplet junctions (16). In addition, aberrant lipid droplet morphology was observed in human seipin deficient fibroblasts and yeast (16;17). These results suggest a role for seipin in the assembly and/or maintenance of lipid droplets, a hallmark of adipocytes. Seipin has also been shown to play an essential role in adipocyte differentiation, as its expression strongly increased during adipogenesis (10). Moreover, RNAi mediated knockdown in mesenchymal cells impaired adipocyte differentiation (10). These studies clearly demonstrate that seipin is critically important in adipocyte differentiation, maintenance and metabolism; hence disruption of normal seipin protein function is likely to result in lipodystrophy.

Interestingly, our organic acids screening in urine of the proband showed elevated levels of several organic acids, including derivatives of the citric acid cycle such as fumaric acid, citric acid and 2-ketoglutaric acid as well as ethylmalonic acid, a metabolite found to be elevated in urine of patients with SCAD deficiency and mitochondriopathy (18). To our knowledge this is the first report showing abnormal levels of urinary organic acids in a patient with CGL2, indicative for mitochondrial dysfunction. Interestingly, mitochondrial dysfunction has also been reported in obesity and type II diabetes (19). A commonality in obesity and lipodystrophy is the lack of sufficient lipid storage capacity in adipose tissue resulting in ectopic accumulation of lipids, mainly in liver and muscle. Therefore, the aetiology of mitochondrial dysfunction in both disorders might be the nutrient overflow in these organs. In line with this an excess of glucose and fatty acids caused oxidative stress due to increased reactive oxygen species (ROS) production (20) resulting in mitochondrial damage. Moreover, a recent study showed that mitochondrial dysfunctions result from increased ROS production in mice fed a high fat and sugar diet (21). These results would implicate that diet adaptations (i.e low fat and sugar) might ameliorate the metabolic disturbances in patients with congenital generalized lipodystrophy. Indeed, the patient presented here was started on a low fat diet supplemented with medium chain triglycerides, protein, essential fatty acids and vitamins resulting in an impressive decrease in serum lipid concentration and improvement of liver function. In addition, as the insulin sensitizing TZD pioglitazone improves mitochondrial function and enhance oxidative phosphorylation (22;23) patients with congenital generalized

lipodystrophy might benefit from pioglitazone treatment.
In conclusion, here we show for the first time elevated urinary organic acid levels in a patient with congenital generalized lipodystrophy due to a novel mutation in *BSCL2*, suggestive for mitochondrial dysfunction. Future studies are required to establish whether metabolic screening is a useful additional tool for diagnosis and monitoring of therapy efficacy in lipodystrophy patients.

Acknowledgements
We thank Dr. K. Wagner for the seipin plasmid construct, Berthil Prinsen and Monique de Sain-van der Velden (Department of Metabolic & Endocrine Diseases, UMC Utrecht, Utrecht, The Netherlands) for their help with the metabolite screening.

References

1. Hegele RA, Joy TR, Al Attar SA, Rutt BK 2007 Thematic review series: Adipocyte Biology. Lipodystrophies: windows on adipose biology and metabolism. J Lipid Res 48:1433-1444
2. Garg A 2004 Acquired and inherited lipodystrophies. N Engl J Med 350:1220-1234
3. Van Maldergem L, Magre J, Khallouf TE, Gedde-Dahl T, Jr., Delepine M, Trygstad O, Seemanova E, Stephenson T, Albott CS, Bonnici F, Panz VR, Medina JL, Bogalho P, Huet F, Savasta S, Verloes A, Robert JJ, Loret H, De Kerdanet M, Tubiana-Rufi N, Megarbane A, Maassen J, Polak M, Lacombe D, Kahn CR, Silveira EL, D'Abronzo FH, Grigorescu F, Lathrop M, Capeau J, O'Rahilly S 2002 Genotype-phenotype relationships in Berardinelli-Seip congenital lipodystrophy. J Med Genet 39:722-733
4. Agarwal AK, Arioglu E, De Almeida S, Akkoc N, Taylor SI, Bowcock AM, Barnes RI, Garg A 2002 AGPAT2 is mutated in congenital generalized lipodystrophy linked to chromosome 9q34. Nat Genet 31:21-23
5. Magre J, Delepine M, Khallouf E, Gedde-Dahl T, Jr., Van Maldergem L, Sobel E, Papp J, Meier M, Megarbane A, Bachy A, Verloes A, D'Abronzo FH, Seemanova E, Assan R, Baudic N, Bourut C, Czernichow P, Huet F, Grigorescu F, De Kerdanet M, Lacombe D, Labrune P, Lanza M, Loret H, Matsuda F, Navarro J, Nivelon-Chevalier A, Polak M, Robert JJ, Tric P, Tubiana-Rufi N, Vigouroux C, Weissenbach J, Savasta S, Maassen JA, Trygstad O, Bogalho P, Freitas P, Medina JL, Bonnicci F, Joffe BI, Loyson G, Panz VR, Raal FJ, O'Rahilly S, Stephenson T, Kahn CR, Lathrop M, Capeau J 2001 Identification of the gene altered in Berardinelli-Seip congenital lipodystrophy on chromosome 11q13. Nat Genet 28:365-370
6. Kim CA, Delepine M, Boutet E, El Mourabit H, Le Lay S, Meier M, Nemani M, Bridel E, Leite CC, Bertola DR, Semple RK, O'Rahilly S, Dugail I, Capeau J, Lathrop M, Magre J 2008 Association of a homozygous nonsense caveolin-1 mutation with Berardinelli-Seip congenital lipodystrophy. J Clin Endocrinol Metab 93:1129-1134
7. Agarwal AK, Barnes RI, Garg A 2004 Genetic basis of congenital generalized lipodystrophy. Int J Obes Relat Metab Disord 28:336-339
8. Parton RG, Simons K 2007 The multiple faces of caveolae. Nat Rev Mol Cell Biol 8:185-194
9. Razani B, Combs TP, Wang XB, Frank PG, Park DS, Russell RG, Li M, Tang B, Jelicks LA, Scherer PE, Lisanti MP 2002 Caveolin-1-deficient mice are lean, resistant to diet-induced obesity, and show hypertriglyceridemia with adipocyte abnormalities. J Biol Chem 277:8635-8647
10. Payne VA, Grimsey N, Tuthill A, Virtue S, Gray SL, Dalla NE, Semple RK, O'Rahilly S, Rochford JJ 2008 The human lipodystrophy gene BSCL2/seipin may be essential for normal adipocyte differentiation. Diabetes 57:2055-2060
11. Lundin C, Nordstrom R, Wagner K, Windpassinger C, Andersson H, von Heijne G, Nilsson I 2006 Membrane topology of the human seipin protein. FEBS Lett 580:2281-2284
12. Ausubel FM, Brent R, Kingston R, Moore D, Seidman JJ, Smith J, Struhl K 1993 Current Protocols in Molecular Biology. New York: John Wiley & Sons
13. Windpassinger C, Auer-Grumbach M, Irobi J, Patel H, Petek E, Horl G, Malli R, Reed JA, Dierick I, Verpoorten N, Warner TT, Proukakis C, Van den BP, Verellen C, Van Maldergem L, Merlini L, De Jonghe P, Timmerman V, Crosby AH, Wagner K 2004 Heterozygous missense mutations in BSCL2 are associated with distal hereditary motor neuropathy and Silver syndrome. Nat Genet 36:271-276
14. van de Graaf SF, Chang Q, Mensenkamp AR, Hoenderop JG, Bindels RJ 2006 Direct interaction with Rab11a targets the epithelial Ca2+ channels TRPV5 and TRPV6 to the plasma membrane. Mol Cell Biol 26:303-312
15. Ito D, Fujisawa T, Iida H, Suzuki N 2008 Characterization of seipin/BSCL2, a protein associated with spastic paraplegia 17. Neurobiol Dis 31:266-277
16. Szymanski KM, Binns D, Bartz R, Grishin NV, Li WP, Agarwal AK, Garg A, Anderson RG, Goodman JM 2007 The lipodystrophy protein seipin is found at endoplasmic reticulum lipid droplet junctions and is important for droplet morphology. Proc Natl Acad Sci U S A 104:20890-

20895
17. Fei W, Shui G, Gaeta B, Du X, Kuerschner L, Li P, Brown AJ, Wenk MR, Parton RG, Yang H 2008 Fld1p, a functional homologue of human seipin, regulates the size of lipid droplets in yeast. J Cell Biol 180:473-482
18. Blau N, Duran M, Blaskovics ME, Gibson KM 2003 Physician's guide to the laboratory diagnosis of metabolic diseases. Springer-Verlag Berlin Heidelberg
19. Hojlund K, Mogensen M, Sahlin K, Beck-Nielsen H 2008 Mitochondrial dysfunction in type 2 diabetes and obesity. Endocrinol Metab Clin North Am 37:713-31, x
20. Evans JL, Goldfine ID, Maddux BA, Grodsky GM 2002 Oxidative stress and stress-activated signaling pathways: a unifying hypothesis of type 2 diabetes. Endocr Rev 23:599-622
21. Bonnard C, Durand A, Peyrol S, Chanseaume E, Chauvin MA, Morio B, Vidal H, Rieusset J 2008 Mitochondrial dysfunction results from oxidative stress in the skeletal muscle of diet-induced insulin-resistant mice. J Clin Invest 118:789-800
22. Bogacka I, Xie H, Bray GA, Smith SR 2005 Pioglitazone induces mitochondrial biogenesis in human subcutaneous adipose tissue in vivo. Diabetes 54:1392-1399
23. Schutz B, Reimann J, Dumitrescu-Ozimek L, Kappes-Horn K, Landreth GE, Schurmann B, Zimmer A, Heneka MT 2005 The oral antidiabetic pioglitazone protects from neurodegeneration and amyotrophic lateral sclerosis-like symptoms in superoxide dismutase-G93A transgenic mice. J Neurosci 25:7805-7812
24. Rinaldo P 2008 Laboratory guide to the methods in biochemical genetics. 2008 ed. SpringerBerlin; 137

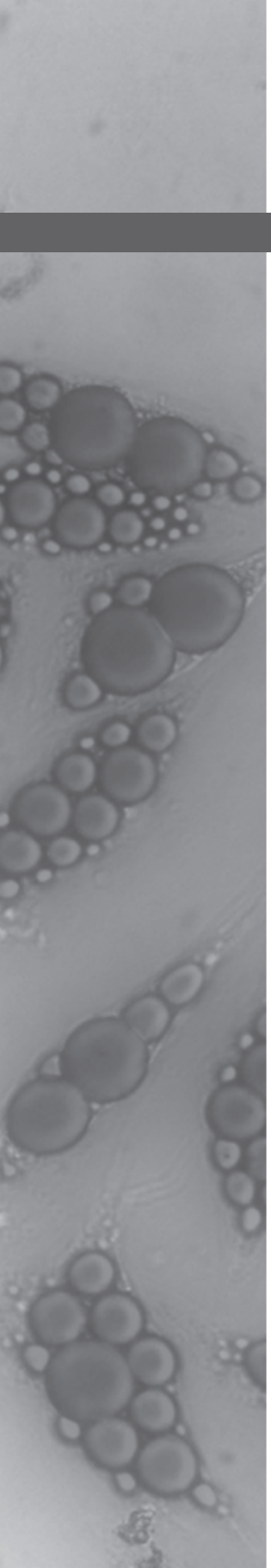

Chapter 8

General Discussion

Introduction "the fat paradox?"

Due to a sedentary lifestyle and high calorie intake, the prevalence of obesity rapidly increases in industrialized countries. This is a major health concern because of the herewith associated complications such as hypertension, insulin resistance, hypertriglyceridemia and type II diabetes. Interestingly, not only an excess of fat as observed in overweight and obese subjects, but also the absence of fat as in subjects with lipodystrophy is associated with these complications. So, apparently a normal amount and/or distribution of fat are required for the maintenance of whole body metabolism.

Lipodystrophies

Lipodystrophy, either inherited or acquired, is characterized by a generalized or partial loss of adipose tissue as described in Chapter 1. Patients with lipodystrophy represent the ultimate *in vivo* experiment-of-nature with regard to human adipose tissue development and function. Therefore, elucidating the physiological role of gene products affected in lipodystrophies as well as investigating the consequences of drugs that cause lipodystrophy as a side effect might provide some possible mechanistic links or pathways that account for common pathophysiological mechanisms. Genes affected in the inherited lipodystrophies include genes encoding nuclear envelope structural components (*LMNA*), a metalloprotease involved in lamin A processing (*ZMPSTE24*), a nuclear receptor (*PPARG*), an integral ER membrane protein (*BSCL2*), a structural component of lipid droplets and plasma membranes (*CAV1*), a lipid biosynthetic enzyme (*AGPAT2*) and a downstream effector of insulin signalling (*AKT2*). The location of these proteins in the adipocyte is depicted in Figure 1B.

Generalized lipodystrophy

In Chapter 7 we describe a novel homozygous mutation in *BSCL2* in a patient with congenital generalized lipodystrophy type 2 (CGL2). The *BSCL2* gene encodes an integral ER membrane protein named seipin and is mainly expressed in adipose tissue. A role for seipin in the formation of lipid droplets, a hallmark of adipocytes, was suggested as it was mainly found at ER-lipid droplet junctions. In addition, yeast and human seipin deficient fibroblasts showed abnormal lipid droplets (1;2). Furthermore, a very recent study suggested an important role for seipin in adipogenesis as seipin expression increases during differentiation of human and mouse primary adipocytes, while RNAi-mediated knockdown of seipin in mesenchymal cells impaired adipogenesis (3). Remarkably, mesenchymal cells lacking seipin failed to induce the expression of the adipogenic transcription factor SREBP1c during early adipogenesis, whereas expression of other adipogenic

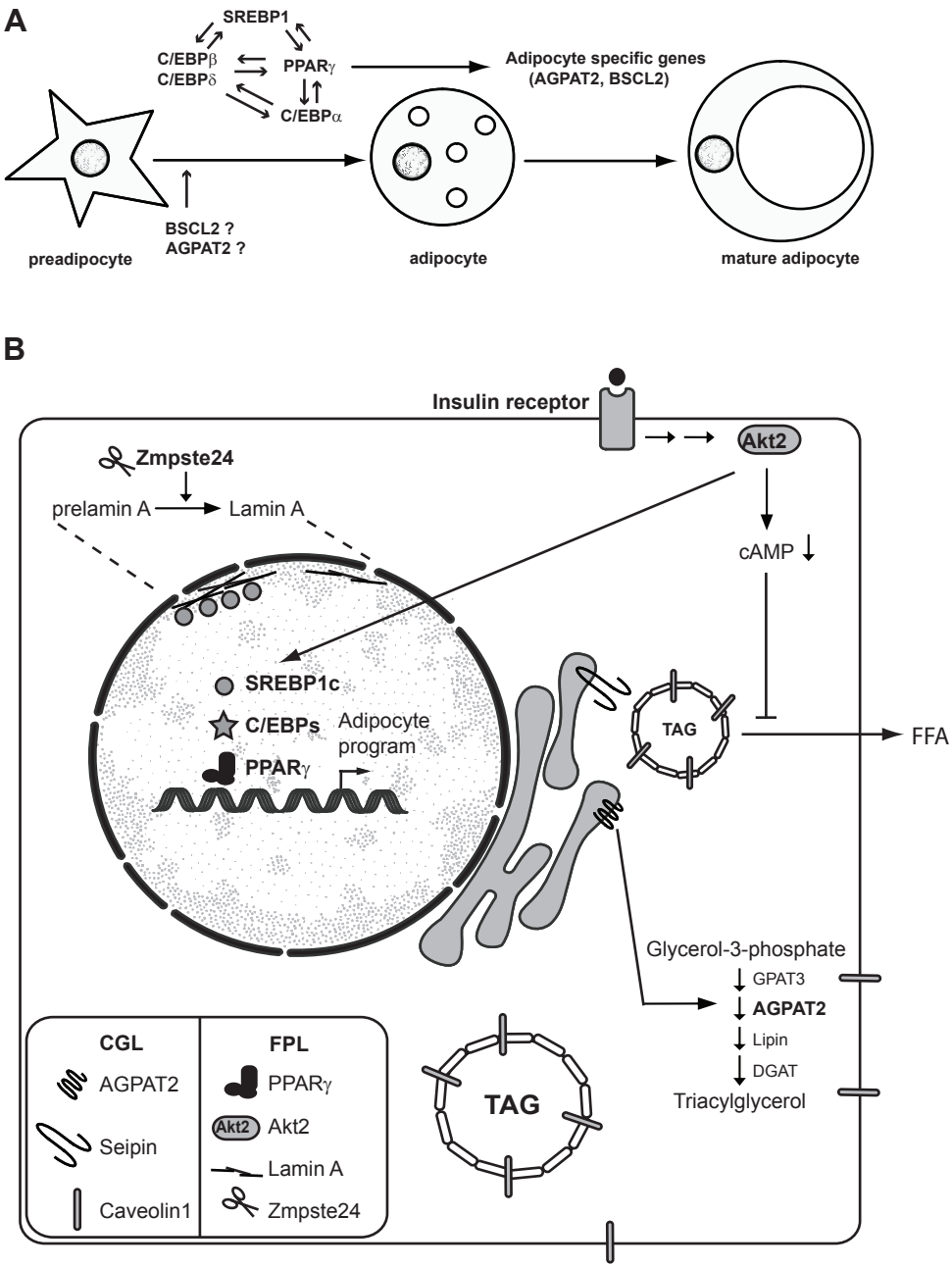

Figure 1. Adipogenesis and location of proteins affected in inherited lipodystrophies.
A. Schematic representation of adipocyte differentiation showing the sequential induction of important adipogenic transcription factors. B. Model showing the location of different gene products affected in inherited lipodystrophy and their (potential) role in (pre)adipocytes. The box in the left corner shows the proteins affected in generalized and partial lipodystrophies.

transcription factors such as C/EBPβ, C/EBPδ and PPARγ was similar compared to control cells (3). In contrast, the expression of these genes as well as other adipocyte-specific genes was reduced at later stages of adipocyte differentiation. SREBP1c directly activates transcription of PPARγ via consensus E-box motifs in the *PPARG* promoter (4) and indirectly by enhanced production of endogenous ligand for PPARγ (5). PPARγ acts to sustain expression of PPARγ and C/EBPs and together these adipogenic transcription factors orchestrate the expression of adipocyte-specific genes necessary for adipocyte function and maintenance. Of note, genome wide profiling of C/EBP and PPARγ binding sites in 3T3-L1 adipocytes revealed binding sites near the *SREBP1c*, *PPARγ* and *C/EBPα*, genes suggesting that these transcription factors regulate each others expression. Furthermore, PPARγ and C/EBP sites were found near the *BSCL2* gene, suggesting that PPARγ and/or C/EBP regulate the expression of the seipin protein in adipocytes (6). Taken together these data indicate that seipin is essential for the development of mature adipocytes, suggesting that the absence of adipose tissue observed in CGL2 is the consequence of a cell-autonomous defect in adipogenesis.

Other forms of congenital generalized lipodystrophy are caused by mutations in *AGPAT2* (CGL1) or *CAV1* (CGL3). *AGPAT2* encodes 1-acyl-glycerol-3-phosphate-acyltransferase 2, a key enzyme in the biosynthesis of glycerophosphoslipids and triacylglycerols. A recent study demonstrated that AGPAT2 is a resident integral ER membrane protein and that its expression as well as its enzymatic activity is massively induced during adipogenesis (7). Furthermore, knockdown of AGPAT2 in preadipocytes prevented the early induction of key transcriptional activators of adipogenesis, such as PPARγ and C/EBPβ and delayed expression of multiple adipocyte-specific genes. Although a recent study showed the direct regulation of AGPAT2 by PPARγ (8), AGPAT2 knockdown experiments in preadipocytes suggest that AGPAT2 operates upstream of these transcription factors. It is possible that normal AGPAT2 expression is essential for the induction of adipogenesis and that the regulation of AGPAT2 in later stages of differentiation by PPARγ is necessary for the function and maintenance of adipocytes. The recently generated AGPAT2 knock-out mouse confirmed the critical role of AGPAT2 in adipogenesis, as adipose tissue was completely absent in these mice (9).

Most but not all patients with CGL harbour mutations in *BSCL2* or *AGPAT2*, suggesting additional loci for this disease. Very recently a nonsense mutation in *CAV1* (G38X) in a patient with CGL has been reported. In line with this, loss of Caveolin in mice leads to lipodystrophy (10). *CAV1* encodes caveolin1, a protein typically found in membrane invaginations, known as caveolae, but also in lipid droplets. It is highly expressed in adipose tissue and strongly induced during 3T3-L1 differentiation (11). In response to an excess of FFAs, caveolin1 translocates to lipid droplets in MEFs (12), suggesting a role in the storage and/or transport of FFAs in lipid droplets. Interestingly, heterozygous frameshift mutations in *CAV1* (1134fsdelA-X137 and -88delC) have recently been reported in patients with

partial lipodystrophy (13). In contrast, $CAV^{+/-}$ mouse displayed no phenotype (10) and three subjects harbouring the heterozygous G38X mutation were clinically unaffected (14). This suggests the existence of mutations in other genes next to the heterozyogous frameshift mutation in *CAV1*. No mutations were detected in *LMNA*, *PPARγ*, *BSCL2* or *AGPAT2*, suggesting that other gene-gene and/or gene-environment interactions are responsible for the phenotype.
Furthermore, as some patients with a CGL phenotype did not harbour mutations in *CAV1, BSCL2* or *AGPAT2*, additional loci are likely to exist.

Partial lipodystrophy
As described in Chapter 1, partial lipodystrophy is caused by mutations in different genes (inherited lipodystrophy) as well as by certain drugs (acquired lipodystrophy). Several mutations in PPARγ have been reported in patients with FPLD3. In Chapter 3 we examined the functional consequences of the FPLD3-associated PPARγ R425C mutation located in the LBD and in Chapter 4 we reported a novel mutation in the DBD of PPARγ (R194W). Both PPARγ mutations disrupt normal protein function, albeit through different mechanisms. Since PPARγ has been shown to be necessary and sufficient for adipogenesis, it is not surprising that loss-of-function mutations in PPARγ result in lipodystrophy.
For other forms of partial lipodystrophy a direct mechanistic link between adipocyte differentiation/function and the disease causing mutation is less obvious, as these include mutations in *LMNA*, *ZMPSTE24* and *AKT2*. FPLD2 is caused by heterozygous mutations in the *LMNA* gene, which are clustered in exon 8 and 11. The most frequently found FPLD2-associated lamin A mutation results in a substitution of an arginine at position 482 in a neutral amino acid (R482Q/L/W). Consistent with this notion, our screening of the *LMNA* gene in two patients with a FPLD2 phenotype revealed a mutation at this site as well (R482W; unpublished observations). The FPLD2-associated lamin A mutations are all located in the C-terminal tail, which has been shown to interact with the adipogenic transcription factor SREBP1c *in vitro* (15). However, Capanni *et al.* demonstrated that not mature lamin A, but prelamin A interacts with the active form of SREBP1c *in vivo* (16). Furthermore, in fibroblasts derived from FPLD2 patients they observed an accumulation of prelamin at the nuclear envelope, which colocalized with SREBP1c. As sequestration of SREBP1c at the nuclear rim decreases the pool of active SREBP1c within the nucleus, this is likely to affect PPARγ expression. Consistent with this, prelamin accumulation due to overexpression of an uncleavable prelamin mutant in 3T3-L1 preadipocytes resulted in decreased PPARγ expression. In addition, treatment of 3T3-F442 preadipocytes with the protease inhibitor Indinavir, which triggers prelamin accumulation, has also been reported to result in SREBP1c retention at the nuclear rim and impaired adipogenesis (17). Consistent with this notion, this drug, which is used in the treatment of HIV, causes lipodystrophy as a side effect in these patients. These results indicate that retention of SREBP1c at the

nuclear rim is due to an excess of prelamin, irrespective of *LMNA* mutations. In line with this accumulation of prelamin has only been found in laminopathies associated with lipodystrophy, such as Hutchinson-Gilford Progeria Syndrome (HGPS) and mandibuloacral Dysplasia type A (MADA), but not in Emery-Dreifuss muscular dystrophy in which lipodystrophy is not observed (18). This also suggests that inhibition of enzymes involved in prelamin processing is likely to result in impaired adipogenesis and probably lipodystrophy. Prelamin is processed to mature lamin by a sequence of reactions of which the first two steps, farnesylation and proteolytic cleavage, are exerted by the zinc metalloprotease, ZMPSTE24 (19). Consistent with this hypothesis, treatment of 3T3-L1 preadipocytes with farnesylation inhibitors resulted in accumulation of prelamin and inhibited adipocyte differentiation (16). Moreover, prelamin accumulation was also observed in fibroblasts of a patient with lipodystrophy-associated Mandibuloacral Dysplasia type B (MADB)(20), which is due to mutations in *ZMPSTE24* (see Chapter 1) and loss of ZMPSTE24 in mice resulted in lipodystrophy as well (21).
Since TZDs rescue adipocyte differentiation in pre-adipocytes accumulating prelamin A, this indicates that the block in adipogenesis is upstream of PPARγ activation and can be circumvented by direct activation of PPARγ. Thus, prelamin accumulation which results in retention of SREBP1c at the nuclear rim thereby decreasing the pool of active SREBP1c is likely to reduce PPARγ activation resulting in impaired adipocyte differentiation.
As mentioned in Chapter 1, partial lipodystrophy has also been associated with heterozygous missense mutations in the *AKT2* gene, encoding a serine/threonine kinase involved in insulin signalling (22;23). The first identified mutation (R274H) was detected in a 34 year old female with severe insulin resistance and partial lipodystrophy (22). Like the patients harbouring this mutation, Akt2 knockout mice displayed insulin resistance (24;25) and age-dependent loss of adipose tissue (25). Furthermore, overexpression of the catalytic inactive Akt2 mutant in 3T3-L1 preadipocytes impaired adipogenesis, while overexpression of wild type protein enhanced adipocyte differentiation (22). Interestingly, Le Lay *et al.* demonstrated that SREBP1c is an important mediator of the insulin transcriptional effects in adipocytes (26). Furthermore, they showed that in adipocytes the adipogenic transcription factor C/EBPβ is under the control of insulin-stimulated SREBP1c. Defective insulin signalling due to a catalytic inactive Akt2 protein might therefore indirectly affect SREBP1c, resulting in reduced expression of the adipogenic transcription factors C/EBPβ and PPARγ and subsequently impair adipogenesis. Although the catalytic inactive Akt2 suggests a role of Akt2 in adipogenesis, a recent study showed that Akt1 and not Akt2 plays a major role in adipogenesis (27). In addition, two other *AKT2* missense mutations (R208K and R467W) were reported in subjects with insulin resistance, of which only one showed partial lipodystrophy (23). Surprisingly, the insulin stimulated kinase activity of these mutant proteins (R208K and R467W) were similar to wild type. Thus, while *AKT2* mutations are

unlikely to explain the development of insulin resistance and lipodystrophy, the catalytic inactive mutant (R274H) and the Akt2 knockout mice demonstrate the critical role of Akt2 in the maintenance of insulin sensitivity and adipogenesis. Additional studies are required to investigate whether the insulin resistance and/or lipodystrophy associated mutations in the *AKT2* gene directly affect insulin signaling and/or adipogenesis.

A common pathophysiological mechanism resulting in lipodystophy?

In the past decade a large number of novel mutations in genes contributing to lipodystrophy have been reported. The generation of mouse models, studies with cells obtained from patients, as well as a number of *in vitro* studies advanced our understanding of the physiological roles of most of these gene products. This allows us to envisage some possible mechanistic links or common pathways underlying lipodystrophy. As PPARγ has been shown to be necessary for adipogenesis to occur, a reduced expression is likely to result in decreased adipocyte differentiation and a subsequent reduction in fat mass. Remarkably, PPARγ has been reported to regulate the expression of AGPAT2 and seipin. As these proteins affect essential functions of adipocytes such as TAG synthesis and lipid droplet size, respectively, mutations in these proteins might result in degeneration of adipocytes. Alternatively, these proteins might be important in adipogenesis as knockdown in adipocytes resulted in decreased expression of adipogenic transcription factors, including C/EBPs and PPARγ suggesting that these proteins might even operate upstream of PPARγ during adipogenesis (Figure 1A). These proteins thus affect both adipocyte differentiation and function. A common denominator in the pathophysiology of at least some lipodystrophies seem to be the lipogenic transcription factors SREBP, as the mutated gene products affect the expression, the localization and/or function of this protein (Figure 1B). Surprisingly, SREBP1c$^{-/-}$ mice display a normal phenotype, suggesting redundancy between SREBP1a and SREBP1c (28). Although most SREBP1$^{-/-}$ mice die in the neonatal period the surviving mice are normal at birth and develop normally. This might be explained by a compensatory mechanism for SREBP2, as SREBP2 levels were increased in different tissues in these mice compared to wild type animals (29). Apparently such a compensation mechanism is absent in SREBP2$^{-/-}$ mice as these mice are embryonically lethal.

In conclusion, adipogenic transcription factors regulate each others expression and together orchestrate the process of adipocyte differentiation. It is a delicate process requiring the induction of different factors at different timepoints (Figure 1A). This process is impaired in lipodystrophy and caused either by mutations in different genes or by drugs. A central player in the pathophysiology of at least some of these lipodystrophies seems to be SREBP1c (Figure 1B). To establish the role of SREBP1c in adipose tissue development, adipose tissue specific SREBP1c knock-out mice are needed.

The impact of genetic variation in PPARγ on insulin sensitivity

PPARγ plays a major role in the modulation of insulin sensitivity as becomes evident from a number of PPARγ mutations associated with insulin resistance. Moreover, PPARγ is the molecular target of the insulin sensitizing TZDs. Mutations in PPARγ have been shown to affect its function and the recently reported crystal structure of the PPARγ/RXRα heterodimer bound to DNA provides novel insights in how some mutations influence PPARγ function as described in Chapter 2.
The most frequently found genetic variant of PPARγ is the P12A polymorphism in the AF-1 region of the PPARγ2 protein. A recruit-by-phenotype approach (30) and two large meta-analyses (31;32) showed a protective role for the P12A variant in the development of diabetes. Numerous association studies between this polymorphism BMI (33-35) and insulin resistance have been performed, but were never conclusive as gene-environment interactions, such as diet and physical activity appeared to play a role (36;37). Very recently the generation of a PPARγ2 P12A knock-in mouse model confirmed that the protective role of P12A is highly dependent on gene-nutrient interactions, as Ala/Ala mice were more insulin sensitive on a regular diet, but not on a HFD (38). Altered cofactor recruitment and adiponectin signalling in the homozygous P12A mice were suggested to contribute to the improved insulin sensitivity. Adiponectin is secreted by adipose tissue and plasma adiponectin levels have been shown to positively correlate with insulin sensitivity (39). Interestingly elevated plasma adiponectin levels have been reported in humans homozygous for the Ala allele (40).
Gene-nutrient interactions also seem to play an important role in the development of insulin resistance in subjects with PPARγ mutations associated with FPLD3, as heterozygous P495L knock-in mice only showed a FPLD3-like phenotype when expressed in the hyperphagic ob/ob background (41). In addition, heterozygous L496A knock-in mice developed mild insulin resistance, but only when fed a HFD for as long as 8 months (42). Remarkably, whereas FPLD3 patients with PPARγ truncation mutations are insulin resistant, a subject harbouring the FSX mutation that causes a truncated PPARγ protein displayed a mostly normal metabolic pattern (43). As the latter subject displays normal amounts of adipose tissue, the loss of adipose tissue in FPLD3 is likely to be the cause of insulin resistance. FPLD3 is characterized by loss of adipose tissue from the extremities with preservation of fat in the intra-abdominal region. This suggests that the specific loss of adipose tissue at these anatomical sites determine insulin sensitivity. Consistently, insulin sensitivity in lean human subjects depends on differences in body fat distribution, with lean subjects with more peripheral body fat being more insulin sensitive than subjects with more centrally located fat. Furthermore, TZD treatment in insulin resistant obese subjects increases peripheral fat mass while improving insulin sensitivity. This suggests that PPARγ is predominantly active in peripheral fat depots and might explain the selective loss of adipose tissue at these sites in patients with FPLD3. The

notion that subjects compound heterozygous for PPARγ FSX and a mutation in the *PPP1R3* that encodes an enzyme playing a keyrole in the regulation of glycogen storage in muscle, are insulin resistant, indicates that gene-gene interactions might play a role in the development of insulin resistance as well (44).
Interestingly, the PPARγ mutations described hitherto all result in reduced transcriptional activity. Unlike these mutations, the PPARγ P113Q mutation displayed an increased transcriptional activity. Mutation of this P113 has been shown to impair the inhibitory phosphorylation of the adjacent serine (S112), which explains the increased transcriptional activity. As TZD mediated PPARγ activation improves insulin sensitivity, this might suggest that hyperactivation of PPARγ due to defective S112 phosphorylation would increase insulin sensitivity. Indeed, S112A mice on a high fat diet have been shown to be more insulin sensitive compared to wild type mice (45). Contrary, subjects harbouring the P113Q mutation that also blocks S112 phosphorylation are insulin resistant. These differences might be due to a subtle difference in the effect of these mutations on the protein structure. Alternatively, additional factors, like gene and/or environmental factors, may influence insulin sensitivity in humans. PPARγ P113Q knock-in mouse on different diets are needed to solve this.
Furthermore, although the PPARγ mutations are relatively rare and affect only a small number of patients, metabolic studies in these patients together with knock-in mouse models on different diets might be useful models to unravel the underlying mechanisms contributing to the development of insulin resistance.

The role of PPARγ in lipid metabolism in adipocytes

PPARγ is a master regulator of adipocyte differentiation as it has been shown to be necessary and sufficient to induce adipogenesis *in vitro* and *in vivo*. PPARγ also plays an essential role in mature adipocytes at least in part by maintaining the expression of genes that confer the characteristics of mature adipocytes (46) and has been shown to be necessary for survival of adipocytes *in vivo* (47). Very recently genome-wide profiling of PPARγ binding sites combined with genome-wide profiling of RNA polymerase II occupancy (RNAPII) during 3T3-L1 adipogenesis showed a strong enrichment of genes involved in lipid and glucose metabolism during differentiation (6;8). In the last decade, the direct regulation of a number of genes by PPARγ has been confirmed, such as genes encoding proteins involved in lipid uptake (LPL, CD36 and OLR), lipid droplet proteins (perilipin and S3-12), enzymes involved in lipolysis (ATGL and HSL) and glyceroneogenesis (PEPCK, GyK).

PPARγ mediates the regulation of antilipolytic genes
A hallmark of adipocytes is the storage of lipids. In the normal physiological

state, excess of fuel substrates are partitioned in adipose tissue, where it is stored as triglycerides. In times of energy demand, these triglycerides are hydrolized to FFA and glycerol, and the FFAs released in the bloodstream can subsequently be used by other organs as fuel substrates. The regulation of lipolysis provides a main switch between lipid storage and lipid mobilization in times of energy demand and is tightly regulated by hormones, cytokines and other metabolites. PPARγ has been shown to regulate the expression of key enzymes in lipolysis, such as ATGL and HSL. Next to the regulation of lipolytic genes, PPARγ regulates the expression of antilipolytic genes in adipocytes as demonstrated by the direct regulation of the antilipolytic G-protein-coupled receptor 81 (GPR81) in Chapter 5. Furthermore the rapid and simultaneous increase of GPR81 and GPR109A and GPR109B, which are colocalized on human chromosome 12 in human mature adipocytes, suggests direct regulation of all three genes by PPARγ. Like the activation of the insulin receptor by insulin, activation of these receptors results in a reduction of intracellular cAMP levels and eventually inhibits lipolysis (Figure 3A). Interestingly, very recently it has been demonstrated that activation of another G-protein-coupled receptor, GPR43, reduced lipolysis and suppressed plasma FFA levels *in vitro* and *in vivo* (48). This receptor is highly expressed in subcutaneous, mesenteric and epididymal fat and its expression significantly increases during differentiation as well as after TZD treatment (49). For these reasons, we hypothesized that the expression of GPR43 is regulated by PPARγ. Preliminary data supports this hypothesis as ChIP-seq analysis in 3T3-L1 cells revealed a significant increase in PPARγ and RXR binding in the promoter of Gpr43 in adipocytes (day 6), which was negligible in pre-adipocytes (day 0) as shown in Figure 2A (8). Furthermore genome wide profiling of polymerase II occupancy (RNAPII), which provide a direct readout of transcriptional activation by transcription factors showed that RNAPII occupancy of Gpr43 increased during differentiation (Figure 2B), which is consistent with the notion that Gpr43 expression increased during differentiation (49). These data indicate that induction of Gpr43 expression is mediated by PPARγ. Additional experiments are required to strengthen our hypothesis. Since actetate, a GPR43 ligand, has been shown to reduce plasma FFA levels in humans (50;51) and GPR109a is the receptor for the antidyslipidemic drug nicotinic acid (52) it is tempting to speculate that part of the TZD effects are via the PPARγ-mediated induction of these GPCRs. To establish the relative contribution of these G-protein-coupled receptors in the lipid lowering effects of TZDs, the effects on FFA levels after TZD treatment in GPCR knock-out mice needs to be investigated.

Do TZDs regulate a specific subset of PPARγ target genes?

Administration of the insulin sensitizing TZDs to obese and/or insulin resistant subjects has been shown to reduce plasma FFA levels and thereby ameliorate insulin sensitivity (53;54). Since TZDs cause an increase in subcutaneous fat, at least part of these effects may be explained by the stimulatory effect of TZDs on

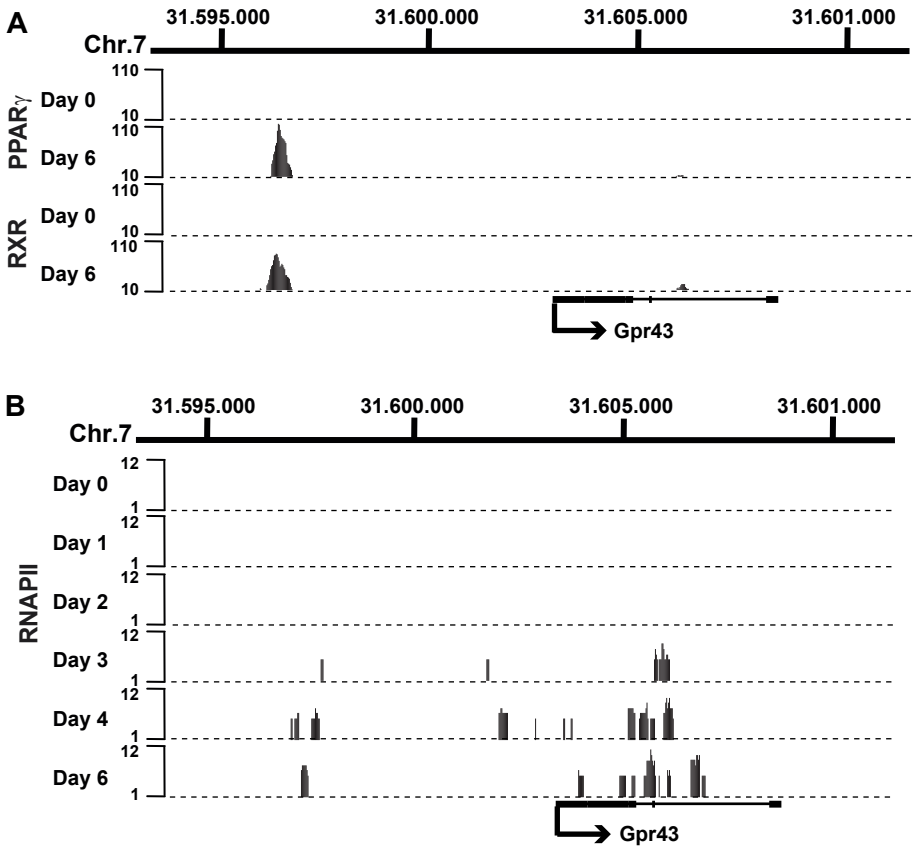

Figure 2. PPARγ:RXR binding and RNAPII occupancy at Gpr43 locus in adipocytes.
A, ChIP-seq data of 3T3-L1 pre-adipocytes (day 0) and adipocytes (day 6) viewed in the UCSC browser showing PPARγ and RXR binding sites for Gpr43. B, RNA polymerase II (RNAPII) occupancy at the Gpr43 gene at day 0, 1, 2, 3, 4 and 6 of 3T3-L1 differentiation. Data are kindly provided by Ronni Nielsen (8).

adipocyte differentiation, thereby increasing lipid storage capacity in adipose tissue. Interestingly, Li *et al.* investigated whether adipocyte differentiation induced by a constitutive active PPARγ or TZD resulted in different gene expression profiles (55). Although the extent of adipocyte differentiation was similar and rosiglitazone up-regulated many of the same genes as VP16-PPARγ induced adipogenesis, some genes were differently regulated. This suggests that TZDs might induce a subtle adipocyte phenotype difference by differential gene regulation. In line with this, rosiglitazone treatment of 3T3-F442 adipocytes rapidly and robustly induced PEPCK expression, whereas other well-known PPARγ target genes such as LPL, HSL and FAS were mildly induced (56). Of note, in our micro-analysis in human adipocytes

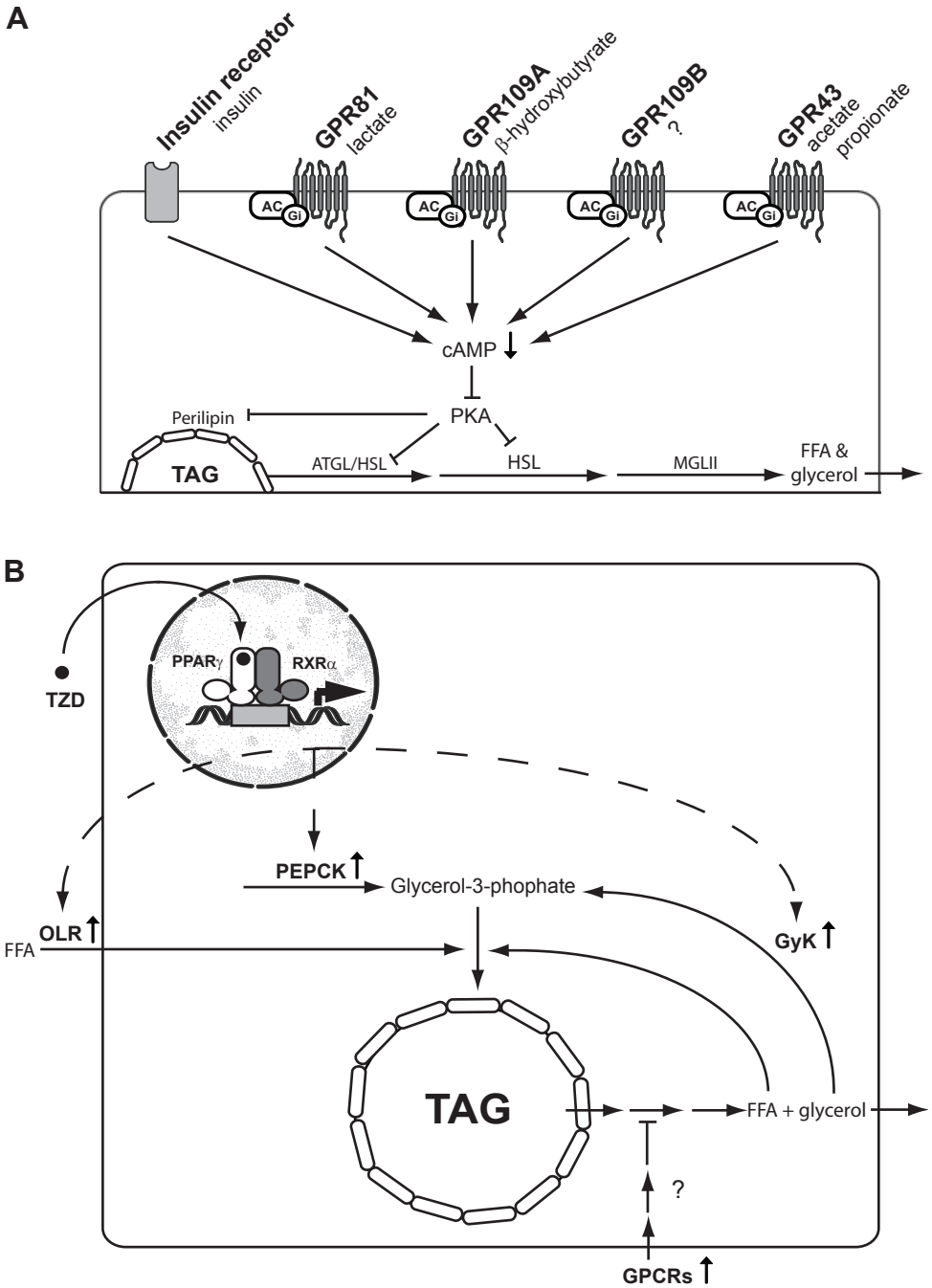
A
Insulin receptor
insulin
GPR81
lactate
GPR109A
β-hydroxybutyrate
GPR109B
?
GPR43
acetate
propionate
AC
Gi
cAMP
PKA
Perilipin
TAG
ATGL/HSL
HSL
MGLII
FFA &
glycerol
B
TZD
PPARγ
RXRα
PEPCK
Glycerol-3-phophate
OLR
FFA
GyK
TAG
FFA + glycerol
?
GPCRs

⇦ **Figure 3. Model for futile cycling of FFAs induced by TZDs in adipocytes.**
A, Activation of the insulin receptor and/or antilipolytic GPCRs inhibit lipolysis. Activation of G_i-coupled GPR81, GPR109A, GPR109B and GPR43 results in the inhibition of adenylyl cyclases. Like activation of the insulin receptor this will consequently result in a decrease in intracellular cAMP levels and Protein kinase A will be less active. PKA will no longer phosphorylate hormone sensitive lipase (HSL) and perilipin, which are involved in hydrolysis of TAG into FFA and glycerol resulting in a reduction FFA and glycerol release in the bloodstream. B, Administration of TZDs to adipocytes results in a rapid and robust increase of PEPCK, OLR and GyK. OLR enhances the uptake of FFAs, which can together with the FFAs liberated by basal lipolysis be used for the esterification into TAG. PEPCK is a key enzyme in glyceroneogenesis, which is the synthesis of glycerol-3-phophate (G3P) from non-carbohydrate precursors. GyK phosphorylates glycerol to G3P. Although the contribution of GyK is probably minor, together with PEPCK it produces G3P which serves as backbone for the re-esterification of FFAs in TAG. Enhanced FFA uptake together with recycling of FFA deliberated by lipolysis results in a net reduction of plasma FFA levels. Since antilipolytic GPCRs are also induced by TZD mediated PPARγ activation, these recptors might play a role in the lipid-lowering effects of TZDs as well.

treated with rosiglitazone for 6 hours, PEPCK1 (*PCK1*) was also among the genes with the highest fold induction (Chapter 6, Table 1). In addition, the PPARγ target genes GyK and OLR1 (oxidized LDL receptor 1), which are expressed at low levels in adipocytes, have been shown to be dramatically upregulated by TZDs (57;58). In contrast the expression level of the classical PPARγ target gene FABP4 (also known as Ap2) is already high in adipocytes and only mildly induced by TZDs. Although endogenous PPARγ/RXR binds ligand-independently in the promoter of these genes, cofactors are differentially recruited at these sites: in the absence of ligand PPARγ recruits coactivators in the promoter of *FABP4*, while recruiting corepressors in the promoter of *GyK* and *OLR1*. TZDs facilitate the exchange of coactivators for corepressors in the *GyK* and *OLR1* promoter, resulting in transcription of these genes. Additional studies are required to investigate whether TZDs modulate PEPCK expression and potential other TZD-specific induced PPARγ genes by a similar mechanism.
Induction of PEPCK, GyK and OLR1 by TZDs might cooperatively augment the futile cycling of FFAs in adipocytes ultimately decreasing plasma FFAs and thereby contributing to the insulin sensitizing properties of TZDs (Figure 3B). PEPCK and GyK are both involved in the production of glycerol-3-phosphate (G3P), a substrate for FFA re-esterification into TAG. In addition, induction of OLR1 has been demonstrated to enhance uptake of FFAs in adipocytes (58). The relevance of Gyk in humans is questionable as its expression is very low in human adipocytes, even in the presence of TZDs (59). In addition, glyceroneogenesis, the synthesis of G3P in which PEPCK is the key enzyme, has been shown to account for most of the FFA lowering effect of TZDs in cultured adipocytes (60). In keeping with the increased adiposity in humans after TZD treatment, overexpression of PEPCK in adipose tissue of mice resulted in obesity. Interestingly, unlike other animal models of obesity, these obese transgenic mice never develop insulin resistance (61). Although these data strongly support an important role for TZD-mediated

induction of PEPCK in the insulin sensitizing effects of these drugs, other genes might be involved as well. Since TZD treatment of adipocytes robustly induced the protein expression of GPR81 and PPARγ seems to regulate the expression of other antilipolytic GPCRs, these genes might also play a role in the lipid-lowering effects of TZDs. As mentioned earlier studies on GPCR knock-out mouse models treated with TZDs are needed to solve this. Furthermore, genome-wide cofactor profiling combined with micro-array studies might help to establish if TZDs modulate a specific subset of adipocyte PPARγ target genes by differential cofactor binding.

Anti-inflammatory response of TZDs

Enlarged adipocytes have been reported to secrete large amounts of pro-inflammatory cytokines, such as IL6 and TNFα. Consistent with this levels of IL6 and TNFα in culture medium of mature human adipocytes (SGBS) were strongly elevated compared to undifferentiated cells (preliminary data). The action of cytokines on adipocytes has two dramatic effects: an increase in lipolysis and a decreased triglyceride synthesis resulting in elevated levels of FFAs. Since elevated levels of FFA are associated with insulin resistance, the proinflammatory state of enlarged adipocytes might contribute to insulin resistance. In line with this, TNFα and TNFα receptor knockout mice show improved insulin sensitivity (62). The insulin sensitizing TZDs have been reported to have potent anti-inflammatory activity and suppress NK-κB activity (63). Treatment of human subjects with insulin-sensitizing TZDs has been shown to reduce TNFα expression (54;64) and LPS-stimulated IL6 secretion was reduced in mature 3T3-L1 adipocytes after treatment with the TZD pioglitazone (65). Conspicuously, KEGG pathway analysis of the downregulated genes in our micro-array analysis in hMADs treated with the TZD rosiglitazone for 6 hours revealed a strong enrichment for genes involved in cytokine-cytokine receptor interaction (Table 1). This supports the anti-inflammatory action of TZDs in adipocytes. One of the downregulated genes is CCL2, which encodes chemokine (C-

KEGG pathway	p-value
Cytokine-cytokine receptor interaction	1.10E-12
Focal adhesion	6.80E-10
MAPK signalling pathway	4.40E-5
Regulation of actin cytoskeleton	7.30E-5
Wnt signalling pathway	9.90E-5
TGF-beta signalling	1.20E-5

Table 1. KEGG pathway analysis down-regulated genes in micro-array analysis.
Downregulated genes in transcriptome analysis of differentiated hMADs treated with rosiglitazone for 6 hours were subjected to KEGG pathway analysis and revealed a strong enrichment of genes involved in cytokine-cytokine receptor interactions.

C motif) ligand-2 (also named MCP-1 (monocyte chemoattractant protein)). MCP1 functions as a chemo-attractant that enhances macrophage infiltration into adipose tissue in obese human (66) and mouse (67) and is, like IL6 and TNFα, secreted by hypertrophied adipocytes. CCR2 is an important receptor for MCP1 and CCR2$^{-/-}$ mouse are partly protected from high fat diet induced insulin resistance and exhibit reductions in adipose tissue macrophage recruitment and inflammatory gene expression (68). The notion that the effect is not complete suggests the existence of additional chemoattractant ligand-receptor pairs. A very recent study showed that MCP1 and MCP3 (CCL7) were significantly upregulated in primary adipocytes isolated from WAT of both ob/ob and HFD induced obese mice (69). Furthermore, FFA induced upregulation of MCP1 and MCP3 was reduced by a NF-κB inhibitor indicating that the regulation of these chemokines is mediated by NF-κB. Treatment with the TZD rosiglitazone reduced MCP1 and MCP3 expression in both 3T3-L1 adipocytes and WAT of obese mice, supporting an inhibitory role for PPARγ in NF-κB mediated cytokine production. Thus, hypertrophied adipocytes secrete pro-inflammatory cytokines, such as TNFα, IL6, MCP1 and MCP3, of which at least TNFα activates NF-κB, thereby reinforcing the expression of the pro-inflammatory cytokines. Moreover, TNFα attenuates PPARγ mRNA and protein levels (70;71) resulting in reduced lipid uptake and enhanced lipolysis, thereby raising plasma FFA levels and contributing to insulin resistance (Figure 4A). TZDs suppress NF-κB mediated cytokine secretion and mediate the induction of PPARγ target genes resulting in FFA sequestration in adipocytes thereby reducing plasma FFA levels and improving insulin sensitivity (Figure 4B).
In conclusion, our micro-array analysis in hMADs treated with rosiglitazone for 6 hours confirmed the TZD-mediated downregulation of the pro-inflammatory cytokines MCP1 (CCL2) and MCP3 (CCL7), supporting the anti-inflammatory effect of TZDs in adipocytes. Furthermore this study might help to identify new factors potentially contributing to the inflammatory state of enlarged adipocytes.

Final remarks

Both obesity and lipodystrophy are associated with major complications such as insulin resistance and cardiovascular disease, illustrating the importance of adipose tissue in normal lipid and glucose homeostasis. An important regulator in adipocyte differentiation, maintenance and function is PPARγ, as has become evident from natural occurring mutations in PPARγ and the identification of PPARγ as the molecular target of the insulin sensitizing TZDs. In the past decade, a large number of studies have advanced our understanding on the role of PPARγ in adipocyte biology. As the prevalence of obesity rapidly increases and a major complication is insulin resistance, a lot of research focuses on the development of drugs ameliorating insulin sensitivity. Although TZDs were promising insulin

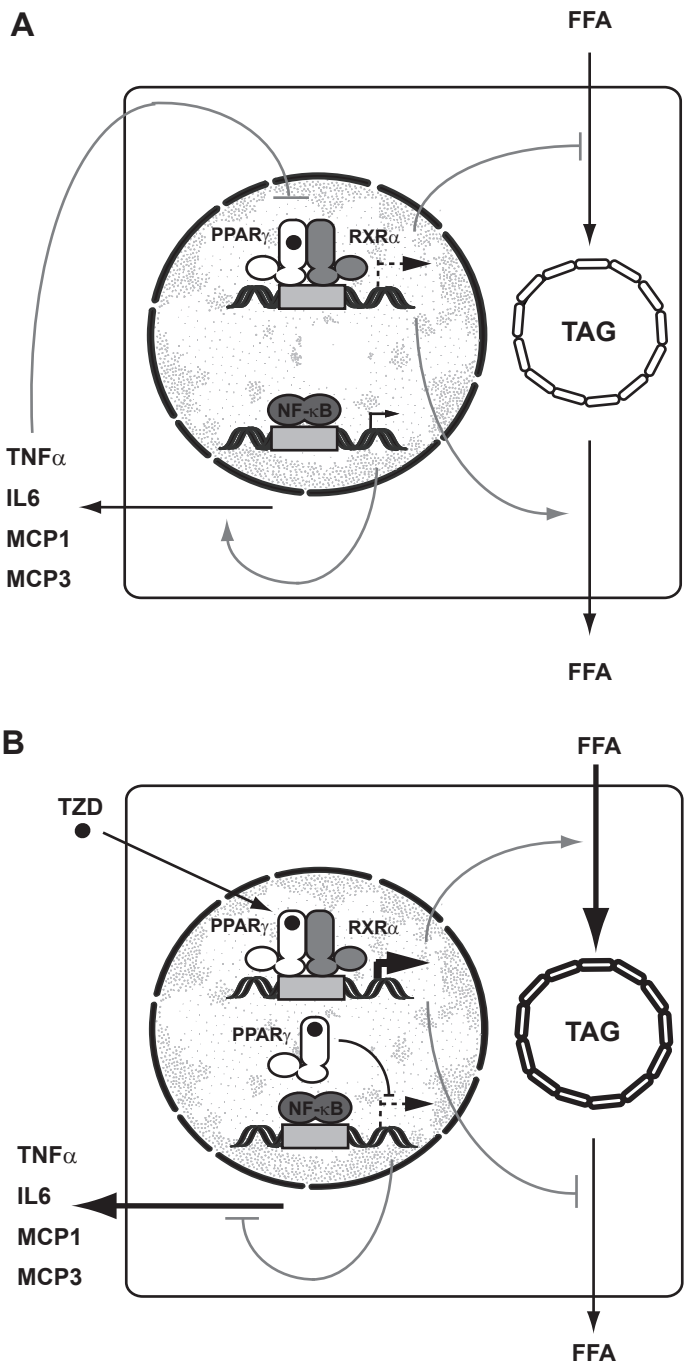

Figure 4. Model of anti-inflammatory action of TZDs.
A, In enlarged adipocytes NF-κB activation results in the production of pro-inflammatory cytokines, of which at least TNFα has been shown to inhibit PPARγ and activate NF-κB thereby reinforcing the production of pro-inflammatory cytokines. Inhibition of PPARγ eventually results in inhibition of FFA uptake and enhanced lipolysis ultimately elevating plasma FFA levels. B, In the presence of a TZD, PPARγ is activated and induces the expression of genes involved in FFA trapping in the adipose tissue resulting in a net reduction of plasma FFA levels. Furthermore, PPARγ inhibits NF-κB activation resulting in a reduction of pro-inflammatory cytokines released.

sensitizing drugs, some of the TZDs are already discarded because of undesired side-effects (72). Nowadays, research focuses on specific PPARγ modulators, so called SPARMs which in theory would only exert the beneficial effects (73). For this purpose a better understanding of ligand dependent PPARγ modulation on specific PPARγ target genes is needed.

References

1. Szymanski KM, Binns D, Bartz R, Grishin NV, Li WP, Agarwal AK, Garg A, Anderson RG, Goodman JM 2007 The lipodystrophy protein seipin is found at endoplasmic reticulum lipid droplet junctions and is important for droplet morphology. Proc Natl Acad Sci U S A 104:20890-20895
2. Fei W, Shui G, Gaeta B, Du X, Kuerschner L, Li P, Brown AJ, Wenk MR, Parton RG, Yang H 2008 Fld1p, a functional homologue of human seipin, regulates the size of lipid droplets in yeast. J Cell Biol 180:473-482
3. Payne VA, Grimsey N, Tuthill A, Virtue S, Gray SL, Dalla NE, Semple RK, O'Rahilly S, Rochford JJ 2008 The human lipodystrophy gene BSCL2/seipin may be essential for normal adipocyte differentiation. Diabetes 57:2055-2060
4. Fajas L, Schoonjans K, Gelman L, Kim JB, Najib J, Martin G, Fruchart JC, Briggs M, Spiegelman BM, Auwerx J 1999 Regulation of peroxisome proliferator-activated receptor gamma expression by adipocyte differentiation and determination factor 1/sterol regulatory element binding protein 1: implications for adipocyte differentiation and metabolism. Mol Cell Biol 19:5495-5503
5. Kim JB, Wright HM, Wright M, Spiegelman BM 1998 ADD1/SREBP1 activates PPARgamma through the production of endogenous ligand. Proc Natl Acad Sci U S A 95:4333-4337
6. Lefterova MI, Zhang Y, Steger DJ, Schupp M, Schug J, Cristancho A, Feng D, Zhuo D, Stoeckert CJ, Jr., Liu XS, Lazar MA 2008 PPAR{gamma} and C/EBP factors orchestrate adipocyte biology via adjacent binding on a genome-wide scale. Genes Dev 22:2941-2952
7. Gale SE, Frolov A, Han X, Bickel PE, Cao L, Bowcock A, Schaffer JE, Ory DS 2006 A regulatory role for 1-acylglycerol-3-phosphate-O-acyltransferase 2 in adipocyte differentiation. J Biol Chem 281:11082-11089
8. Nielsen R, Pedersen TA, Hagenbeek D, Moulos P, Siersbaek R, Megens E, Denissov S, Borgesen M, Francoijs KJ, Mandrup S, Stunnenberg HG 2008 Genome-wide profiling of PPAR{gamma}:RXR and RNA polymerase II occupancy reveals temporal activation of distinct metabolic pathways and changes in RXR dimer composition during adipogenesis. Genes Dev 22:2953-2967
9. Cortes VA, Curtis DE, Sukumaran S, Shao X, Parameswara V, Rashid S, Smith AR, Ren J, Esser V, Hammer RE, Agarwal AK, Horton JD, Garg A 2009 Molecular mechanisms of hepatic steatosis and insulin resistance in the AGPAT2-deficient mouse model of congenital generalized lipodystrophy. Cell Metab 9:165-176
10. Razani B, Combs TP, Wang XB, Frank PG, Park DS, Russell RG, Li M, Tang B, Jelicks LA, Scherer PE, Lisanti MP 2002 Caveolin-1-deficient mice are lean, resistant to diet-induced obesity, and show hypertriglyceridemia with adipocyte abnormalities. J Biol Chem 277:8635-8647
11. Scherer PE, Lisanti MP, Baldini G, Sargiacomo M, Mastick CC, Lodish HF 1994 Induction of caveolin during adipogenesis and association of GLUT4 with caveolin-rich vesicles. J Cell Biol 127:1233-1243
12. Cohen AW, Razani B, Schubert W, Williams TM, Wang XB, Iyengar P, Brasaemle DL, Scherer PE, Lisanti MP 2004 Role of caveolin-1 in the modulation of lipolysis and lipid droplet formation. Diabetes 53:1261-1270
13. Cao H, Alston L, Ruschman J, Hegele RA 2008 Heterozygous CAV1 frameshift mutations (MIM 601047) in patients with atypical partial lipodystrophy and hypertriglyceridemia. Lipids Health Dis 7:3
14. Kim CA, Delepine M, Boutet E, El Mourabit H, Le Lay S, Meier M, Nemani M, Bridel E, Leite CC, Bertola DR, Semple RK, O'Rahilly S, Dugail I, Capeau J, Lathrop M, Magre J 2008 Association of a homozygous nonsense caveolin-1 mutation with Berardinelli-Seip congenital lipodystrophy. J Clin Endocrinol Metab 93:1129-1134
15. Lloyd DJ, Trembath RC, Shackleton S 2002 A novel interaction between lamin A and SREBP1: implications for partial lipodystrophy and other laminopathies. Hum Mol Genet 11:769-777
16. Capanni C, Mattioli E, Columbaro M, Lucarelli E, Parnaik VK, Novelli G, Wehnert M, Cenni V, Maraldi NM, Squarzoni S, Lattanzi G 2005 Altered pre-lamin A processing is a common mechanism leading to lipodystrophy. Hum Mol Genet 14:1489-1502

17. Caron M, Auclair M, Donadille B, Bereziat V, Guerci B, Laville M, Narbonne H, Bodemer C, Lascols O, Capeau J, Vigouroux C 2007 Human lipodystrophies linked to mutations in A-type lamins and to HIV protease inhibitor therapy are both associated with prelamin A accumulation, oxidative stress and premature cellular senescence. Cell Death Differ 14:1759-1767
18. Maraldi NM, Capanni C, Lattanzi G, Camozzi D, Facchini A, Manzoli FA 2008 SREBP1 interaction with prelamin A forms: a pathogenic mechanism for lipodystrophic laminopathies. Adv Enzyme Regul 48:209-223
19. Sinensky M, Fantle K, Trujillo M, McLain T, Kupfer A, Dalton M 1994 The processing pathway of prelamin A. J Cell Sci 107 (Pt 1):61-67
20. Shackleton S, Smallwood DT, Clayton P, Wilson LC, Agarwal AK, Garg A, Trembath RC 2005 Compound heterozygous ZMPSTE24 mutations reduce prelamin A processing and result in a severe progeroid phenotype. J Med Genet 42:e36
21. Pendas AM, Zhou Z, Cadinanos J, Freije JM, Wang J, Hultenby K, Astudillo A, Wernerson A, Rodriguez F, Tryggvason K, Lopez-Otin C 2002 Defective prelamin A processing and muscular and adipocyte alterations in Zmpste24 metalloproteinase-deficient mice. Nat Genet 31:94-99
22. George S, Rochford JJ, Wolfrum C, Gray SL, Schinner S, Wilson JC, Soos MA, Murgatroyd PR, Williams RM, Acerini CL, Dunger DB, Barford D, Umpleby AM, Wareham NJ, Davies HA, Schafer AJ, Stoffel M, O'Rahilly S, Barroso I 2004 A family with severe insulin resistance and diabetes due to a mutation in AKT2. Science 304:1325-1328
23. Tan K, Kimber WA, Luan J, Soos MA, Semple RK, Wareham NJ, O'Rahilly S, Barroso I 2007 Analysis of genetic variation in Akt2/PKB-beta in severe insulin resistance, lipodystrophy, type 2 diabetes, and related metabolic phenotypes. Diabetes 56:714-719
24. Cho H, Mu J, Kim JK, Thorvaldsen JL, Chu Q, Crenshaw EB, III, Kaestner KH, Bartolomei MS, Shulman GI, Birnbaum MJ 2001 Insulin resistance and a diabetes mellitus-like syndrome in mice lacking the protein kinase Akt2 (PKB beta). Science 292:1728-1731
25. Garofalo RS, Orena SJ, Rafidi K, Torchia AJ, Stock JL, Hildebrandt AL, Coskran T, Black SC, Brees DJ, Wicks JR, McNeish JD, Coleman KG 2003 Severe diabetes, age-dependent loss of adipose tissue, and mild growth deficiency in mice lacking Akt2/PKB beta. J Clin Invest 112:197-208
26. Le Lay S, Lefrere I, Trautwein C, Dugail I, Krief S 2002 Insulin and sterol-regulatory element-binding protein-1c (SREBP-1C) regulation of gene expression in 3T3-L1 adipocytes. Identification of CCAAT/enhancer-binding protein beta as an SREBP-1C target. J Biol Chem 277:35625-35634
27. Yun SJ, Kim EK, Tucker DF, Kim CD, Birnbaum MJ, Bae SS 2008 Isoform-specific regulation of adipocyte differentiation by Akt/protein kinase Balpha. Biochem Biophys Res Commun 371:138-143
28. Liang G, Yang J, Horton JD, Hammer RE, Goldstein JL, Brown MS 2002 Diminished hepatic response to fasting/refeeding and liver X receptor agonists in mice with selective deficiency of sterol regulatory element-binding protein-1c. J Biol Chem 277:9520-9528
29. Shimano H, Shimomura I, Hammer RE, Herz J, Goldstein JL, Brown MS, Horton JD 1997 Elevated levels of SREBP-2 and cholesterol synthesis in livers of mice homozygous for a targeted disruption of the SREBP-1 gene. J Clin Invest 100:2115-2124
30. Tan GD, Neville MJ, Liverani E, Humphreys SM, Currie JM, Dennis L, Fielding BA, Karpe F 2006 The in vivo effects of the Pro12Ala PPARgamma2 polymorphism on adipose tissue NEFA metabolism: the first use of the Oxford Biobank. Diabetologia 49:158-168
31. Altshuler D, Hirschhorn JN, Klannemark M, Lindgren CM, Vohl MC, Nemesh J, Lane CR, Schaffner SF, Bolk S, Brewer C, Tuomi T, Gaudet D, Hudson TJ, Daly M, Groop L, Lander ES 2000 The common PPAR gamma Pro12Ala polymorphism is associated with decreased risk of type 2 diabetes. Nat Genet 26:76-80
32. Ludovico O, Pellegrini F, Di Paola R, Minenna A, Mastroianno S, Cardellini M, Marini MA, Andreozzi F, Vaccaro O, Sesti G, Trischitta V 2007 Heterogeneous effect of peroxisome proliferator-activated receptor gamma2 Ala12 variant on type 2 diabetes risk. Obesity (Silver Spring) 15:1076-1081
33. Masud S, Ye S 2003 Effect of the peroxisome proliferator activated receptor-gamma gene Pro12Ala variant on body mass index: a meta-analysis. J Med Genet 40:773-780

34. Beamer BA, Yen CJ, Andersen RE, Muller D, Elahi D, Cheskin LJ, Andres R, Roth J, Shuldiner AR 1998 Association of the Pro12Ala variant in the peroxisome proliferator-activated receptor-gamma2 gene with obesity in two Caucasian populations. Diabetes 47:1806-1808
35. Swarbrick MM, Chapman CM, McQuillan BM, Hung J, Thompson PL, Beilby JP 2001 A Pro12Ala polymorphism in the human peroxisome proliferator-activated receptor-gamma 2 is associated with combined hyperlipidaemia in obesity. Eur J Endocrinol 144:277-282
36. Luan J, Browne PO, Harding AH, Halsall DJ, O'Rahilly S, Chatterjee VK, Wareham NJ 2001 Evidence for gene-nutrient interaction at the PPARgamma locus. Diabetes 50:686-689
37. Franks PW, Luan J, Browne PO, Harding AH, O'Rahilly S, Chatterjee VK, Wareham NJ 2004 Does peroxisome proliferator-activated receptor gamma genotype (Pro12ala) modify the association of physical activity and dietary fat with fasting insulin level? Metabolism 53:11-16
38. Heikkinen S, Argmann C, Feige JN, Koutnikova H, Champy MF, Dali-Youcef N, Schadt EE, Laakso M, Auwerx J 2009 The Pro12Ala PPARgamma2 variant determines metabolism at the gene-environment interface. Cell Metab 9:88-98
39. Hu E, Liang P, Spiegelman BM 1996 AdipoQ is a novel adipose-specific gene dysregulated in obesity. J Biol Chem 271:10697-10703
40. Mousavinasab F, Tahtinen T, Jokelainen J, Koskela P, Vanhala M, Oikarinen J, Keinanen-Kiukaanniemi S, Laakso M 2005 Common polymorphisms in the PPARgamma2 and IRS-1 genes and their interaction influence serum adiponectin concentration in young Finnish men. Mol Genet Metab 84:344-348
41. Gray SL, Nora ED, Grosse J, Manieri M, Stoeger T, Medina-Gomez G, Burling K, Wattler S, Russ A, Yeo GS, Chatterjee VK, O'Rahilly S, Voshol PJ, Cinti S, Vidal-Puig A 2006 Leptin deficiency unmasks the deleterious effects of impaired peroxisome proliferator-activated receptor gamma function (P465L PPARgamma) in mice. Diabetes 55:2669-2677
42. Freedman BD, Lee EJ, Park Y, Jameson JL 2005 A dominant negative peroxisome proliferator-activated receptor-gamma knock-in mouse exhibits features of the metabolic syndrome. J Biol Chem 280:17118-17125
43. Tan GD, Savage DB, Fielding BA, Collins J, Hodson L, Humphreys SM, O'Rahilly S, Chatterjee K, Frayn KN, Karpe F 2008 Fatty acid metabolism in patients with PPARgamma mutations. J Clin Endocrinol Metab 93:4462-4470
44. Savage DB, Agostini M, Barroso I, Gurnell M, Luan J, Meirhaeghe A, Harding AH, Ihrke G, Rajanayagam O, Soos MA, George S, Berger D, Thomas EL, Bell JD, Meeran K, Ross RJ, Vidal-Puig A, Wareham NJ, O'Rahilly S, Chatterjee VK, Schafer AJ 2002 Digenic inheritance of severe insulin resistance in a human pedigree. Nat Genet 31:379-384
45. Rangwala SM, Rhoades B, Shapiro JS, Rich AS, Kim JK, Shulman GI, Kaestner KH, Lazar MA 2003 Genetic modulation of PPAR gamma phosphorylation regulates insulin sensitivity. Dev Cell 5:657-663
46. Tamori Y, Masugi J, Nishino N, Kasuga M 2002 Role of peroxisome proliferator-activated receptor-gamma in maintenance of the characteristics of mature 3T3-L1 adipocytes. Diabetes 51:2045-2055
47. Imai T, Takakuwa R, Marchand S, Dentz E, Bornert JM, Messaddeq N, Wendling O, Mark M, Desvergne B, Wahli W, Chambon P, Metzger D 2004 Peroxisome proliferator-activated receptor gamma is required in mature white and brown adipocytes for their survival in the mouse. Proc Natl Acad Sci U S A 101:4543-4547
48. Ge H, Li X, Weiszmann J, Wang P, Baribault H, Chen JL, Tian H, Li Y 2008 Activation of G protein-coupled receptor 43 in adipocytes leads to inhibition of lipolysis and suppression of plasma free fatty acids. Endocrinology 149:4519-4526
49. Hong YH, Nishimura Y, Hishikawa D, Tsuzuki H, Miyahara H, Gotoh C, Choi KC, Feng DD, Chen C, Lee HG, Katoh K, Roh SG, Sasaki S 2005 Acetate and propionate short chain fatty acids stimulate adipogenesis via GPCR43. Endocrinology 146:5092-5099
50. Suokas A, Kupari M, Heikkila J, Lindros K, Ylikahri R 1988 Acute cardiovascular and metabolic effects of acetate in men. Alcohol Clin Exp Res 12:52-58
51. Laurent C, Simoneau C, Marks L, Braschi S, Champ M, Charbonnel B, Krempf M 1995 Effect of acetate and propionate on fasting hepatic glucose production in humans. Eur J Clin Nutr 49:484-

491
52. Gille A, Bodor ET, Ahmed K, Offermanns S 2008 Nicotinic acid: pharmacological effects and mechanisms of action. Annu Rev Pharmacol Toxicol 48:79-106.:79-106
53. Lenhard JM, Kliewer SA, Paulik MA, Plunket KD, Lehmann JM, Weiel JE 1997 Effects of troglitazone and metformin on glucose and lipid metabolism: alterations of two distinct molecular pathways. Biochem Pharmacol 54:801-808
54. McTernan PG, Harte AL, Anderson LA, Green A, Smith SA, Holder JC, Barnett AH, Eggo MC, Kumar S 2002 Insulin and rosiglitazone regulation of lipolysis and lipogenesis in human adipose tissue in vitro. Diabetes 51:1493-1498
55. Li Y, Lazar MA 2002 Differential gene regulation by PPARgamma agonist and constitutively active PPARgamma2. Mol Endocrinol 16:1040-1048
56. Glorian M, Duplus E, Beale EG, Scott DK, Granner DK, Forest C 2001 A single element in the phosphoenolpyruvate carboxykinase gene mediates thiazolidinedione action specifically in adipocytes. Biochimie 83:933-943
57. Guan HP, Ishizuka T, Chui PC, Lehrke M, Lazar MA 2005 Corepressors selectively control the transcriptional activity of PPARgamma in adipocytes. Genes Dev 19:453-461
58. Chui PC, Guan HP, Lehrke M, Lazar MA 2005 PPARgamma regulates adipocyte cholesterol metabolism via oxidized LDL receptor 1. J Clin Invest 115:2244-2256
59. Tan GD, Debard C, Tiraby C, Humphreys SM, Frayn KN, Langin D, Vidal H, Karpe F 2003 A "futile cycle" induced by thiazolidinediones in human adipose tissue? Nat Med 9:811-812
60. Tordjman J, Chauvet G, Quette J, Beale EG, Forest C, Antoine B 2003 Thiazolidinediones block fatty acid release by inducing glyceroneogenesis in fat cells. J Biol Chem 278:18785-18790
61. Franckhauser S, Munoz S, Pujol A, Casellas A, Riu E, Otaegui P, Su B, Bosch F 2002 Increased fatty acid re-esterification by PEPCK overexpression in adipose tissue leads to obesity without insulin resistance. Diabetes 51:624-630
62. Uysal KT, Wiesbrock SM, Marino MW, Hotamisligil GS 1997 Protection from obesity-induced insulin resistance in mice lacking TNF-alpha function. Nature 389:610-614
63. Shoelson SE, Lee J, Goldfine AB 2006 Inflammation and insulin resistance. J Clin Invest 116:1793-1801
64. Souza SC, Yamamoto MT, Franciosa MD, Lien P, Greenberg AS 1998 BRL 49653 blocks the lipolytic actions of tumor necrosis factor-alpha: a potential new insulin-sensitizing mechanism for thiazolidinediones. Diabetes 47:691-695
65. Yamaguchi M, Nishimura F, Naruishi H, Soga Y, Kokeguchi S, Takashiba S 2005 Thiazolidinedione (pioglitazone) blocks P. gingivalis- and F. nucleatum, but not E. coli, lipopolysaccharide (LPS)-induced interleukin-6 (IL-6) production in adipocytes. J Dent Res 84:240-244
66. Curat CA, Miranville A, Sengenes C, Diehl M, Tonus C, Busse R, Bouloumie A 2004 From blood monocytes to adipose tissue-resident macrophages: induction of diapedesis by human mature adipocytes. Diabetes 53:1285-1292
67. Xu H, Barnes GT, Yang Q, Tan G, Yang D, Chou CJ, Sole J, Nichols A, Ross JS, Tartaglia LA, Chen H 2003 Chronic inflammation in fat plays a crucial role in the development of obesity-related insulin resistance. J Clin Invest 112:1821-1830
68. Weisberg SP, Hunter D, Huber R, Lemieux J, Slaymaker S, Vaddi K, Charo I, Leibel RL, Ferrante AW, Jr. 2006 CCR2 modulates inflammatory and metabolic effects of high-fat feeding. J Clin Invest 116:115-124
69. Jiao P, Chen Q, Shah S, Du J, Tao B, Tzameli I, Yan W, Xu H 2009 Obesity-related upregulation of monocyte chemotactic factors in adipocytes: involvement of nuclear factor-kappaB and c-Jun NH2-terminal kinase pathways. Diabetes 58:104-115
70. Tang XQ, Guilherme A, Chakladar A, Powelka AM, Konda S, Virbasius JV, Nicoloro SMC, Straubhaar J, Czech MP 2006 An RNA interference-based screen identifies MAP4K4/NIK as a negative regulator of PPAR gamma, adipogenesis, and insulin-responsive hexose transport. Proc Natl Acad Sci U S A 103:2087-2092
71. Christianson JL, Nicoloro S, Straubhaar J, Czech MP 2008 Stearoyl-CoA desaturase 2 is required for peroxisome proliferator-activated receptor gamma expression and adipogenesis in cultured

3T3-L1 cells. J Biol Chem 283:2906-2916
72. Gervois P, Fruchart JC, Staels B 2007 Drug Insight: mechanisms of action and therapeutic applications for agonists of peroxisome proliferator-activated receptors. Nat Clin Pract Endocrinol Metab 3:145-156
73. Balint BL, Nagy L 2006 Selective modulators of PPAR activity as new therapeutic tools in metabolic diseases. Endocr Metab Immune Disord Drug Targets 6:33-43

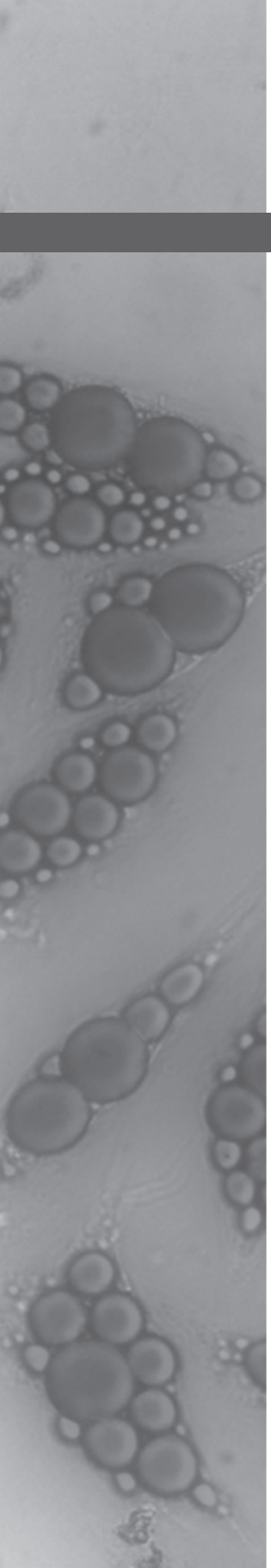

Chapter 9

Summary

The ligand-inducible nuclear receptor Peroxisome Proliferator Activated Receptor γ (PPARγ) plays an important role in the differentiation, maintenance and function of adipocytes. In addition it is the molecular target of the insulin-sensitizing thiazolidinedione (TZD) drugs. However, how the activation of PPARγ by TZDs leads to insulin-sensitization remains poorly understood. For this reason we studied the effects of rare natural occurring PPARγ mutations in patients with familial partial lipodystrophy (FPLD3). In addition, we discovered novel genes that are regulated by TZDs and probably contribute to the insulin-sensitizng effects of TZDs.

In **Chapter 1**, we describe lipid metabolism in adipocytes and the role of PPARγ in this process. Furthermore, we provide an overview of the different forms of lipodystrophy and genetic variation in PPARγ.

A number of studies focussed on the effects of natural occurring mutations on PPARγ function. In **Chapter 2** we provide an overview of the results of these studies and combine this with novel insights obtained by the elucidation of the 3D-structure of the full length PPARγ/RXRα heterodimer bound to DNA.

The functional consequences of two of the FPLD3-associated PPARγ mutations are described in Chapter 3 and 4. The mutation (R425C) described in **Chapter 3** is located in the ligand binding domain of PPARγ and affects its function at multiple levels, such as ligand and DNA binding resulting in reduced transcriptional activity. Crystallographic modelling of the 3D-structure of the PPARγ LBD predicted that these defects are the consequence of disruption of a conserved salt bridge and the subsequent formation of an alternative salt bridge. In **Chapter 4** we report a novel mutation (R194W) in the DNA binding domain of PPARγ in a patient with FPLD3. This arginine (R194) is located in the DNA binding domain and contacts the phosphate backbone of DNA. Therefore mutation of this arginine disrupts DNA binding resulting in a transcriptionally inactive PPARγ protein.

In order to get more insight in the mechanisms underlying the TZD effects, we performed a transcriptome analysis in human adipocytes treated with the TZD rosiglitazone for 6 hours. Using this method we identified two novel genes that are regulated by TZD-mediated PPARγ activation. In **Chapter 5** we show that PPARγ regulates the expression of the antilipolytic *GPR81* gene. This gene encodes a G-protein-coupled receptor that is exclusively expressed in adipocytes. Activation of this receptor results in the inhibition of adipocyte lipolysis. One of the beneficial effects of TZDs is a lowering of plasma free fatty acids thereby improving insulin sensitivity. We propose therefore that PPARγ-mediated regulation of GPR81 contributes to this effect. Another gene regulated by rosiglitazone-mediated PPARγ activation is RNF125, described in **Chapter 6**. RNF125 is an E3-ubiqituin ligase. The substrate for RNF125 in adipocytes is currently unknown and therefore the relevance of the regulation of this gene in adipocytes by TZDs needs to be further explored.

We identified a novel mutation in the *BSCL2* gene in a patient with congenital

generalized lipodystrophy type 2 (CGL2), described in **Chapter 7**. This mutation is located in the splice site of exon 5 and results in the formation of aberrant proteins. *BSCL2* encodes seipin, an integral ER protein that has been shown to play an essential role in adipogenesis and the formation of lipid droplets, a hallmark of adipocytes. In the urine of this patient we found abnormal levels of organic acids, indicating that mitochondrial dysfunction may form an intrinsic part of this congenital defect.
In **Chapter 8** we discuss and integrate the results described in the previous chapters in the current literature.

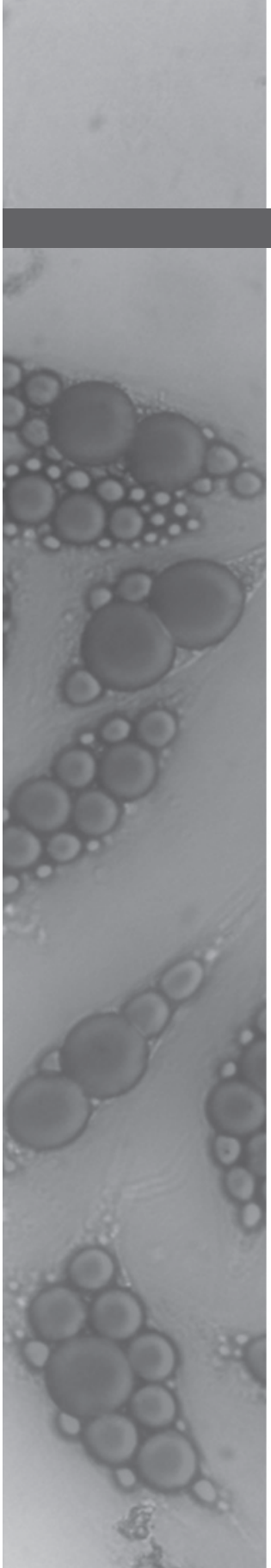

Nederlanse samenvatting voor niet ingewijden

In de westerse samenleving neemt het percentage van mensen met overgewicht (25<BMI<30) en obesitas (zwaarlijvigheid; BMI>30) steeds verder toe, zelfs onder kinderen. Had in de jaren '70 nog 15% van de kinderen in de Verenigde Staten overgewicht, in 2003 was al 36% te zwaar en dit zal alleen nog maar verder toenemen. Hoewel de Verenigde Staten nog steeds koploper zijn, in de Europese landen (m.n. Engeland) en Japan is het percentage in de afgelopen 30 jaar ook verdubbeld. Het is interessant om te zien dat deze toename gelijk opgaat met de toename van de portiegroottes van bijvoorbeeld een hamburger en een beker cola bij fastfoodketens in de jaren '70 en nu. Een overmatig, voornamelijk suiker- en vetrijk, dieet is dan ook een van de oorzaken van het ontstaan van overgewicht. Een andere oorzaak is te vinden in een tekort aan lichaamsbeweging doordat steeds meer kinderen met de auto overal naartoe worden gebracht en in hun vrije tijd voornamelijk voor de tv en/of de computer zitten.

De vet paradox

Overgewicht en obesitas vormen een groot gezondheidsrisico, omdat het gepaard gaat met complicaties zoals een verhoogde bloeddruk, dyslipidemie (te lage concentraties "goed" cholesterol (HDL) en te hoge concentraties "slecht" cholesterol (LDL)) in het bloed) wat kan leiden tot hart- en vaatziekten. Ook kan het verhoogde bloedsuikerspiegels en insuline-ongevoeligheid veroorzaken, wat kan leiden tot type II diabetes ('ouderdoms suikerziekte"). Vroeger kwam zoals de bijnaam al doet vermoeden, type II diabetes voornamelijk voor bij oudere mensen. Tegenwoordig hebben al veel jonge mensen en zelfs kinderen type II diabetes en een van de grootste oorzaken hiervoor is overgewicht. Ongeveer 80% van mensen met type II diabetes hebben dan ook overgewicht/obesitas.
Echter, niet alleen overgewicht/obesitas kan leiden tot type II diabetes, ook een tekort aan vetweefsel, zoals het geval is in lipodystrofie, gaat gepaard met type II diabetes en andere complicaties die geassocieerd zijn met obesitas. Lipodystrofie is een stoornis in de vethuishouding in het lichaam en wordt gekarakteriseerd door een totale afwezigheid van vetweefsel (gegeneraliseerde lipodystrofie) of door de plaatselijke afwezigheid en/of toename van vetweefsel (partiële lipodystrofie)). Het kan aangeboren (genetisch) zijn en veroorzaakt door foutjes (mutaties) in bepaalde genen of door het gebruik van sommige medicijnen (verworven), zoals het geval is bij de behandeling van patiënten met HIV.
Dit geeft aan dat een normale hoeveelheid en/of een normale verdeling van het vetweefsel in het lichaam van essentieel belang is voor een gezonde stofwisseling in het lichaam.

Vetstofwisseling in vetcellen

Vetcellen (adipocyten) zijn unieke cellen in het lichaam, omdat ze de mogelijkheid hebben om een overschot aan brandstoffen (suikers (glucose) en vetten (FFA)) in het bloed, zoals het geval is na een maaltijd, op te slaan als triacylglycerol (TAG) in vetdruppels (zie Figuur 1). De opgeslagen triacylglycerolen kunnen op hun beurt weer afgebroken worden en afgegeven aan de bloedbaan om vervolgens door de lever omgezet te worden in brandstoffen die gebruikt kunnen worden door andere organen als daar om gevraagd wordt, bijvoorbeeld tijdens duursporten of vasten. De afbraak van deze triacylglycerolen (lipolyse) wordt onder andere geregeld door adrenaline en insuline. Adrenaline wordt gemaakt in de bijnier en is het meest bekende molecuul dat de lipolyse in vetcellen stimuleert. Insuline echter remt de lipolyse in vetcellen. Dit hormoon wordt gemaakt in de alvleesklier als reactie op verhoogde suikerspiegels na voedselinname en zorgt ervoor dat deze suikers opgenomen worden in insuline-gevoelige organen zoals spieren, vetweefsel en lever, zodat de suikerspiegels in het bloed constant blijven. Dit is erg belangrijk,

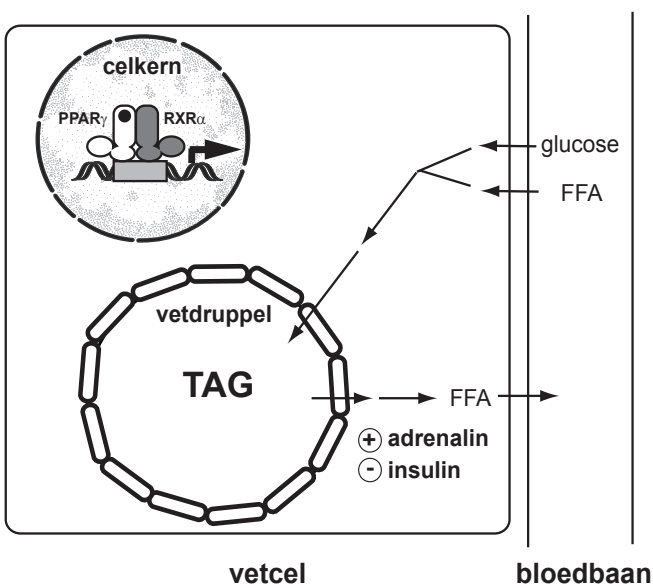

Figure 1. Schematische weergave van de vetstofwisseling in vetcellen.
Suikers (glucose) en vetten (FFA) worden uit de het bloed opgenomen in de vetcel. Hier worden ze opgeslagen als triacylglycerol (TAG) in vetdruppels. Deze TAGs kunnen op hun beurt weer afgebroken worden (lipolyse) en afgegeven aan de bloedbaan om vervolgens in de lever omgezet te worden in brandstoffen bruikbaar voor andere organen als dat nodig is, bijvoorbeeld tijdens vasten of sporten. Lipolyse wordt onder andere geregeld door hormonen als adrenaline, wat lipolyse stimuleert en insuline wat lipolyse juist remt. PPARγ bevindt zich in de celkern en bindt samen met RXRα aan specifieke plekken in het DNA. Als bepaalde moleculen aan PPARγ binden, dan wordt het geactiveerd dat leidt tot het aanschakelen van de specifieke genen in het DNA.

omdat te hoge bloedsuikerspiegels schadelijk zijn voor het lichaam. De functie van een groot aantal van de factoren (eiwitten) die betrokken zijn bij de opslag van suikers en vetten in vetcellen en de afbraak hiervan wordt gereguleerd door PPARγ.

PPARγ

PPARγ is een eiwit dat zich in de celkern (nucleus) van voornamelijk vetcellen bevindt (Figuur 1). Het kan hier op specifieke plekken in het DNA binden en functioneert als het ware als een "schakelaar". Als bepaalde moleculen (liganden) aan PPARγ binden dan wordt het geactiveerd wat leidt tot het aanschakelen van specifieke genen in het DNA. Een gen codeert voor een eiwit en bevat ook de informatie die de cel nodig heeft om te weten hoe het dit eiwit moet maken. Door het aanschakelen van specifieke genen reguleert PPARγ de functie van een aantal eiwitten welke vetcellen tot vetcellen maken. Bovendien is PPARγ het aangrijpingpunt in de vetcel voor geneesmiddelen van de zogenaamde Thiazoledinedione klasse (TZDs), welke worden voorgeschreven aan patiënten met insuline-ongevoeligheid. Deze TZDs functioneren als synthetische liganden van PPARγ en dragen bij aan het verbeteren van de insuline-gevoeligheid ("insulin-sensitizing") in het lichaam.

Hoe PPARγ precies functioneert en hoe de gunstige effecten van TZDs door middel van activatie van PPARγ tot stand komen was nog niet duidelijk. Om deze reden hebben we ten eerste de effecten van zeldzame foutjes (mutaties) in het DNA dat codeert voor PPARγ bestudeerd. Vervolgens hebben we een aantal genen ontdekt die onder controle bleken te staan van TZDs, en die mogelijk bijdragen aan de gunstige effecten van TZDs in patiënten.

In **hoofdstuk 1** wordt de vetstofwisseling in adipocyten, evenals de rol van PPARγ hierin besproken. Verder wordt er een overzicht gegeven van de verschillende vormen van genetische lipodystrofie en de genetische variatie in PPARγ.

Verscheidene studies zijn er gedaan naar de effecten van deze mutaties op het functioneren van PPARγ. In **hoofdstuk 2** wordt een overzicht gegeven van de resultaten van deze studies en gecombineerd met de nieuwe inzichten verkregen uit de recente 3D-structuur van PPARγ en zijn partner RXRα op DNA.

De functionele consequenties van twee van de FPLD3-geassocieerde PPARγ mutaties worden beschreven in de hoofdstukken 3 en 4. De in **hoofdstuk 3** beschreven mutatie (R425C) ligt in het ligand-bindingsdomein van PPARγ en tast verschillende functies, zoals ligand- en DNA- binding aan, waardoor bepaalde genen niet meer goed geactiveerd kunnen worden. Structuuranalyse liet zien dat deze defecten het gevolg zijn van het verbreken van een zoutbrug, die essentieel is voor het behoud van de structuur van het eiwit. In **hoofdstuk 4** hebben we een nieuwe mutatie (R194W) in PPARγ in een patiënt met FPLD3 gerapporteerd. Deze arginine (R194) bevind zich in het DNA-bindingsdomein en draagt bij aan de interactie van PPARγ met DNA. Mutatie van deze arginine zorgt er dan ook voor

dat PPARγ niet meer aan DNA kan binden en vanzelfsprekend niet meer de genen die essentieel zijn voor adipocyten kan activeren.
Om meer inzicht te verkrijgen in de werkingsmechanismen van TZDs, hebben we een micro-array in humane adipocyten behandeld met de TZD rosiglitazone uitgevoerd. Dit heeft ertoe geleid dat we twee nieuwe genen hebben gevonden die onder invloed van rosiglitazone door PPARγ gereguleerd worden. In **hoofdstuk 5** hebben we laten zien dat PPARγ het anti-lipolytische *GPR81* gen reguleert. Dit gen codeert voor de celmembraan receptor GPR81 die zich uitsluitend in adipocyten bevindt. Activatie van deze receptor zet een cascade van reacties in gang, dat uiteindelijk resulteert in een remming van de afbraak van opgeslagen vetten in vrije vetzuren en glycerol (lipolyse) en de uitscheiding hiervan in de bloedbaan. Een van de gunstige effecten van TZDs in patiënten is dat ze de concentratie vrije vetzuren in het bloed verlagen en daarmee de insuline-gevoeligheid verbeteren. Mogelijk draagt de PPARγ-gemedieerde regulatie van GPR81 hieraan bij. Een ander gen dat onder invloed van rosiglitazone door PPARγ gereguleerd wordt is *RNF125* en wordt beschreven in **hoofdstuk 6**. RNF125 is een E3-ubiquitine ligase. E3-ubiquitine ligases zetten ubiqituine-groepen aan specifieke eiwitten waarna ze worden afgebroken of naar een andere plek in de cel worden gestuurd. Nader onderzoek is nodig om te bepalen aan welke eiwitten RNF125 ubiqituine-groepen zet en waarom dit gen door PPARγ gereguleerd wordt in adipocyten.
In een patiënt met complete lipodystrophy (congenitale gegeneraliseerde lipodystrophy type II (CGL2)) hebben we een nieuwe mutatie gevonden in het *BSCL2* gen welke wordt beschreven in **hoofdstuk 7**. Deze mutatie bevindt zich in de splice-site van exon 5 en resulteert in de vorming van afwijkende eiwitten. *BSCL2* codeert voor seipin, een integraal ER eiwit, welke een rol speelt in het differentiatieproces van adipocyten en de vorming van vetdruppels, een karakteristieke eigenschap van adipocyten. In de urine van deze patiënt hebben we afwijkende concentraties organische zuren gemeten, wat een indicatie is voor mitochondriële dysfuctie in deze patiënt.
In **hoofdstuk 8** hebben we bevindingen van onze studies, beschreven in de voorgaande hoofdstukken, bediscussieerd en geïntegreerd in de huidige literatuur.

Conclusies

Zowel obesitas als lipodystrofie gaat gepaard met complicaties zoals insuline-ongevoeligheid, type II diabetes en verhoogde bloeddruk, wat aangeeft dat vetweefsel een essentiële rol speelt in het handhaven van een gezonde stofwisseling in het lichaam. Een belangrijke regulator in vetceldifferentiatie en -functie is PPARγ, zoals is gebleken uit natuurlijke mutaties in PPARγ en de identificatie van PPARγ als het moleculaire target van de insuline-sensitizerende TZDs. In de afgelopen

10 jaar hebben vele studies ertoe bijgedragen dat onze kennis betreffende de rol van PPARγ in adipocyt-biologie sterk is toegenomen. Omdat het aantal mensen met overgewicht en obesitas nog steeds flink toeneemt en dit gepaard gaat met insuline-ongevoeligheid, is veel onderzoek gericht op het ontwikkelen van nieuwe medicijnen die de insuline-gevoeligheid verbeteren. De TZDs waren veelbelovende insuline-sensitizers, maar sommige zijn al weer uit de handel genomen vanwege ongewenste bijwerkingen. Daarom is het huidige onderzoek gericht op de ontwikkeling van zogenaamde SPARMs (specifieke PPARγ modulators), welke mogelijk alleen leiden tot de gunstige effecten. Om dit te kunnen realiseren is het belangrijk dat we goed begrijpen hoe specifieke liganden de functie van PPARγ beïnvloeden.

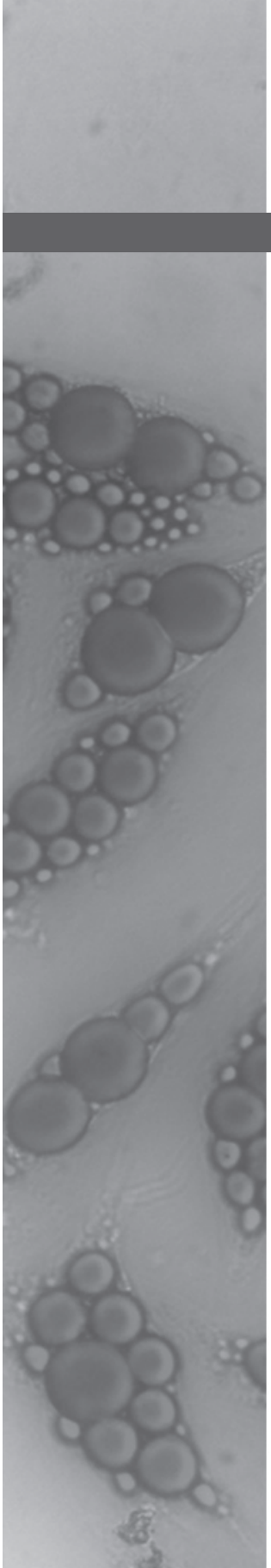

Dankwoord

De aio-periode is voor mij in alle opzichten erg leerzaam geweest. Het is me vaak opgevallen dat er veel overeenkomsten zijn met mijn passie, de bergsport. Om bergen te beklimmen, zowel te voet als op de ski is het noodzakelijk te beschikken over specifieke kennis, vaardigheden en eigenschappen. De kennis en vaardigheden maak je je eigen tijdens cursussen, waarbij een goede coaching door je instructeurs essentieel is. Ook het samenwerken met je medecursisten is erg belangrijk: je leert van elkaar, en je moet gebruik kunnen maken van elkaar kennis en kunde. Daarnaast zijn bepaalde eigenschappen vereist, zoals doorzettingsvermogen, creativiteit en nieuwsgierigheid. De voldoening bij het bereiken van de top is groot. Tegelijkertijd lonkt de volgende top al weer! In die zin is een top ook niet het doel, maar wel een heel plezierige tussenstop.
Op deze manier wil ik iedereen die op welke wijze dan ook (dat laat ik aan jullie verbeelding over) heeft bijgedragen aan de totstandkoming van dit proefschrift heel erg bedanken. Een aantal mensen wil ik in het bijzonder noemen.

Allereerst mijn co-promotor en directe begeleider Eric Kalkhoven en mijn promotor Professor Ruud Berger. Beste Eric, heel erg bedankt voor je inzet en goede begeleiding, een betere "instructeur" heb ik me niet kunnen wensen. Je deur stond altijd voor me open en met je kennis en aanstekende enthousiasme wist je me altijd weer te motiveren en inspireren. Ook heb ik het vertrouwen dat je in me stelde en de kans die je me hebt gegeven om congressen te bezoeken en naar Denemarken te gaan, erg gewaardeerd. Beste Ruud, ondanks dat de dagelijkse begeleiding niet in jouw handen lag vond ik het altijd verbazingwekkend hoe goed je op de hoogte was van het reilen en zeilen van mijn onderzoek. Ik ben erg onder de indruk van je metabole kennis en heb je betrokkenheid en je goede ideeën met betrekking tot mijn onderzoek erg op prijs gesteld. Bedankt!
Beste Leo, graag wil ik je bedanken voor je interesse in mijn onderzoek, de kritische vragen tijdens de werkbesprekingen, je tips en ideeën om manuscripten te verbeteren.
Joost, bedankt voor je interesse en het oplossen van mijn computerprobleempjes.
Jo, Inge en Arjan, bedankt voor jullie input tijdens de werkbesprekingen.
Ciao bella, lieve Maaike, we kennen elkaar sinds het begin van de studie en hebben sindsdien veel samen meegemaakt. Niet alleen hebben we samen 7 maanden in Milaan stage gelopen, ook hebben we 4 maanden door Azië gezworven en een maand in Vietnam gefietst. We zijn min of meer tegelijk begonnen met ons promotie-onderzoek en zullen ons proefschrift een week na elkaar verdedigen. Ik vind het daarom zeer bijzonder en superleuk dat je mijn paranimf wilt zijn.
Hey, pssstt...paranimf, lieve Nicole, toen ik in de adipo-groep kwam heb jij me onder je hoede genomen en me wegwijs gemaakt in het lab. Het was altijd supergezellig om met je samen te werken en ik heb het erg leuk gevonden dat je me in Denemarken hebt opgezocht. Hopelijk kom je ook eens in Lausanne langs. Zodra ik een goede cappuccinobar heb gevonden laat ik het je meteen weten.
Lieve Leyla, kamergenootje, samen hebben we de afgelopen 4 jaar veel aio lief en

leed gedeeld. Ontzettend bedankt voor de gezellige gesprekken, je luisterend oor en je steun. Veel succes met de afronding van je proefschrift en het vinden van een leuke baan. Hopelijk blijven we elkaar zien in de toekomst.
Graag wil ik mijn (ex)collega's van de adipogroep, Olivier, Yuan, Brenda, Arjen, Henk, Ismayil, Anneke, Veerle en Joep enorm bedanken voor hun hulp, adviezen, interesse en gezelligheid. Olivier, screenmaster, het was erg fijn en leerzaam om met je samen te werken. Je pragmatische aanpak, betrokkenheid en passie voor wetenschappelijk onderzoek en je bijzondere hobby's zullen me altijd bijblijven. Xiâo Yúan, thanks for the nice Chinese dinners and all your hugs. Good luck with finishing your thesis and when you are visiting your friend in Lausanne, please come by for dinner. Arjen, ik heb altijd erg gelachen om je droge humor en het heeft even geduurd, maar nu heb ik eindelijk in de gaten wanneer je me in de maling probeert te nemen. Henk, Wampex-organisator, het is verbazingwekkend hoe snel jij ons zo gek hebt gekregen om de hele nacht door de Friese modder te banjeren. Ik vind het heel leuk dat jij mijn RNF125 project gaat voortzetten en ben ervan overtuigd dat het tot een mooie publicatie zal leiden. Anneke, het was erg leuk en leerzaam om je te begeleiden. Bedankt voor je inzet en gezelligheid.
Wouter, je was een zeer gezellige kamergenoot en goede vraagbaak. Bedankt voor de leuke en interessante gesprekken en je hulp bij mijn lay-out problemen (gelukkig was jij wel geduldig). Succes met je onderzoek. Sabine, ex-kamergenote, bedankt voor je interesse en de gezelligheid. Succes met het afronden van je promotie.
Mijn (ex)collega-AIO's, "medecursisten", Peter, Hannelie, Janneke, Lieke, Willianne, Rafaella, Gemma, Stiaan, Wendy, Prim, Patricia en ook de (ex)post-docs, Stan, Saskia, Bart en Annemieke wil ik bedanken voor de leerzame en leuke tijd. Peter, bedankt voor je hulp met indesign. Hannelie, ik heb altijd erg genoten van onze gezellige fietstochtjes na het werk. De klok is naar de zomertijd, dus we kunnen weer.... Bart, ex-collega en fietsmaatje, jij ook bedankt voor de gezellige fietstochtjes. Helaas woon je nu in Grun en kunnen Hannelie en ik niet meer in je wiel kruipen. En natuurlijk wil ik mijn labgenoten die ik nog niet genoemd heb en de mensen van de Speciële Endocrinologie en Metabole Diagnostiek bedanken voor de leuke en gezellige tijd. Mariëtte, het was altijd leuk om naar je enthousiaste reisverhalen te luisteren en bedankt voor de reistips en het lenen van de Kirgizië reisgids. Truus, bedankt voor het regelen van mijn bestellingen en voor de blaadjes van de KNRM. Als ik nog eens met het skûtsje vast kom te liggen, dan wordt ik zeker donateur! Monique de Gooijer, bedankt voor het regelen van allerlei praktische zaken.
Professor Susanne Mandrup, thanks for the nice and fruitful collaboration and the opportunity you gave me to stay in your lab for two months to learn ChIP-assays. I would also like to thank the people of Susanne's lab for their help, ideas and the nice time. Anne, thanks a lot for your help with the ChIP assays, the viruswork and things outside the lab. Good luck with finishing your PhD and your future career! Ronni and Thomas, ChIP-seq masters, thanks for all your help with the ChIP-seq analysis. Jørgen Bjerring, thanks for arranging the practical stuff.

Mijn externe begeleiders Sander Kersten en Jeanette Leusen wil ik graag bedanken voor hun interesse en adviezen bij mijn aio-evaluaties. Sander, tevens bedankt voor je hulp bij de micro-arrays, welke de start zijn geweest van hoofdstuk 5 & 6 en dat je me in december vorig jaar de presentatie van Prof. Auwerx in Amsterdam getipt hebt. Dit heeft ertoe bijgedragen dat hij nu mijn toekomstige werkgever is. Guido Hooijveld, bedankt voor je hulp bij de micro-array analyse. Shohreh Keshtkar, bedankt voor je bijdrage aan het GPR81 verhaal.
Alexandre Bonvin en Aalt-Jan van Dijk, bedankt voor de fijne samenwerking en de mooie resultaten en 3D-plaatjes die terug te vinden zijn in hoofdstuk 2 en 3.
Houshang Monajemi, bedankt voor de leuke samenwerking, welke geresulteerd heeft in het R194W paper. Veel succes met je nieuwe baan in het UMCU.
Monique de Vroede en Nanda, bedankt voor de fijne samenwerking en de goede tips voor het verbeteren van het Seipin manuscript.
Koen, het was erg leuk je te helpen bij je Menin-paper en hopelijk wordt het nu snel geaccepteerd. Veel succes bij het afronden van je promotie.

Tevens wil ik al mijn vrienden bedanken voor hun steun, telefoontjes, kaartjes, gezellige feestjes, weekendjes, fietstochtjes en vakanties, waarna ik weer met hernieuwde energie aan het werk kon. Floor en Giel, bedankt voor het lekkere eten en de gezelligheid na de spinning. Aafke, bedankt voor al onze gezellige avondjes. Hopelijk vind je ook snel een passende baan! Lieve Ils, Noor, Annet en Charis, we kennen elkaar al sinds de kleuterschool en ik vind het dan ook zeer bijzonder dat we elkaar nog altijd zien en gezellig weekendjes weg gaan. Diewke, Birgit, Mathilde en Els, sorry dat ik de laatste keren soms verstek heb laten gaan, maar ik beloof beterschap. Onze weekendjes weg moeten we er zeker in houden, in ieder geval hebben we weer 2 nieuwe bestemmingen; Kopenhagen en Lausanne.
And last, but not least, wil ik graag mijn ouders en broers bedanken voor hun onvoorwaardelijke liefde, steun, interesse, begrip en luisterend oor. Jasper, lieve broer, ik vind het heel jammer dat jij en Jutta nu in Australië zitten en niet bij de verdediging aanwezig kunnen zijn. Hopelijk zie ik jullie eind juli weer en kunnen we misschien nog een weekje op het Wad zeilen met het skûtsje. In ieder geval is de afstand Lausanne-Untergruppenbach iets kleiner dan Utrecht-Untergruppenbach. Hey ouwe!, broertje, lieve Maarten, ik was erg blij toen je een jaar geleden bij me om de hoek kwam wonen. Het was heerlijk om samen te fietsen, eten, koffie en biertjes te drinken en ik vind het dan ook jammer dat ik nu 900 km verderop ga wonen. Binnenkort krijg je je snelle nieuwe auto en dan moet je maar met je fietsje en snowboard langskomen. Lieve paps en mams, ik weet niet goed wat ik voor jullie kan schrijven, behalve dat ik jullie erg dankbaar ben dat jullie er altijd voor me zijn. Ik houd van jullie!

En voor diegenen voor wie mijn onderzoek een beetje abracadabra was, hopelijk verschaft mijn Nederlandse samenvatting voor niet ingewijden helderheid!

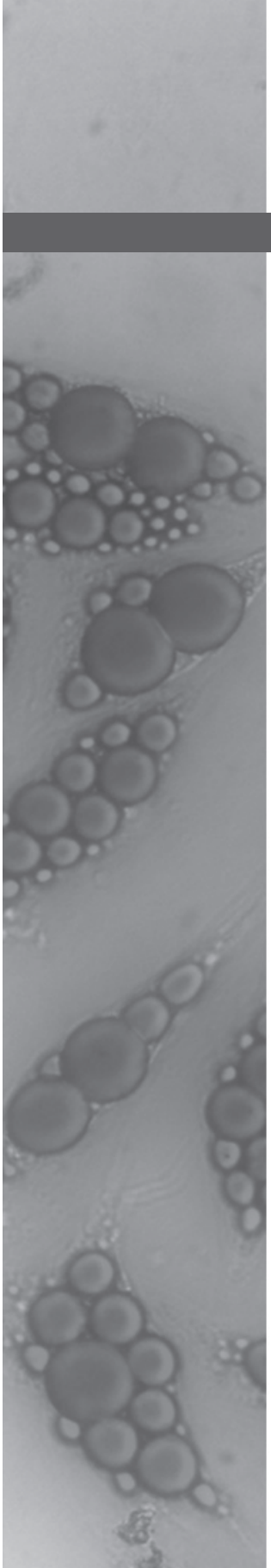

About the Author

Ellen Jeninga was born on April 6, 1980 in Obdam (The Netherlands). She finished secondary school (Athenaeum, St. Ludger College Doetinchem) in 1998. In the same year she started her study Biomedical Sciences at the University of Utrecht. During her study she fulfilled training periods at the Department of Hematology, University Medical Center Utrecht (UMCU), under supervision of Dr. J.A. Remijn and Prof. dr. P.G. de Groot and at the Department of Immunohematology and Cell Biology, Mario Negri Institute, Milan, Italy, under supervision of Dr. J. Golay, Dr. M. Introna and Prof. dr. A. Hagenbeek. In June 2003 she obtained her masters degree in Biomedical Sciences. From June 2003 until November 2004 she worked as data-entry and episode employee at Stichting Nivel in Utrecht and travelled for some months in Australia and Asia. From November 2004 until February 2009 she was employed as PhD student at the Department of Metabolic and Endocrine Diseases at the UMCU. During this period she performed the research presented in this thesis under supervision of Dr. E. Kalkhoven and Prof. dr. R. Berger. In September 2009 she will start as a post-doctoral fellow in the Laboratory of Integrative Systems Physiology (Prof. dr. J. Auwerx) at the Swiss Federal Institutes of Technology in Lausanne (EPFL), Switzerland.

~

Ellen Jeninga werd geboren op 6 april 1980 te Obdam. Ze behaalde haar VWO diploma op het St. Ludger College te Doetinchem in 1998. In hetzelfde jaar begon zij aan haar studie Biomedische Wetenschappen aan de Universiteit van Utrecht. Tijdens haar studie werden stages gevolgd bij de Afdeling Hematologie, Universitair Medisch Centrum Utrecht (UMCU), onder begeleiding van Dr. J.A. Remijn en Prof. dr. P.G. de Groot en bij de Afdeling Immunohematologie en Celbiologie, Mario Negri Instituut, Milaan, Italië, onder begeleiding van Dr. J. Golay, Dr. M. Introna and Prof. dr. A. Hagenbeek. In juni 2003 werd het doctoraal examen Biomedische wetenschappen behaald. Van juni 2003 tot november 2004 was zij werkzaam als data-entry en episode medewerkster bij de Stichting Nivel in Utrecht en heeft zij enige maanden in Australië en Azië rondgereisd. Van november 2003 tot februari 2009 was zij werkzaam als assistent-in-opleiding bij de afdeling Metabole en Endocriene Ziekten van het UMCU. Gedurende deze periode werd onder begeleiding van Dr. E. Kalkhoven en Prof. dr. R. Berger onderzoek verricht dat tot dit proefschrift heeft geleid. In september 2009 zal zij starten als een post-doctoraal onderzoeker in het Laboratorium Integratieve Systeem Fysiologie (Prof. dr. J. Auwerx) aan de Technische Rijksuniversiteit Lausanne (EPFL), Zwitserland.